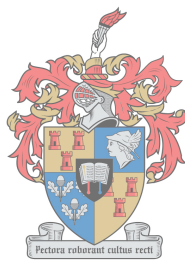


Contribution of Highly Active Anti-Retroviral Therapy to the Development of Non-alcoholic Fatty Liver Disease with Concomitant Cardiovascular Dysfunction in an Obese Rat Model

by
Dr Festus Maina Kamau



Dissertation presented for the degree of Doctor of Philosophy (Medical Physiology) in the Faculty of Medicine and Health Sciences at Stellenbosch University



Supervisors: Dr Ruduwaan Salie and Dr Peter Waweru
Co-supervisor: Prof Hans Strijdom

March 2018

Declaration

By submitting this dissertation electronically, I declare that the entirety of the work contained therein is my own, original work, that I am the sole author thereof (save to the extent explicitly otherwise stated), that reproduction and publication thereof by Stellenbosch University will not infringe any third-party rights and that I have not previously in its entirety or in part submitted it for obtaining any qualification.

Festus Maina Kamau

March 2018

Copyright © 2018 Stellenbosch University

All rights reserved

Abstract

Introduction:

HIV/AIDS mortality is declining due to successful highly active anti-retroviral therapy (HAART). However, obesity, non-alcoholic fatty liver disease (NAFLD) and cardiovascular disease (CVD) in treated HIV-infected populations are rising. Impaired peroxisome proliferator-activated receptor (PPAR α/γ) activity is partly implicated.

Aims:

To assess the contribution of a protease inhibitor (Lopinavir/Ritonavir (LPV/r) and nucleoside reverse transcriptase inhibitor (Azidothymidine (AZT)/lamivudine (3TC)) HAART regimen in the development of NAFLD and CVD in rats with high caloric diet (HCD)-induced obesity, and to investigate dual PPAR α/γ stimulation in limiting HAART-induced NAFLD and CVD.

Methods:

Wistar rats were randomised into rat chow and HCD groups (n=88/group; 16 weeks). From week 10, each group was further sub-divided into: vehicle/control, HAART, HAART+PPAR α/γ agonist (Saroglitazar) and Saroglitazar only (n=22/group) administered via oral gavage. **Endpoints:** Daily food/water consumption, weekly total body mass (TBM), random+fasting blood glucose measurements (n=8/group); hearts exposed to either 20min global ischaemia/10min reperfusion for Western blot (WB) analysis (n=6/group) or 35min regional ischaemia/60min reperfusion (n=8/group) for haemodynamic and infarct size (IS) determinations. Liver samples were histologically assessed (n=12/group) and analysed by WB. Intraperitoneal (IP) fat was weighed. Fasting serum lipids, insulin and oxidative stress markers were measured (n=8/group). WB analyses of important signalling proteins in pre/post-cardiac ischaemia, liver and aorta tissues. Thoracic aorta (n=8/group) segments were subjected to isometric tension studies.

Results:

The HCD resulted in obesity (increased: TBM, %IP fat (HCD control 6.50 \pm 0.40% vs. lean control 3.60 \pm 0.3%; p<0.0001), liver mass, insulin and triglycerides (TGs). Additionally, HCD induced insulin resistance (IR). HAART+Saroglitazar led to reduced %IP fat in lean and HCD groups. HAART-induced IR, elevated cardiac mass and insulin in obese rats were limited by Saroglitazar co-treatment. HCD+HAART-induced oxidative stress (elevated conjugated dienes), was limited in combined HAART+Saroglitazar.

Liver histology: HAART induced moderate hepatic steatosis in ~67% of obese rats and moderate inflammation in ~25% of cases. Combined HAART+Saroglitazar limited these changes and upregulated adenosine monophosphate-activated protein kinase (AMPK) and protein kinase B (PKB/Akt) activity, which were downregulated by HAART in HCD.

Heart/aorta studies: Untreated obese rats had smaller %IS compared to lean control rats (19.1 \pm 1.6 vs. 26.1 \pm 1.6, respectively; p<0.05). IS for HCD+HAART animals were smaller (despite poor cardiac performance) compared to untreated obese rats. Post-ischaemia activity of extracellular-signal-regulated

kinase (Erk1/2), PKB/Akt, AMPK and endothelial nitric oxide synthase (eNOS) was downregulated, whereas expression of p22-phox and caspase-3 was accentuated. HAART+Saroglitazar upregulated (1.5-fold) the expression of Erk1/2, PKB/Akt, AMPK and eNOS, and downregulated caspase-3 and p22-phox.

Obese+HAART rats demonstrated poor aortic relaxation accompanied by downregulated eNOS and PKB/Akt, and upregulated p22-phox. However, Saroglitazar+HAART in obese animals improved aortic relaxation by ~30%, accompanied by upregulation of eNOS, and PKB/Akt, and downregulated p22-phox.

Discussion and conclusion:

HAART-induced NAFLD and CVD in obesity were limited by PPAR α/γ agonist co-administration. HAART treatment for six weeks was not a cardiovascular risk factor *per se*, but it potentiated HCD-induced cardiovascular effects. Monitoring cardiovascular risk factors in obese+HAART patients is crucial, and our findings suggest that there is therapeutic potential in co-treatment with PPAR α/γ agonists. The metabolic, functional and signalling disturbances in the liver, heart and aorta tissues in obese+HAART rats are interlinked, and partially limited by co-treatment with a dual PPAR α/γ agonist.

Opsomming

Inleiding:

Daar is 'n daling in die HIV/VIGS sterftesyfer a.g.v. suksesvolle hoogs-aktiewe antiretrovirale terapie (HAART). Vetsug, nie-alkoholiese vetterige lewersiekte (NAFLD) en kardiovaskulêre siekte (KVS) in behandelde HIV-geïnfekteerde populasies is aan die styg. Ingekorte peroksisoom proliferator-geaktiveerde reseptor (PPAR α/γ) funksie is deels hiervoor verantwoordelik.

Doelwitte:

Om die bydraes van 'n protease inhibitor (Lopinavir/Ritonavir (LPV/r) en nukleosied omgekeerde transkriptase inhibitor (Azidothymidine (AZT)/lamivudine (3TC)) as deel van HAART in die ontwikkeling van NAFLD en KVS in rotte met 'n hoë kaloriesdieet (HCD)-geïnduseerde vetsug te bepaal, asook tweeledige PPAR α/γ -stimulasie in die vermindering van HAART-geïnduseerde NAFLD en KVS te bepaal.

Metodes:

Wistar rotte is lukraak in 'n gewone rot-dieet en 'n HCD groep (n=88/groep; 16 weke) ingedeel. Vanaf Week 10 is elke groep verder onderverdeel in: oplosmiddel/kontrole, HAART, HAART+PPAR α/γ agonis (Saroglitazar) en slegs Saroglitazar (n=22/groep) wat via 'n gastriese buis toegedien was.

Eindpunte:

Daaglikse kos/water verbruik, weeklikse totale liggaamsgewig (TBM), lukrake+vastende bloedglukose (n=8/groep); harte wat blootgestel is aan óf 20min globale isgemie/10min herperfusie, wat vir Western blot (WB) ontleding aangewend is, of 35min streksisgemie/60min herperfusie (n=8/groep), wat vir hemodinamiese en infarkt-grootte (IS) bepalinge aangewend is. Lewermonsters is histologies ondersoek (n=12/groep) en ontleed deur WB. Intraperitoneale (IP) vet is geweeg. Vastende serumlipiede, oksidatiewe spanningsmerkers en insulien is gemeet (n=8/groep). WB ontledings van belangrike seintransduksieproteïene in pre/post-isgemiese hart-, lewer- en aortaweefsel uitgevoer. Torakale aortasegmente (n=8/groep) is aan isometriese spanningstudies blootgestel.

Resultate:

Die HCD het tot vetsug gelei (verhoogde: TBM, %IP vet (HCD kontrole 6.50 \pm 0.40% vs. gewone-dieet kontrole 3.60 \pm 0.3%; p<0.0001), lewermassa, insulien en trigliseriedes). Verder het HCD tot insulienweerstandigheid (IR) gelei. HAART+Saroglitazar het tot verlaagde %IP vet in kontrole en HCD groepe gelei. HAART het IR veroorsaak, terwyl verhoogde hartmassa en insulien in vetsugtige rotte deur ko-behandeling met Saroglitazar verlaag is. HCD+HAART het vrye-vetsuur-oksidasie (verhoogde gekonjugeerde diëne) geïnduseer, wat deur gekombineerde HAART+Saroglitazar verminder is.

Lewerhistologie: HAART het matige lewersteatose in ~67% van vetsugtige rotte en matige inflammasie in ~25% veroorsaak. Hierdie veranderinge is deur gekombineerde HAART+Saroglitazar verlig en AMPK en PKB/Akt aktiwiteit is opgereguleer, wat deur HAART afgereguleer is.

Hart/aorta studies: Onbehandelde vetsugtige rotte het kleiner IS as kontrole gehad (19.1 ± 1.6 vs. 26.1 ± 1.6 , onderskeidelik; $p < 0.05$). Die IS vir rotte op HAART+HCD was kleiner (ondanks swak hartfunksie) vs. hul onbehandelde eweknieë. Die post-isgemiese aktiwiteit van Erk1/2, PKB/Akt, AMPK en eNOS is afgereguleer, terwyl uitdrukking van p22-phox en kaspase-3 verhoog is. Die uitdrukking van Erk1/2, PKB/Akt, AMPK en eNOS is deur HAART+Saroglitazar opgereguleer (1.5-voudig) en PKB/Akt en p22-phox is afgereguleer.

Vetsugtige+HAART rotte het swak aortiese verslapping getoon ~30%, wat met afgereguleerde eNOS en PKB/Akt en opgereguleerde p22-phox geassosieer was. Tog het Saroglitazar+HAART in vetsugtige rotte tot verbeterde aortiese verslapping, gepaard met opgereguleerde eNOS en PKB/Akt, asook afgereguleerde p22-phox gelei.

Bespreking en gevolgtrekking:

HAART-geïnduseerde lewersteatose en KVS in vetsugtige rotte is deur ko-behandeling met 'n PPAR α/γ agonis verlig. HAART *per se* was nie 'n kardiovaskulêre risikofaktor nie, maar het die HCD-geïnduseerde kardiovaskulêre effekte vererger. Dis noodsaaklik om die kardiovaskulêre risikofaktore in vetsugtige+HAART pasiënte te monitor, en ons bevindinge toon dat ko-behandeling met PPAR α/γ agoniste terapeutiese potensiaal het. Die metaboliese, funksionele en seintransduksieversteurings in die lewer, hart en aortaweefsel in vetsugtige+HAART rotte is ineengeskakel en word gedeeltelik verlaag deur ko-behandeling met 'n tweeledige PPAR α/γ agonis.

Dedication

This treatise is dedicated to the immunocompromised; stay strong, we are working on solutions...

Acknowledgements

I would like to sincerely thank my supervisors: Dr. Peter Waweru, Dr. Ruduwaan Salie and Prof. Hans Strijdom for your guidance, and support. Incredible team work enabled us to succeed. Additionally, you have been friendly, patient, very understanding and offered me a conducive environment to perform my tasks.

Secondly, I would like to acknowledge my family: Starting with my beloved Grace, my loving dad, mum and my siblings for being with me emotionally and encouraging me through prayers. I thank God for keeping us close despite the long distance.

I would also like to thank other senior colleagues who have offered their expertise and time in course of this project. I'm indebted to Dr. Dee Blackhurst for allowing me to work in her lab and being a good teacher. Special thanks to Reggie for working long hours with me in his (histology) lab. I am grateful to Dr. Christo Muller for guiding me through my histology work.

I offer my special gratitude to Prof. A Lochner for her warm kindness and always being there to offer assistance whenever needed and being an advisor to our team. Also, I would like to thank Prof. Huisamen for being a good teacher and listener whenever I needed clarifications on my work. Special thanks to Prof. Stefan du Plessis for being an excellent Division head; whenever I needed help with administrative issues, you were always there not only to encourage, but also to make sure that everything ran smoothly. I would also like to express my gratitude to Prof. Nico Gey van Pittius for availing funds to support my studies in the year 2017.

I would also like to thank Dr. Amanda for all the sacrifices you have made to ensure our project was successful. Also, many thanks to Miss Skosana, Miss Emiliana and all the staff members in our division for creating a wonderful working environment.

Many thanks to all my colleagues for being wonderful friends. Special thanks to those I worked closely with in the heart lab, just to mention: Frans Everson, Dr. Karthik, Zibele, Sybrand and Marguerite. Not only did you ensure that our lab work ran smoothly, but also, you provided wonderful company.

Table of contents

Title / cover page	-
Declaration.....	i
Abstract.....	ii
Opsomming.....	iv
Dedication	vi
Acknowledgements	vii
Table of contents	viii
List of abbreviations	xiii
List of units of measurement.....	xx
List of Figures.....	xxi
List of Tables	xxvi
List of Addenda	xxvii
Chapter 1 : Introduction and literature review	1
1.1 General introduction	1
1.2 Cardiovascular disease	2
1.2.1 Introduction.....	2
1.2.2 Epidemiology.....	3
1.2.3 Pathophysiology of myocardial infarction.....	5
1.2.4 Role of endothelium.....	5
1.2.5 CVD in metabolic syndrome	6
1.3 HIV/AIDS	7
1.3.1 Introduction.....	7
1.3.2 Epidemiology of HIV/AIDS.....	8
1.3.3 HIV structure	9
1.3.4 HIV life cycle and treatment targets	10
1.3.5 2'-deoxy-3'-thiacytidine; (3TC)	12
1.3.6 3'-azido-3'-deoxythymidine (AZT).....	13
1.3.7 LPV	14
1.3.8 Basis of ARV combination against HIV.....	15
1.3.9 CVD in HIV and HAART	16
1.3.10 HIV, HAART and overweight/obesity	17
1.4 Non-alcoholic fatty liver disease (NAFLD).....	17

1.4.1	Introduction.....	17
1.4.2	Epidemiology of NAFLD.....	18
1.4.3	Pathophysiology of NAFLD.....	19
1.4.4	The intersection: HAART, NAFLD and CVD.....	21
1.5	Signalling molecules in hepatic, vascular and cardiac homeostasis.....	25
1.5.1	Peroxisome proliferator-activated receptors alpha / gamma (PPAR α / γ).....	25
1.5.2	Peroxisome proliferator-activated receptors gamma co-activator 1 alpha (PGC1- α).....	26
1.5.3	Nuclear factor-kappa B (NF κ B).....	28
1.5.4	Protein kinase B (PKB) / Akt.....	29
1.5.5	AMPK.....	31
1.5.6	Role of AMPK in CVD and metabolic syndrome.....	33
1.5.7	Other important signalling molecules.....	34
1.6	Problem statement and study rationale.....	35
1.7	Research questions.....	36
1.7.1	Hypotheses.....	37
1.8	Research aims and objectives.....	37
Chapter 2 : Methodology.....		39
2.1	Introduction.....	39
2.2	Study design.....	39
2.3	Ethics clearance and protocol approval.....	39
2.4	Infrastructure.....	40
2.4.1	Personnel involved in the various research study activities.....	40
2.5	Research activities.....	41
2.5.1	Experimental animal selection, housing and grouping.....	41
2.5.2	Feeding and treatment programme.....	42
2.5.3	Animal monitoring.....	44
2.5.4	Overnight fasting.....	45
2.5.5	Euthanasia.....	45
2.5.6	Blood glucose measurement.....	46
2.5.7	Incision, serum collection and isolation of organs.....	46
2.5.8	Isolated working heart perfusion system.....	47
2.5.9	TTC staining and infarct size analysis.....	49
2.5.10	Cardiac haemodynamic performance data collection.....	50
2.5.11	Vascular reactivity, aortic ring studies.....	51
2.5.12	Analysis of fasted serum samples.....	53
2.5.13	Protein expression and phosphorylation measurements - Western blot analysis.....	54
2.5.14	Liver tissue histology.....	60

2.6	Data management and statistical analysis	64
Chapter 3 : Results.....66		
3.1	Introduction.....	66
3.2	Feeding and treatment programme: - food and water consumption monitoring	68
3.2.1	Standard rat chow	68
3.2.2	HCD consumption	70
3.2.3	Water consumption	71
3.3	Total body mass monitoring	72
3.3.1	Total body mass of the animals at the onset of the programme.....	72
3.3.2	Total body mass changes during the first 10 weeks of the feeding programme.....	73
3.3.3	Total body mass monitoring during the treatment programme	74
3.4	Biometric data on the day animals were sacrificed	75
3.4.1	Mean total body mass during euthanasia	75
3.4.2	Visceral / intra-peritoneal (IP) fat mass.....	76
3.4.3	Cardiac mass.....	77
3.4.4	Liver mass.....	79
3.5	Blood and serum parameters.....	80
3.5.1	Blood glucose levels	80
3.5.2	Lipid profile	82
3.5.3	Serum markers of lipid peroxidation	86
3.6	Liver enzymes assays	89
3.6.1	Serum alkaline phosphatase (S-ALP)	90
3.7	Fasting serum insulin concentrations	91
3.8	Homeostasis model assessment for insulin resistance (HOMA-IR).....	91
3.9	Isolated working rat heart perfusion data.....	92
3.9.1	Heart rate (HR)	93
3.9.2	Qa: aortic outflow	94
3.9.3	Qe: coronary flow rate	95
3.9.4	Total cardiac output	95
3.9.5	Wt: work total	96
3.9.6	sp and dp	97
3.10	Myocardial infarct size analysis	97
3.11	Liver tissue histology results.....	99
3.12	Vascular reactivity / aortic ring study results	104
3.12.1	Phenylephrine-induced aortic contraction	105
3.12.2	Acetylcholine-induced aortic relaxation.....	106

3.12.3	Nonlinear regression for log transformation of acetylcholine dose vs. percentage aortic relaxation.....	108
3.13	Protein expression and phosphorylation measurements - Western blot analysis results	110
3.13.1	Heart tissue protein determination.....	110
3.13.2	Aortic tissue protein determination.....	124
3.13.3	Liver tissue protein determination	130
Chapter 4	Discussion	137
4.1	Introduction.....	137
4.2	Feeding programme.....	137
4.2.1	Food intake.....	137
4.2.2	Water consumption	138
4.3	Body mass monitoring	138
4.4	Visceral fat.....	140
4.5	Organ mass	141
4.5.1	Heart mass.....	141
4.5.2	Liver mass.....	142
4.6	Food intake, body mass and IP mass	143
4.7	Biochemical Analyses.....	144
4.7.1	Blood glucose levels	144
4.7.2	Fasting serum insulin and HOMA-IR.....	145
4.7.3	Mechanisms of PPAR α and PPAR γ that mediate their biological effects.....	146
4.8	Serum lipid profile	147
4.8.1	Serum total cholesterol, TC	148
4.8.2	HDL-C	148
4.8.3	LDL-C.....	149
4.8.4	Serum phospholipids.....	149
4.8.5	TGs.....	150
4.8.6	Serum lipids and atherosclerosis.....	150
4.9	Serum markers of lipid peroxidation	151
4.9.1	CD and TBARS	151
4.10	Working heart perfusion studies	152
4.10.1	HR.....	152
4.10.2	Coronary flow rate (Q _e) and aortic diastolic / systolic pressure.....	152
4.10.3	Aortic output (Q _a), total cardiac output (CO) and total work (W _t).....	153
4.10.4	Left ventricular infarct size analysis	154
4.11	Aortic ring isometric tension studies.....	155
4.11.1	Phenylephrine-induced aortic contraction	155

4.11.2	Acetylcholine-induced aortic relaxation	157
4.12	Liver tissue histology	159
4.12.1	Diet and NAFLD.....	160
4.12.2	HAART and NAFLD.....	160
4.13	Signalling proteins	161
4.13.1	AMPK.....	161
4.13.2	PKB/Akt.....	165
4.13.3	eNOS.....	169
4.13.4	MAPKs: p38 and Erk 1 / 2.....	170
4.13.5	PGC 1 α and PPAR α	172
4.13.6	I κ B α	173
4.13.7	NADPH p22-phox, cleaved caspase 3 and cleaved PARP.....	174
4.14	Summary.....	176
Chapter 5	: Final conclusion	181
5.1	Conclusion	181
5.2	Study limitations	182
5.3	Future directions.....	184
5.4	Research outputs so far	185
Chapter 6	: Bibliography	192

List of abbreviations

3TC	2,3' dideoxy- 3-thiacytidine (Lamivudine)
Ab	Antibody
ABCA 1	ATP-binding cassette transporter 1
ACC	Acetyl-CoA carboxylase
ACS	Acute coronary syndrome
ADP	Adenosine diphosphate
ALP	Alkaline phosphatase
ALT	Alanine amino transferase
AMI	Acute myocardial infarction
AMP	Adenosine monophosphate
AMPK	5' Adenosine monophosphate-activated protein kinase
ANOVA	Analysis of variance
APO A	Apolipoprotein A
APO B	Apolipoprotein B
AR	Area at risk
ARV	Antiretroviral
AST	Aspartate aminotransferase
ATP	Adenosine triphosphate
AZT	Azidothymidine (Zidovudine)
bFGF	basic fibroblast growth factor
BMI	Body mass index
BPA	Bradford protein Assay
bpm	Beats per minute
BRIP	Biomedical Research and Innovation Platform
BSA	Bovine serum albumin
CAC	Coronary artery calcification
CAD	Coronary artery disease
CAMKK	Calmodulin-dependent protein kinase kinase 2

cAMP	Cyclic AMP
cART	Combined/ combination anti-retroviral therapy
CCR5	C-C chemokine receptor type 5
CD4	Cluster of differentiation subtype 4
CDC	Centre for Disease Control
CDs	Conjugated dienes
CHD	Coronary heart disease
Cleaved PARP	Cleaved poly (ADP-ribose) polymerase
CO	Cardiac output
CRP	C-reactive protein
CT	Computerized tomography
CVD	Cardiovascular disease
CXCR4	C-X-C chemokine receptor type 4
DALYs	Disability adjusted life years
DIO	Diet-induced obesity
DM	Diabetes mellitus
DNA	Deoxyribonucleic acid
dp	Diastolic pressure
ECG	Electrocardiogram
ECL	Enhanced chemiluminescence
EDTA	Ethylenediaminetetraacetic acid
EGF	epidermal growth factor
EGTA	Ethyleneglycoltetraacetic acid
ELISA	Enzyme-linked immunosorbent assay
eNOS	Endothelial nitric oxide synthase
ERK 1 / 2	Extracellular-signal-regulated kinase
ESC	European Society of Cardiology (ESC)
FA	Fatty acids
FBS	Fasting blood sugar

FFA	Free fatty acids
FMHS	Faculty of Medicine and Health Sciences
FP	Feeding programme
GF	Growth factors
GGT	Gamma-glutamyl transferase
GLUT 1 / 4	Glucose transporter 1 / 4
Gp	Glycoprotein particles
GSK-3	Glycogen synthase kinase 3
GST-P	Glutathione S-transferase P
H/E	Haematoxylin and eosin
H ₂ O ₂	Hydrogen peroxide
HAART	Highly active antiretroviral therapy
HCD	High calorie / caloric diet
HDL	High-density lipoprotein
HED	Human equivalent dose
HF	Heart failure
HFD	High fat diet
HIV / AIDS	Human immunodeficiency virus / acquired immunodeficiency syndrome
HIVAC	HIV-associated cardiomyopathy
HOMA-IR	Homeostatic model assessment of insulin resistance
HR	Heart rate
HTLV-1	Human T-cell lymphotropic virus type 1
I/R	Ischaemia-reperfusion
IGF-1	Insulin like growth factor-1
IHD	Ischaemic heart disease
IL	Interleukin
InSTI	Integrase strand inhibitors
IP	Intraperitoneal
IR	Insulin resistance

IRS	Insulin receptor substrate
IS	Infarct size
I κ B α	Inhibitor of nuclear kappa B (subtype alpha)
JNK	c-Jun N-terminal kinase
KHB	Krebs-Henseleit buffer
L-NAME	L-N ^G -Nitroarginine methyl ester
LADCA	Left anterior descending coronary artery
LDL-C	Low-density lipoproteins cholesterol
LFT	Liver function tests
LKB1	Liver kinase B1
LMICs	Low-and-middle income countries
LPL	Lipoprotein lipase
LPR	Lipoprotein receptor-related protein
LPV	Lopinavir
LPV/r	LPV boosted with ritonavir
LV	left ventricle
MAPK	Mitogen-activated protein kinase
MI	Myocardial infarction
MRI	Magnetic resonance imaging
n	Sample size
Na ₃ VO ₄	Sodium orthovanadate
NaCl	Sodium chloride
NADPH p22-phox	Nicotinamide adenine dinucleotide phosphate-oxidase, p22 phox subunit
NAFLD	Nonalcoholic fatty liver disease
NAS	Nonalcoholic steatosis
NASH	Nonalcoholic steatohepatitis
NCD	Non-communicable diseases
NF κ B	Nuclear factor kappa B
NNRTI	Non-nucleoside reverse transcriptase inhibitors

NO	Nitric oxide
NOS	Nitric oxide Synthase
NOX	Nicotinamide adenine dinucleotide phosphate-oxidase
NRTIs	Nucleoside reverse transcriptase inhibitors
NtRTIs	Nucleotide reverse transcriptase inhibitors
OIs	Opportunistic infections
ORO	Oil red O
PAGE	Polyacrylamide gel electrophoresis
PARP	Poly (ADP) ribose polymerase
PDE3B	Phosphodiesterase 3B
PDGF-R	Platelet-derived growth factor receptor
PEPCK	Phosphoenopyruvate carboxylase
PGC	Peroxisome proliferator-activated receptor gamma co-activator
PGC-1 α	Peroxisome proliferator-activated receptor gamma co-activator 1-alpha
PI	Protease inhibitors
PI3K	3-phosphoinositide kinase
PIP3	Phosphatidylinositol 3,4,5, triphosphate
PKB/Akt	Protein kinase B
PKC	Protein kinase C
PKD1	Protein kinase D1
PLWH	People living with HIV / AIDS
PMSF	Phenylmethylsulfonyl fluoride
PP2A	Phosphatase 2A
PPAR	Peroxisome proliferator-activated receptors
PPAR α	Peroxisome proliferator-activated receptor alpha
PPAR γ	Peroxisome proliferator-activated receptor gamma
PPRE	Peroxisome proliferator response element
PUFA	Polyunsaturated fatty acids
PVAT	Perivascular adipose tissue

PVDF	Polyvinylidene fluoride
Qa	Aortic outflow
Qe	Coronary outflow
RA	Retinoic acid
RBS	Random blood sugar
RHD	Rheumatic heart disease
RISK	Reperfusion injury salvage kinase
RNA	Ribonucleic acid
ROMICAT	Rule out myocardial infarction using computer assisted tomography
ROS	Reactive oxygen species
RP	Retrograde perfusion
RT	Reverse transcriptase
RXR	Retinoid x receptor
S1P	Sphingosine-1-phosphate
SAMRC	South Africa Medical Research Council
SANS	South African National Standards
SAPK	Stress-activated protein kinase
SAVC	South African Veterinary Council
SD	Standard diet
SDS	Sodium dodecyl sulphate
SGOT	Serum glutamic oxaloacetic transaminase
sp	Systolic pressure
SREBP	Sterol regulatory element-binding protein
STAT	Signal transducer and activator of transduction
STZ	Streptozotocin
SU	Stellenbosch University
T1DM	Type 1 diabetes mellitus
T2DM	Type 2 diabetes mellitus
TBARS	Thiobarbituric acid reactive substances

TBM	Total body mass
TBS-Tween	Tris buffered saline with tween®
TC	Total cholesterol
TEMED	1,2, Bis (dimethyl amino) ethane
TG	Triglycerides
TNF	Tumour necrosis factor
TTC	Triphenyltetrazolium chloride
TZD	Thiazolidinedione
UCP	Uncoupling protein
USA	United States of America
UTHSCSA	University of Texas, Health Science Centre, San Antonio Texas
VA	Viable area
VCAM	Vascular endothelial cell adhesion molecule
VEGF	Vascular endothelial growth factors
VLDL-C	Very low-density lipoproteins cholesterol
WB	Western blot
WHO	World Health Organisation
Wt	Total work

List of units of measurements

%	Percentage
°C	Degree Celsius
dL	Decilitre
g	Gram
IU	International units
kDa	Kilo Dalton
kg	Kilogram
L	Litre
m	Metre
M	Molar
mg	Milligram
min	Minute
mL	Millilitre
mm	Millimetre
mmHg	Millimetres of mercury
mmol	Millimol
mW	Milliwatt
ng	Nanogram
nM	Nanomolar
v	Volume
μ	Micro
μL	Microlitre
μM	Micromolar
μmol	Micromol

List of Figures

Figure 1.1 General classification of cardiovascular risk factors.....	4
Figure 1.2 Structure of the HIV virion.....	10
Figure 1.3 Life cycle of the HIV and various stages targeted by different classes of ARVs	12
Figure 1.4 Structures of (a) 3TC, and (b) the endogenous nucleoside deoxycytidine.....	13
Figure 1.5 Structure of 3'-azido-3'-deoxythymidine	14
Figure 1.6 Structure of LPV.....	14
Figure 1.7 Structure of Ritonavir.....	14
Figure 1.8 Schematic interplay of various factors that mediate hepatic changes in the spectrum of NAFLD.	20
Figure 1.9 PIs and NRTIs alteration of lipid metabolism, mitochondrial damage and eventual hepatic damage with increased cardiovascular risk.....	22
Figure 1.10 A summary of the interrelationships between ARV toxicity and major mediators of both cardiac and liver disease.....	25
Figure 1.11 Activation and various mechanisms regulated by AMPK	32
Figure 2.1 Schematic representation of randomised grouping and various experimental interventions	44
Figure 2.2 Rat grimace scale.....	44
Figure 2.3 Landmarks for rat intraperitoneal injection.....	45
Figure 2.4 Global ischaemia / reperfusion perfusion protocol	48
Figure 2.5 Regional ischaemia-reperfusion protocol.....	49
Figure 2.6 Left ventricular transverse section following TTC staining.....	50
Figure 2.7 Isometric tension protocol for aortic ring studies.....	52
Figure 2.8 Isometric tension measurement protocol (L-NAME).....	53
Figure 2.9 Normalisation of the 'Chemi Hi sensitive blots'	60
Figure 3.1 Mean standard rat chow consumption between lean and HCD groups before onset of drug treatment	68
Figure 3.2 Comparison of mean standard rat chow consumption between lean and HCD groups during the first four weeks of drug treatment.	69
Figure 3.3 Trend of mean rat chow consumption	69
Figure 3.4 Mean HCD consumption.....	70
Figure 3.5 Trend of mean HCD consumption	70

Figure 3.6 Mean volume of water consumption before onset of drug treatment.....	71
Figure 3.7 Mean volume of water consumption during the drug treatment programme.....	71
Figure 3.8 Trend of mean daily water consumption two weeks before onset of drug treatment and during the first four weeks of treatment.....	72
Figure 3.9 Mean total body mass after random assignment into either standard rat chow or HCD groups.....	73
Figure 3.10 Weekly mean total body mass during the feeding programme before onset of drug treatment....	73
Figure 3.11 Weekly mean total body mass during the drug treatment phase.....	74
Figure 3.12 Mean total body mass group during euthanasia.....	76
Figure 3.13 Mean percentage intraperitoneal fat.....	77
Figure 3.14 Mean absolute cardiac mass.....	78
Figure 3.15 Mean normalised heart mass by tibial length.....	79
Figure 3.16 A) Mean absolute liver mass B) Mean normalised liver mass by tibial length.....	80
Figure 3.17 Mean fasting blood glucose.....	81
Figure 3.18 Mean random blood glucose.....	81
Figure 3.19 Mean fasting blood glucose and mean random blood glucose.....	82
Figure 3.20 Mean fasting serum total cholesterol.....	82
Figure 3.21 Mean fasting serum triglycerides.....	83
Figure 3.22 A) Mean high-density lipoprotein cholesterol B) Mean low-density lipoprotein cholesterol.....	84
Figure 3.23 Mean fasting serum PL and TGs levels.....	85
Figure 3.24 Mean fasting serum PL levels.....	85
Figure 3.25 Mean fasting serum HDL3 levels.....	86
Figure 3.26 Mean fasting serum HDL2 levels.....	86
Figure 3.27 Mean fasting serum CD levels.....	87
Figure 3.28 Mean normalised serum CD levels.....	88
Figure 3.29 Mean fasting serum TBARS levels.....	88
Figure 3.30 Mean normalised serum TBARS levels.....	89
Figure 3.31 Mean serum alkaline phosphatase (S-ALP) levels.....	90
Figure 3.32 Mean fasting serum insulin concentration.....	91
Figure 3.33 Mean HOMA-IR.....	92

Figure 3.34 Mean pre-and post-ischaemia heart rate.....	94
Figure 3.35 Mean pre-and post-ischaemia aortic outflow	94
Figure 3.36 Mean pre-and post-ischaemia Qe and percentage Qe recovery.	95
Figure 3.37 Mean pre-and post-ischaemia total cardiac output (CO) and percentage CO recovery	96
Figure 3.38 Mean pre-and post-ischaemia total work (Wt) and percentage Wt recovery.....	96
Figure 3.39 Mean pre-and post-ischaemia sp and percentage sp recovery.....	97
Figure 3.40 Mean pre-and post-ischaemia dp and percentage dp recovery.....	97
Figure 3.42 Mean left ventricular infarct sizes	99
Figure 3.43 Mean percentage infarct size in comparison to infarct area + area at risk	99
Figure 3.44 Representative liver tissue photomicrographs demonstrating, (A) H & E stain (B) ORO stain (C) Immunohistochemical stain with anti-(GST-P) antibody	102
Figure 3.45 Representative liver tissue photomicrographs demonstrating steatosis and steatohepatitis.....	103
Figure 3.46 Mean phenylephrine cumulative dose-induced aortic tension response curves.....	105
Figure 3.47 Mean phenylephrine cumulative dose-induced aortic tension	106
Figure 3.48 Mean acetylcholine cumulative dose-induced aortic relaxation response curves.....	107
Figure 3.49 Mean acetylcholine-induced maximal aortic relaxation R_{max}	108
Figure 3.50 Nonlinear regression curves generated from the log (X) transform of acetylcholine-induced aortic relaxation.....	108
Figure 3.51 Nonlinear regression (curve fit) for log transform of mean acetylcholine-induced aortic relaxation (EC_{50})	109
Figure 3.52 A and B- Mean pre-ischaemia cardiac total AMPK.....	111
Figure 3.53 A and B. Mean pre-ischaemia phospho-AMPK.....	111
Figure 3.54 A and B. Mean pre-ischaemia phospho-AMPK.....	112
Figure 3.55 A and B. Mean post-ischaemia phospho-AMPK	112
Figure 3.56 A and B Mean post-ischaemia phospho-AMPK	113
Figure 3.57 A and B. Mean post-ischaemia total eNOS.....	114
Figure 3.58 A. and B. Mean post-ischaemia phospho-eNOS.....	114
Figure 3.59 A, B and D Mean post-ischaemia phospho-eNOS / total eNOS ratio C. Mean post-ischaemia phospho-eNOS.....	115
Figure 3.60 A and B. Mean total post ischaemia total PKB.....	116

Figure 3.61 A-C Mean post-ischæmia phospho-PKB and D mean post-ischæmia phospho-PKB / total PKB ratio	117
Figure 3.62 A and B. Mean pre-ischæmia phospho-Erk 1 / 2: total Erk 1 / 2 ratio.....	118
Figure 3.63 Mean post-ischæmia total expression of Erk 1 / 2.....	118
Figure 3.64 A and B-mean post-ischæmia phospho-Erk1 / 2	119
Figure 3.65 A and B Mean post-ischæmia-reperfusion total p38.....	120
Figure 3.66 A and B Mean post-ischæmia-reperfusion total phospho-p38	120
Figure 3.67 A Mean pre-ischæmia p22-phox expression and B mean post-ischæmia expression of cardiac p22-phox	122
Figure 3.68 A and B. Mean post -ischæmia cleaved caspase 3 expression	123
Figure 3.69 A and B. Mean post-ischæmia expression of cleaved PARP	124
Figure 3.70 Mean aortic phospho-eNOS / total eNOS ratio.....	125
Figure 3.71 Mean aortic total PKB / Akt expression.....	126
Figure 3.72 Mean aortic phospho-PKB / Akt expression.....	126
Figure 3.73 Mean aortic phospho-PKB / Akt : total PKB / Akt ratio.....	127
Figure 3.74 Mean aortic phospho-Erk 1 / 2 / total Erk 1 / 2	127
Figure 3.75 Mean aortic I κ B α	128
Figure 3.76 Mean aortic PGC 1 α expression.....	128
Figure 3.77 Mean aortic p22-phox expression	129
Figure 3.78. A and B Mean hepatic total PKB / Akt.....	131
Figure 3.79 A and B. Mean hepatic phospho-PKB / Akt : total PKB / Akt ratio.....	131
Figure 3.80 Mean hepatic phospho-PKB / Akt : total PKB / Akt ratio	132
Figure 3.81 A and B Mean hepatic phospho-Erk1 / 2	133
Figure 3.82 A and B Mean hepatic phospho-Erk 1 / 2 : total Erk 1 / 2 ratio.....	133
Figure 3.83 Mean phospho-Erk 1 / 2	134
Figure 3.84 Mean hepatic expression of p22-phox.....	134
Figure 3.85 A and B. Mean hepatic expression of caspase 3	135
Figure 3.86 Mean hepatic phospho-AMPK / total AMPK ratio.....	136
Figure 4.1 Mechanisms of HIV-1 protease inhibitor-induced insulin resistance	145

Figure 4.2 Biological effects of (A) PPAR γ , (B) PPAR α and (C) PPAR β stimulation	147
Figure 4.3 Mechanisms of atherosclerosis.....	151
Figure 4.4 Mechanisms via which PPAR γ activation by thiazolidinediones (TZDs) leads to improved systemic insulin sensitivity through AMPK mediated signalling.....	163
Figure 4.5 PI3K and PKB/Akt mediated vascular effects	167
Figure 4.6 PKB/Akt-mediated intracellular insulin signalling	168
Figure 4.7 Short-term and long-term consequences of PARP activation	175

List of Tables

Table 2.1 Composition of standard and high fat / calorie diet.....	42
Table 2.2 Categorization of the eight experimental groups.....	43
Table 2.3 Different components used in preparation of lysis buffer	56
Table 2.4 Bovine serum albumin, (BSA) standard concentrations for Bradford Protein Assay.	57
Table 2.5 Preparation of running and stacking gels for PAGE.....	58
Table 2.6 Standard processing protocol for H & E staining.....	61
Table 2.7 Standard H & E protocol	62
Table 2.8 Histological features of NAFLD for the liver H & E and ORO stained liver sections and the scoring criteria used.....	64
Table 3.1 Experimental groups.....	66
Table 3.2 Results outline.....	67
Table 3.3 Weekly mean total body mass (g) of the eight experimental groups during the treatment phase....	75
Table 3.4 Mean serum ALT, AST, LD and GGT enzymes (IU / L) / experimental group	90
Table 3.5 Mean heart rate / experimental group	93
Table 3.6 Mean left ventricular infarct sizes (%)	98
Table 3.7 Results of liver tissue histology using a modified scoring criterion for NAFLD.....	101
Table 3.8 Phenylephrine induced maximal aortic contraction.....	104
Table 3.9. Mean expression of pre-and post-ischaemia I κ B α , PGC-1 α and PPAR α	121
Table 3.10 Mean hepatic expression of PGC-1 α , I κ B α and PPAR α	130
Table 4.1 A and B Summary of the main study findings.....	177

List of Addenda

Addendum A, 1 Certificate of rat chow analysis.....	186
Addendum A, 2 Certificate of HCD analysis	187
Addendum B HCD preparation	188
Addendum C Description of phenylephrine and acetylcholine drug preparation for organ (aorta) bath perfusion system	189
Addendum D Antibodies	190
Addendum E Rat mortality report.....	191

Chapter 1 : Introduction and Literature Review

1.1 General introduction

Reports by the World Health Organisation (WHO) indicate that although over 36 million people are living with human immunodeficiency virus / acquired immunodeficiency syndrome (HIV/AIDS) globally, mortality associated with the infection has drastically dropped from 2.4 million deaths in the year 2005 to 1.5 million deaths in 2015 (World Health Organisation 2015). Similarly, the prevalence of non-communicable diseases (NCDs) such as Cardiovascular Disease (CVD) and metabolic syndrome is on the rise in the low-to-middle income countries (LMICs) especially in sub-Saharan Africa, a region that is already burdened with a high prevalence of communicable diseases such as HIV/AIDS. However, current trends indicate that the reduction in HIV/AIDS-associated mortality in the last decade is attributable to widespread treatment of HIV infected individuals with antiretroviral drugs (ARVs) (Chung et al. 2009; Mocroft et al. 2003).

The successful use of highly active anti-retroviral therapy (HAART) has altered the natural history of this fatal infection into a manageable chronic medical condition, and there is strong clinical and epidemiological evidence that this has been associated with emergence of other non-AIDS-related adverse conditions such as non-alcoholic fatty liver disease (NAFLD), insulin resistance, diabetes mellitus (DM), overweight / obesity, hypertension and CVD (Durand et al. 2011; Guehi et al. 2016). Current developments indicate that these non-AIDS events, attributed to chronic ARV use, also contribute to morbidity and mortality (Leite & Sampaio 2010; Lumsden & Bloomfield 2016). For example, the rates of hospitalization due to coronary heart diseases have been shown to be higher in HIV-infected patients than in non-HIV-infected persons and the incidence of acute myocardial infarct has been shown to follow similar trends (Friis-Møller et al. 2003a; Friis-Møller et al. 2003b).

It is projected that by the year 2030, NCDs will account for over 75% of global mortality and CVD is estimated to be the number one cause of deaths (ahead of all other NCD) in the developing world population (Beaglehole & Bonita 2008). Recent studies indicate that the prevalence of overweight / obesity in patients on HAART is higher than in the general population (Gain et al. 2013; Crum-Cianflone et al. 2010; Crum-Cianflone et al. 2011). Unpublished preliminary data from the EndoAfrica prospective cohort study currently underway in the Western Cape province (South Africa) show high rates of overweight / obesity (increased body mass index (BMI) and waist circumference) in HIV-infected study participants (with or without HAART), ranging

between 30% - 50% (personal communication: Prof H Strijdom, EndoAfrica project coordinator). These findings provide evidence that an increasing number of patients living with HIV/AIDS are overweight or obese, yet studies focusing on the effects of antiretroviral drugs in the context of overweight/obesity are scarce. Furthermore, there is no clearly defined therapy to counter these metabolic derangements.

The intricate interplay among HIV/AIDS, HAART, metabolic derangements and CVD, however, make it extremely difficult to dissect out the underlying pathophysiological mechanisms. Consequently, to date, there is no clearly devised therapy to alleviate the complications. This study therefore, set out to address this paucity of knowledge by exploring HAART-associated metabolic derangements and resultant cardiac and vascular dysfunctions using an experimental model of high calorie diet for induction of obesity in Wistar rats treated with ARVs. Additionally, the study investigated the role of dual peroxisome proliferator-activated receptors alpha (PPAR α) and peroxisome proliferator-activated receptors gamma (PPAR γ) stimulation as potential therapeutic targets to limit HAART-induced metabolic derangements, and cardiovascular dysfunction.

This chapter focuses on the literature demonstrating the intricate interplay among HAART, hepatic steatosis, obesity, CVD and offers insight into the role played by PPAR α / γ signalling, among other intracellular cascades, as a concrete background for this study. Although the HI-virus is implicated in these pathologies, it is not the focus of this study as we primarily aimed to investigate the effects of ARVs. Consequently, no humanized HIV-1 animal models were employed.

1.2 Cardiovascular disease, CVD

1.2.1 Introduction

CVD is a broad umbrella term used for any form of disease of the heart and / or blood vessels. In this treatise, the term CVD will be used to define the clinical entity that results from impaired cardiac function following compromised perfusion. The primary cause of the impaired perfusion is narrowing of the coronary vessel / vessels resulting in either focal or diffuse myocardial infarction (MI) also referred to as ischaemic heart diseases (IHD) (Ferdinandy et al. 2007). Coronary heart disease (CHD) / coronary artery disease (CAD) refers to the underlying vascular pathology where a fibrofatty plaque forms in the coronary lumen narrowing the vessel diameter resulting in altered blood flow, i.e., reduced or complete obstruction of blood flow (Castelli 1988). To ascertain accurate diagnosis of MI, the European Society of Cardiology (ESC) and American College of Cardiology joint task force drew a consensus document to redefine criteria based on electrocardiographic (ECG), biochemical and pathologic findings of (acute, evolving or recent MI) (Antman et al. 2000). However, the broad scope of CVDs is still considered by WHO ([Http://www.who.int/cardiovascular_diseases/en/](http://www.who.int/cardiovascular_diseases/en/) n.d. "Accessed: 08/08/2017") and other bodies encompassing various categories such as: -

- i) CHD referring to pathologies of the blood vessels responsible for myocardial perfusion.

- ii) Cerebrovascular disease: These are disorders of the blood vessels that perfuse the brain resulting in either ischaemic or haemorrhagic stroke.
- iii) Peripheral arterial disease: These are disorders of blood vessels perfusing the upper and lower extremities
- iv) Rheumatic heart disease (RHD): Refers to disorders of the cardiac muscles and valves resulting from rheumatic fever.
- v) Congenital heart diseases: These are malformations of the heart valvular and vascular structures existing at birth.
- vi) Deep venous thrombosis and pulmonary embolism: These are disorders of coagulation in the venous system which can dislodge and embolise to the heart and pulmonary vessels leading to ischaemia.

Of all the NCDs, CVD has the highest global cause-mortality rate and shows an upward trend in the developing world (Wang et al. 2016).

1.2.2 Epidemiology

CVD ranks as the leading single cause of mortality and loss of disability-adjusted life years (DALYs) globally and although studies show declining trends in high income countries, CVD mortality rates are on the rise in LMICs (Wang et al. 2016; Vedanthan et al. 2014). The WHO estimates that globally, CVDs account for about 17.5 million deaths (31% of all deaths) each year with over 75% of these deaths occurring in LMICs (<http://www.who.int/mediacentre/factsheets/fs317/en/>. “Accessed: 29/08/2017”). The rising prevalence of NCDs in the developing world poses a double burden of health challenges because of the co-existing communicable diseases. Furthermore, of all CVD cases, CHD accounts for most of the cases across the various geographical regions (Yusuf et al. 2004; Yusuf et al. 2001). Although the lifetime risk of overall CVD for persons above the age of 30 years without known CVD is approaching 50%, the prevalence of CVD in low socio-economic settings is rising in younger age groups (Pujades-Rodriguez et al. 2014).

1.2.2.1 Risk factors

Extensive studies have identified and classified an array of cardiovascular risk factors (conditions that increase the risk of CVD development), and ardent campaigns continue to educate the public at large and those already diagnosed with CVD on prevention measures with an aim of mitigating the CVD burden. The Framingham prospective cohort study has provided invaluable data over long follow-up periods (Kannel et al. 1961). Moreover, studies have shown that with proper adherence to risk modifying / mitigating measures, CAD morbidity and mortality rates can be successfully reversed (Piepoli et al. 2016; Moran et al. 2014).

Cardiovascular risk factors have been profiled (Kannel et al. 1976) and broadly classified into two categories: classical / traditional risk factors and new / emerging risk factors (Figure 1.1). The traditional risk factors are further sub-classified as non-modifiable (age, gender and hereditary factors) and modifiable (hypertension, dyslipidaemia, cigarette (tobacco) smoking, obesity, type 2 diabetes mellitus (T2DM) and sedentary life style)

(Hackam & Anand 2003). The metabolic / lipid related factors (modifiable) that predispose to atherosclerosis include high apolipoprotein B / apolipoprotein A1 (ApoB / ApoA1), low-density lipoprotein (LDL), oxidised LDL and lipoprotein-associated phospholipase A (2) (Pai et al. 2004). The emerging risk factors are further classified into inflammatory markers (Blake & Ridker 2002), haemostasis / thrombosis markers such as fibrinogen (Kannel et al. 1987) and others as shown in Figure 1.1 below. The underlying principle here is that the various conditions favour development of atherosclerotic fibrous and fatty plaques and thrombosis, thus predisposing the coronary vessels to occlusion and subsequent reduction in myocardial perfusion.

Metabolic derangements associated with various medical conditions have been described as a major risk factor to development of CVD either acting independently or accelerating already existing risk factors (Kannel & McGee 1979). The link between overweight/obesity, diabetes and metabolic syndrome to increased risk of CVD is clear (Pérez Rodrigo 2013; Del Ben et al. 2012). Emerging evidence shows that HIV patients on HAART are also at increased risk of metabolic dysregulation, development of NAFLD and therefore are predisposed to higher risk of CVD compared to untreated HIV patients and the general population (Crum-Cianflone et al. 2009; Crum-Cianflone et al. 2010; Lakey et al. 2013; Durand et al. 2011). Apart from being associated with liver-related morbidity and mortality, NAFLD and HAART also increase the risk of cardiomyopathy and CHD (Goland et al. 2006; Friis-Møller et al. 2003a).

General classification of cardiovascular risk factors

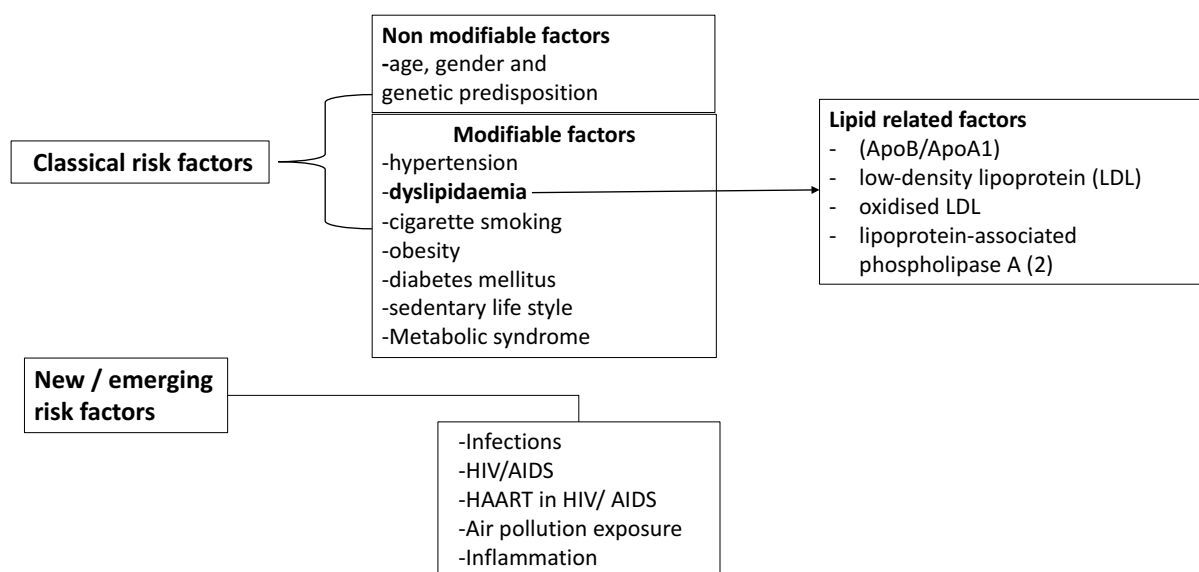


Figure 1.1 General classification of cardiovascular risk factors. Abbreviations: - Apo (Apolipoprotein), IL (Interleukin). (Blake & Ridker 2002), (Kannel et al. 1987).

1.2.2.2 CVD Prevention

The 6th Joint task force of the ESC on CVD prevention guidelines stated that addressing modifiable risk factors via healthy dietary practices, blood pressure monitoring, smoking cessation and body weight reduction are key in reducing the attributable deaths due to CVD (Piepoli et al. 2016). Therefore, mortality associated with CVD

is largely preventable. However, successful risk reduction is dependent on lifestyle modification and behavioural change which are major challenges to effect despite widespread health education.

1.2.3 Pathophysiology of myocardial infarction

Atherosclerosis of the coronary vessels results in impaired cardiomyocyte perfusion that creates an imbalance between substrate/ oxygen supply and energy demands. When this imbalance is severely altered, for example due to complete obstruction of the coronary flow, the cardiomyocytes undergo ischaemic injury (Pascual & Coleman 2016). Depending on the duration and extent of the obstructed flow, cardiomyocytes undergo varying degrees of damage that ultimately compromises the ventricular contractility resulting in failure of the heart as a pump (Doenst et al. 2013). This mechanical failure is largely attributed to altered cardiomyocyte mitochondrial metabolism (Fillmore et al. 2014) resulting in impaired energy generation. Myocardial ischaemia is characterised by the loss of cardiomyocytes through necrosis following prolonged durations of impaired perfusion. Acute myocardial ischaemia (AMI) clinically presents with the classic chest pain (angina pectoris), electrocardiogram (ECG) changes, and changes in biomarkers (troponin and creatine kinase-MB), which form the basis of the diagnostic criteria (Antman et al. 2000).

When cardiomyocytes undergo severe (prolonged) ischaemia, their mode of death can be identified as either through oncosis, (coagulation or contraction band necrosis) or through apoptosis (programmed cell death). Accordingly, the sections that have undergone infarction are usually classified microscopically (focal necrosis) depending on the size of the MI. When the size of the infarct is less than 10 percent of the left ventricle (LV), it is classified as small, medium when the size is between 10-30% of the LV or large when it is more than 30 percent of the LV. Also by location of the infarct either (anterior, lateral, inferior, posterior or septal) or combined locations (Antman et al. 2000). The injury suffered by the myocardium is twofold: first resulting from ischaemia, and secondly, when blood flow is re-established (reperfusion), either with or without clinical intervention, the myocardium undergoes an additional form of insult referred to as reperfusion injury. Reperfusion injury is attributed to inflammation, oxidative stress and further impaired mitochondrial function (Ferdinandy et al. 2007; Vilahur & Badimon 2014; Doenst et al. 2013).

1.2.4 Role of endothelium

The endothelium, a monolayer of specialised cells lining vascular lumen, is a crucial vascular structure that is strategically located between the circulating blood and vascular smooth muscle. It plays a key role in vascular homeostasis because it is not only a source of various mediators that are key in regulation of vascular tone and growth (Folkman 1995), but also is involved in the maintenance of normal platelet function, haemostasis and inflammation. Therefore, a complex relationship exists between the endothelium and CVD because atherosclerotic forms of CVD result from functional and structural changes in the coronary endothelium and smooth muscle layer (Lüscher & Vanhoutte 1991).

One of the most extensively studied endothelium-derived mediators is nitric oxide (NO). NO is a lipophilic gaseous signalling molecule synthesized by endothelial nitric oxide synthase (eNOS) from L-arginine, and is essential in mediating smooth muscle relaxation thereby regulating vascular tone (Palmer et al. 1988). Moreover, its release into the lumen inactivates platelets protecting against abnormal coagulation and thrombosis. Impaired endothelial function, and NO signalling not only predispose to vascular constriction (Panza et al. 1990) and coagulation, but also lead to altered vascular smooth muscle proliferation and migration enhancing proatherogenicity and susceptibility to hypertension, thrombosis and eventual atherosclerotic CVD (Badimon et al. 1993). Compromised eNOS activity is also associated with increased cardiovascular risk (Qian & Fulton 2013).

The deleterious effects of endothelial damage / dysfunction manifest not only in MI, but also in, among others, stroke and renal vasculopathies (Félétou & Vanhoutte 2006). The endothelium is susceptible to the deleterious effects of various compounds either endogenously secreted or exogenously administered. Pharmacological agents, such as ARVs have been shown to increase susceptibility to endothelial damage and subsequent increased risk of CVD (Zhou et al. 2005).

1.2.5 CVD in metabolic syndrome

There is a growing body of clinical and epidemiological evidence that HAART and NAFLD not only increase the risk of liver failure, but are also associated with metabolic and cardiovascular complications. For example, patients who develop NAFLD from chronic use of HAART, have been shown to be at an increased risk of heart failure as a result of cardiomyopathy, CHD or dysrhythmias (Ballestri et al. 2014; Golland et al. 2006; Targher et al. 2005). Therefore, the metabolic derangements in NAFLD aggravate the traditional cardiovascular risk factors associated with the metabolic syndromes. Additionally, NAFLD and metabolic syndrome are closely associated with T2DM, obesity. NAFLD is therefore considered a reliable indicator of abnormal ectopic fat accumulation characterised by chronic inflammatory states (Ballestri et al. 2014; Bhatia et al. 2012).

The ectopic accumulation of fat in non-adipose tissues e.g. the liver and skeletal muscle often leads to lipotoxicity in these tissues (Tamilarasan et al. 2012). Pathologic lipid accumulation in the liver results in several metabolic derangements that often have deleterious pathophysiologic consequences. These include, but are not limited to: -

- i) abnormal glucose metabolism characterised by increased hepatic gluconeogenesis and glycogenolysis which eventually lead to non-insulin-dependent DM increased oxidative stress, (Videla et al. 2004; Araya et al. 2004), endothelial dysfunction (Targher et al. 2005) and hypercoagulability (Knaapen et al. 2013).
- ii) abnormal lipid and lipoprotein metabolism leading to an accelerated rate of atherosclerosis.

The foregoing discussion partly explains why NAFLD ultimately leads to a dysfunctional cardiometabolic phenotype (Ballestri et al. 2014). In addition, cardiovascular mortality is the main cause of premature death in NAFLD (Bhatia et al. 2012).

These functional changes are often accompanied by structural changes in the myocardium and precede overt metabolic changes or CVD (Hallsworth et al. 2013). The mechanisms leading to myocardial damage are therefore multifactorial and are mediated by pro-inflammatory processes, pH changes, generation of excess reactive oxygen species (ROS) and calcium overload (Féletou & Vanhoutte 2006). The mechanisms involved in risk posed by ARVs remain poorly understood (Reyskens et al. 2013). However, HAART-induced metabolic and cardiovascular dysfunction have also been partly attributed to reduced expression of genes coding for PPARs and mitochondrial proteins (Giralt et al. 2006) that ultimately impair cardiac energy metabolism.

1.3 HIV/AIDS

1.3.1 Introduction

Great advances have been made since the first description of unusual cluster of infections, (*Pneumocystis carinii* pneumonia) and malignancies (Kaposi sarcoma) in previously healthy men who had sex with other men in the United States of America (USA) (Gottlieb et al. 1981). These symptoms were ascribed to immunological failure defined as acquired immunodeficiency syndrome abbreviated as (AIDS), that were later revised by the Centre for Disease Control (CDC) in USA (Centre for Disease Control 1985) for a comprehensive case definition. Research into the aetiology of immune deterioration led to isolation of human T-cell lymphotropic virus (HTLV) in AIDS patients (Gallo et al. 1983; Gallo et al. 1984) and the eventual identification of a cytopathic retrovirus (Barre-Sinoussi et al. 1983) that was termed as human immunodeficiency virus (HIV) (Gallo et al. 1984) due to its association with immunological defence shutdown leading to a plethora of opportunistic infections (OIs), malignancies and eventually death. Additionally, diminished levels of cluster of differentiation 4 (CD4) lymphocytes were shown to correlate with declining immunocompetency (Brien 1996; Cloyd et al. 2000).

Over the years, the infection has generated a lot of interest from various researchers, organisations and governments, and consequently, combined efforts have made great strides towards improving diagnostic tests, viral transmission prevention strategies and most importantly, availability of potent antiviral drugs.

Although no cure for the virus has been devised to date, meaningful progress, albeit challenging, has been achieved using pharmacological antiviral agents. Identification of HIV was followed by the development of ARV drugs 4 years later and the first drug, Azidothymidine (AZT), was introduced and its efficacy demonstrated in patients with AIDS-related complex (Barnes 1986). AZT-treated patients had a reduction in the development of OIs, coupled with an increased number of CD4 cells and weight gain. In addition, the

overall mortality rate was significantly reduced in the AZT-treated group (Fischl et al. 1987). AZT gave the first ‘ray of hope’ in the fight against AIDS.

To date, many other ARVs have been developed and subsequent studies on efficacy and effectiveness of these drugs against HIV have shown better response when two or more drugs are combined, thus weakening the viral resistance that develops with single drug use (Egger et al. 1997; Tisdale et al. 1993; Larder et al. 1995). Therefore, since 1996, it has become a standard practice to use different ARVs referred to as combination antiretroviral therapy (cART), or highly active antiretroviral therapy (HAART) for the best outcome (Mocroft et al. 2003). HAART has altered the natural history of HIV/AIDS because of immune recovery resulting in longevity in people living with HIV (PLWH).

Another outstanding benefit of sustained immunocompetence achieved by HAART is a marked reduction in rates of the viral transmission (Günthard et al. 2016). Mortality during the post-HAART era dropped markedly compared to the pre-HAART era as evidenced in the EuroSIDA study (Mocroft et al. 2003). Today, HIV infection is considered a chronic medical condition when proper ART is adhered to. Furthermore, HIV infected adults on various HAART regimens have a life expectancy approaching that of the general population (Samji et al. 2013).

Although HAART has successfully been demonstrated to reduce HIV/AIDS morbidity and mortality, chronic use of these drugs has led to emergence of a new burden of non-HIV/AIDS-related complications that are of growing concern in PLWH. To date, HIV infection has a global spread with the highest prevalence in Africa and particularly the sub-Saharan Africa region (World Health Organisation 2015). With epidemiological transition, where NCDs are on the rise in the region, the continent now faces a double burden of disease where both infectious and non-infectious diseases pose a huge economic burden to these struggling economies.

1.3.2 Epidemiology of HIV/AIDS

Since the first cases of HIV/AIDS were described, the infection has spread globally reaching a pandemic magnitude as the ‘most destructive microbial scourge in history’ as described by Fauci (2007). There are more than 35 million PLWH and since the onset of the epidemic, around 78 million people (71-87 million) people have become infected, with 39 million (35-43 million) people dying of HIV/AIDS-related complications. These infections affect people of all ages. In the sub-Saharan Africa region, over 4.5 % of persons aged between 15-49 years are HIV positive; this represents the highest prevalence globally (World Health Organisation, World health statistics 2017). Therefore, the burden of HIV infection is grave, declining the quality of life among the sufferers and impacting serious socio-economic challenges to individuals and governments.

In sub-Saharan Africa, AIDS-related deaths fell by 39% since 2005 and related infections declined by 33%. Use of HAART has also increased; with 35-39% of all people with HIV having access to ARVs. Globally, by mid-2016, 18.2 million PLWH were receiving ARV therapy (World Health Organisation, World health statistics 2017). However, the coverage is still low, with only 24% of all HIV positive children receiving the

lifesaving treatment (UNICEF 2004). The WHO has set a target to end the AIDS pandemic by the year 2030 and therefore there is still a huge gap to contain the infection especially in the developing world.

Efforts aimed at prevention of transmission of HIV, early diagnosis and initiation of HAART have yielded considerable gains in the reduction of transmission and mortality rate. Consequently, the advent of HAART has led to improved quality of life and life expectancy in those infected with the virus. ARV treatment significantly improved the mortality rate compared to HAART naïve patients 5.2 versus 20.9 deaths / 100 person years in an extensive study comparing 41,213 HIV patients exposed to HAART for over 72 months (Bozzette et al. 2008). Long term use of ARV has however been associated with negative health effects thus raising concerns about non-AIDS-related morbidity and mortality as a result of HAART-mediated metabolic derangements, development of liver complications and CVD.

1.3.3 HIV structure

HIV-1 is a single stranded positive sense ribonucleic acid (RNA) virus that belongs to the subgroup lentiviridae that primarily infects immune cells leading to loss of cell-mediated immunity against multiple pathogens and eventual susceptibility to OIs and malignancies (Barre-Sinoussi et al. 1983). It is a T-helper (CD4) tropic virus where it replicates, subsequently leading to loss of their vital function in the defence against pathogens (Gallo et al. 1984). There are two subtypes of HIV namely: HIV 1 and HIV 2. HIV 1 is highly virulent and has a global distribution, whereas HIV 2 is confined to west African and some parts of the Portugal region and has reduced pathogenicity (Gilbert et al. 2003; Reeves 2002). In this treatise, the abbreviation HIV will be used to refer to HIV subtype 1 unless otherwise stated.

The outer surface of the virus is an envelope that has several glycoproteins embedded that attach to host cell surface receptors (Kwong et al. 1998). Additionally, it has a capsid core where the viral genetic material encoded in RNA is contained (Chan et al. 1997). The HIV RNA has only nine genes that code for the viral proteins, i.e., structural (those incorporated in the envelope and core) and enzymes (reverse transcriptase (RT), integrase and protease) (Amarasinghe et al. 2000). The capsid also contains key viral enzymes namely: integrase and protease, responsible for viral integration into host cell DNA and post-translational polypeptide cleavage respectively. A simplified HIV structure is shown below, Figure 1.2. A more detailed description of their function is given below under viral life cycle (section 1.3.4).

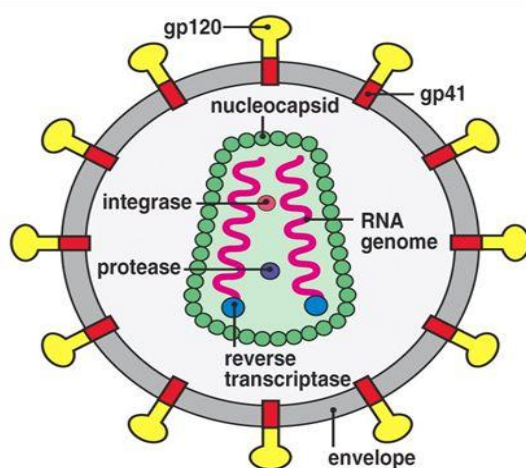


Figure 1.2 showing the structure of the HIV virion. An envelope, with glycoprotein (gp) particles, encapsulates a nucleocapsid which contains the viral genetic material. (Reitz & Gallo 2015).

1.3.4 HIV life cycle and treatment targets

For the HIV to replicate and produce infectious virions, it must be transferred from one infected individual to uninfected person via a medium that does not alter the viral pathogenicity. Transmission of HIV occurs primarily through transfer of body fluids, i.e., blood, semen, vaginal/rectal secretions and breast milk. The transmitting media is either directly injected into the blood stream, for example through blood transfusion (Moore et al. 2001), contaminated needles (Baggaley et al. 2006) or fluids encountering mucous membrane or damaged tissues common in penile-vaginal/ penile-rectal transmissions (Craiel et al. 1988; Marks et al. 2006).

Once the virus is introduced, it goes through various stages from the initial attachment to the new host cell surface receptors to the release of new infectious viruses (Maartens et al. 2014). Although outside the scope of this study, the HIV life cycle is described below highlighting the ARV targets. It is composed of seven stages, namely: binding/attachment, fusion, reverse transcription, integration, replication, assembly and budding (Figure 1.3). These stages are targeted by various ARV drugs to disrupt the viral life cycle, hence averting host cell damage and release of infectious virions as described below.

i) Binding/attachment

The viral glycoprotein particles (gp 120) attach to CD4 cell surface receptors and co-receptors, C-C chemokine receptor type 5 (CCR5) and C-X-C chemokine receptor type 4 (CXCR4) (McDougal et al. 1986). This stage is targeted by drugs that inhibit chemokine receptors, also known as entry inhibitors, e.g. Maraviroc, which acts as by negatively modulating the co-receptor (Tan et al. 2013).

ii) Fusion

Once the virus is attached, conformational changes occur that join the viral envelop to the CD4 cell membrane allowing the HIV capsid to enter the host cell. This is a critical stage and is targeted by ARV fusion inhibitors,

e.g., Enfuvirtide restricting the entry of viral genetic material into the host cells (Chan et al. 1997; Kwong et al. 1998; Wyatt & Sodroski 1998).

iii) Reverse transcription

Once the capsid enters the cell, the viral enzyme, RT is released and converts its genetic material, HIV RNA, into complementary HIV DNA (reverse transcription) to pave way for viral incorporation into the host cell nucleus (Charneau et al. 1994). Inhibition of reverse transcription renders the viral genetic material irrelevant since the viral RNA cannot be integrated into the CD4 cell nucleus to replicate (St Clair et al. 1987). There are two types of ARV drugs that act at this stage, Nucleoside (nucleotide) RT Inhibitors (N(t)RTIs) and non-Nucleoside RT Inhibitors (NNRTIs).

a) Nucleoside RT inhibitors (NRTI) and nucleotide RT inhibitors (NtRTI) are nucleoside and nucleotide analogues which competitively inhibit RT, e.g., Azidothymidine (AZT), abacavir, 3TC, emcitarabine, and tenofovir (Balzarini et al. 1998). A brief description of AZT and 3TC and their mode of action is given below as they formed the backbone of the HAART regimen investigated in this study.

b) NNRTIs inhibit reverse transcription by binding to an allosteric site of RT and non-competitively inhibiting its activity (Hsiou et al. 1996). They are further classified into 1st generation: e.g., nevirapine and efavirenz and 2nd generation: etravirine and rilpivirine (Usach et al. 2013).

iv) Integration

Successfully reverse-transcribed complementary HIV DNA strands are then integrated (inserted) into the host cell DNA to form a provirus ready for transcription. This step is facilitated by the viral enzyme, integrase, (Esposito & Craigie 1999) that is targeted by integrase nuclear strand transfer inhibitors (INSTI) thereby inhibiting viral enzyme integrase annulling integration of viral DNA into the infected cell DNA (Robinson et al. 1996). These include: raltegravir, elvitegravir and dolutegravir.

v) Replication (transcription and translation)

With the viral DNA incorporated into the host cell DNA, the cell can be activated to start transcribing multiple copies of viral RNA that are translated into long chains of HIV proteins using the host cell machinery (Locker et al. 2011).

vi) Assembly

Newly formed long HIV polypeptides sequences containing viral proteins and RNA are assembled to form immature non-infectious particles (Sundquist & Kra 2012). To convert these immature particles, the long polypeptide chains are cleaved using the HIV-1 enzyme aspartyl protease to form individual enzymes responsible for production of other viruses. This enzyme can be inhibited by specific inhibitors that form a key component of HAART. Protease inhibitors (PIs), block the ability of the enzyme aspartyl protease to cleave the viral polypeptide into functional enzymes thereby interfering with continued infection since the viral particles are immature (Brik & Wong 2003). Examples of PIs include Lopinavir (LPV), indinavir, nelfinavir, amprenavir, ritonavir, darunavir and atazanavir. A brief description of LPV and ritonavir is given below

because they formed part of the HAART administered to the experimental animals. Once the virus is assembled, it undergoes the last stage of budding.

vii) Budding

Budding or emergence refers to the eventual release of the virus from the host cell. This occurs through the release of the assembled virus from the host cell surface enveloping itself with a swatch of the cell membrane (Sundquist & Kra 2012). The envelope contains the viral surface proteins that bind to receptors on other immune surface cell receptors for continued infection.

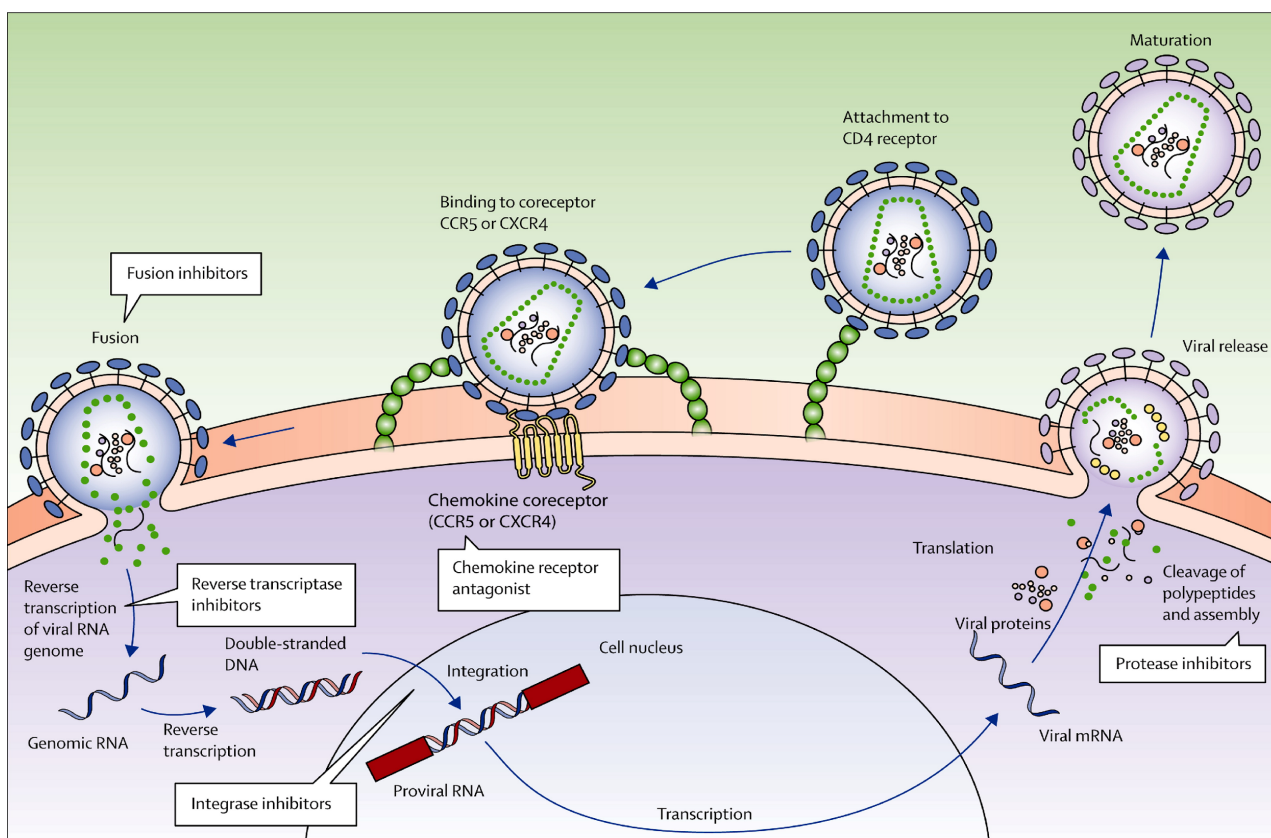


Figure 1.3 showing the life cycle of the HIV and various stages targeted by different classes of ARVs (Maartens et al. 2014).

1.3.5 2'-deoxy-3'-thiacytidine; (3TC)

Lamivudine (2'-deoxy-3'-thiacytidine; 3TC) is a dideoxynucleoside analogue of cytidine that inhibits the HIV 1 and HIV 2 RT enzyme. It is the negative isomer of a cytidine analogue where the 3' carbon of the ribose ring has been replaced by a sulphur atom (Kewn et al. 1997) as shown on Figure 1.4 a and b, below.

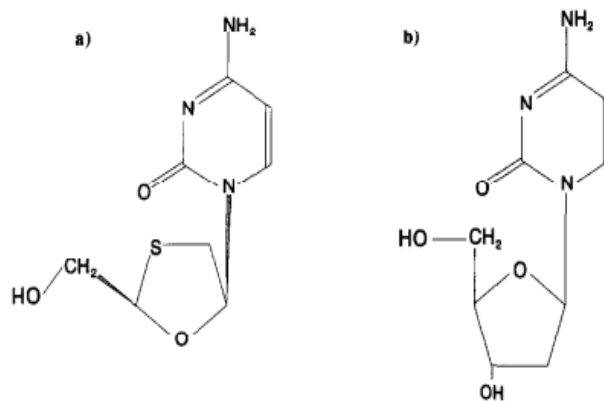


Figure 1.4 Structures of (a) 3TC, and (b) the endogenous nucleoside deoxycytidine (Kewn et al. 1997).

The drug, in its active triphosphate form, competes with corresponding endogenous nucleoside triphosphates for binding to RT. Once incorporated into viral DNA, chain elongation terminates due to absence of a 3'-hydroxy group to which 3'-5'-phosphodiester linkages are made; thereby curtailing viral replication (St Clair et al. 1987; Mitsuya & Broder 1986).

The use of 3TC as a monotherapy is limited by rapid high-level viral resistance to the drug arising from a mutation at codon 184. The mutation is a consequence of substitution of one amino acid (from methionine into an isoleucine) within the highly conserved motif YMDD in the catalytic site of the HIV-1 RT (Boucher et al. 1993). However, compared to other NRTIs, 3TC has a better toxicity profile. (Bridges et al. 1996). Additionally, when used in combination with other nucleoside analogues, for example AZT, they produce a synergistic inhibitory effect to the HIV-1 RT achieving sustained lower viraemia than in single drug use (monotherapy) (Larder et al. 1995). For this reason, 3TC has been approved as a co-formulation with AZT as a fixed dose tablet.

1.3.6 3'-azido-3'-deoxythymidine (AZT)

AZT is a thymidine analogue 3'-azido-3'-deoxythymidine (Figure 1.5) that, as a triphosphate, competitively (with other endogenous nucleosides) inhibits the HIV-1 RT (Mitsuya et al. 1985). It is non-selectively phosphorylated by the cellular thymidine kinase to azidothymidine triphosphate and subsequently binds to the HIV-1 RT and once incorporated into the DNA strand, the chain elongation process is terminated (Furman et al. 1986).

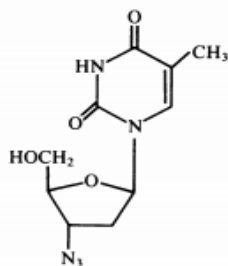


Figure 1.5 Structure of 3'-azido-3'-deoxythymidine, AZT (Lin & Prusoff 1978).

The HI-viral resistance to AZT when used as a monotherapy occurs rapidly within six to 12 months of treatment because of multiple mutations of the HIV-1 RT (Kellam et al. 1992). However, when used in combination with other nucleoside analogues (for example with 3TC), the HIV-1 does not develop any resistance (Tisdale et al. 1993; Larder et al. 1995), thereby achieving a synergistic inhibitory effect and effective viral replication control.

1.3.7 LPV

LPV is peptidomimetic aspartyl PI (Figure 1.6) which has been incorporated in many regimens due to its potent activity against HIV-1 (Sham et al. 1998). However, due to its low bioavailability resulting from rapid first-pass biometabolism by the cytochrome P450 enzyme, it is formulated with low-dose ritonavir. Ritonavir, (Figure 1.7) not only inhibits HIV-1 protease, but also inhibits the cytochrome P450 3A4 enzyme thereby resulting in improved pharmacokinetics of LPV when co-administered (Bertz et al. 2001).

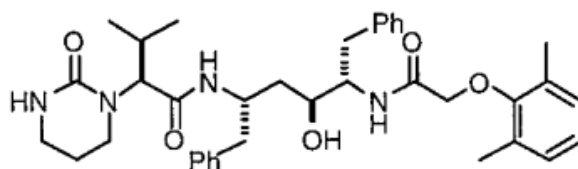


Figure 1.6 Structure of LPV (Sham et al. 1998).

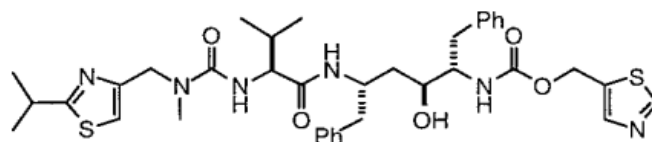


Figure 1.7 Structure of ritonavir (Kempf et al. 1995).

Although ritonavir has high oral bioavailability and a long plasma half-life, (Kempf et al. 1995), its clinical use as a monotherapy is limited due to the rapid development of mutations at valine 82 (Val 82) to alanine, threonine or phenylalanine resulting in drug resistance (Molla et al. 1996). When used in combination with LPV (LPV/r), the net result is improved HIV-1 protease inhibition against Val 82 mutation with longer serum

half-life (Sham et al. 1998). Furthermore, this combination has been shown to have superior antiviral activity compared to other HAART regimens containing nelfinavir, and is also well tolerated (Walmsley et al. 2002).

1.3.8 Basis of ARV combination against HIV

The foregoing discussion clearly demonstrates that treatment of HIV is complicated by the ability of the virus to alter its genetic makeup and therefore mount resistance against various antiretroviral agents. Furthermore, the development of a mutation against a specific drug may cause cross resistance against a different drug when used as a monotherapy (Kellam et al. 1992; Boucher et al. 1993). Therefore, combination therapy (two or more ARV agents) was introduced to mitigate HIV-1 resistance and the outcome was encouraging (Larder et al. 1995; Walmsley et al. 2002).

To date, various modifications have been made to regimens regarding when to initiate therapy (early vs late), the number of drugs (monotherapy vs combination therapy, with or without PIs). An array of clinical studies (both cohort and blinded trials) have consistently showed that intensive combined therapy results in the reduction of both mortality and morbidity associated with major OIs and a decline in HIV transmission rates (Palella Jr et al. 1998; Egger et al. 1997; Chung et al. 2009). These studies are supported by WHO data and national / international AIDS monitoring bodies from various regions and countries (World Health Organisation 2017). Consequently, use of cART has been adopted as standard therapy for HIV/AIDS management globally.

In summary, HAART has achieved the following milestones in combating HIV/AIDS: -

- i) Profound suppression of viral replication leading to marked reduction of viral load / viraemia (reduction in viral RNA copies/ml of blood).
- ii) Repletion of CD4+ cells leading to improved immunity against multiple pathogens responsible for OIs in advanced AIDS.
- iii) Marked reduction in rates of HIV transmission.

The criteria of when to initiate HAART has also undergone several revisions in the last 20 years from the earlier count of < 350 CD4+ cells / μ L raised to <500 CD4+ cells / μ L and current recommendations supported by the WHO and the international antiviral society instruct that all patients with detectable viraemia (HIV+) should be initiated on HAART regardless of the CD4+ cell count (Günthard et al. 2016).

Various protocols have been developed but most combinations are composed of two NRTIs and one NNRTI (first line) or one PI and two NRTIs (second line) (Panel on antiretroviral guidelines for adults and adolescent 2017). Other combinations consist of an INSTI or a fusion inhibitor. First line therapy refers to the regimen first prescribed after HIV diagnosis is made. Thereafter, these patients are followed up and monitored for virological, immunological or clinical failure of the regimen. If the regimen is not tolerated or fails, a switch is made to the second line therapy. The current recommended second line regimen for adults is a combination of 2NRTIs and 1 INSTI or 2 NRTIs and boosted PI/ INSTI among others. Recommendations for various regimens are according to protocols based on age, tolerance and other drug interactions.

HAART has yielded marked clinical outcomes as a result of improved immune function evidenced by increase in CD4 cell count, the reduction of viral load and overall decline in morbidity (Chung et al. 2009) leading to delayed progression of HIV infection to AIDS.

Although the advent of HAART has been associated with positive effects on morbidity and mortality in HIV infected patients, its chronic use is associated with the development of metabolic derangements such as dyslipidaemia, increased blood pressure, and insulin resistance (Reyskens & Essop 2014; Lipshultz et al. 2012). Prevalence of overweight and obesity in HAART populations is rising (Amorosa et al. 2005) and has been attributed to immune recovery and unhealthy dietary practices (Crum-Cianflone et al. 2010; Crum-Cianflone et al. 2011).

It is emerging that these non-AIDS-related complications contribute to the rising trends in NCDs and metabolic complications in HIV populations. These metabolic changes are also often accompanied by the development of various forms of NAFLD including hepatic steatosis, hepatic steatohepatitis and the more lethal hepatic fibrosis leading to portal hypertension (Vodkin & Loomba 2015; Vodkin et al. 2015). The mechanisms leading to these non-AIDS-related complications are still incompletely understood.

1.3.9 CVD in HIV and HAART

The interdependency between HIV and cardiovascular dysfunction poses a serious public health challenge worldwide. It has been projected that HIV/AIDS and IHD will be in the top three causes for global mortality and global DALYs by the year 2030 (Mathers & Loncar 2015).

HIV-associated cardiomyopathy (HIVAC) was described in the early 1980s as one of the stage IV AIDS defining illnesses. Patients infected with the virus developed congestive cardiomyopathy primarily due to left ventricular systolic dysfunction. Consequently, HIVAC was attributed to the viral myocarditis, OIs and overt immunological failure (Cohen et al. 1986). Introduction of ART has led to improvement in severity of the systolic dysfunction in these patients but the resulting chronicity is complicated by development of left ventricular diastolic dysfunction convoluting the pathology (Schuster et al. 2008). HIVAC has been termed as ‘a tale of two worlds’ (Lumsden & Bloomfield 2016) because untreated patients (low socio-economic status) have a more severe systolic dysfunction HIVAC with a poor prognostic course than those with well controlled viraemia presenting with the subacute diastolic dysfunction HIVAC. Accordingly, HIV infection is now considered a risk factor for heart failure (Butt et al. 2011).

In the post-HAART era, there has been a shift towards a heightened risk of CHD that is independent of demographic characteristics or traditional cardiovascular risk factors. The risk is even higher in those taking ARVs than in HAART naïve patients (Friis-Møller et al. 2007; Durand et al. 2011). ARV's such as PIs and NRTIs are associated with varying degrees of endothelial dysfunction and atherosclerosis thereby predisposing HIV patients to CVD (Zhou & Gurley 2006; Zhou et al. 2005; Lipshultz et al. 2012). The mechanisms involved include: endothelial oxidative stress (Reyskens & Essop 2014) and activation of mononuclear cell recruitment, an early event in the development of atherosclerosis (Dressman et al. 2003) and altered endothelial signalling,

ERK 1/2, p38 phosphorylation (Chen et al. 2005; Chen et al. 2009), resulting in increased permeability to lipoproteins and other macromolecules (Bell et al. 1974). However, studies encompassing vascular function in ARV therapy in this context are limited and further studies are crucial to elucidate the mechanisms involved in endothelial dysfunction.

1.3.10 HIV, HAART and overweight/obesity

During the pre-HAART era, HIV infection was characterised by severe immunosuppression, OIs, severe wasting and progressive health deterioration that eventually resulted in wasting syndrome and death. However, when immunity is re-established by use of these drugs coupled with improved nutrition (which is a major component of HAART in patient management), the weight loss is reversed. In a longitudinal cohort study, HIV infected adults on cART for a period of one year showed an increase in the BMI after initiation of treatment and were classified as either being overweight or obese. HIV infected female subjects on cART gained more weight compared to the male counterparts in this American study (Lakey et al. 2013). Similarly, a Swiss cohort study reported comparable trends in weight gain among HIV patients on HAART (Egger et al. 1997).

Today, the timing of HAART initiation has been revised and current WHO protocols recommend onset of therapy when a patient is diagnosed with the infection (World Health Organisation 2016). The increase in the prevalence of overweight/obesity among HIV infected populations has been attributed to the early initiation of HAART and more widespread cART coverage. The weight gain, and similarly higher prevalence of dyslipidaemia is highest in those patients initiated on HAART when the CD4 cell count is low (Crum-Cianflone et al. 2010). Furthermore, studies have established that the weight gain in PLWH on ART is directly proportional to the presence and severity of dyslipidaemia, hepatic steatosis, cardiovascular risk (Maia & De Mattos 2010) and hypertension (Crum-Cianflone et al. 2008; Crum-Cianflone et al. 2011) and therefore increased risk for CVD.

1.4 Non-alcoholic fatty liver disease (NAFLD)

1.4.1 Introduction

NAFLD defines a large spectrum of liver conditions ranging from simple asymptomatic steatosis (fatty liver) to non-alcoholic steatohepatitis (NASH) and cirrhosis (Chalasani et al. 2012), and is today considered as the most prevalent liver disease in adults affecting up to a third of the general population worldwide (Williams et al. 2011). Pathogenesis of NAFLD is described by the “tale of two hits” (Day & James 1998). Firstly, triglycerides (TGs) and free fatty acids (FFAs) accumulate within hepatocytes due to insulin resistance, enhanced dietary influx and excessive lipogenesis by hepatocytes. Secondly, lipid peroxidation and mitochondrial damage lead to hepatocyte inflammation and eventual damage. NAFLD is attributed to the rising prevalence of diabetes, obesity, HIV/AIDS and the prolonged use of cARVs (McGovern et al. 2006; Siddiqui

et al. 2015), and is now widely recognised as forming the hepatic component of metabolic syndrome (Byrne 2012).

NAFLD is defined as the presence of cytoplasmic lipid droplets, either by histology or imaging, in more than 5% of hepatocytes or TG levels exceeding the 95th percentile for lean, healthy individuals without secondary causes of steatosis such as significant alcohol consumption (alcohol intake < 20 grams / day for female and 30 grams / day for male), use of steatogenic drugs, hereditary disorders and negative for viral and autoimmune liver disease (Hashimoto 2006; Kawano & Cohen 2013). It encompasses a wide spectrum of steatotic liver damage ranging from simple fat accumulation to steatohepatitis, necrosis and fibrosis (Chalasani et al. 2012).

There are several metabolic risk factors common to both NAFLD and CVD. Accordingly, pathological lipid accumulation in the hepatocytes has been identified as an important cardiovascular risk factor (Bhatia et al. 2012; Targher et al. 2005; Targher et al. 2016). NAFLD is not only a common cause of chronic liver disease/liver-related mortality, but is also directly linked to development of insulin resistance and subsequent predisposition to T2DM (Leite et al. 2009) because of abnormal ectopic accumulation of lipids. Therefore, hepatic steatosis forms a key link between various metabolic risk factors and NCD disease states.

There are two clinical manifestations of NAFLD: non-alcoholic fatty liver (NAFL) and non-alcoholic steatohepatitis (NASH). NAFL is defined by presence of steatosis without hepatocyte injury such as inflammation or ballooning and tends to have a benign course, whereas NASH has evident hepatocyte ballooning and necroinflammation and can progress to cirrhosis which in rare cases gives rise to hepatocellular carcinoma (Hashimoto et al. 2014).

1.4.2 Epidemiology of NAFLD

1.4.2.1 Incidence and prevalence in the general population

Epidemiological and clinical studies on the incidence and prevalence of NAFLD across different demographics are limited and results indicate varying data depending on the populations studied, the diagnostic methods (imaging versus histology) and definitions used. A prospective cohort study from a healthy Japanese population set to determine the frequency and risk factors of NAFLD showed that the prevalence of hypertransaminasaemia (elevated serum levels of serum transaminases), used as a surrogate of NAFLD, was 9.3% (incidence rate of 31 cases per 1000 person-years). The risk factors associated with this elevation were: male sex, elevated BMI, hypertension, low high-density lipoprotein cholesterol (HDL-C) and glucose intolerance/ DM (Suzuki et al. 2005). A similar Japanese study aiming at characterizing the longitudinal relationship between the metabolic syndrome and NAFLD showed a higher incidence of 86 cases of NAFLD per 1000 person-years, although no distinction was drawn between NAFL and NASH (Hamaguchi et al. 2005). The study showed metabolic syndrome as a strong predictor of NAFLD and that NAFLD was less likely to regress in study subjects who had metabolic syndrome. A British retrospective study reported a much lower incidence of 29 NAFLD cases per 100,000 person years of which, 23.5 had non-cirrhotic hepatitis and 5 had

cirrhotic hepatitis (Whalley et al. 2007). These discrepancies indicate that there is need for further studies to provide an accurate global assessment of NAFLD incidence.

Population based studies on the prevalence of NAFLD are challenging because of the invasive nature of the gold standard diagnostic technique, liver biopsy and histology. Therefore, most of the studies on the prevalence of NAFLD are based on liver biopsies performed on potential liver transplant donors or autopsy specimens or imaging techniques like magnetic imaging resonance (MRI) and ultrasonography. The prevalence of NAFLD in developed countries also vary depending on the diagnostic modality (Angulo 2007). On average, most US studies report a NAFLD prevalence of 10-35%, and biopsy proven prevalence of NASH of 3-5% (Vernon et al. 2011). A Korean study on potential liver donors reported a NAFLD prevalence of 51.4% (steatosis >5%) and 10.4% (steatosis >30%). Additionally, 2.2% of participants showed features consistent with NASH (Lee et al. 2007). The risk factors associated with this prevalence were: age >30 years, obesity, hypertriglyceridaemia and diabetes. There is a paucity of NAFLD epidemiological data from developing countries. However, an Indian study reported a significant prevalence of NAFL in non-obese, non-affluent populations (Das et al. 2010). The majority of studies from developing countries have focused on viral-related liver pathologies.

1.4.2.2 Incidence and prevalence in high risk groups

There is overwhelming evidence that obesity is associated with a high incidence and prevalence of NAFLD. A Chilean prospective cohort study conducted on obese patients undergoing gastric bypass surgery revealed a NAFLD prevalence 63%, where 37% of participants had simple steatosis, 26% had NASH and 1.6% had cirrhosis on liver biopsy histological assessments. Furthermore, these patients had elevated aspartate aminotransferase (AST) levels and high homeostatic model assessment of insulin resistance (HOMA-IR) index (Boza et al. 2005). The prevalence of NAFLD has been reported to be as high as 90% in morbidly obese persons (Steatosis 91%, NASH 37%, cirrhosis 1.7%) (Machado et al. 2006).

Other conditions associated with a high prevalence of NAFLD include DM, hypertriglyceridaemia, and metabolic syndrome. Leite et al. (2009) reported a NAFLD prevalence of 69.4% in T2DM patients diagnosed via abdominal ultrasonography. An Edinburgh study reported a NAFLD prevalence of 42.6% in patients with T2DM (Williamson et al. 2011). Similar findings have been reported by a wide range of other studies (Prashanth et al. 2009; Vernon et al. 2011). Hypertriglyceridaemia has been reported as the lipid profile component most often associated with fatty liver with an odds ratio of 5.9 (Assy et al. 2000). Furthermore, these patients also fit the criteria for metabolic syndrome. HIV patients who are on antiretroviral therapy form the other group at high risk of developing NAFLD (discussed below, see section 1.4.4).

1.4.3 Pathophysiology of NAFLD

As mentioned previously, NAFL and NASH have a multifactorial aetiology ranging from metabolic, genetic, environmental and gut microbial factors. The spectrum of the pathology is also wide as it can present as simple

non-progressive hepatic steatosis to cirrhotic hepatitis inducing hepatocellular carcinoma. It is not known why some patients have a progressive course and yet others remain with isolated simple steatosis for long durations. Studies have shown that metabolic changes in the visceral adipose tissue alter lipid metabolism that eventually lead to hepatic lipid alterations resulting in steatosis. Additionally, development of a pro-inflammatory milieu coupled with oxidative stress, and pro-apoptotic signalling predispose to hepatic necro-inflammation that progressively leads to fibrosis and cirrhosis, a major risk factor for hepatocellular carcinoma (Rinella 2015) as illustrated in the Figure 1.8 below.

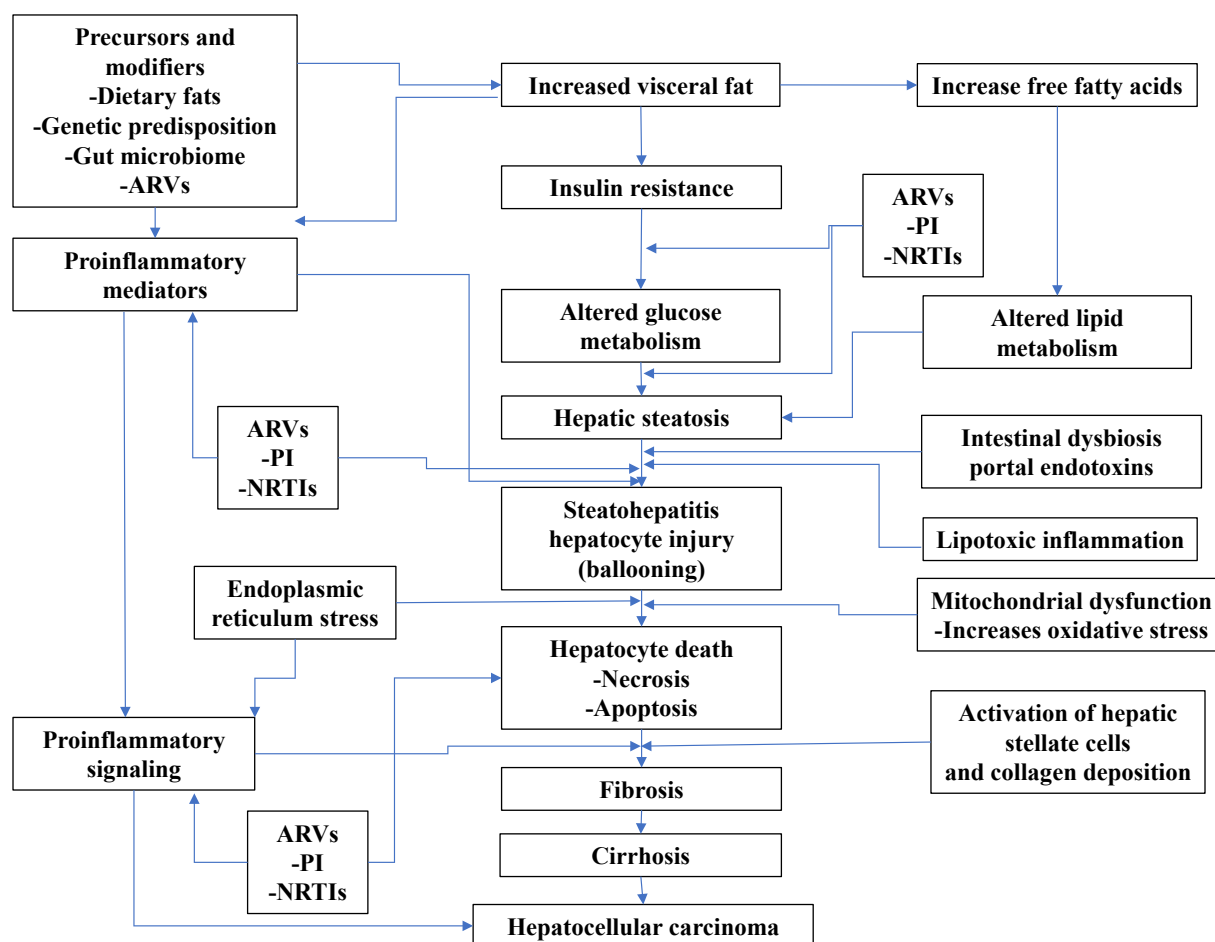


Figure 1.8 showing a schematic interplay of various factors that mediate hepatic changes in the spectrum of NAFLD. Abbreviations, ARV (antiretroviral), PI (protease inhibitors) NRTI (nucleoside reverse transcriptase inhibitors) (Rinella 2015).

Hepatocyte injury in NAFLD has been explained by the ‘two hit hypothesis’ (Day & James 1998) as previously mentioned. The first hit occurs because of insulin resistance, which is enhanced by excessive dietary fat influx and increased hepatic lipogenesis resulting in accumulation of TGs and FFAs in the hepatocytes. Following this, the second hit occurs as lipid laden hepatocytes increase lipid peroxidation, coupled with mitochondrial dysfunction, accumulation of ROS and inflammation resulting in, necro-inflammation and hepatocyte damage. FFAs and TNF- α are potent stimuli of c-Jun N-terminal kinase (JNK) which leads to degradation of insulin

receptor substrate 1 (IRS 1) through direct phosphorylation ultimately resulting in insulin resistance because of impaired downstream insulin signalling (Hirosumi et al. 2002).

Inflammation is induced by cytokines, hepatic interleukin 6, (IL-6), tumour necrosis factor- α (TNF- α) and pattern recognition toll like receptors (Wieckowska et al. 2008). Inflammatory mediators (TNF- α , FFAs and other cytokines) stimulate nuclear factor- $\kappa\beta$ (NF- $\kappa\beta$) which leads to increased transcription of pro-inflammatory genes aggravating hepatitis and hepatic insulin resistance. These two pathways not only aggravate hepatocyte inflammation, but also cause insulin resistance in the liver, muscle and adipocytes (Cai et al. 2005; Hirosumi et al. 2002). Furthermore, lipid-laden hepatocytes undergoing inflammation exhibit deranged expression of transcription factors that eventually lead to promotion of hepatic stellate cell proliferation and lipid peroxidation which are associated with the induction of fibrogenesis (Hazra et al. 2004; Lemoine et al. 2006; Diehl 2005). Another major factor that has been extensively studied in the pathogenesis of NAFLD, is increased oxidative stress via ROS. Excess production of ROS in damaged hepatocytes has been shown to be a potent factor in the induction of cytokine release and subsequently initiation of immune mechanisms that further damage hepatocytes (Than & Newsome 2015) as illustrated in Figure 1.8, above.

1.4.4 The intersection: HAART, NAFLD and CVD

As longevity in HIV patients increases due to wide use of HAART, the rise in the prevalence of other comorbidities has elicited special attention, especially liver-related complications (Vodkin & Loomba 2015). Although HIV infection is known to directly impact negatively on hepatocytes, the focus of this study will be on the epidemiology and pathophysiological mechanisms of HAART and ectopic lipid accumulation in the hepatocytes as the role of HIV in liver disease is beyond the scope of this study.

The prevalence of liver disease in HIV-seropositive populations receiving HAART varies, but studies have reported over 50% mortality resulting from end-stage liver damage and the discontinuation of HAART in up to 31.8% of patients due to hepatotoxicity (Bica et al. 2001). Other studies have consistently shown similar strong associations between liver-related mortality and morbidity in HIV patients on HAART (Price et al. 2014; Crum-Cianflone et al. 2009). NAFLD has been shown to be highly prevalent in HAART and HIV-infected patients are at an increased risk of developing fatty liver disease due to the viral infection itself and the added risk of antiretroviral medications. Other factors associated with the development of NAFLD in these patients include elevated TGs, high BMI and hip: waist ratio, metabolic syndrome and duration of the illness and medication (Crum-Cianflone et al. 2009; Crum-Cianflone et al. 2008).

Antiretroviral agents accentuate the 'two hit' risk factors due to increased hepatic TG accumulation and mitochondrial damage leading to oxidative stress and stimulation of pro-inflammatory pathways as illustrated below (Figure 1.9). The prevalence of NASH and fibrosis is also higher in HAART-treated patients vs. HAART naïve patients (Bhatia et al. 2012); additionally, they are also at higher risk of developing CVD than untreated patients (Cunha et al. 2017; Durand et al. 2011). Due to overt metabolic derangements and hepatic

damage, these patients also present with elevated amino transferases, alkaline phosphatase and serum TGs (Morse et al. 2015; Vodkin et al. 2015).

The development of NAFLD can be caused by all or several members in three antiretroviral classes i.e., NRTIs e.g., AZT; NNRTIs e.g., Efavirenz; and PIs e.g., LPV/r (McGovern et al. 2006; Mehta et al. 2005). NRTIs possess a specific class effect of causing mitochondrial toxicity secondary to the depletion of mitochondrial RNA and this often leads to hepatic steatosis, lactic acidosis and cardiomyocyte dysfunction (Matthews et al. 2011). These drugs are linked to hepatic mitochondrial damage through the inhibition of mitochondrial DNA polymerase γ leading to hepatotoxicity, lactic acidosis and steatosis (Lai et al. 1991; Olano et al. 1995; Sundar et al. 1997; Day et al. 2004). Since these drugs (PIs and NRTIs) are administered in combinations, the severity of all these hepatic derangements is aggravated and these perturbations predispose to increased cardiovascular risk as summarised below (Figure 1.9).

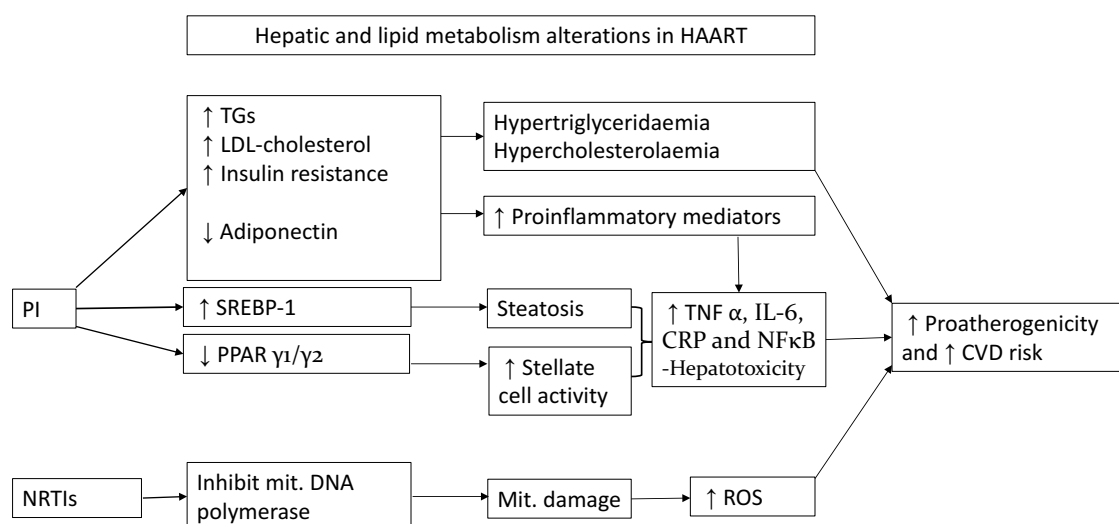


Figure 1.9 showing how PIs and NRTIs alter lipid metabolism, mitochondrial damage and eventual hepatic damage and increased cardiovascular risk. Abbreviations: PI (protease inhibitors), NRTIS (nucleoside reverse transcriptase inhibitors), Mit. (mitochondria), ROS (reactive oxygen species), NF κ B (nuclear factor kappa-light-chain-enhancer of activated B cells), TNF (tumour necrosis factor), CRP (C-reactive protein), TGs (triglycerides), SREBP (sterol regulatory element-binding protein), LDL (low-density lipoprotein), \uparrow indicate an increase and \downarrow indicate a decline (Day et al. 2004).

There is accumulating evidence that NAFLD increases risks of several cardiovascular complications such as, CAD, atherosclerosis, cardiomyopathy, cardiac hypertrophy, arrhythmias and heart failure (Del Ben et al. 2012). The pathophysiological mechanisms that underlie these interactions remain poorly understood due to the complex interplay with other components of the metabolic syndrome, i.e. obesity and insulin resistance (Ballestri et al. 2014; Gaggini et al. 2013), and therefore NAFLD has been termed as the hepatic component of the metabolic syndrome.

As a component of metabolic syndrome, NAFLD has been associated with a heightened risk of the development of CVD. A recent meta-analysis clearly showed that the presence of NAFLD increased the risk of fatal and non-fatal CVD events and this risk was proportional to the severity of the liver damage (Targher et al. 2016). NASH patients have been reported to develop more cardiovascular events than non-NASH patients, consequently, CAD is the leading cause of death (Treeprasertsuk et al. 2011) in these patients. NAFLD is also associated with the development of high-risk coronary plaques in patients devoid of traditional cardiovascular risk factors (Puchner et al. 2015). A Swedish cohort study showed that although mortality is not increased in patients diagnosed with steatosis, those with NASH had significantly reduced survival rates and the subjects often died from CVD (15%). Other causes of death were from both extrahepatic and hepatic malignancies (Ekstedt et al. 2006). Independent of metabolic syndrome features and other traditional risk factors, a clear association has been shown in NAFLD patients developing CAD, ischaemic strokes and cardiorespiratory failure (Targher et al. 2005; Hamaguchi et al. 2005; Treeprasertsuk et al. 2011; Chen et al. 2010).

The high prevalence of IHD in NAFLD patients and the associated mortality has elicited major concerns and new diagnostic techniques are being explored. The association between NAFLD and the development of high risk coronary atherosclerotic plaques has been clearly defined using computed tomographic (CT) angiography in the “Rule out Myocardial Infarction Using Computer Assisted Tomography” ROMICAT II trial study (Puchner et al. 2015). Consequently, other CT angiographic studies have shown increased coronary artery calcification (CAC) score (>100) independently of other cardiovascular risk factors in NAFLD (Chen et al. 2010).

The fatty liver secretes numerous factors that have been associated with increased risk for CVD, for example excess production of inflammatory cytokines, hyperglycaemia, and dyslipidaemia. The pro-inflammatory mediator, TNF- α , is stimulated by the accumulation of FFAs in the liver (Crespo et al. 2001). Moreover, liver resident macrophages, Kupffer cells, are also activated in NAFLD and they secrete and release more cytokines (TNF- α and IL-6) that eventually induce acute phase proteins (c-reactive protein, CRP) by hepatocytes (Diehl 2005; Choi & Diehl 2005; Wieckowska et al. 2008; Blake & Ridker 2002) leading to hepatocyte damage. Other pro-inflammatory molecules that are increased in NAFLD are uric acid and homocysteine in response to oxidative stress (Dai et al. 2016). All these pro-inflammatory mediators are elevated systemically (Byrne & Targher 2015) portending increased inflammation in distant organs such as the heart, pancreas, visceral fat and the gastrointestinal system. NAFLD patients have significantly reduced levels of plasma adiponectin (Hui et al. 2004) which has been strongly associated with the severity of the hepatic histopathological changes and hepatic steatosis.

The increased plasma levels of CRP, TNF- α , IL-6 and reduced adiponectin favour inflammation and pro-atherosclerosis leading to CVD (Pearson et al. 2003; Pai et al. 2004; Lizardi-Cervera et al. 2007) (Figure 1.10). These cytokines also drive insulin resistance resulting from impaired hepatic insulin receptor function and intracellular signalling cascade. TNF- α , directly phosphorylates insulin receptor substrate-1 (IRS-1) at the

serine 312 residue leading to its degradation curtailing downstream signalling and therefore blunted response to insulin stimulation (Gupta et al. 2007; Rydén & Arner 2007). The proatherogenic nature of NAFLD is multifactorial. The dyslipidaemia characterised by elevated plasma levels of very low-density lipoprotein (VLDL), TGs, reduced HDL cholesterol (Gaggini et al. 2013) coupled with insulin resistance and subsequent increased generation of pro-inflammatory molecules namely uric acid, CRP, IL-6, TNF- α and homocysteine favour development of high risk atherosclerotic plaques.

Patients treated with PIs show varying degrees of hepatic fatty damage and although the pathogenesis is multifactorial, steatosis has been ascribed to the overexpression of sterol regulatory element-binding protein - 1 (SREBP-1), and resultant lipodystrophy/hyperlipidaemia (Riddle et al. 2001). Riddle et al. (2001) showed that, ritonavir treatment induced increased adipose and hepatic fatty acid and cholesterol biosynthesis leading to hypertriglyceridaemia and hypercholesterolaemia in mice. HAART-treated HIV patients develop lipodystrophy and insulin resistance predisposing them to steatohepatitis and fibrosis. In these patients, use of PIs has been shown to decrease the expression of transcription factors regulating lipid metabolism, peroxisome proliferator-activated receptor γ 1 (PPAR γ 1) and PPAR γ 2 (Lemoine et al. 2006). Since PPAR γ is pivotal in the induction of the reversion of activated stellate cells to a quiescent state, it follows that PPAR γ downregulation results in unregulated stellate cells activity leading to hepatic fibrosis (Hazra et al. 2004).

Patients receiving PIs also develop metabolic syndrome, insulin resistance and lipodystrophy and have been shown to have a higher risk for development of T2DM and CVD (Troll 2011) (Figure 1.10). It has, however, been established that overexpression of peroxisome proliferator-activated receptor- gamma coactivator 1 alpha (PGC-1 α) protects cardiomyocytes from NRTI-induced toxicity (Liu et al. 2015) and it was therefore previously suggested that combining HAART with other therapies such as the combined PPAR α / γ agonists (Tonstad et al. 2007) may improve atherogenic dyslipidaemia distinctive of insulin resistance and reduce the development of secondary cardiac dysfunction. It therefore follows that exogenous administration of PPAR agonists may offer a therapeutic benefit in HIV patients on HAART and may serve to reverse or prevent these adipose and hepatic derangements.

To explore this, a 12-week prospective Indian study (Deshpande et al. 2016) was conducted in HIV patients receiving HAART by treating them with Saroglitazar (dual PPAR α and γ agonist) and although they sampled only 50 patients, the clinical trial showed promising results. Saroglitazar-treated patients had significantly reduced serum TGs and VLDL cholesterol compared to the untreated patients (Deshpande et al. 2016). The present study investigates further the potential of this drug, Saroglitazar, in limiting the liver, metabolic and cardiovascular derangements in HAART using an animal model.

The heightened risk of CVD in HAART-treated patients thus warrants further investigations to delineate the pathophysiologic mechanisms involved as well as formulate effective therapy to ameliorate the pathology. As clearly demonstrated above, the interplay between metabolic syndrome, antiretroviral drugs and resultant hepatic and CVD is complex, and remains poorly understood. The foregoing discussion highlights several pathways and signalling molecules implicated in the various pathophysiological conditions described. It is

imperative therefore, to discuss the physiological roles played by these molecules and their involvement in disease states.

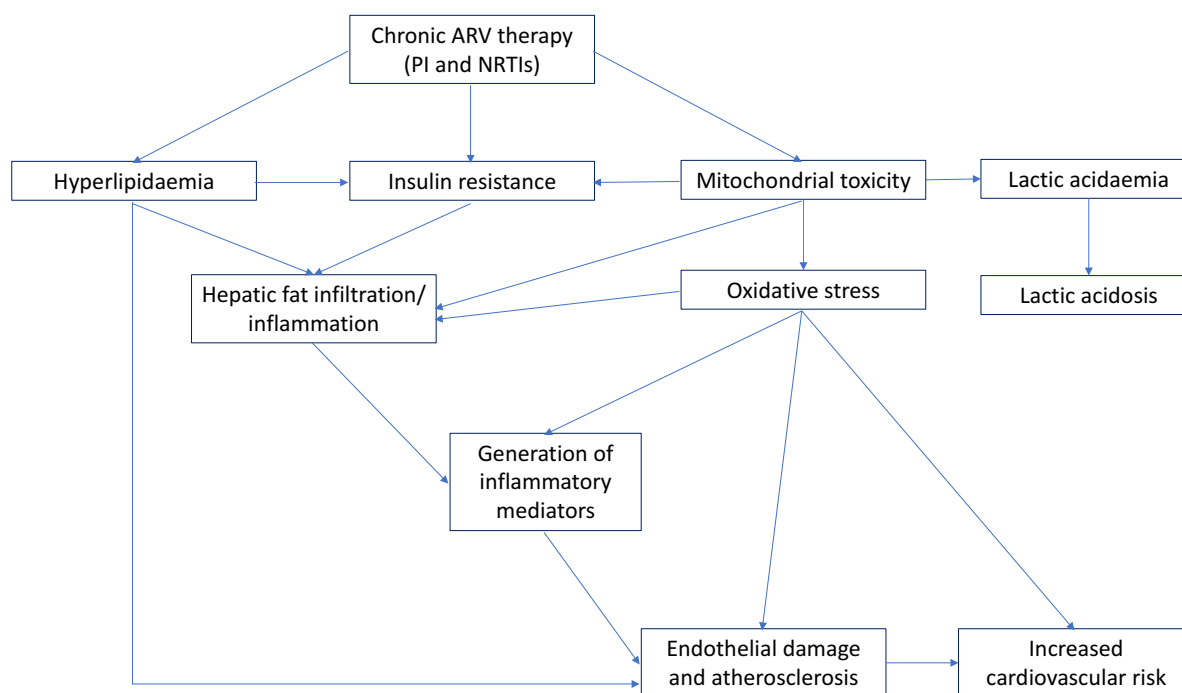


Figure 1.10 A summary of the interrelationships between ARV toxicity and major mediators of both cardiac and liver disease (Day et al. 2004).

1.5 Signalling molecules in hepatic, vascular and cardiac homeostasis

There are diverse molecules implicated in hepatic, vascular endothelial and cardiac homeostasis mediating key roles in cellular responses to various insults. As previously discussed, oxidative stress, inflammatory response, insulin signalling, transcriptional control and cell death among other cellular processes are altered to varying degrees in ART, fatty liver changes, and cardiovascular dysfunction.

1.5.1 Peroxisome proliferator-activated receptors alpha / gamma (PPAR α / γ)

PPARs belong to a superfamily of nuclear steroid receptors that play a role in the transcriptional control of target genes encoding proteins involved in glucose, energy and lipid homeostasis (Dreyer & Krey 1992). Furthermore, PPARs are also key in the control of inflammation through antagonism of nuclear factor-kappa B (NF κ B) (Delerive et al. 2001). PPAR α is highly expressed in liver, skeletal muscle, heart, and vascular tissues as a key mediator of fatty acid metabolism and its synthetic ligands known as fibrates e.g., fenofibrates are used clinically in the management of dyslipidaemia (Ziouzenkova et al. 2002). PPAR γ is expressed in adipose tissues and immune cells, its stimulation mediates adipocyte differentiation and enhances glucose uptake through insulin sensitization (Ferre 2004). This property of insulin sensitization has been exploited pharmacologically through use of thiazolidinediones (PPAR γ agonists) e.g., pioglitazone, in T2DM patients

resulting in improved glucose control. Therefore, combined effects of PPAR α and γ stimulation provide added benefits in the control of lipid and glucose metabolism. Consequently, development of dual PPAR α/γ receptor agonists has led to marked improvement in both glucose and lipid regulation in metabolic syndrome (Tonstad et al. 2007; Ratziu et al. 2008).

HAART-induced metabolic and cardiovascular dysfunction have also been partly attributed to reduced expression of genes coding for PPARs and mitochondrial proteins (Giralt et al. 2006). PIs have been linked to the inhibition of the retinoid x-receptor and PPAR γ and impairment of hepatic chylomicron uptake and TG clearance resulting in lipodystrophy, insulin resistance and NAFLD. (Carr et al. 1998). An *in vitro* study conducted in the H9c2 cardiac cell line, originally derived from embryonic rats, showed that overexpression of PGC-1 α protects cardiomyocytes from NRTI-induced toxicity, suggesting that a pharmacological agent with similar activity would potentially protect against such toxicities (Liu et al. 2015). Consequently, Saroglitazar, a dual PPAR α / γ receptor agonist, improved liver function and lipid profile in patients on HAART from an Indian clinical study (Deshpande et al. 2016). These findings suggest that, combining HAART with other therapies such as PPAR α / γ agonists (Tonstad et al. 2007) may improve atherogenic dyslipidaemia, a hallmark of insulin resistance, and reduce the risk of development of secondary cardiac dysfunction.

1.5.2 Peroxisome proliferator-activated receptors gamma co-activator 1 alpha (PGC1- α)

PGC-1 α is an inducible transcriptional coactivator that promotes an array of genes responsible for the regulation of oxidative metabolism and mitochondrial biogenesis facilitating energy homeostasis in diverse physiological states. PGC-1 α belongs to a small family of transcriptional coactivators, which together with PGC-1 β , have the unusual feature of possessing a transcriptional activation domain and RNA processing motifs in the same molecule (Lin et al. 2002). There are various factors that induce expression of PGC-1 α in different tissues. Fasting states and hypoglycaemia induce expression of PGC-1 α in cardiomyocytes and hepatocytes to mobilise more energy generation. Similarly, in skeletal muscle tissues, hypothermia and exercise also induce its stimulation (Lehman et al. 2000; Rhee et al. 2003).

It is expressed in diverse mitochondria rich tissues such as skeletal muscle, adipocytes, heart, liver, kidney and brain (Finck & Kelly 2006; Leone et al. 2005). Below is a summary of its key roles in hepatic, cardiac and vascular tissues in both physiological and pathophysiological conditions.

As a coactivator, PGC-1 α increases the rate at which transcription occurs by interacting with transcription factors without sequence-specificity in DNA binding. Consequently, its expression leads to increased stimulation of genes responsible for fatty acid oxidation in adipocytes, liver, skeletal muscle and cardiomyocytes (Lehman et al. 2000; Vega & Huss 2000). PGC-1 α also induces gene expression for insulin sensitive glucose transporter (GLUT-4) and increases glucose uptake in skeletal muscle cells (Michael et al. 2001). PGC-1 α gene is also induced robustly by fasting subsequently activating PPAR α target genes involved

in hepatic fatty acid oxidation, ketogenesis and gluconeogenesis (Yoon et al. 2001). On the other hand, hyperinsulinaemia, a common feature of insulin resistance, suppresses PGC-1 α expression in the liver. T1DM models of streptozotocin (STZ)-induced hypoinsulinaemia demonstrated high expression of PGC-1 α (Koo et al. 2004).

The high-energy requirements of cardiomyocytes depend on their mitochondrial capacity to produce ATP, therefore, PGC-1 α is highly expressed early in the developing heart tissue due to the high rate of mitochondrial biogenesis and oxidative metabolism (Lehman et al. 2000). Expression of PGC-1 α regulates several cardiac genes responsible for the electron transport chain, mitochondrial biogenesis and fatty acid β oxidation via coactivation of PPAR α , a key fatty acid receptor regulating lipid and energy metabolism gene expression (Vega & Huss 2000). Another important inducer of PGC-1 α expression is fasting (Lehman et al. 2000) which leads to fatty acid oxidation to replenish energy demands.

Changes in PGC-1 α expression have been reported in several cardiac pathologies that alter cardiomyocyte function. In cardiac hypertrophy, common in prolonged high pressure demands, PGC-1 α expression is diminished leading to a shift from fatty acid oxidation to glycolytic metabolism for energy (Elly 1997). It is still unclear whether this shift is adaptive or maladaptive since ischaemia also significantly lowers mitochondrial function in cardiomyocytes. Studies on PGC-1 α null (PGC-1 α $-/-$) mice demonstrate an abnormal heart rate (HR) control that is associated with cardiac dysfunction (Arany et al. 2005).

Manipulation of PGC-1 α expression in animal models has offered invaluable insight into the role played by the co-activator in heart disease. In a swine model of chronically ischaemic myocardium, the PPAR γ agonist, pioglitazone increased PGC-1 α signalling although no improvements were observed in either blood flow or infarct sizes (Butterick et al. 2016). It has, however, been established that overexpression of PGC-1 α (transcriptional coactivator of PPARs) protects cardiomyocytes from NRTI induced toxicity (Liu et al. 2015). Therefore, the role of PGC-1 α regulatory pathway is key as a potential therapeutic target for cardiomyocyte recovery.

PGC-1 α plays an important role in vascular homeostasis and loss of PGC-1 α activity has been implicated in the pathogenesis of acute coronary syndrome resulting in impaired mitochondrial function. A recent study has clearly demonstrated that PGC-1 α overexpression in CAD protects against increased intraluminal pressure by recruiting both NO and H₂O₂ during flow-mediated dilation (Kadlec et al. 2017). Since in acute coronary syndrome the mediation of dilation shifts from NO to mitochondrial hydrogen peroxide (_{mt}H₂O₂), excess H₂O₂ production poses a proatherogenic risk and further impaired coronary dilation. Furthermore, it has been shown that NO activates mitochondrial biogenesis complementing the role played by PGC-1 α in the different tissues (Nisoli 2003).

The role of PGC-1 α as a protector or mediator in metabolic syndrome, insulin resistance and DM is still unclear. Genetic variations in the PGC-1 α coding gene (Gly482 Ser) have been associated with increased risk of T2DM development and impaired glucose control (Ek et al. 2001). In an Ob/Ob mice model of T2DM, PGC-1 α is highly induced but there are no clear associations with the profound hyperinsulinaemia and insulin

resistance in these mice. However, PGC-1 α expression may promote insulin resistance through an indirect inhibition of protein kinase B / Akt (PKB / Akt) (Koo et al. 2004). PGC-1 α $-/-$ mice also demonstrate increased body fat, diminished hepatic fatty acid oxidation properties and hepatic steatosis ascribed to reduced mitochondrial capacity and an increase in lipogenic gene expression (Leone et al. 2005).

1.5.2.1 PGC-1 α and HAART

NRTIs have been associated with mitochondrial toxicity that ultimately results in cellular pathology. In this regard, a study evaluating hepatic mitochondrial stress response among various NRTIs revealed that zidovudine, stavudine and tenofovir, led to a reduction in ATP levels, increased oxidative damage and an overexpression of PGC-1 α in response to mitochondrial damage (Nagiah et al. 2015; Day et al. 2004). These drugs have been associated with various hepatic pathologies, the commonest being steatosis / steatohepatitis and hepatotoxicity as evidenced by elevation of hepatic aminotransferases ten times higher than the upper limits (Wit et al. 2002). Therefore, it follows that PGC-1 α roles are interlinked in hepatic, cardiac and metabolic diseases and introduction of antiretroviral drugs, both PI and NRTIs, further compound its physiological role.

1.5.3 Nuclear factor-kappa B (NF κ B)

Nuclear factor kappa-light-chain enhancer of activated B cells (NF κ B) is a protein complex belonging to a family which shares a Rel homology domain in their N-terminus with the retroviral oncoprotein v-Rel and thus classified as NF- κ B/ Rel proteins. It was discovered via its interaction with the immunoglobulin light-chain enhancer in B-cells (Jacobs & Harrison 1998). It is expressed in almost all cell types and plays a key role in regulating immune response to infection and responds to various cell stressors as described below.

NF κ B is present in an inactive state in form of sequestered dimers in the cytoplasm. Upon activation, it acts as a rapid primary transcription factor. NF κ B can be activated by several factors, including both endogenous and exogenous ligands as well as a plethora of physical and chemical stresses e.g. hypoxia/ anoxia, hyperoxia, cytokines/ chemokines (TNF α , IL-1B), ROS, protein kinase coactivators, MAPK activators, bacterial (lipopolysaccharides) and viral products. (Bowie & O'Neill 2000). The sequestration of NF κ B dimers in unstimulated cells is accomplished by a family of inhibitors called inhibitors of κ B (I κ B) through masking of nuclear localization signals (Jacobs & Harrison 1998). I κ B α is the major inhibitor of NF κ B and the most extensively studied. NF κ B-I κ B interaction renders NF κ B inactive and remains in latent form in the cytoplasm due to a strong nuclear export signal.

Inducers of NF κ B initiate a cascade of events that activates the I κ B kinase (IKK), which phosphorylates the 2 serine residues located in the IKK regulatory domain, leading to I κ B ubiquitination by the proteasome system and are proteolytically degraded, freeing the NF κ B to enter the nucleus and initiate transcription of appropriate genes (Ghosh & Baltimore 1990). Once NF κ B is activated, it translocates into the nucleus binding to consensus sites in promoter/enhancer regions of specific genes, leading to transcription of factors that promote inflammation such as leucocyte adhesion molecules and cytokines (Chen et al. 2013). NF κ B also induce a feedback loop to stimulate I κ B expression thus inhibiting its own activation (Jacobs & Harrison 1998).

IL-1 β stimulation results in the phosphorylation and degradation of I κ B α (Ghosh & Baltimore 1990) allowing NF κ B to translocate to the nucleus and mediate inflammatory changes associated with macrophages, T cells and microbial bioproducts through gene transcription. Other stimulants include, IL-6, IL-8, MCP-1 and TNF- α (Rogler et al. 1998; Schreiber et al. 1998). In obese states, the presence of excess visceral fat is characterised by low grade systemic inflammation mainly resulting from increased adipocyte stimulation as well as fat resident and recruited macrophage activity. Therefore, the pro- and anti-inflammatory effects of adipokines and cytokines through intracellular signalling pathways mainly involve NF κ B and Jun-N-Terminal kinase (JNK), as well as I κ B (Gil et al. 2007).

NF κ B has been implicated in the induction and development of atherosclerosis by transducing pathogenic stimulation to the expression of genes that promote recruitment and activation of inflammatory cells in plaques (Monaco et al. 2004). Furthermore, NF κ B activation in cardiac ischaemia and reperfusion starts shortly after initiation of ischaemia and is augmented during reperfusion. The main stimulus for NF κ B activation in this process are ROS and pro-inflammatory cytokines generated during the insult (Saini et al. 2005). Consequently, inhibition of NF κ B in I/R studies has been shown to improve cardiac function and reduce infarct sizes. Therefore, NF κ B is a key player in the pathophysiology of ischaemia-reperfusion injury and heart failure (Valen et al. 2001).

NF κ B is implicated in hepatocyte protection against ischaemia / reperfusion and TNF α induced apoptosis (Sun & Karin 2008). Furthermore, suppression of NF κ B signalling results in susceptibility to reperfusion injury in the liver (Sun & Karin 2008). Various antiretroviral agents are associated with serum lipoprotein changes such as elevated low-density lipoproteins (LDL). They also induce generation of ROS which are potent inducers of NF κ B, thereby indirectly implicating them in development of steatohepatitis, atherosclerosis and unstable CAD (Valen et al. 2001; Pereira et al. 2015). In addition, NF κ B activates pro-inflammatory responses that elevate cytokine and chemokine expression that eventually result in fibrosis and cirrhosis. Consequently, it is essential to assess I κ B α levels in liver, heart and aorta tissues, since it is indicative of an inflammatory response and NF κ B sequestration status in HAART therapy.

1.5.4 Protein kinase B (PKB) / Akt

Akt also known as protein kinase B (PKB) is one of the key molecules activated downstream of the cell membrane linked enzyme, 3-phosphoinositide kinase (PI3 Kinase / PI3K) signalling pathway. Since its initial description as a proto-oncogene, this serine / threonine kinase has become a major focus of attention because of its critical role in regulating diverse cellular functions including metabolism, growth, proliferation, survival, transcription, and protein synthesis and its role in pathological conditions such as cancer, diabetes and cardiovascular disease (Lawlor & Alessi 2001).

The PKB / Akt family comprises of 3 closely and evolutionary related isoforms Akt 1 / 2 / 3 or PKB α / β / γ . They share many substrates but also show some specificity. They belong to the AGC (protein kinase A, G and C) superfamily of protein kinases. All 3 isoforms share a high degree of amino acid identity and are composed

of 3 functionally distinct regions: - an N-terminal pleckstrin homology (PH) domain, a central catalytic domain and a C-terminal hydrophobic motif (HM). Together, these regions encompass a phosphoprotein of approximately 56 kDa (Scheid & Woodgett 2003).

1.5.4.1 Regulation and activation of PKB /Akt

PKB / Akt is activated by receptor tyrosine kinases such as platelet-derived growth factor receptor (PDG-R), insulin, epidermal growth factor (EGF), basic fibroblast GF (bFGF), and insulin like GF (IGF-1), integrins, B and T cell receptors, cytokine receptors, G-protein coupled receptors and others (Alessi et al. 1996; Deprez et al. 1997). These stimuli induce the production of phosphatidylinositol 3,4,5, triphosphate (PIP3) by PI3K. These lipids serve as docking sites for proteins that harbour the PH domain like Akt and its upstream activator protein kinase D1 (PKD1). At the membrane, PKD1 phosphorylates PKB / Akt at Thr 308 leading to its partial activation (Rykx et al. 2003). Consequently, phosphorylation of Akt at Ser 473 by MTORC2 stimulates its full enzymatic activity. Deactivation of PKB / Akt is via phosphatase 2A (PP2A) at the PH domain and dephosphorylation of PIP3 by tumour suppressor phosphatase (Hanada et al. 2003).

PKB / Akt has a multiplicity of roles contributing to a variety of cellular responses ranging from cellular metabolism, growth and survival. PKB / Akt phosphorylation and activation of GSK3 regulates glycogen synthase in response to insulin stimulation. The cardiac specific isoform of 6-phosphofructose-2 kinase phosphorylated by PKB on Ser 466 promoting glycolysis (Deprez et al. 1997). Additionally, PKB / Akt phosphorylates phosphodiesterase 3B (PDE3B) subsequently leading to regulation of intracellular cyclic nucleotides such as, cAMP and cGMP in response to insulin stimulation (Kitamura et al. 1999).

1.5.4.2 PKB / Akt signalling in CVD and liver disease

PKB / Akt pathway dysregulation is implicated in many pathological conditions such as, cancer, DM, CVD and neurological diseases. Insulin resistance of peripheral tissues results from peripheral tissues failure to increase whole body glucose disposal in response to insulin. This is a common feature of metabolic derangements in common chronic conditions such as obesity, T2DM, and NAFLD. Akt regulates glucose uptake into muscle and fat cells by stimulating translocation of GLUT 4 glucose transporter to the plasma membrane and represses hepatic gluconeogenesis by insulin through suppression of the expression of phosphoenopyruvatecarboxykinase (PEPCK) and glucose-6-phosphatase (Logie et al. 2007). It therefore follows that, dysregulation of PKB / Akt has deleterious effects in both induction, progress and management of T2DM and metabolic syndrome in general.

Different cell types, such as endothelial cells, vascular smooth muscle cells, and cardiomyocytes show alterations in intracellular signalling implicated in energy metabolism, growth and survival in ischaemia and reperfusion. Therefore, PKB / Akt signalling in these cells is key in regulating cardiac growth, contractile function and coronary angiogenesis. Overexpression of Akt has also been implicated in cardiac hypertrophy which is pathological in the long term and this leads to functional impairment such as poor contractility, disrupted angiogenesis and disordered growth of cells eventually resulting in heart failure (Shiojima et al.

2005). In genetically modified mice, the protective role of PKB / Akt has been demonstrated in endothelial cells of Akt 1^{-/-} mice on APOE ^{-/-} displaying severe peripheral vascular disease, atherosclerosis, occlusive coronary artery disease, plaque vulnerability and cardiac dysfunction (Fernández-Hernando et al. 2007).

Akt has been identified as a key player in mediating cardioprotection in both pre-and post-ischaemic conditioned heart perfusion studies. This protection has been attributed to activation of anti-apoptotic pathways, forming the reperfusion injury salvage kinase pathways (RISK) (Hausenloy et al. 2005; Hausenloy & Yellon 2007). Altered signalling in PKB / Akt and eNOS have also been linked to vasculopathies such as atherosclerosis and impaired vascular dilatation (Fernández-Hernando et al. 2007; Fernández-Hernando et al. 2010). In a study investigating the roles and mechanisms of PIs and NRTIs in pulmonary artery endothelial cells, it was clearly demonstrated that these drugs lead to eNOS down-regulation, oxidative stress, and Erk 1 / 2 activation. (Wang et al. 2009). However, mechanisms leading to HAART-associated vasculopathies and CVD remain incompletely understood. Due to the critical role played by PKB / Akt in cellular physiology, it forms an important therapeutic target for various medical conditions and therefore an important topic for current and future research.

1.5.5 AMPK

Adenosine monophosphate activated protein kinase (AMPK) is an enzyme present in the cytoplasm of eukaryotic cells where it plays a key role as a master regulator of cellular energy homeostasis by acting as a sensor of energy status thereby maintaining optimal cellular energy homeostasis (Hardie 2011).

AMPK is a serine/ threonine kinase that exists as a heterodimeric complex comprising of catalytic α subunits, and regulatory β and γ subunits. The α subunit contains a typical serine/threonine kinase domain at the N terminus. The γ subunit contains the regulatory adenine nucleotide-binding site and is composed of four tandem repeats of sequence known as a CBS motif (Nagendran et al. 2013). The β subunit contains a c-terminal domain that forms the conserved core of the $\alpha\beta\gamma$ complex, linking the C-terminal of the α subunit to the N-terminal region of the γ subunit (Wong & Lodish 2006).

Binding of AMP to the α subunit allosterically activates the complex making it a more attractive substrate for phosphorylation on threonine 172 in the activation loop of the α subunit by its major upstream AMPK liver kinase B1 (LKB1) (Shackelford & Shaw 2009). Furthermore, AMPK can also be phosphorylated on the threonine 172 by calcium/calmodulin dependent protein kinase kinase 2 (CAMKK 2) in response to changes in intracellular Ca^{2+} that occur following stimulation by metabolic hormones including adiponectin and leptin (Jensen et al. 2007).

Metabolic stressors that either interfere with the catabolic generation of ATP e.g. glucose deprivation, hypoxia ischaemia and treatment with metabolic poisons, or those stresses that accelerate ATP consumption such as muscle contraction can increase the cellular ADP:ATP ratio and activate AMPK (Nagendran et al. 2013). Additionally, hormones such as leptin, adiponectin, ghrelin, cannabinoids and triiodothyronine, regulate AMPK activity although the actual mechanisms remain unclear (Lage et al. 2008; Jensen et al. 2007).

AMPK positively regulates signalling pathways that replenish cellular ATP supplies and negatively regulates ATP consuming biosynthetic processes. It therefore switches on catabolic pathways that generate ATP while switching off anabolic pathways that consume ATP. This is accomplished through phosphorylation of enzymes directly involved in these processes as well as through transcriptional control of metabolism by phosphorylating transcriptional factors, co-activators and co-repressors. Examples of catabolic pathways that are upregulated include, glucose uptake via activation of both glucose transporter 1 and 4 (GLUT 1 and GLUT 4) (Russell et al. 1999), glycolysis via phosphorylation and activation of 2 of 4 isoforms of 6-phosphofructose-2-kinase and fatty acid uptake via phosphorylation of ACC 2 isoform of acetyl-CoA carboxylate thus lowering malonyl-CoA levels, an inhibitor of FA uptake into mitochondria (Marsin et al. 2000).

Activation of AMPK inhibits several energy consuming anabolic pathways through direct phosphorylation of key metabolic enzymes, i.e. FA synthesis inhibition by phosphorylation of ACC 1, isoprenoid synthesis inhibition by phosphorylation of hydroxymethylglutaryl-CoA reductase, TGs and phospholipid synthesis inhibited by inactivation of glycerol phosphate acyl transferase, glycogen synthesis inhibition by phosphorylation of glycogen synthase and ribosomal RNA synthesis inhibition by phosphorylation of the RNA polymerase 1 transcriptional factors (Hardie et al. 2003). Another key role played by activated AMPK is the up regulation of catabolism through enhancement of mitochondrial function by phosphorylating the transcriptional co-activator of mitochondrial biogenesis, PGC-1 α . (Jäger et al. 2007). Figure 1.11 below summarises how activation of AMPK mediates the regulation of various metabolic processes.

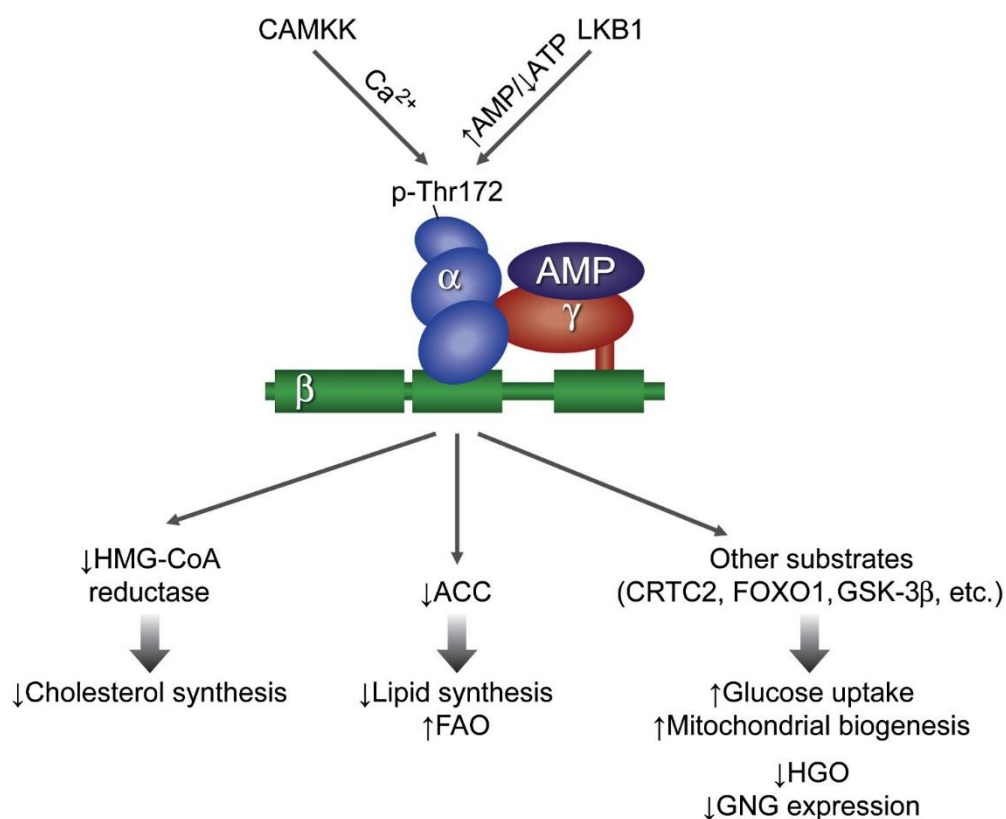


Figure 1.11 showing the activation and various mechanisms regulated by AMPK. Abbreviations: CAMKK 2 (calcium/calmodulin dependent protein kinase kinase 2), LKB1 (liver kinase B1), FAO (fatty acid oxidase),

CRTC2 (CREB (cAMP response element-binding protein) regulated transcription coactivator 2), HGO (hepatic glucose output), ACC (acetyl-CoA carboxylase), Ca²⁺ (Calcium), GNG (gluconeogenic genes), GSK-3 β (glycogen synthase kinase 3 β), \uparrow indicate an increase and \downarrow indicate a decline. Adapted with permission (Zhang et al. 2009).

Therefore, AMPK plays a critical role in co-ordination of cell growth, autophagy and reprogramming cellular metabolism processes (Mihaylova & Shaw 2011; Takagi et al. 2007) that are implicated in cardiovascular dysfunction and metabolic syndrome.

1.5.6 Role of AMPK in CVD and metabolic syndrome

Since the myocardium relies on ATP for contraction, pathologies that interfere with the generation and utilization of ATP severely compromise cardiac function. Ischaemia alters energy and oxygen supply to the myocardium thereby leading to myocyte stress and activation of cellular mechanisms to compensate for the reduction in ATP levels. AMPK has been shown to be upregulated in IHD and is therefore a suitable marker to assess the myocardial response to stressful events such as MI (Baron et al. 2005). Activation of AMPK during myocardial ischaemia increases cellular glucose levels through enhanced glucose uptake and glycolysis; consequently, during reperfusion / post-ischaemic phase, fatty acids are increased to ensure adequate cellular energy supply (Sambandam & Lopaschuk 2003). Furthermore, mediation of glucose uptake and fatty acid oxidation ameliorates cardiac dysfunction post-ischaemia through the prevention of apoptosis and myocardial injury (Russell et al. 2004; Qi & Young 2015).

There is evidence indicating that the activated form of AMPK is significantly reduced in obese mouse and rat models compared to lean ones. Furthermore, high fat diets have been shown to alter both the expression and activity of AMPK (Liu et al. 2006), which is associated with lipotoxicity characterised by hyperinsulinaemia, hypertriglyceridaemia and impaired fatty acid oxidation. Defects in AMPK signalling are responsible for these abnormalities that predispose to development of T2DM (Sriwijitkamol et al. 2006). This may explain the excess myocardial lipid accumulation (lipotoxicity) leading to cardiomyopathy in obese rodents (An & Rodrigues 2006). Reduced levels of activated, phosphorylated AMPK have been associated with increased myocardial lipotoxicity in obese rodents (Wang & Unger 2005). Although the downregulation of AMPK signalling may not be a primary defect preceding metabolic aberrations associated with metabolic syndrome, it is likely that suppressed AMPK signalling in severe obesity is likely to exacerbate aspects of the metabolic syndrome. Therefore, due to AMPK's role as a central regulator of both lipid and glucose metabolism and suppression of cell proliferation, AMPK is considered a potential therapeutic target in management of obesity, T2DM (Zhang et al. 2009), atherosclerosis and some cancers (Motoshima et al. 2006). Furthermore, metformin, a major drug used in the management of T2DM has been shown to improve AMPK activity in metabolic syndrome thereby ameliorating hyperinsulinaemia and fatty acid oxidation in the high fat diet context (Liu et al. 2006).

NRTI-induced mitochondrial toxicity alters cellular energy production thereby leading to metabolic derangements (Brinkman et al. 1999; Lewis et al. 2001). Altered mitochondrial activity in various tissue targets results in specific pathologies such as steatosis and insulin resistance in the liver tissue (Videla et al. 2004), as well as endothelial dysfunction. Furthermore, there is ample evidence supporting involvement of AMPK in cardiac ischaemia-reperfusion injury as a potential therapeutic target (Russell et al. 2004; Qi & Young 2015).

1.5.7 Other important signalling molecules

1.5.7.1 NADPH oxidase subunit, p22-phox

Nicotinamide adenine dinucleotide phosphate-oxidase (NOX) is a cell membrane bound enzyme that plays an important role in cellular immune responses to pathogens by generating superoxides and ROS that ultimately lead to bacterial eradication. The enzyme has several subunits, p22-phox is one of the key components (Regier et al. 2000). The oxidase is not only expressed in immune cells, such as neutrophils and macrophages, but NADPH components, including p22-phox, gp91-phox, p67-phox and p47-phox have also been identified in endothelial cells and vascular smooth muscle cells (Jones et al. 1996). Increased p22-phox mRNA expression coupled with the enzyme hyperactivity have been reported in aortas harvested from hypertensive male Sprague-Dawley rats (Fukui et al. 1997). Therefore, the oxidase has received special attention in vascular and cardiac physiology due to the risk posed by excessive generation of ROS in pathological states. Furthermore, the oxidase has been implicated in aberrant cell proliferation and migration and inflammatory responses in atherosclerotic vascular disorders (Griendling et al. 2000).

Long term use of both PIs and NRTIs has been associated with increased generation of ROS which have detrimental effects on vascular endothelium, cardiomyocytes and hepatocytes. (Videla et al. 2004; Reyskens & Essop 2014; Sharma 2014). The changes in the antioxidant profile in patients on HAART have been partly responsible for NAFLD, increased atherogenic risk and CAD as reported in *in vitro*, *in vivo* and clinical studies (Sundaram et al. 2008; Bavinger et al. 2013; Videla et al. 2004). As a key component of the NADPH oxidase enzyme, p22-phox is an important laboratory marker of superoxide radical generation and subsequent oxidative stress (Dinauer et al. 1990). Furthermore, studies have clearly demonstrated that elevated levels of p22-phox correlate with risk and severity of atherosclerotic CHD (Azumi et al. 1999).

1.5.7.2 Cleaved poly (ADP-ribose) polymerase (PARP) and cleaved caspase 3

Poly (ADP-ribose) polymerase 1 (PARP-1) is a nuclear protein / enzyme present in abundance and plays a key role in sensing DNA breaks and contributes in repairing DNA to ensure that genes remain stable (Mazen et al. 1989). However, when over activated, PARP diminishes cellular NAD^+ and ATP rendering the cell dysfunctional or dead through necrosis. Furthermore, it is a major substrate for the apoptosis mediating caspases 7 and 3 (Tewari et al. 1995). The cleaved PARP fragments suppress PARP-1 activity not only preserving NAD^+ but also mediating release of Ca^{2+} and Mg^{2+} dependent endonucleases (Herceg and Wang 1999). Therefore, PARP is involved in both necrotic and apoptotic cell death.

PARP also enhances other intracellular signalling pathways such as NF κ B thereby facilitating pro-inflammatory responses that further contribute to oxidative DNA and cellular damage as seen in T2DM patients with microangiopathy (Adaikalakoteswari et al. 2007).

The cellular insults described in both fatty liver and HAART induce DNA damage, genomic instability, mitochondrial dysfunction and eventual cell death. For example, HAART is associated with increased rates of cell loss in a variety of tissues as evidenced by pro-apoptotic effects of PIs (Badley 2005; Zhou et al. 2005) in hepatocytes, endothelial and immune cells. Furthermore, NRTIs are associated with mitochondrial toxicity that eventually results in cytotoxicity (Liu et al. 2015; Lewis et al. 2001). Therefore, these two enzymes, cleaved poly (ADP-ribose) polymerase and cleaved caspase 3, which are implicated in cell death in both normal and altered physiology were evaluated in this study.

1.5.7.3 Mitogen-activated protein kinases (MAPKs); Jun N-terminal kinase (JNK), p38 and extracellular-signal-regulated protein kinase (ERK 1/2)

MAPKs are involved in many facets of cellular regulation including regulating the expression of many inflammatory genes (Dean et al. 1999). Three major MAPK pathways, extracellular-signal-regulated protein kinase (ERK), p38 MAPK and c-Jun N-terminal kinase (JNK)/stress activated protein kinase (SAPK), are involved in post-transcriptional regulation of mRNAs encoding for TNF- α , IL-6 and cyclooxygenase (COX)-2 (Ridley et al. 1997; Hitti et al. 2006). However, the possible links and hierarchical relationship between HAART, NAFLD, CVD and MAPK signalling pathways, remain unidentified. Activation of the P38 MAPK cascade is critical for HIV-1 replication in primary T lymphocytes (Cohen et al. 1997). However, drugs that inhibit RT also interfere with p38 signalling (Bakan & Bahar 2009) impairing survival and proliferation of immune and endothelial cells (Yu et al. 2004).

Upregulation of JNK signalling in NAFLD has been postulated to modulate the phosphorylation of proteins in insulin signalling leading to insulin resistance (Malhi et al. 2006). Since PI-based HAART is associated with NAFLD and insulin resistance, investigating this pathway becomes imperative.

1.6 Problem statement and study rationale

Ongoing work has demonstrated that HAART greatly reduces HIV/AIDS-associated mortality and the lifespan of PLWH has been prolonged dramatically. This chronicity has led to the emergence of multisystemic undesired effects which have contributed significantly in the rising incidence of non-AIDS-related morbidity and mortality. CVD and liver-related complications have been identified as some of the major causes of morbidity and mortality associated with HAART. To date, the pathophysiological mechanisms that link HAART use and NAFLD with CHD, aortic valve sclerosis, myocardial dysfunction/hypertrophy and cardiac arrhythmias are incompletely understood.

The complex interactions between HAART, NAFLD, insulin resistance and visceral obesity make it extremely difficult to dissect out the actual causal mechanisms responsible for the increased risk of these types of cardiac

and vascular complications. Furthermore, the rising incidence of AMI with the use of HAART has been reported in various clinical studies (Friis-Møller et al. 2007, Durand et al. 2011, Friis-Møller et al. 2003a, Friis-Møller et al. 2003b), however, there is a paucity of knowledge in the literature as to how PI-based HAART regimens contribute to these chronic conditions. Therefore, it is justified to conduct ischaemia-reperfusion studies and to analyse important signalling pathways implicated in survival and damage to the cardiomyocytes. Additionally, analysis of lipid profile (cholesterol, TGs, LDL and HDL), blood glucose, insulin and markers of lipid peroxidation (conjugated dienes (CD) and thiobarbituric acid reactive substances (TBARS) (normalized with serum phospholipids) will provide valuable information on the extent of alterations of these circulating metabolites in obesity and HAART.

To date, there is no clearly defined targeted therapy to avert these adverse effects and hence a definite need for extensive experimental studies to have a clearer understanding of the underlying mechanisms and explore possible therapeutic targets to ameliorate these detrimental effects.

By assessing the hepatic changes in HAART, the present study aims to link steatosis with cardiac changes observed in ischaemia-reperfusion injury and vasculopathies. This study focused on the cardiac response to ischaemia by assessing the haemodynamic changes in the isolated hearts before, during and after induced ischaemia and infarct size analysis after reperfusion. Vascular reactivity studies were also conducted in an isolated organ bath system with the aim of assessing endothelial and vascular contractility / relaxation of the thoracic aorta. Liver studies were limited to morphological / fat infiltration histological assessments, and enzyme function tests (transaminases and phosphatases) to assess the degree of HAART-mediated hepatic damage. These enzymes have been used as surrogate markers of hepatic steatosis. Furthermore, relevant signalling cascades in the heart, liver and aorta were assessed to delineate the various mechanisms involved.

Therefore, this study focuses on enhancing our understanding on the contribution of HAART to the development of NAFLD with concomitant cardiovascular dysfunction and explores the role of dual PPAR α / γ stimulation as a potential therapeutic target to limit HAART-induced metabolic, and cardiovascular dysfunction.

1.7 Research questions

The study explores the following questions: -

- a. Does the treatment with HAART (LPV/r + AZT/3TC) for six weeks lead to NAFLD with concomitant development of cardiac and vascular dysfunction in lean / obese male Wistar rats compared to non-treated rats?
- b. Does co-treatment of lean / obese male Wistar rats with a dual PPAR α / γ agonist, Saroglitazar, for six weeks limit HAART-induced NAFLD and CVD?

1.7.1 Hypotheses

1.7.1.1 Alternate hypothesis H_A

We hypothesize that the use of second line HAART (LPV/r + AZT/3TC), a PI-based regimen, leads to the development of NAFLD and cardiac / vascular dysfunction and that these effects can be limited by dual PPAR α / γ stimulation.

1.7.1.2 Null hypothesis H_0

The use of second line HAART regimen has no effect on the development of NAFLD and cardiac / vascular dysfunction and PPAR α / γ stimulation has no effects on the model rats treated with LPV/r + AZT/3TC for six weeks.

1.8 Research aims and objectives

The two-overarching aims of this study are: -

- a) To evaluate the contribution of HAART to the development of NAFLD and cardiac dysfunction in a rat model of high caloric diet-induced obesity (DIO).
- b) To investigate the role of PPAR α / γ stimulation as a potential therapeutic target to limit HAART induced hepatic, metabolic and cardiovascular dysfunction.

The specific objectives of the study include: -

- a) To induce obesity (via high-calorie diet) in male Wistar rats by means of an established, previously published high-fat / calorie diet model.
- b) To investigate the effects of HAART and Saroglitazar treatment on the lipid profile, oxidative stress markers, liver enzymes and fasting insulin in serum obtained from high calorie diet and age-matched control rats.
- c) To investigate the effects of HAART and PPAR α / γ agonist (Saroglitazar) treatment on liver morphology as well as the expression and phosphorylation of important signalling proteins in liver tissue from high calorie diet and age-matched control rats.
- d) To determine the haemodynamic effects of HAART and Saroglitazar on isolated perfused hearts from obese and age-matched control rats exposed to cardiac ischaemia-reperfusion.
- e) To identify the effects of HAART and Saroglitazar treatment on the expression and phosphorylation of important cell signalling cascades in isolated and perfused hearts from obese and age-matched control rats exposed to ischaemia-reperfusion.
- f) To investigate the endothelial and smooth muscle function of aortic rings from obese and age-matched control rats treated with HAART and Saroglitazar by use of an organ bath system.
- g) To assess the effects of HAART and Saroglitazar treatment on the expression and phosphorylation of important cell signalling cascades in isolated aorta tissue from obese and age-matched control rats.

Having reviewed HAART implication in metabolic, hepatic and cardiovascular dysfunction, and having outlined clear aims and objectives of the present study, the next chapter (chapter 2) gives a description of the study activities and methods that were employed to answer the research questions.

Chapter 2 : Methodology

2.1 Introduction

This chapter describes the various methods and techniques undertaken to accomplish the aims of the study.

The main research activities conducted in this study include: -

- i) Randomised grouping of experimental animals.
- ii) Animal care and monitoring for a duration of 16 weeks.
- iii) Treatment with the experimental drugs.
- iv) Animal sacrificing and organ/tissue harvesting.
- v) *Ex vivo* cardiac perfusion studies.
- vi) Liver histology studies.
- vii) Serum analyses.
- viii) Protein determination using Western blot technique.
- ix) Vascular reactivity studies.
- x) Data analysis.

2.2 Study design

This study employed a randomised controlled experimental design where experimental animals were randomly allocated into eight different groups and subsequently subjected to the various treatment and feeding programmes.

2.3 Ethics clearance and protocol approval

Ethics approval for this project was granted by the Stellenbosch University Research Ethics Committee: Animal Care and Use via committee review procedures; Protocol #: SU-ACUD15-00019 and animals were handled in accordance with international and South African standards for the care and use of animals for research and scientific purposes. All persons who handled the animals obtained authorization as per the South African National Standards (SANS 10386:2008, <http://www.sun.ac.za/research>, “Accessed: 22/08/2017)) and by the South African Veterinary Council (SAVC) (<http://www.savc.org.za/>, “Accessed: 22/08/2017).

The study adhered strictly to the principles of “replacement, reduction and refinement”. Therefore, only the required number of animals were used in this study and the numbers were calculated to ensure that the aims of the study were accomplished efficiently.

The choice of rats as our experimental animals was after careful consideration. They were chosen because they are easily accessible in the accredited university animal facility and they have been used in our laboratories for the various research activities listed above. Furthermore, they are of great value in this study because the findings will generate translatable results that will provide relevant and important knowledge. At the end of treatment and feeding programme, animals were humanely sacrificed using a universally acceptable method as described below, (Section 2.5.5).

2.4 Infrastructure

The cardiovascular research experiments and Western blot studies were conducted under the auspices of the Cardiovascular Research Group housed in the Division of Medical Physiology, Faculty of Medicine and Health Sciences (FMHS), Stellenbosch University (SU).

Histological experiments were conducted in collaboration with the Division of Anatomy and Histology, Stellenbosch University and the Biomedical Research and Innovation Platform (BRIP), South African Medical Research Council (SAMRC), Tygerberg, South Africa.

Serum lipid and oxidative stress analyses were conducted in collaboration with Dr. Dee Blackhurst from the Division of Chemical Pathology, University of Cape Town.

Laboratory animals were bred, housed and supplied by the animal housing facility, Faculty of Medicine and Health Sciences, SU.

2.4.1 Personnel involved in the various research study activities

- a) Random allocation of animals to various study groups – candidate (Festus Kamau) and SU animal facility staff.
- b) Animal monitoring (daily food and water consumption and weekly total body weight measurement – candidate.
- c) Cleaning of animal cages and changing of animal beddings – SU animal facility staff.
- d) Drug preparations – candidate.
- e) Oral gavaging of the experimental animals – Mr Noel Markgraaf (SAVC certified).
- f) Euthanasia, blood collection and organ harvesting – candidate.
- g) Cardiac perfusion studies – candidate.
- h) Aortic ring studies – candidate assisted by Miss Imperial Emiliana (MSc.).
- i) Liver histology experiments – candidate and Mr Reggie Williams (Histology technician).
- j) Liver enzyme analysis – PathCare veterinary pathology laboratory, Western Cape, Cape Town. South Africa.
- k) Serum analyses (lipid analysis, oxidative stress markers analysis, fasting insulin analysis) - candidate and Dr Dee Blackhurst (Division of Chemical Pathology, University of Cape Town).
- l) Liver immunohistochemistry – BRIP, SAMRC.

- m) Western blot studies – candidate.
- n) Data management and analysis - candidate in collaboration with Biostatistics Unit, SU.
- o) Supervisors – Dr Ruduwaan Salie, Dr Peter Waweru and co-supervisor Prof Hans Strijdom. Team advisor – Prof. Amanda Lochner.

2.5 Research activities

2.5.1 Experimental animal selection, housing and grouping

Male pathogen free Wistar rats (*Rattus norvegicus*) were the animals of choice in this study because they have been used extensively in cardiovascular experimental studies in our laboratory with reproducible and reliable data (Salie et al. 2014; Webster et al. 2017). They are readily available, locally bred and our laboratory has suitable systems for conducting the *ex vivo* cardiovascular experiments of interest in this study. Although we recognise the limitations associated with use of male rats only, this choice was carefully considered because combining male and female rats in this study, would have required a significantly higher sample size (and cost) to account for the female hormonal variations that are attended by confounding physiological changes that affect both the endocrine and cardiovascular systems (Moran et al. 2000).

We obtained rats 3-4 weeks after they were weaned i.e. approximately 7 weeks of life, with an average body weight of 157.2 ± 5.1 g (mean \pm SEM). To achieve appropriate sample sizes for the various experiments of interest, a total number of 176 rats were used (Figure 2.1). However, the study sought for ethics approval of 200 rats to account for expected losses during the treatment procedures. Since all the animals could not be followed up simultaneously, they were staggered into 10 groups each consisting of 20 rats. Twenty rats were introduced every week for ease of follow-up and subsequent procedures. Allocation to various groups was done randomly to avoid selection bias.

The rats were randomly assigned into different cages (5 rats per cage) and fed on a standard rat chow diet. Additionally, the animals had access to clean drinking water *ad libitum* to acclimatize for 7 days. Thereafter, they were fed, treated and monitored in the same room for the entire experimental study duration. During the one week of acclimatization, their water and food intake were monitored daily and recorded, they were housed under the following conditions: standard day-night cycles of 12 hours, temperatures of 22 °C and 40 % humidity. After a successful week of acclimatization, the rats were on average 8 weeks old and weighed 180.2 ± 2.28 g (mean \pm SEM). This age corresponds to the late adolescence/ young adulthood phase in humans (Sengupta 2012). The age was intentionally chosen for initiation of the experimental procedures because the feeding programme we used, has been shown to have optimal effect at this age (Webster et al. 2017). Subsequently, as described below, the treatment regimen protocols were calculated to correspond to adult human doses.

2.5.2 Feeding and treatment programme

The cages (each accommodating 5 rats) were randomly assigned into 2 groups and initiated on a feeding programme composed of either *ad libitum* standard rat chow (lean group) or *ad libitum* standard rat chow and high calorie diet (HCD group). To induce obesity, rats were fed specially formulated HCD (previously published) composed of 11.5% fat, 8.3% protein, 42% carbohydrate and 20% sucrose (Salie et al. 2014). Standard diet (rat chow) was composed of 4.8% fat, 17.1% protein, 34.6% carbohydrates and 5.3% sucrose. Please refer to Table 2.1 showing the composition of the diets. The diets were analysed by Microchem specialized laboratory services (Accredited by South African National Accreditation System, SANAS), Cape Town, South Africa (Addenda A 1 and A 2 Diet Analysis Certificates). Food and water were supplied *ad libitum* to all the groups throughout the study duration.

Table 2.1 Composition of standard and high fat / calorie diet: g (grams), kJ (kilojoules).

	Fat (g/100g)	Saturated fat (g/100g)	Cholesterol (mg/100g)	% Protein	% Carbohydrates	% Sucrose	kJ/ 100g
Lean / Standard diet (ordinary rat chow)	4.8	0.9	2.2	17.1	34.6	6.6	1272
Specially formulated High Calorie Diet (HCD)	11.5	7.6	13	8.3	42	24.4	1354

2.5.2.1 Preparation of HCD

The HCD was prepared using normal rat chow, sucrose, cooking fat (HolsumTM), full cream, and sweetened condensed milk (Addendum B, HCD preparation).

The diets were continued for a total duration of 16 weeks and for the last 6 weeks, animals were treated with the experimental drugs. During the entire feeding and treatment period, rats were weighed and the cage dressings / beddings (pine shavings / corncob) changed weekly. Additionally, animals were monitored daily for their general state of health and their water (ml) and food (g) intake was recorded daily.

2.5.2.2 Treatment

From week 11 of the diet programme, the two groups of cages (HCD versus lean) were randomised further into 4 subgroups and initiated on treatment as follows: -

- i) Vehicle, distilled water (control group)
- ii) HAART (LPV / Ritonavir (LPV/r) + Zidovudine / Lamivudine (AZT/3TC)
- iii) LPV/r + AZT/3TC + Saroglitazar
- iv) PPAR α / γ agonist, Saroglitazar

Therefore, each treatment group was comprised of control lean and HCD rats as shown on the table 2.2 below.

Table 2.2 Categorization of the eight experimental groups (1-8), LPV/r (LPV boosted with ritonavir), AZT (Azidothymidine), 3TC (Lamivudine), HAART (Highly active antiretroviral therapy), Saro (Saroglitazar).

Experimental intervention	Standard rat diet (normal rat chow) - lean	High calorie diet (HCD)
Vehicle, distilled water (Control)	1) Lean Control	2) HCD Control
LPV/r + AZT/3TC (HAART)	3) Lean HAART	4) HCD HAART
HAART + PPAR α / γ agonist, Saroglitazar (HAART + Saro)	5) Lean HAART + Saroglitazar	6) HCD HAART + Saroglitazar
Saroglitazar	7) Lean Saroglitazar	8) HCD Saroglitazar

The drug prescriptions were obtained from a registered veterinarian as per the SAVC and SANS. The drugs were obtained as follows: -

- i) LPV / r (200mg /50mg) as combined film coated tablets traded as *AluviaTM* (*AbbVie (Pty) Ltd South Africa*).
- ii) Zidovudine / Lamivudine each tablet containing (zidovudine 300mg and lamivudine 150mg) traded as *COMBIVIR[®]* (*GlaxoSmithKline South Africa (Pty) Ltd*).
- iii) Saroglitazar, [(S)- α -ethoxy-4-{2-[2-methyl-5-(4-methylthio) phenyl]-1H-pyrrol-1-yl]-ethoxy}-benzenepropanoic acid magnesium salt], 4 mg tablets traded as *LipaglynTM* (*Zydus Discovery: A division of Cadila Healthcare Limited, India*).

Each drug tablet was weighed, crushed and then measured to the required dose before making a suspension (turbid mixture) in distilled water which was used as a vehicle. The daily drug doses administered were 68.57/17.14 mg/kg/day of LPV/r, 51.43/25.71 mg/kg/day of AZT/3TC and 0.40 mg/kg/day of Saroglitazar; corresponding to human doses (11.43/2.86 mg/kg/day, 8.57/4.29 mg/kg/day and 0.06 mg/kg/day, respectively) calculated using the body weight/ surface area normalisation formula below (Nair et al. 2016).

$$\text{HED (mg / kg)} = \text{Animal does (mg / kg)} \times (\text{Animal } K_m / \text{Human } K_m)$$

$$\begin{aligned} \text{HED is Human Equivalent Dose, } K_m \text{ is Correction factor} \\ \text{Rat } K_m = 6.2, \text{ Human } K_m = 37 \end{aligned}$$

Rat to human body weight/ surface area normalisation formula for drug dose calculations.

The average weekly rat weight was used to calculate the drug doses (total volume 1 mL) and the administration was conducted daily between 0900h and 1100h via oral gavage for six weeks by a SAVC certified veterinary technician. The food and water intake were monitored daily for two weeks before onset of treatment and continued for 4 weeks during treatment to ensure that the treatment did not adversely affect food and water

intake in compliance with animal ethics. Below is a schematic presentation of randomization and various experimental interventions undertaken (Figure 2.1).

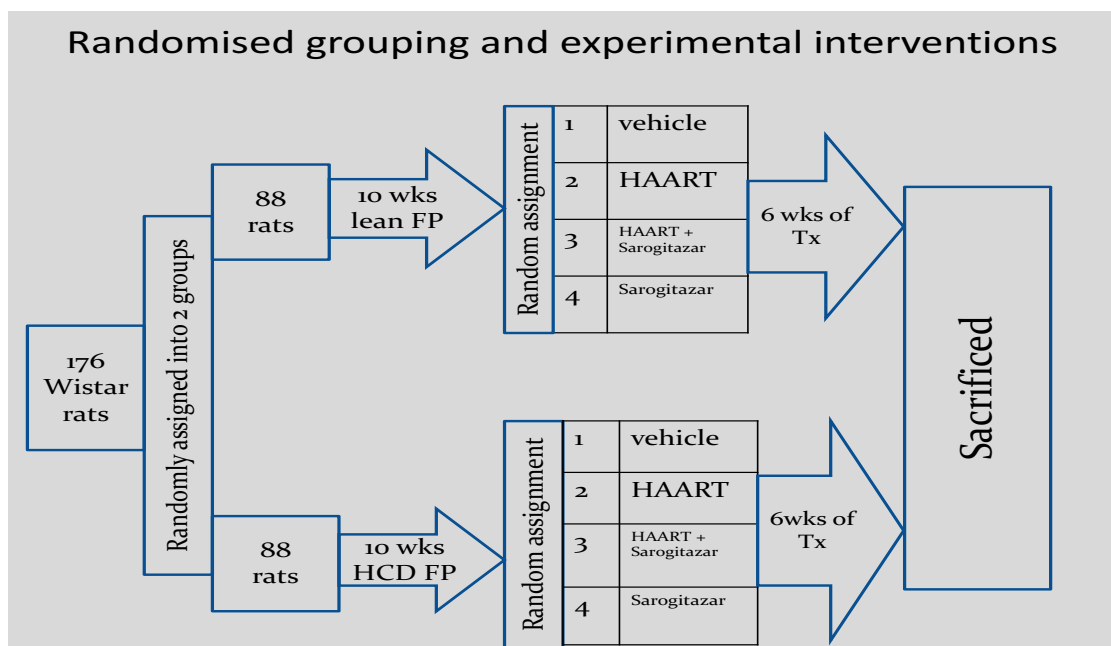


Figure 2.1 Schematic representation of randomised grouping and various experimental interventions. Abbreviations wks: weeks, Tx: treatment, FP: feeding programme.

2.5.3 Animal monitoring

During the treatment phase of the study, apart from weight monitoring, rats were closely monitored for any adverse effects and where distress was noted, appropriate measures were taken. Food and water intake monitoring was done daily to ensure that the gavage procedure did not interfere with feeding and thereby adversely affecting the outcome of the study. Although stool and urine volumes were not quantified, their colour and consistency were closely monitored. The rat grimace scale shown below (Figure 2.2), was applied to assess the level of distress / pain following oral gavage.



Figure 2.2 Rat grimace scale, (Sotocinal et al. 2011).

Rats that showed moderate to obvious distress were isolated and monitored closely and those that showed persistent distress associated with reduced feeding (> 50 %) for more than 48 hours were not gavaged and therefore dropped from the study. After completion of the treatment programme, the animals were transported from the central animal unit to the temporary animal holding facility (for not more than 5 days) in the Division of Medical Physiology for subsequent experimentation. This stay was kept short to ensure that the transfer did not adversely affect the animal welfare. Furthermore, *ad libitum* food and water administration was continued until the rats were sacrificed. However, some rats were fasted overnight for serum lipid profile analysis as described below.

2.5.4 Overnight fasting

From each group described above, 8 rats, ($n = 8$ / group) were randomly selected and fasted for 10-14 hours before euthanasia. They were placed in special cages (metabolic cages) and supplied with water only *ad libitum*. Serum samples obtained from these rats were stored at -80 degrees Celsius ($^{\circ}$ C) and subsequently utilised for the measurement of fasting insulin levels, lipids (i.e., total serum cholesterol (TC), TGs, phospholipids (PL), high density lipoproteins (HDL-C, HDL₂, HDL₃)), and markers of lipid peroxidation (conjugated dienes (CD) and thiobarbituric acid reactive substances (TBARS)). Heart tissue samples ($n = 6$ / group) were also harvested from these animals and snap frozen for subsequent Western blot analyses.

2.5.5 Euthanasia

Rats were euthanised through intraperitoneal (IP) injection of 160 mg/kg of sodium pentobarbitone (*Euthanaze*[®], Bayer (Pty) Ltd. Animal Health Division, South Africa) using a sterile 26-gauge hypodermic needle. The site of injection was at the lower right quadrant of the abdomen to ensure that the urinary bladder, cecum, liver and other abdominal tissues were not damaged (Zatroch et al. 2017) as shown below (Figure 2.3).

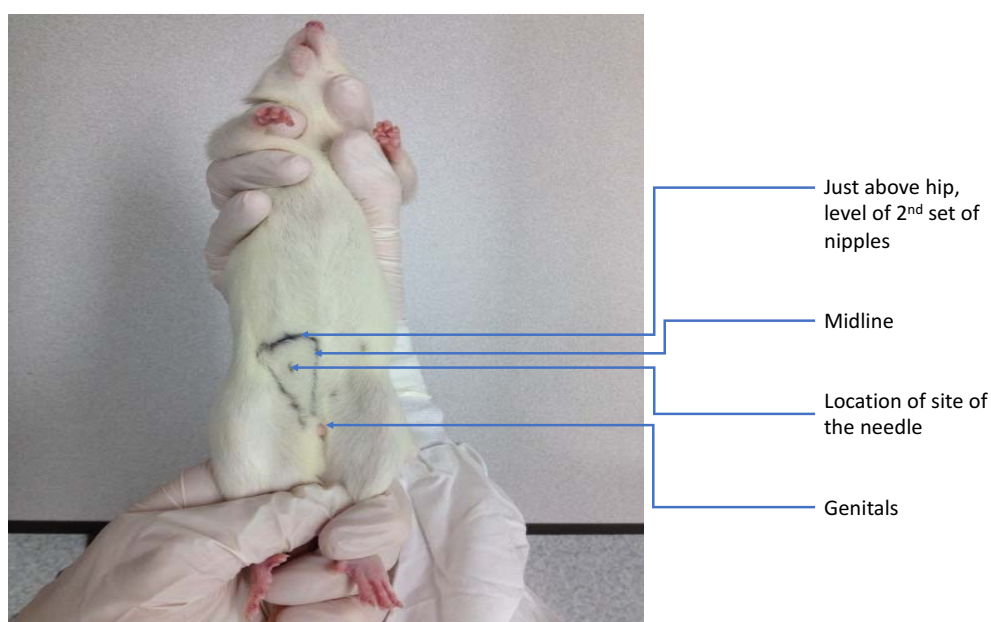


Figure 2.3 Landmarks for rat intraperitoneal injection.

After injection, the animals were weighed and kept in a warm environment (to prevent hypothermia) away from bright light to minimize discomfort before the animals were in a fully (deep) anaesthetised state. To ascertain a state of deep anaesthesia, a pedal withdrawal reflex to pain stimuli was performed and its absence signalled successful euthanasia.

2.5.6 Blood glucose measurement

Blood glucose levels were measured in both fasted and non-fasted rats (n = 8 / group). A tail prick was done during anaesthesia and blood glucose levels were measured in millimoles / litre (mmol/L) using a conventional glucometer (*GlucoPlusTM Cipla MedPro (Pty) Ltd. SouthAfrica*). The fasting blood glucose and fasting serum insulin measurements were used to calculate the homeostasis model assessment for insulin resistance (HOMA-IR). HOMA-IR is a validated method of assessing insulin resistance and β cell function in Wistar rats (Antunes et al. 2014) and was calculated using the formula: fasting serum insulin concentration ($\mu\text{IU} / \text{L}$) * blood glucose (mg / dl) / 405 (Mathews et al.1985).

2.5.7 Incision, serum collection and isolation of organs

A transverse sub-sternal incision was made and extended sub-diaphragmatically and the chest cavity was accessed via opening of the diaphragm and incising bilaterally towards the costochondral joints. The heart was rapidly excised after severing the aorta and pulmonary trunk and was submerged in fresh ice cold modified Ringer's Lactate/ Krebs-Henseleit buffer (KHB) (containing NaCl 119 mM; NaHCO₃ 24.9 mM; KCl 4.7 mM; KH₂PO₄ 1.2 mM; MgSO₄.7H₂O 0.59 mM; Na₂SO₄ 0.59 mM; CaCl₂ 1.25 mM; glucose 10 mM) to arrest metabolism and stop contractions. Excess fat and connective tissue around the heart and ascending aorta were carefully dissected out and hearts were weighed maintaining them in ice cold KHB before they were mounted on the isolated rat heart perfusion system.

After heart excision, blood collected within the chest cavity was collected using a pipette and placed into plain vacutainers (*Serum clot activator vacuette, greiner bio-one, Germany*) and left to stand for 25-35 minutes on dry ice before centrifugation at 3,000 revolutions / minute (3,000 rpm) for 20 minutes. Thereafter, the supernatant (serum) was carefully drawn and transferred into pyrogen free cryotubes (*Cryo.STM, greiner bio-one, Germany*) and stored at -80 °C for subsequent serum analyses.

Serum from non-fasted rats was analysed for liver enzymes i.e., alkaline phosphatase (ALP), alanine aminotransferase (ALT), aspartate aminotransferase (AST), lactate dehydrogenase and gamma-glutamyl transferase (GGT) (*Analysis done by: PathCare veterinary Pathology Laboratory, Western Cape, Cape Town South Africa*).

The liver tissue was carefully dissected and weighed and thereafter the right lobe was divided into three pieces: where one piece was immediately freeze clamped and stored in liquid nitrogen for subsequent Western blot analysis, the second piece was stored in liquid nitrogen for frozen section histological analysis and the third

piece was preserved in 10% neutral buffered formalin for standard haematoxylin and eosin (H/E) staining followed by histological analysis.

The thoracic cavity was rinsed with ice cold KHB to clear blood clots and the thoracic aorta was accessed after meticulously dissecting out the pulmonary structures and oesophagus. The proximal part of the aorta (the point where the heart was severed) was identified and using non-toothed tissue dissecting forceps, the peri-aortic tissue (fat) was gently held and the vessel together with the perivascular tissues were dissected out from the vertebral bed. The entire thoracic aorta was harvested and quickly placed in ice cold Ringer's Lactate solution for isometric tension studies (see section 2.5.11.2) and Western blot analyses. After performing a laparotomy through extension of the midline incision, the visceral / peritoneal fat was harvested and weighed as an indicator of fat deposition following experimental interventions.

The left tibia was also harvested and the length measured using a Vernier calliper (150mm 530-101) to relate the tibial length to heart weight for accurate quantification of the cardiac hypertrophy if any. The absolute heart mass (mg) of each experimental animal was divided by its tibial length (mm) to obtain a normalised cardiac mass index (mg / mm). Thereafter, the mean indices were computed per group. This has been described as a more accurate index than comparing the heart mass to total body weight (Yin et al. 1982).

2.5.8 Isolated working heart perfusion system

The isolated hearts arrested in KHB were mounted on the Neely-Morgan perfusion system according to principles described by Neely and colleagues in 1967 (Liebermeister et al. 1967). The system contains warm crystalloid solution, KHB (36° C) that is gassed with 95 % oxygen and 5 % carbon dioxide to maintain pH at 7.4. The aorta was mounted on the aortic cannula on the system to allow retrograde perfusion at 100 cm of H₂O for 15 minutes for stabilisation. The left atrium/pulmonary trunk was cannulated and after 15 minutes of retrograde flow, the flow was changed to antegrade/ working mode where the heart was perfused at a preload of 15 cm H₂O and the left ventricle ejected against an afterload of 100 cm H₂O. The temperature was monitored throughout the perfusion protocol using a thermometer probe placed in the coronary sinus. The myocardial temperature was maintained at 36.5° C during ischaemia. After 15 minutes of working mode (left ventricle pumping against 100 cm H₂O), the flow was reversed to retrogradely perfuse the heart (Langendorff mode) for another 25 minutes before induction of myocardial ischaemia. Two types of ischaemia were induced as described below. The 25 minutes of retrograde perfusion was aimed at enhancing stabilization to achieve reproducible results for the infarct sizes and signalling proteins investigated (Stensløkken et al. 2009). On the other hand, reperfusion phases for both global and regional ischemia-reperfusion have been optimized in our laboratory (Marais et al. 2005; Salie et al. 2012) and were approved by experts in the field (personal communication: Professor A. Lochner).

2.5.8.1 Global ischaemia

After the stabilisation phase, a set of hearts (n = 6 / group) were randomly selected for global ischaemia / reperfusion studies and subsequent Western blot determinations of protein expression / activation. To induce

global ischaemia, perfusion to the heart was completely cut off (coronary flow rate of 0 ml/ min) by closing both the aortic and left atrial flows for 20 minutes (Bell et al. 2011). Temperature was monitored and kept constant at 36.5° C throughout the global ischaemia phase. At the end of global ischaemia, the hearts were retrogradely perfused for 10 minutes, snap frozen and preserved in liquid nitrogen for subsequent Western blot analyses (Figure 2.4).

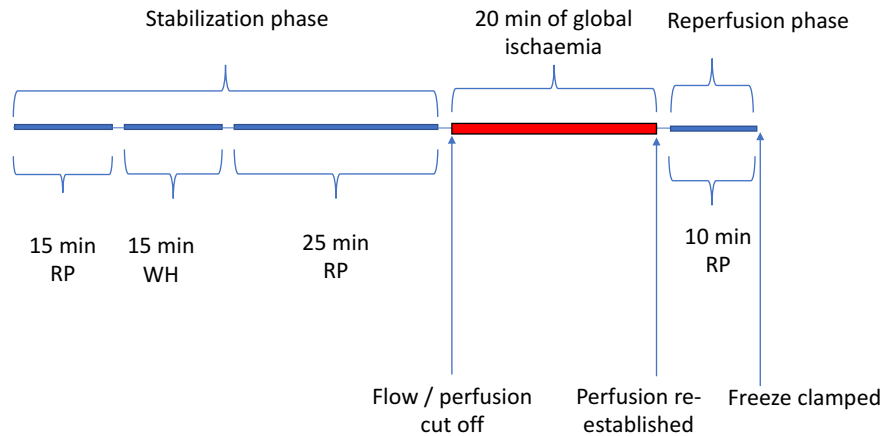


Figure 2.4 Global ischaemia / reperfusion perfusion protocol. RP: retrograde perfusion, WH: working heart, Min: minutes.

2.5.8.2 Regional ischaemia-reperfusion studies

In another set of *ex vivo* working heart experiments, (n = 8 / group), hearts were exposed to a regional ischaemia-reperfusion protocol (Figure 2.5). After stabilising the hearts for 55 minutes (15 retrograde perfusion, 15 working heart mode and 25 of retrograde flow), the left anterior descending coronary artery (LADCA) was ligated for 35 minutes using a silk surgical suture and the temperature kept constant at 36.5° C throughout the ischaemia phase. LADCA ligation reduced the coronary flow to approximately 1/3 of pre-ischaemia flow rate. After 35 minutes, the ligature was loosened and hearts reperfed retrogradely for 10 minutes and thereafter switched to working heart for 20 minutes. The perfusion protocol was completed after perfusing the hearts in Langendorff mode for another 30 minutes (Bell et al. 2011).

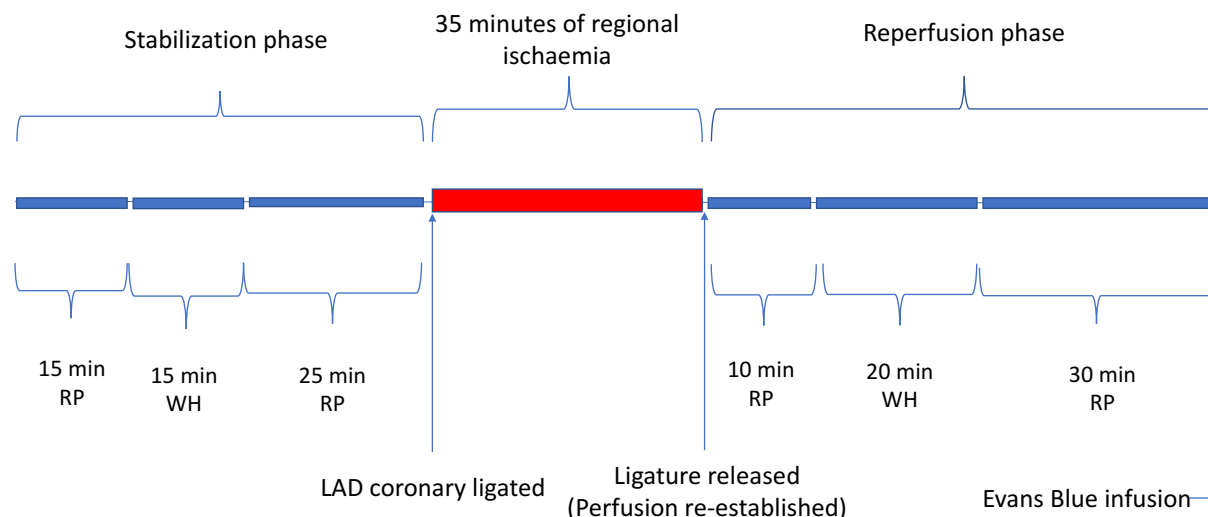


Figure 2.5 Regional ischaemia-reperfusion protocol. RP: retrograde perfusion, WH: working heart, LAD: left anterior descending coronary artery, Min: minutes.

At the end of the protocol, the silk suture was securely tied (to occlude the LADCA) and 0.5 - 0.8 millilitres of a 0.5% Evans blue ($C_{34}H_{24}N_6Na_4O_{14}S_4$, Sigma, St. Louis, USA) dye suspension was slowly injected via the aortic cannula. Thereafter, hearts were frozen overnight (in a closed container at $-10^{\circ}C$) before staining with 2,3,5 triphenyltetrazolium chloride (TTC, $C_{19}H_{15}ClN_4$; Merck (Pty) Ltd. Germany).

2.5.9 TTC staining and infarct size analysis

TTC staining salt solutions (Merck KGaA, Darmstadt, Germany) were prepared according to the protocol described below, (Bohl et al. 2009).

Preparation of staining solutions

Chemicals used:

-Solution I: 100mM $NaH_2PO_4 \cdot 2H_2O$ (15.6 g/L dH_2O)

-Solution II: 100mM Na_2HPO_4 (14.2 g/L dH_2O)

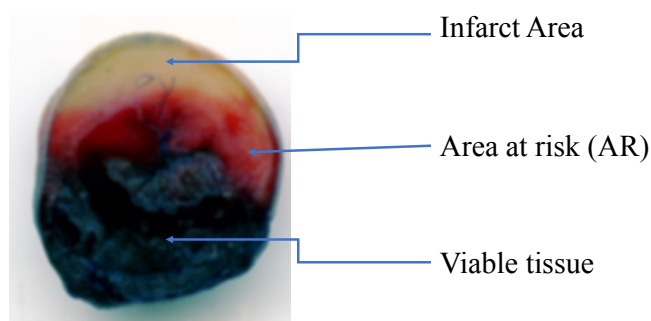
-2, 3, 5 -triphenyltetrazoliumchloride, $C_{19}H_{15}ClN_4$

The salt solution for staining was prepared by taking 20 ml of Solution I and 80 ml of Solution II mixed and pH set at 7.4.

To prepare TTC staining solution.

5 ml of this solution (Solution I and II) was placed in a tube and 0.05 g of tetrazolium salt added and covered in aluminum foil (light sensitive). This solution was used to stain one heart and therefore, the volume of the solution was prepared according to the number of hearts ready for staining.

Each frozen heart was cut transversely into 5-6 slices, each approximately 2 mm thick using a sharp blade and placed in a tube containing 5 ml of the above solution (0.05 g of TTC in buffer solution I and II) and shaken a few times during the 30 minutes of staining. The colour development was monitored (damaged, but not infarcted, tissues take on a deep red colouration whereas infarcted tissue areas are not stained and have a white colour) and at the end of 30 minutes, the salt solution was poured off and 4 % formaldehyde solution (24.3 ml/100 ml distilled water) was added and left to stand for an hour to fix the stain. Thereafter, the slices were placed between glass plates and images scanned for computerized planimetry. From these digital images, the areas were drawn and infarct size (pale), area at risk (bright red) and viable tissue (blue) were determined (Figure 2.6) using an image analysis software (Image Tool, *University of Texas, Health Science Centre, San Antonio Texas, UTHSCSA*). The infarcted area (infarct size) of the left ventricle (n = 8/group) was expressed as a percentage of the area at risk + infarct area as shown below, Figure 2.6.



$$\text{Infarct size (IS)} = \frac{\text{Infarct area}}{\text{Area at risk} + \text{Infarct area}} \times 100$$

Figure 2.6 Left ventricular transverse section following TTC staining. Infarct area (pale in colour), area at risk (AR, bright red) and viable tissue (deep blue) from a slice of heart tissue (lean control) stained with TTC after undergoing ischaemia reperfusion.

2.5.10 Cardiac haemodynamic performance data collection

As described in the protocols above, during the isolated working heart protocol, performance of the heart was monitored and data collected for analysis. Coronary (Q_e) and aortic (Q_a) flow rates in millilitre/minute (ml/min) were measured manually. These two parameters were used to calculate the total cardiac output (CO) by obtaining their sum ($Q_e + Q_a = \text{CO}$).

The aortic pressure (mmHg) was obtained through a side branch of the aortic cannula which was connected to a Viggo-spectramed pressure transducer. The peak systolic pressure (sp), diastolic pressure (dp) and heart rate (HR) were obtained from the recordings made by the computerized pressure transduction system. These measurements were recorded before (during stabilisation) and after ischaemia (during reperfusion).

Functional recovery of the hearts was determined by expressing post-ischaemic aortic output as a percentage of pre-ischaemic aortic output, n = 8 / group. Furthermore, total work (Wt) performance by the left ventricle

(calculated by the transduction system) was also recorded before and after ischaemia and percentage total work recovery determined. Other parameters recorded include, the maximal rate at which the left ventricle pressure rose (dp/dT max) and fell (dp/dT min), mean left ventricular power (TW, mWatts) and kinetic power (Wk).

2.5.11 Vascular reactivity, aortic ring studies

2.5.11.1 Harvesting of the aorta

After the thoracic cavity was rinsed with ice cold KHB to clear blood clots, the thoracic aorta was identified after meticulously dissecting out the other thoracic tissues. The proximal part of the aorta (the point where the heart was severed) was identified and using non-toothed tissue dissecting forceps, the peri-aortic tissue (fat) was gently held and the vessel was dissected out from the vertebral bed. The entire thoracic aorta was harvested and quickly placed in ice cold KHB in a 100-mm petri dish where all the perivascular adipose tissue (PVAT) was meticulously shaved off taking care not to damage the vascular wall and the endothelium. From here, a short segment of the aorta measuring 3.5 to 4 millimetres was cut out and mounted in an organ bath system.

2.5.11.2 The isometric tension measurement protocol

The vascular reactivity studies were conducted using an organ bath (25 mL) for the aortic ring segments (Powerlab 4/30 ADINSTRUMENTS: *Bella Vista, New South Wales, Australia*) and a tension transduction system, isometric force transducer (TRI202PAD, *Panlab, Cornellà, BCN, Spain*). The system has two horizontal stainless-steel hooks; the lower hook is stationary and the upper one is attached to a force-displacement transducer for measuring isometric tension. The output from the force transducer was recorded on a LabChart® 7 data acquisition and analysis software (*Dunedin, New Zealand*).

The technique was based on previously published protocols (Jespersen et al. 2015 and Privett et al. 2004). Before mounting the aortic rings, the organ bath and the string with attached steel hook were rinsed four times with boiled distilled water. The organ bath was filled up with fresh KHB, warmed to 36.5° C – 37° C and monitored with a thermometer probe. The buffer was gassed with 95% O₂/ 5% CO₂ at a steady flow and the system was calibrated. The aortic ring was mounted between the two horizontal stainless-steel hooks and tension kept minimal (< 0.2 g) just adequate to hold the tissue in place, otherwise too much tension would stretch and destroy the ring. The ring was left for 5 minutes before the tension was gradually increased to 0.5 g within 10 minutes. At this point the organ bath was drained and refilled cautiously with pre-warmed KHB. Thereafter the tension was increased to 1.5 g and buffer changed again at 20 minutes (Jespersen et al. 2015).

After 30 minutes of equilibration, the volume of the buffer was accurately measured to 25 mL because the drugs were administered into the bath and their concentrations were calculated based on a final volume of 25 mL. 100 nM of phenylephrine was added (2.5 µL of 1 mM phenylephrine stock) and the tissue was monitored until it achieved maximum contraction marked by a plateau (Figure 2.7) at which point 10 µM acetylcholine was added (25 µL of Stock A) (see Addendum C) and left to attain full relaxation. For a normal healthy rat, the aorta should achieve at least 70% relaxation following maximal contraction. The tissue bath was the rinsed

three times and refilled (25 ml) and aorta stabilised for 30 minutes at a tension of 1.5 g changing the buffer every 10 minutes.

Aortic ring contraction was induced by step-wise administration of cumulative doses of phenylephrine (100 nM; 300 nM; 500 nM; 800nM and 1 μ M) (Figure 2.7). These doses were administered into the bath solution in single boluses after maximal tension was reached for the previous dose. Following the injection of the last 1 μ M dose (highest concentration of phenylephrine), and the aorta ring attaining maximal cumulative tension, induction of relaxation was commenced by administration of increasing concentrations of acetylcholine (30nM, 100nM, 300 nM, 1 μ M and 10 μ M) (Figure 2.7). Similarly, successive doses were administered following maximal relaxation for the previous dose. The final relaxation following the last concentration of acetylcholine marked the end of the protocol. For the description of the drug doses and their concentrations (stock preparations) see Addendum C.

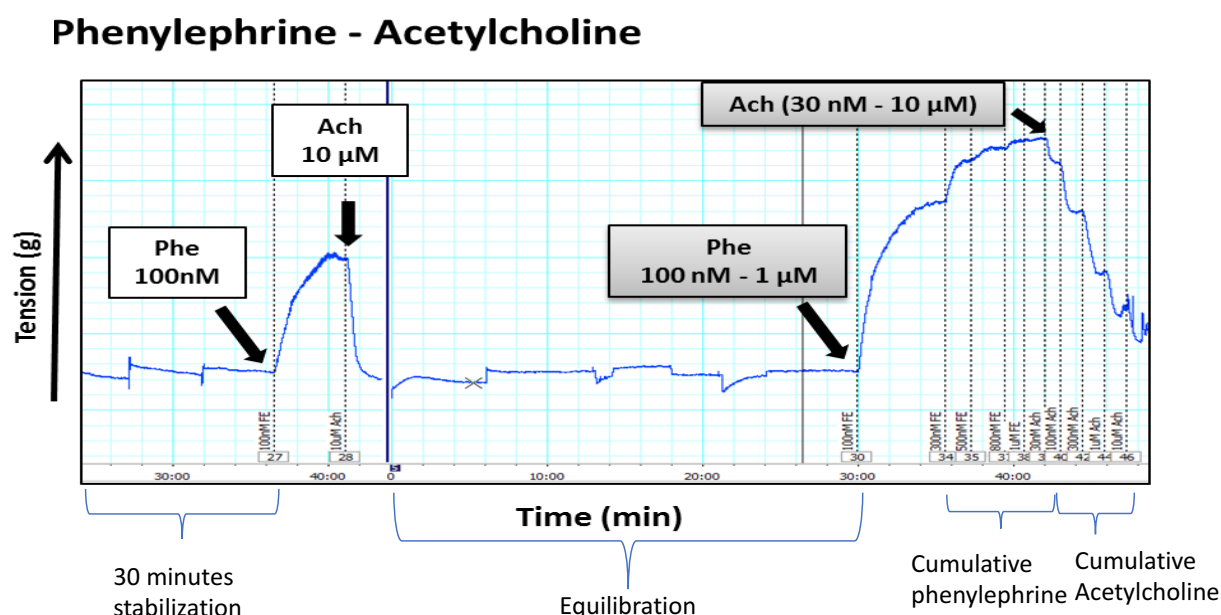


Figure 2.7 Recording showing the isometric tension protocol for aortic ring contraction and relaxation following administration of phenylephrine (Phe) and acetylcholine (Ach) respectively.

At the end of the protocol, the graph recording was saved and analysed for vascular contractility and relaxation. Contraction was expressed as percentage change in gram tension of the aortic ring per dose of phenylephrine whereas relaxation resulting from cumulative acetylcholine administrations was expressed as percentage relaxation of maximum phenylephrine-induced contraction.

To ascertain that acetylcholine-induced aortic ring relaxation via an endothelium and nitric oxide-dependent mechanism, another experiment was conducted using a non-selective inhibitor of nitric oxide synthase (Dodd-o et al. 1997), L-nitroarginine methyl ester (L-NAME) (EMD Chemicals, Inc. San Diego CA, USA an affiliate of Merck KGaA, Darmstadt, Germany). 250 μ L of 100 μ M of L-NAME was added to the 25 mL of KHB (to

make L-NAME concentration of 1 μM) 15 minutes prior to cumulative doses of phenylephrine and the effect was abolishment of acetylcholine mediated relaxation as shown below (Figure 2.8).

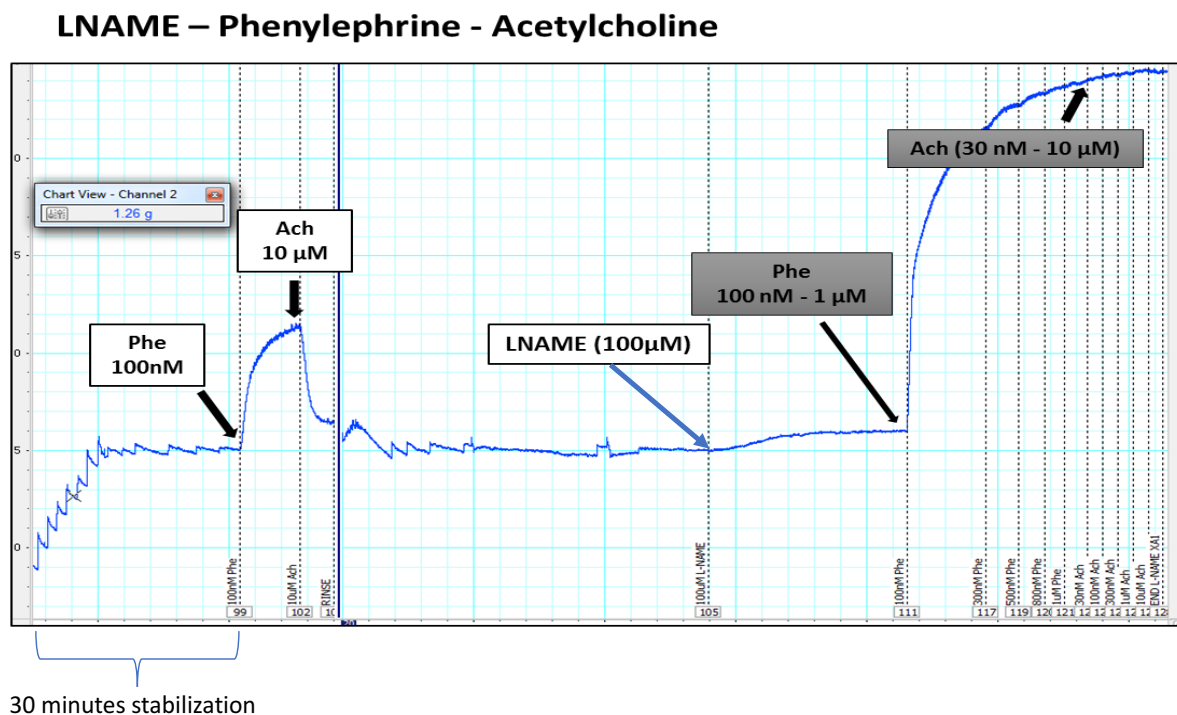


Figure 2.8 . Recording showing isometric tension measurement protocol using L-nitroarginine methyl ester (L-NAME), phenylephrine (Phe) and acetylcholine (Ach).

2.5.12 Analysis of fasted serum samples

The serum samples ($n = 8$ / group) were analysed in the Division of Chemical Pathology, University of Cape Town for lipid levels, fasting insulin and markers of lipid peroxidation/ oxidative stress; CD and TBARS.

HDL-C and its subclasses HDL₂ and HDL₃ ($\mu\text{mol} / \text{L}$) concentrations were analysed as per the protocol described by Gidez et al. (1982) whereby total HDL-C was separated from the APO-B lipoprotein through precipitation with sodium heparin-manganese chloride. Following this, HDL₂ was precipitated from the supernatant using dextran sulfate leaving HDL₃ in the supernatant. Consequently, HDL₂ concentrations were determined by subtracting the HDL₃ from HDL-C.

Serum TC and TGs concentrations (mmol/L) were assessed using enzymatic colorimetric kits (LabAssay™ Cholesterol (catalogue number 294-65801), LabAssay™ TG (catalogue number 290-63701), and PL (LabAssay™ Phospholipid (catalogue number 296-63801) (*Wako Chemicals, Germany*) using a SPECTRA-max Plus 384 spectrophotometer with SoftMax Pro 4.8 microplate data acquisition and analysis software (*Molecular Devices Corporation, Labotec Industrial Technologies, South Africa*).

CD concentrations ($\mu\text{mol} / \text{L}$) were calculated at absorbance of 234 nm following cyclohexane dilution as described by Esterbauer et al. (1989) and Pryor and Caste (1984). TBARS concentrations ($\mu\text{mol} / \text{L}$) were determined with spectrophotometry at an absorbance of 532 nm after addition of thiobarbituric acid reagent

(*Sigma-Aldrich, USA*) to a mixture of butylated hydroxytoluene (BHT) (*Fluka Chemie-Switzerland*), ethanol (*Merck, SA*) and orthophosphoric acid (*Sigma-Aldrich, USA*) (Jentzsch et al. 1996).

Fasting insulin levels were analysed using the RayBio® rat insulin enzyme linked immunosorbent assay kit (ELISA), (*RayBiotech, Norcross, USA*) as per the manufacturer's instructions and results were expressed in $\mu\text{IU/mL}$ and used to calculate the Homeostasis Model Assessment index for Insulin Resistance (HOMA-IR).

2.5.13 Protein expression and phosphorylation measurements - Western blot analysis

Protein immunoblot techniques were employed to detect proteins of interest and determine their expression and phosphorylation. Gel electrophoresis was used to separate proteins per their different molecular weights and transferred to a polyvinylidene fluoride (PVDF) membranes where they were probed / detected using specific antibodies.

The following proteins were analysed: -

Detection of total and phosphorylated proteins (to assess activation)	Detection of protein expression
-AMPK	- I κ B α
-eNOS	- PGC-1 α
-PKB/Akt	- PPAR-alpha
-Erk 1 / 2	- NADPH, P22-phox
-P38	- Caspase 3
	- Cleaved PARP

The tissues and specific proteins analysed (justification, see section 1.5) are summarised as follows: -

- i) Liver tissue (n = 8 / group): - Western blot analysis of (total and phosphorylated) proteins involved in hepatic oxidative stress (NADPH p22-phox), inflammatory/insulin signalling/ stress response (I κ B α , AMPK, ERK 1/2, PKB/Akt, p38), transcriptional control (PGC 1 α) and apoptosis (cleaved PARP and caspase 3).
- ii) Vascular (aorta) tissue (n = 8 / group): - Proteins involved in endothelial oxidative stress (NADPH p22-phox), inflammatory/ stress response (I κ B α , AMPK, ERK 1/2, PKB/Akt, p38), vascular tone (eNOS) and apoptosis (cleaved PARP and caspase 3).
- iii) Cardiac tissue: Baseline protein analysis using hearts harvested from fasted rats (n = 8 / group, these hearts were rinsed in ice cold KHB before they were snap frozen and stored at -80° C), and protein analysis following global ischaemia-reperfusion (n = 8 / group, as described in Figure 2.4): - Proteins involved in oxidative stress (NADPH p22-phox), response to ischaemia-reperfusion (I κ B α , AMPK, ERK 1/2, PKB/Akt, p38), transcriptional control (PGC 1 α) and apoptosis (cleaved PARP and caspase 3).

The protocol for the Western blot technique is described below.

2.5.13.1 Lysate preparation

To extract proteins from frozen liver, heart and aortic tissues, lysates were prepared through mechanical and enzymatic processes. First, lysis buffer was prepared using the ingredients listed below.

- Tris-Hydrochloric acid (Tris-HCl): pH buffer
- EDTA (ethylenediaminetetraacetic acid), $[\text{CH}_2\text{N}(\text{CH}_2\text{CO}_2\text{H})_2]_2$: it is used in lysis buffer as a protease inhibitor.
- EGTA (ethylene glycol tetraacetic acid): it is used in lysis buffer as a protease inhibitor.
- NaCl (Sodium chloride): increases osmolality to facilitate lysis and keeps proteins soluble
- β -glycerophosphate: non-specific phosphatase inhibitor
- Tetra-Na-Pirophosphate: non-specific phosphatase inhibitor
- Na_3VO_4 (sodium orthovanadate): it is an inhibitor of tyrosine phosphatases, alkaline phosphatases and a number of ATPases. The aim is to preserve the phosphorylation of proteins of interest by inhibiting endogenous phosphatases present in cell lysate mixture.
- Triton X-100: is a non-ionic surfactant that breaks protein-protein bonds maintained by means of Van Der Waals forces.
- Leupeptin: protease inhibitor.
- Aprotinin: inhibits serine proteases.
- PMSF (phenylmethanesulphonylfluoride or phenylmethylsulphonyl fluoride): irreversible serine protease inhibitor.
- SDS (sodium dodecyl sulphate): dissociating agent that denatures proteins to individual polypeptides.

From the above ingredients, the lysis buffer for liver and heart tissues was prepared per the concentrations and volumes shown below, Table 2.3.

Table 2.3 showing different components used in preparation of lysis buffer. For abbreviations, see section 2.5.13.1.

	Stock	10 ml	20 ml	30 ml	50 ml
20 mM Tris-HCl 1 mM EGTA	200 mM 10mM	1 ml	2 ml	3 ml	
1 mM EDTA	100 mM	100 µl	200 µl	300 µl	500 µl
150 mM NaCl	1 M	1.5 ml	3 ml	4.5 ml	7.5 ml
1 mM β-glycerophosphate		0.002g	0.004g	0.006g	0.01g
2.5 mM tetra-Na-Pirophosphate		0.01g	0.02g	0.03g	0.05g
1 mM Na ₃ VO ₄ (0.018g/10ml)	10 mM	1 ml	2 ml	3 ml	5 ml
* 50 µg/ml PMSF	100 mM	30 µl	60 µl	90 µl	150 µl
10 µg/ml Leupeptin		10 µl	20 µl	30 µl	50 µl
10 µg/ml Aprotinin		10 µl	20 µl	30 µl	50 µl
1% Triton X-100	10%	1 ml	2 ml	3 ml	5 ml

For preparation of aortic tissue lysis buffer, 50 nM (0.0213 g/ 10 ml of buffer solution) of sodium fluoride (NaF) and 0.1% of sodium dodecyl sulphate (SDS) was added to the above chemicals. After preparation of the lysis buffer, 700 µL was transferred in 2 ml Eppendorf tubes for each sample tissue and kept in ice.

2.5.13.2 Tissue homogenisation

From each frozen tissue sample, a small piece was obtained and pulverized using a liquid nitrogen-precooled mortar and pestle. Subsequently 55-65 mg of the pulverized powder was mixed into the 700 µL lysis buffer to which seven stainless-steel beads (SSB16, 1.6 mm in diameter; 1 lb.) (*Next Advance, USA*) were added and then homogenised using the bullet blenderTM (*Next advance, USA*) at 4 °C. The bullet blender was set at homogenisation power of eight and one-minute duration for three cycles with five-minute intervals between the cycles. The homogenised samples were left to set for 20 minutes before centrifugation for 20 minutes at 15,000 revolutions per minute (rpm) or 12074 x g (*Sigma Laborzentrifugen, type 1-4 K, Germany*). Thereafter, the supernatant was transferred to Eppendorf tubes and maintained on ice before the Bradford assay was performed.

2.5.13.3 Bradford protein assay (BPA)

The Bradford assay (Bradford, 1976) was used to determine protein concentration in the supernatant. Bradford stock was prepared by dissolving 500 mg coomassie brilliant blue in 250 ml 95 % ethanol; 500 ml phosphoric acid was added and the final volume made up to 1L with distilled water and mixed. From this stock, Bradford solution was prepared by diluting 1:10 with distilled water and filtered twice using Wathman filter papers (0.4 µm pores).

10 μL of each sample supernatant was added to 90 μL of distilled water into sorval tubes to prepare the first 10 times dilution. From the 10 X diluted set, another 10 μL volume was drawn and added to another set of duplicate tubes with 90 μL of distilled water for the second 10 x dilution.

To prepare standards, 100 μL Bovine serum albumin (BSA) of known concentration (5 mg/ ml) was diluted five times (400 μL of distilled water was added) and prepared in increasing concentrations and 900 μL of Bradford solution added as shown below (Table 2.4).

Table 2.4 Bovine serum albumin, (BSA) standard concentrations for BPA.

BSA concentration ($\mu\text{g/ml}$)	BSA Volume (μL)	Distilled water Volume (μL)	Bradford Solution (μL)
0	0 (blank)	100	900
1.25	5	95	900
2.5	10	90	900
5	20	80	900
10	40	60	900
15	60	40	900
20	80	20	900

900 μL of Bradford solution was added also to the duplicate set of diluted samples and mixed (using a vortex) and left to stand for 15 minutes before absorbance at wavelength of 595 nm was measured using a spectrophotometer (Cat. 4001/4, *Spectronic Instruments, USA*). From the absorbance, protein concentrations were calculated against the BSA standard curve (absorbance against concentration) using the equation $y = mx + c$.

From the above concentrations, the volume of supernatant to load was calculated against a standard concentration and total volume of 40 μg / 12 μL loaded in each agar gel well. One third of the volume of lysates was composed of the Laemmli sample buffer (62.5mM Tris-HCl (pH 6.8), 4 % SDS and 10 % glycerol, 0.03 % bromophenol blue and 5 % β -mercaptoethanol) and the volume difference was topped up with the lysis buffer. For liver and cardiac tissues, a protein concentration of 40 μg was calculated and 12 μL of volume loaded whereas for aorta tissue, 20 μg of protein at 15 μL was loaded per well since the protein concentration was low. The prepared lysate samples were boiled in a water bath for five minutes to denature proteins and were preserved at -80 $^{\circ}\text{C}$.

2.5.13.4 Protein separation by gel electrophoresis

The frozen lysates were boiled again for four minutes and centrifuged for five minutes before proteins were separated by sodium dodecyl sulphate polyacrylamide gel electrophoresis (SDS-PAGE). 10 % loading gel and 4 % stacking gel were prepared using the chemicals and concentrations shown below (Table 2.5).

Table 2.5 showing preparation of running and stacking gels for PAGE. (Tris- HCl: Tris hydrochloric acid, SDS: Sodium Dodecyl Sulphate, APS: Ammonium persulphate, TEMED: 1,2 Bis (dimethylamino) ethane – N’N’N’N-tetramethylethylenediamine, Stain free: 2,2,2-trichloroethanol, from Sigma-Aldrich (St. Louis, MO, USA).

Reagent	Running gel		Stacking gel	
	Stock	10 % running gel	Stock	4 % stacking gel
Millipore water	-	4.85 mL	-	3.05 mL
Stain free	99 %	50 µL	-	-
Tris-HCl (pH 8.8)	1.5 M	2.5 mL	0.5 M	1.25 mL
SDS	10 %	100 µL	10 %	50 µL
Acrylamide	40 %	2.5 mL	40 %	500 µL
APS	10 %	50 µL	10 %	50 µL
TEMED	99 %	20 µL	99 %	10 µL

Using the Bio-Rad Mini Gel Protean System (*BIO-RAD laboratories, USA*) the running gel was then cast between two glass plates 0.75 mm and left for 20-30 minutes to set before adding the stacking gel on top and applying the plastic combs for setting the 15 wells needed for sample loading. The gel was left for 10-15 minutes to set before transfer into a protean system U-shaped core latch and filled with transfer buffer where the combs were carefully taken out filling the wells with the buffer to prevent them from collapsing. The set up was then placed in a tank and samples were loaded into the wells.

The first well was loaded with five µL pre-stained protein ladder (molecular weight marker) (*Thermo Scientific, Lithuania, European Union*). Thereafter, the samples were loaded, starting with the control sample and subsequent experimental samples (n = 3 / group). The running buffer (composed of 250 mM Tris, 190mM glycine and 1 % sodium dodecyl sulphate) was added to the outer compartment and the system connected to electrodes (matching the anode to anode and cathode to cathode) and set to run at 100 V, 200 mA for 10 minutes and then 200 V, 200mA for 50 minutes. After the protein separation / gel electrophoresis was complete, the proteins were transferred to a membrane.

2.5.13.5 Gel to PVDF membrane protein transfer

A Millipore transfer membrane / polyvinylidene fluoride (PVDF) microporous membrane (*Immobilon®-P Merck KGaA, Darmstadt, Germany*) was used to bind proteins from the gel through a transfer system. The membrane was cut to an appropriate size and was first soaked in methanol for 3 minutes and equilibrated in the transfer buffer (25m Tris-HCl, 192 mM glycine and 20% v/v methanol) for 15 minutes before the protein transfer was commenced. Thereafter, the gel was placed on top of a stack of two blotting papers and a sponge (presoaked in the transfer buffer) and the PVDF membrane was placed on top of the gel and rolled gently to

ensure that no air bubbles were trapped in between. Two blotting papers were placed on top of the membrane and another presoaked sponge on top and the sandwich was secured in the transfer cassette.

The cassette was placed in the transfer tank (filled with the transfer buffer) and an ice pack placed behind the cassette to ensure that the transfer was at approximately $< 10^{\circ}\text{C}$. The system was connected to electrophoresis power supply (*Amersham pharmacia biotech, Cape Town, South Africa*) and transfer was set at 200 V and 200 mA for an hour. Following this, the membrane was retrieved and placed in methanol for 30 seconds and visualized using the ChemidocTM (Bio-Rad) imaging system to confirm that the transfer was successful. The image was captured and saved using the ImageLabTM 5.2.1 image acquisition and analysis software (*BIO-RAD Inc. Hercules, California, U.S.A*) for subsequent normalisation of the blots.

The membranes were washed using 0.1% Tween® 20 in Tris buffered saline (TBS Tween) three times and non-specific protein binding sites were blocked with 5 % fat free milk (5 mL / 100 mL TBS tween) for two hours on a gentle shaker. Subsequently, they were washed three times (washing in intervals of five minutes while shaking them gently) before incubation with the primary antibody.

2.5.13.6 Primary and secondary antibody incubation

The membranes were incubated in primary antibody specific for the antigen of interest at 4°C for 10-14 hours under gentle agitation. The antibodies were diluted as per the manufacturer's instructions at a ratio of 1:1000 (5 μL of primary antibody to 5000 μL TBS-Tween). However, eNOS and PGC-1 α primary and secondary antibodies were diluted in signal boost (Cat:KP31812, *EMD Millipore Corp., Billerica, MA USA*), (see Addendum D for the list of all antibodies and their dilutions).

After primary incubation period, the membranes were washed to get rid of unbound primary antibody and incubated for one hour (room temperatures) with a horseradish peroxidase-linked anti-rabbit secondary antibody (*AEC Amersham, Buckinghamshire, United Kingdom*) (1:4000 TBS-tween). After the incubation, the membranes were washed in TBS-Tween for 15 minutes under gentle agitation before incubation with enhanced chemiluminescence (ECL) agent (*AEC Amersham, Buckinghamshire, United Kingdom*) for 5 minutes. The principle is that the anti-rabbit antibody binds to the primary antibody and since it is linked to horseradish peroxidase, when exposed to a chemiluminescent agent the reaction produces luminescence in proportion to the amount of protein. The emitted light can then be captured by a camera for qualitative and quantitative analysis.

After the incubation with ECL, the membranes were transferred to the ChemidocTM (*Bio-Rad*) imaging system and images were captured using the ImageLabTM 5.2.1 image acquisition and analysis software. The images were saved and the corresponding images with total proteins were used for normalisation.

2.5.13.7 Normalisation and analysis

To quantify the amount of specific protein contained in each Chemi-Hi blot, the images captured after ECL exposure were compared to the total stain free membranes, total lane protein – stain free blot and all the

corresponding columns were normalised using ImageLab™ 5.2.1 image analyser. Therefore, there was no need for the use of a house keeping antibody to control for equal protein loading since every protein blot was controlled by the corresponding total stain free blot lane as shown in Figure 2.9 below. The software detects bands and calculates normalisation volume intensities for each band using a normalisation factor (control). The normalised volume intensities were then recorded for analysis and interpretation. The normalised volume intensity for the control/ standard column was set as one (1) and all the other intensities were calculated relative to it. Subsequently, the mean \pm SEM (densitometry units) per group were analysed.

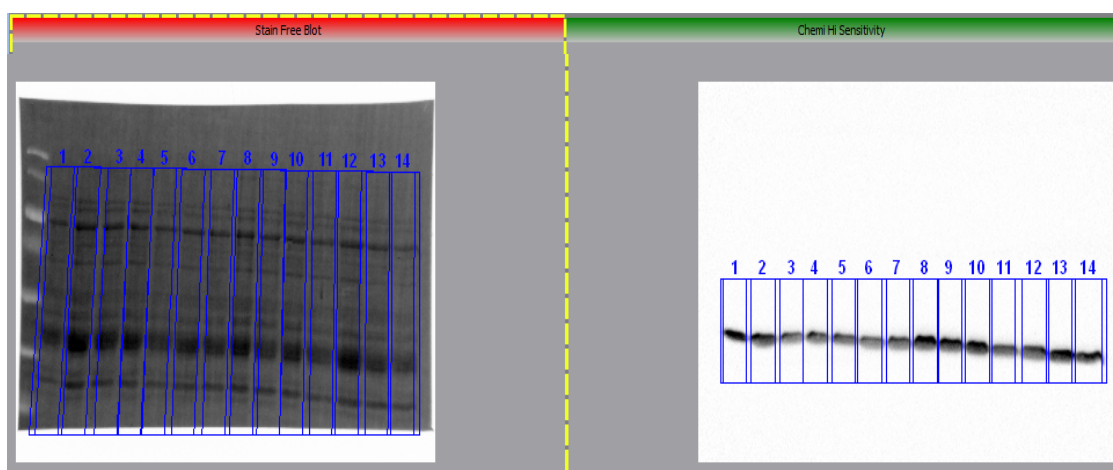


Figure 2.9 showing the normalisation of the 'Chemi Hi sensitive blots' to the 'total lane protein-Stain free blot' using ImageLab™ 5.2.1 image analyser. The generated normalised volume intensities were analysed for interpretation.

2.5.14 Liver tissue histology

Liver samples were harvested and one set was preserved in 10 % buffered neutral formaldehyde for standard haematoxylin and eosin (H & E) staining procedures and the other was snap frozen for preparation of frozen sections for oil red O (ORO) staining. The aim of the H & E staining was for hepatic morphological characterization where the cell nucleus stains blue (haematoxylin) and the cytoplasm stains pink (eosin).

Below is a description of how the tissues were prepared, stained and the analyses interpreted.

2.5.14.1 Tissue collection and fixation

Liver tissues were collected immediately after the rats were euthanised and two samples were obtained for histological purposes. One set of samples (n = 12 / group) was fixed in 10 % buffered formaldehyde to prevent tissue degradation because of putrefaction and retain tissue structure. They were retained in the formalin solution for a minimum of two days for complete fixation. These tissues were processed for H&E staining.

2.5.14.2 Tissue processing

The fixed tissues were sectioned into smaller pieces, placed in embedding cassettes and clearly labelled. They were processed using an automated processing system (*Duplex processor, Shandon Elliot; Optolabor (Pty) Ltd, Johannesburg, South Africa*) where they were then dehydrated using increasing concentrations of alcohol, cleared with xylene and infiltrated with paraffin wax as shown in Table 2.6 below.

Table 2.6 showing the standard processing protocol for H & E staining.

Step	Solution	Time (min)	Temperature (°C)
1	10% Formalin	30	Room Temperature
2	70% Ethanol	30	Room Temperature
3	96% Ethanol	30	Room Temperature
4	96% Ethanol	30	Room Temperature
5	99.9% Ethanol	30	Room Temperature
6	99.9% Ethanol	30	Room Temperature
7	99.9% Ethanol	30	Room Temperature
8	Xylene	30	Room Temperature
9	Xylene	30	Room Temperature
10	Paraffin	60	60
11	Paraffin	60	60
12	Paraffin	60	60

2.5.14.3 Embedding

After the tissues sections were processed, they were embedded in paraffin wax at 60 °C using Leica EG 1160 embedder (*Leica Biosystems, Germany; supplied by SIMM Instruments (Pty) Ltd, Cape Town, South Africa*). The wax mold was placed on an iced surface for it to set and subsequently stored at temperatures ranging from 20-25 °C before sectioning.

2.5.14.4 Tissue block sectioning

Using a Leica RM 2125 RT microtome, (*Leica Biosystems, Germany; supplied by SIMM Instruments (Pty) Ltd, Cape Town, South Africa*), uniform sections of 5 µm in thickness were sectioned from pre-cooled blocks and thereafter, sections were warmed in a water bath (40 °C) for the tissues to stretch before transferring on glass slides.

2.5.14.5 Staining

The slides were incubated at 60 °C for 2 minutes for the wax to melt before they were stained. Eosin solution and filtered haematoxylin solutions were placed into the automated stainer, Leica Auto Stainer XL (*Leica*

Biosystems, Germany; supplied by SIMM Instruments (Pty) Ltd, Cape Town, South Africa). See Table 2.7 below for the protocol.

Table 2.7 showing a standard H & E protocol.

Step	Solution	Time	Repetitions
1	Oven (60°C)	2 min	Once
2	Xylene	5 min	Twice
3	Ethanol (99%)	2 min	Twice
4	Ethanol (96%)	2 min	Once
5	Ethanol (70%)	2 min	Once
6	Tap water	2 min	Once
7	Haematoxylin	8 min	Once
8	Running water	5 min	Once
9	Eosin	4 min	Once
10	Running water	1 min	Once
11	Ethanol (70%)	30 sec	Once
12	Ethanol (96%)	30 sec	Twice
13	Ethanol (99%)	30 sec	Once
14	Xylene	1 min	Once

2.5.14.6 Mounting

To improve the visual quality of the slide under a microscope, DPX mountant (*Sigma-Aldrich, USA*) was used to apply the glass cover slip on the stained liver sections and left to dry at room temperatures for two days before light microscopy analysis.

2.5.14.7 Oil red O (ORO) staining

Another set of liver tissues was snap frozen and preserved in liquid nitrogen for ORO staining. The aim of staining with ORO is to stain fats/lipids within the liver tissue and characterise the hepatic fat infiltration. ORO (xylene-azo-xylene-azo- β -naphthol) stains neutral lipids giving them an orange-red tint and the stain is more stable when mixed with an isopropanol solution (Lillie 1944).

The tissues were sectioned into smaller pieces and embedded on tissue freezing medium using a Leica CM1850 UV Cryostat, microtome (*Leica Biosystems, Germany; supplied by SIMM Instruments (Pty) Ltd, Cape Town, South Africa*), they were trimmed and sectioned to obtain uniform 12 μ m thick sections. The trimming and sectioning was done at temperatures of $-14\text{ }^{\circ}\text{C} \pm 2\text{ }^{\circ}\text{C}$ to prevent tissues from drying. The sections were transferred on to positively charged, coated polylysine 1.1 mm-thick microscope slides. The slides were left to set for 30 minutes at room temperatures before staining. The stain was prepared as shown below using ORO isopropyl solution and dextrin solution.

Oil red O (ORO) solution

ORO (<i>Sigma-Aldrich</i>)	0.9 g
Absolute isopropyl alcohol	180 mL

Stirred and left overnight

Dextrin Solution

Dextrin (<i>Sigma-Aldrich</i>)	1.2 g
Distilled water	120 mL

Working solution

ORO solution	180 mL
Dextrin solution	120 mL

Allowed to stand for a day and filtered before use

Preparation of ORO-Dextrin solution.

The slides were placed directly into the filtered 0.5 % ORO in dextrin and stained for 20 minutes before rinsing with running water. Following this, they were counterstained with 0.25 % crystal violet (*Kimix chemicals, South Africa*), rinsed with running water and a coverslip was mounted using an aqueous mounting medium (*Sigma-Aldrich, USA*). This is a modified protocol from the original description of ORO in haematoxylin (Lillie and Ashburn 1943) because we observed that the haematoxylin counterstain faded faster and after application of the mounting medium the nucleus could not be characterised.

2.5.14.8 Immunohistochemistry

Liver sections were also prepared for immunohistochemistry. The tissues sections were probed using anti-placental rabbit glutathione S transferase (GST-P) antibody (standard immunohistochemical staining process for paraffin embedded sections) (Shi et al. 2007) and counterstained with haematoxylin before mounting for subsequent microscopic assessment to identify presence / absence of GST-P- positive foci.

2.5.14.9 Microscopy

Standard light microscopy techniques were used to assess the morphology and severity of fatty changes (steatosis). The degree of steatosis was determined by estimating the proportion of hepatocytes containing fat droplets per medium power field; <1 / 3 mild, 1 / 3–2 / 3 moderate and >2 / 3 severe, (n = 12 / group). The morphology of the hepatocytes was assessed for any inflammatory, fibrotic and or necrotic changes. Nonalcoholic steatohepatitis (NASH) was defined as the presence of hepatic fat infiltration and inflammation with hepatocyte ballooning (indicator of hepatocyte injury) with or without fibrosis (Chalasani et al. 2012).

A scoring criteria system for NASH was developed by adopting the key features described in the clinical NASH diagnostic criteria based on liver histology (Kleiner et al. 2005) as shown below (Table 2.8). The microscopic evaluation was done by three blinded scorers and results interpreted accordingly. A score of 0 and 2 denoted no steatohepatitis, and borderline steatohepatitis, respectively, whereas a score of 3 revealed definite steatohepatitis.

Table 2.8 showing the histological features assessed during histological evaluation of NAFLD for the liver H & E and ORO stained liver sections and the scoring criteria used.

Microscopic feature	Definition	score
Steatosis	Parenchymal involvement by Steatosis	
	< 5 %	0
	5 – 33 %	1
	33 – 66 %	2
	> 66 %	3
Microvesicular steatosis	Contiguous patches	
	Absent	0
	Present	1
Fibrosis	None	0
	Present	1/2
Inflammation	No foci	0
	< 2 foci/ 200 x field	1
	2-4 foci/ 200 x field	2
	> 4 foci/ 200 x field	3
Liver cell ballooning	None	0
	Few Balloon cells	1
	Prominent ballooning	2
Pigmented macrophages/Meganeucleus/ glycogenated nuclei	none	0
	many	1

2.6 Data management and statistical analysis

Results were expressed as mean \pm standard error of the mean (SEM); for multiple group comparisons, one-way analysis of variance (ANOVA) was used (GraphPad Prism® Plus Version 6.0) and post-hoc testing for differences between selected groups was done using Bonferroni's method. A p-value of <0.05 was considered statistically significant.

Vascular reactivity data were analysed using two-way analysis of variance (two-way ANOVA) and Bonferroni's post-hoc test. Relaxation response data were log transformed and phenylephrine mediated vascular contractility was analysed as tension (g) against the dose concentrations. The EC₅₀ (the drug concentration inducing 50% of the maximal response, was determined by nonlinear regression model analysis following the log X (dose) vs. response transformation of the percentage relaxation (%) or tension (g) using an 'agonist-dose-response-curve' and results were expressed as mean \pm SEM of the EC₅₀.

Statistical analysis was done in consultation with a statistician from the Biostatistics Unit, Stellenbosch University.

The subsequent chapter, (chapter 3), presents the results obtained after undertaking all the activities described above.

Chapter 3 : Results

3.1 Introduction

Following the introduction of the high calorie diet (HCD) and / standard (lean) diet and subsequent drug treatment, the findings of this randomised controlled experimental study will be based on the categorization of the eight experimental groups treated with vehicle (control), HAART ((Highly Active Antiretroviral Therapy), comprised of LPV/r (LPV boosted with ritonavir) + AZT (Azidothymidine) and 3TC (Lamivudine)), HAART + Saroglitazar and Saroglitazar (Table 3.1). The results are presented as follows: feeding / treatment monitoring parameters, biometric data recorded after the animals were sacrificed, blood and serum analyses, cardiac perfusion and infarct size analyses, liver investigations, aortic reactivity studies and signalling studies from the three tissue types (heart, liver and aorta) as outlined below (Table 3.2).

Table 3.1 Experimental groups treated with vehicle (control), HAART (highly active antiretroviral therapy): LPV/r (LPV boosted with Ritonavir), AZT (Azidothymidine / Zidovudine), 3TC (Lamivudine) and dual PPAR α/γ agonist, Saroglitazar.

Standard rat diet / normal rat chow (lean)	High calorie diet (HCD)
1) Lean control	2) HCD control
3) Lean HAART	4) HCD HAART
5) Lean HAART + Saroglitazar	6) HCD HAART + Saroglitazar
7) Lean Saroglitazar	8) HCD Saroglitazar

Table 3.2 Results will be reported based on the following outline.

Results Layout			
Rat treatment and feeding program monitoring parameters			
a) Weight at onset of study			
b) Food intake		-Rat chow (g/rat/day)	
		-HCD (g/rat/day)	
		-Water intake (mL/rat/day)	
c) Weekly total body weight monitoring (g)			
Biometric data after sacrificing the rats			
a) Total body weight (g)			
b) Intraperitoneal fat mass (mg)			
c) Heart mass		- Total heart mass (mg)	
		- Heart mass normalized by tibial length (mg/mm)	
d) Liver mass (mg)			
Blood and serum parameters			
a) Spot tail prick		- Random blood sugar (mmol/L)	
		- Fasting blood sugar (mmol/L)	
b) Fasted rat serum	- Lipid profile	- TC	
		- HDL-C, - HDL ₂ and - HDL ₃	
		- Phospholipids (PL)	
		- Triglycerides (TGs)	
		- Lipid peroxidation markers	
		- Conjugated Dienes (CD) - TBARS	
c) Non-fasted rat serum	-Liver enzymes	- S-ALT	- S-LD - S-AST - S-GGT - S-ALP
Cardiac parameters			
a) Isolated working heart model functional data		- Baseline functional parameters - Functional recovery post ischemia	
b) Infarct size analysis			
c) Signaling proteins analysis			
Aortic study parameters			
a) Vascular reactivity studies		- Contractility	
		- Relaxation	
b) Signaling proteins analysis			
Liver studies			
a) Histological data			
b) Signaling proteins analysis			

3.2 Feeding and treatment programme: - food and water consumption monitoring

Although the animals were group-housed (5 rats/ cage), data on food and water consumption are presented as g/rat/day (food) and mL/rat/day (water) because the number of rats in several cages reduced after onset of treatment. This was as a result of random deaths (see Addendum E) associated with gavaging-related complications and therefore the ideal cage comparisons were not feasible.

3.2.1 Standard rat chow

Consumption of standard rat chow was monitored daily during weeks 9 and 10 before the introduction of the drug treatment, and monitoring continued for a further 4 weeks during the treatment phase. HCD groups consumed significantly less chow compared to the lean groups throughout the feeding and drug treatment programme. Before onset of treatment, the mean standard rat chow consumption of the lean group was significantly higher compared to HCD group (15.75 ± 0.22 g/rat/day and 0.64 ± 0.03 g/rat/day respectively, $p < 0.0001$; $n = 88$ / group (Figure 3.1). Similarly, this trend continued throughout the first month of drug treatment. On average, all the lean treated groups consumed significantly more rat chow compared to the average mass of rat chow consumed by the HCD groups during treatment period (15.66 ± 0.22 g/rat/day and 0.59 ± 0.03 g/rat/day respectively, $p < 0.0001$; $n = 22$ / group) (Figure 3.2).

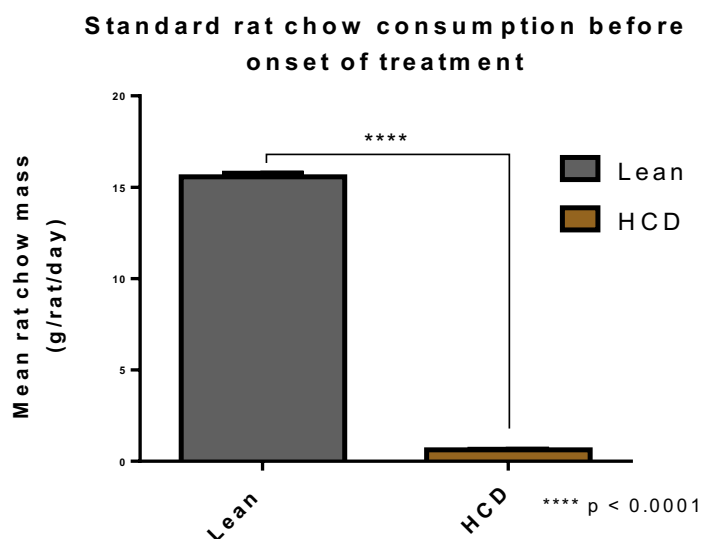


Figure 3.1 Mean standard rat chow consumption (g/rat/day) between lean and HCD groups before onset of drug treatment.

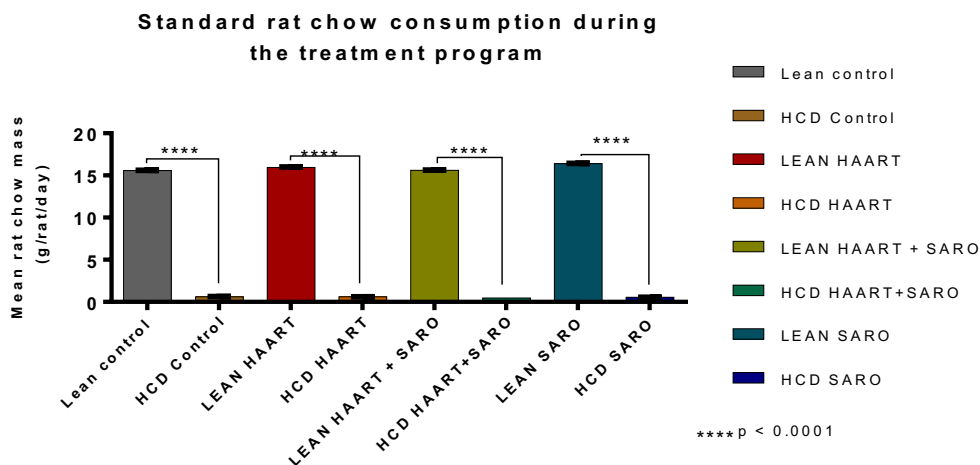


Figure 3.2 Comparison of mean standard rat chow consumption between lean and HCD groups during the first four weeks of drug treatment.

The trend in the mass of standard rat chow consumption remained constant in all the experimental groups (lean and HCD groups) before and during treatment. Lean control: 15.7 ± 0.20 g/rat/day, Lean HAART: 15.96 ± 0.18 g/rat/day, Lean HAART + Saro: 16.61 ± 0.18 g/rat/day, Lean Saro: 16.42 ± 0.13 g/rat/day. All the HCD groups significantly consumed less amount of chow (HCD control: 0.62 ± 0.03 g/rat/day, HCD HAART 0.58 ± 0.04 g/rat/day, HCD HAART + Saro 0.47 ± 0.02 g/rat/day, HCD Saro 0.54 ± 0.02 g/rat/day) compared to the lean groups p < 0.0001, n = 22 / group (Figure 3.3).

However, there was a slight drop in the amount of chow consumed in all the groups (16.4 ± 1.6 % g/rat/day – 19.3 % ± 1.8 % g/rat/day) after onset of treatment via oral gavage (shown using an arrow, Figure 3.3). This drop was only sustained for 3 - 5 days and study animals reverted to their pre-treatment mass of standard rat chow consumed.

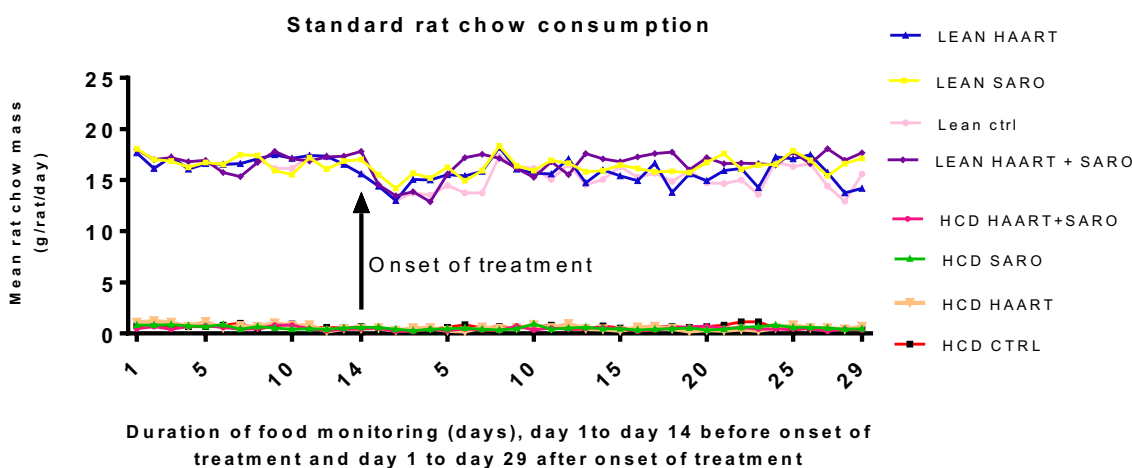


Figure 3.3 Trend of mean rat chow consumption (g/rat/day) / experimental group two weeks before onset of drug treatment and during the first four weeks of treatment.

3.2.2 HCD consumption

There were no differences in the mean mass of HCD consumed by each rat per day in the various groups for the first 28 days of the treatment programme, HCD control: 32.29 ± 0.35 g/rat/day, HCD HAART 33.42 ± 0.32 g/rat/day, HCD HAART + Saro: 32.23 ± 0.47 g/rat/day, HCD Saro 31.43 ± 0.45 g/rat/day, $n = 22$ / group (Figure 3.4).

The trend in the mass of the HCD consumption remained constant in all the experimental groups (HCD HAART, HCD HAART + Saroglitazar and HCD control) before and during treatment. However, there was a slight drop in the mass consumed in all the groups ($\downarrow 22.3 \pm 2.2$ %) after onset of treatment via oral gavage (shown using an arrow, Figure 3.5). This drop was only sustained for 5 days and study animals reverted to their pre-treatment HCD mass.

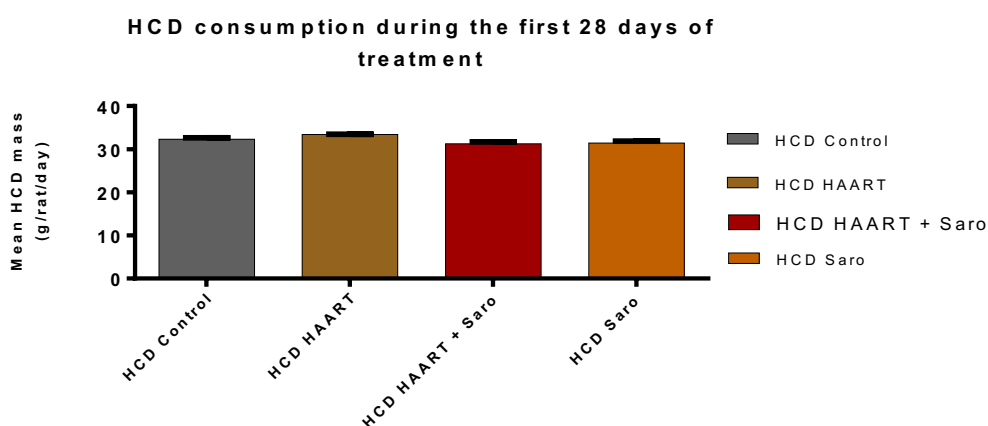


Figure 3.4 Mean HCD consumption (g/rat/day) per experimental group during the first four weeks of treatment.

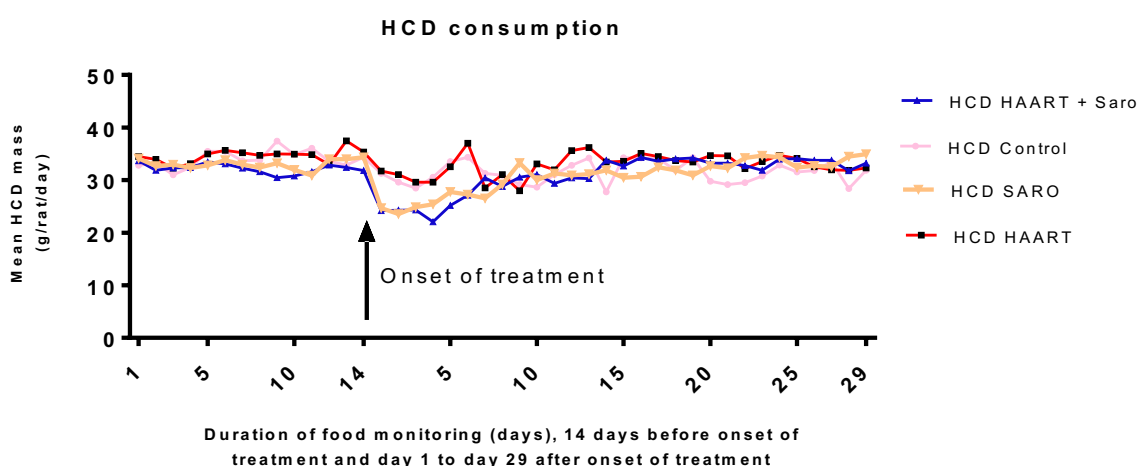


Figure 3.5 Trend of mean HCD consumption (g/rat/day) / experimental group two weeks before onset of drug treatment and during the first four weeks of treatment.

3.2.3 Water consumption

Water intake of all the experimental animals was monitored daily for two weeks before onset of treatment and for four weeks during the treatment phase. Before onset of treatment, the lean group consumed more water compared to HCD group, 29.88 ± 0.27 mL/rat/day vs. 14.03 ± 0.21 mL/rat/day respectively, $p < 0.0001$; $n = 88$ / group (Figure 3.6). Similarly, during treatment, the average water consumption per rat per day was higher for the lean treated groups compared to their respective HCD groups. Lean control: 28.18 ± 0.31 mL/rat/day vs. HCD control: 12.52 ± 0.24 mL/rat/day, lean HAART: 29.04 ± 0.40 mL/rat/day vs. HCD HAART: 13.68 ± 0.19 mL/rat/day, lean HAART + Saro: 30.22 ± 0.23 mL/rat/day, vs. HCD HAART + Saro: 14.30 ± 0.21 mL/rat/day, lean Saro: 29.88 ± 0.27 mL/rat/day, vs. HFD Saro: 14.72 ± 0.24 mL/rat/day; $n = 22$ rats / group, $p < 0.0001$ in all groups compared; $n = 22$ / group (Figure 3.7).

However, there were no differences in the volume of water consumed between the respective lean groups and similarly all the HCD groups consumed equal volumes of water (Figure 3.8).

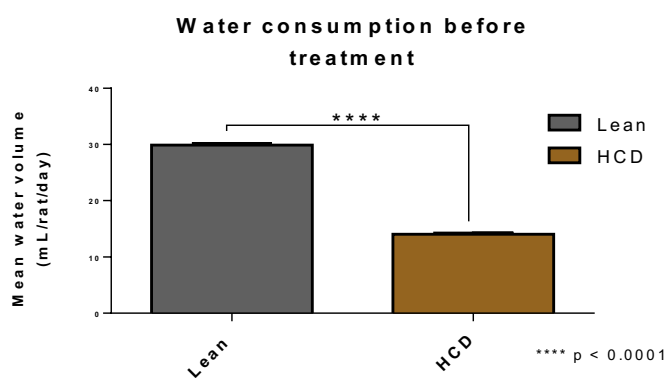


Figure 3.6 Mean volume of water consumption (mL/rat/day) / experimental group before onset of drug treatment.

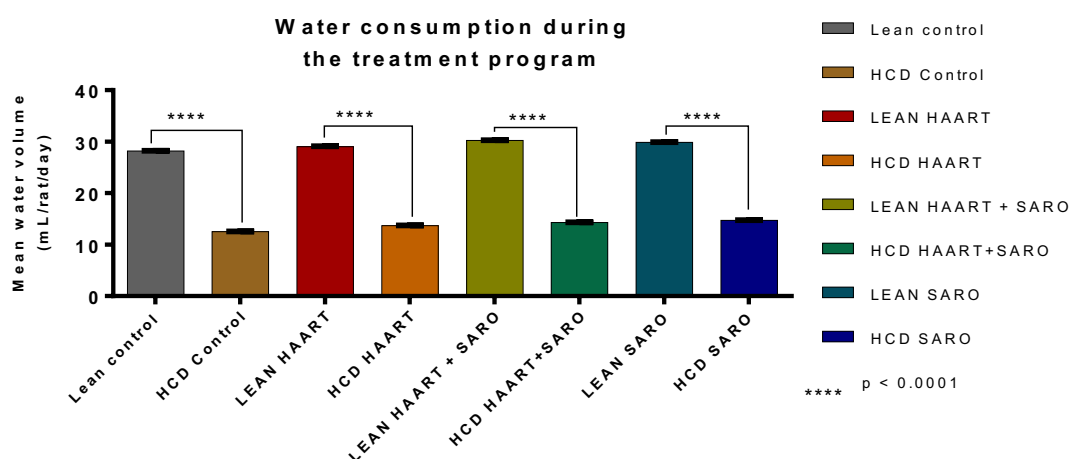


Figure 3.7 Mean volume of water consumption (mL/rat/day) / experimental group during the drug treatment programme.

On average, HCD groups consumed significantly less water ($\downarrow 48.2 \pm 1.8 \%$) compared to the lean rats. Additionally, the slight drop observed in the food consumption after onset of treatment was evident too in the volume of water consumed in all experimental groups. However, by fifth day of treatment the volume intake per rat reverted to pre-treatment levels (Figure 3.8).

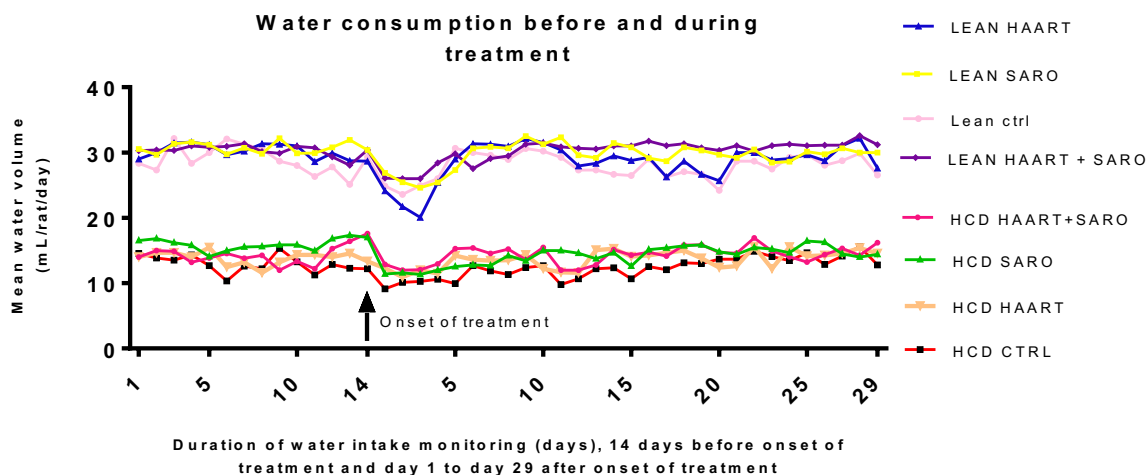


Figure 3.8 Trend of mean daily water consumption (mL/rat/day) / experimental group two weeks before onset of drug treatment and during the first four weeks of treatment.

3.3 Total body mass monitoring

3.3.1 Total body mass of the animals at the onset of the programme

The initial total body mass (g) of all the rats included in this study (176) was 180.20 ± 2.28 g (mean \pm SEM). There was no statistically significant difference in the mean total body mass \pm SEM / group after random allocation of rats into either lean / standard rat chow or HCD groups at the onset of the feeding programme, Lean: 182.00 ± 3.22 g; HCD: 179.38 ± 3.24 g, $n = 88$ / group, (Figure 3.9).

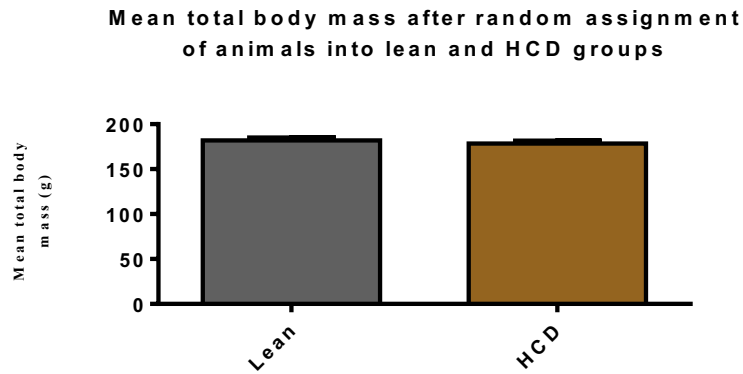


Figure 3.9 Mean total body mass / experimental group (g) after random assignment into either lean (standard diet / rat chow) or HCD groups.

3.3.2 Total body mass changes during the first 10 weeks of the feeding programme

Weekly monitoring of the total body mass of each experimental animal showed that the mass increased gradually in both lean and HCD groups for the first 10 weeks and from the 6th week of feeding programme, the HCD group recorded a significantly higher mean total body mass compared to the lean group (HCD 309.72 ± 8.72 g vs. lean 280.76 ± 9.03 g, $p < 0.05$; (10.3 % difference), $n = 88$ / group) and this difference further widened by week 10 (HCD group 354.56 ± 10.51 vs. lean group 317.68 ± 8.81 g, $p < 0.01$; (11.9 % difference), $n = 88$ / group) (Figure 3.10). The mean percentage increase in total body mass from week 1 to week 10 was higher for the HCD group compared to the lean group (96.17 ± 4.87 % vs. 74.22 ± 5.01 %, $p < 0.01$, respectively; $n = 88$ / group).

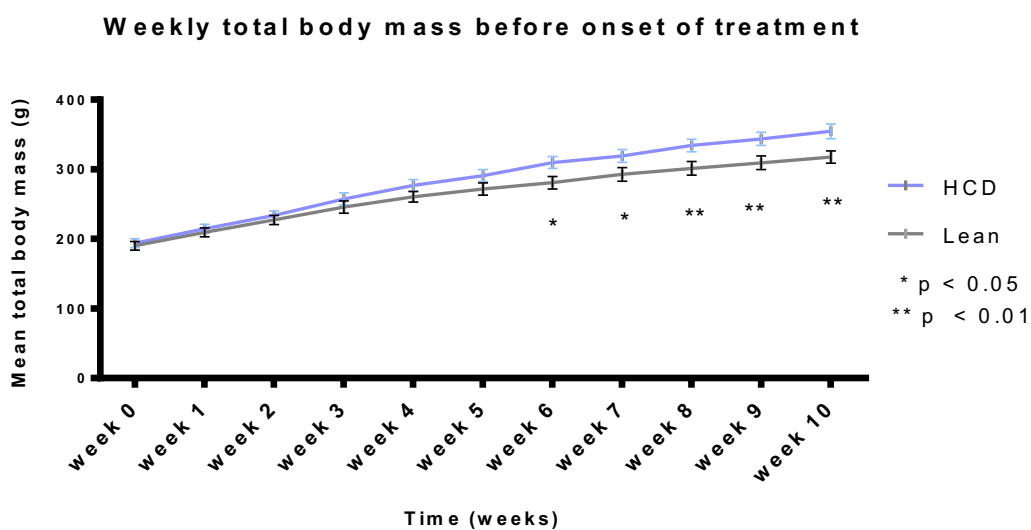


Figure 3.10 Weekly mean total body mass (g) in lean and HCD groups during the feeding programme before onset of drug treatment.

3.3.3 Total body mass monitoring during the treatment programme

During the drug treatment period, the differences in total body mass persisted between the HCD and lean treated groups. All the treated HCD groups had a significantly higher mean total body mass compared to their respective treated lean counterparts (Figure 3.11). Table 3.3 shows the weekly mean \pm SEM (g) total body mass in each experimental group during the treatment programme. The p-values (Figure 3.11 and Table 3.3) represent weekly comparisons between HCD and the respective lean control groups, i.e. HCD control vs. lean control, HCD HAART vs. lean HAART, HCD HAART + Saro vs. lean HAART + Saro and HCD Saro vs. lean + Saro. No significant differences in the mean total body mass was observed among the lean treated groups and similarly, the mean total body mass among the HCD groups showed no differences (Figure 3.11).

On average, the HCD groups were 15.7 ± 3.3 % (50 ± 8.2 g) heavier compared to the lean groups at the end of the full feeding and drug treatment programme of 16 weeks.

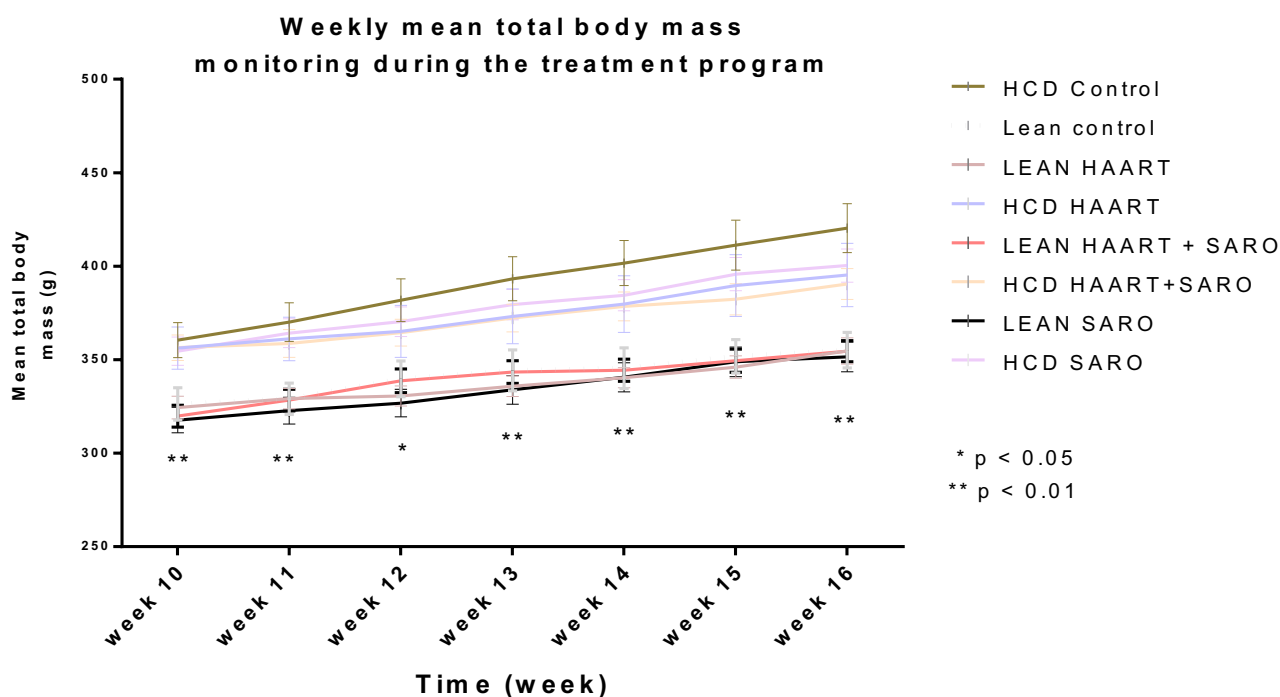


Figure 3.11 Weekly mean total body mass (g) / experimental group during the drug treatment phase.

Table 3.3 Weekly mean total body mass (g) of the eight experimental groups during the treatment phase and mean percentage increase in body mass from week 10-16. Each HCD group mean total body mass was significantly higher than their corresponding lean control group (** $p < 0.01$; * $p < 0.05$ (groups compared shown above); $n = 22$ / group).

	Lean control	HCD Control	LEAN HAART	HCD HAART	LEAN HAART + SARO	HCD HAART + SARO	LEAN SARO	HCD SARO
week 10	326.30 ± 8.62	360.50 ± 9.31 **	324.40 ± 6.00	356.22 ± 11.21 **	319.83 ± 5.82	356.40 ± 6.81 **	317.61 ± 6.83	354.52 ± 7.62 **
week 11	329.10 ± 8.42	370.14 ± 10.32 **	329.16 ± 5.39	361.13 ± 11.58 **	328.42 ± 5.72	358.59 ± 7.44 **	322.72 ± 7.10	364.19 ± 7.70 **
week 12	339.82 ± 9.60	381.80 ± 11.51 **	330.61 ± 5.43	365.20 ± 14.00 *	338.70 ± 6.34	364.50 ± 7.18 **	326.80 ± 7.44	370.34 ± 7.91 **
week 13	344.31 ± 10.94	393.34 ± 11.82 **	335.82 ± 5.48	373.24 ± 14.62 **	343.42 ± 6.00	372.2 ± 7.42 **	333.80 ± 7.58	379.52 ± 8.10**
week 14	345.54 ± 10.9	401.70 ± 12.14 **	340.32 ± 5.43	379.80 ± 15.24 **	344.44 ± 6.00	378.4 ± 7.66 **	340.59 ± 7.82	384.39 ± 8.32 **
week 15	351.78 ± 8.91	411.32 ± 13.30 **	346.00 ± 6.00	389.64 ± 16.51 **	349.39 ± 6.11	382.28 ± 8.20 **	348.80 ± 7.91	395.72 ± 9.01 **
week 16	355.14 ± 9.60	420.39 ± 13.10 **	354.66 ± 7.00	395.31 ± 17.00 **	354.55 ± 5.64	390.38 ± 8.22 **	351.41 ± 8.00	400.33 ± 8.94 **
% change (week 10-16)	8.87 ± 0.48	16.24 ± 0.66	10.42 ± 0.49	12.86 ± 1.02	9.84 ± 0.52	10.24 ± 0.62	9.78 ± 0.64	13.21 ± 0.74

3.4 Biometric data on the day animals were sacrificed

3.4.1 Mean total body mass during euthanasia

The total body mass (g) was recorded for each animal before they were sacrificed. The mean body mass (mean ± SEM, g) recorded for each experimental group (rats that were not fasted) is shown in Figure 3.12. All the HCD groups had significantly higher mean total body mass compared to their corresponding lean groups. HCD Control: 418.62 ± 9.61 g, vs. Lean Control: 356.00 ± 8.00 g, $p < 0.01$; HCD HAART: 411.84 ± 8.21 g, vs. Lean HAART: 356.90 ± 6.72 g, $p < 0.01$; HCD HAART + Saro: 392.41 ± 8.92 g, vs. Lean HAART + Saro: 364.89 ± 7.33 g, $p < 0.05$; HCD Saro 415.3 ± 10.92 g, vs. Lean Saro: 348.11 ± 10.48 g, $p < 0.01$. $n = 14$ / group (Figure 3.12).

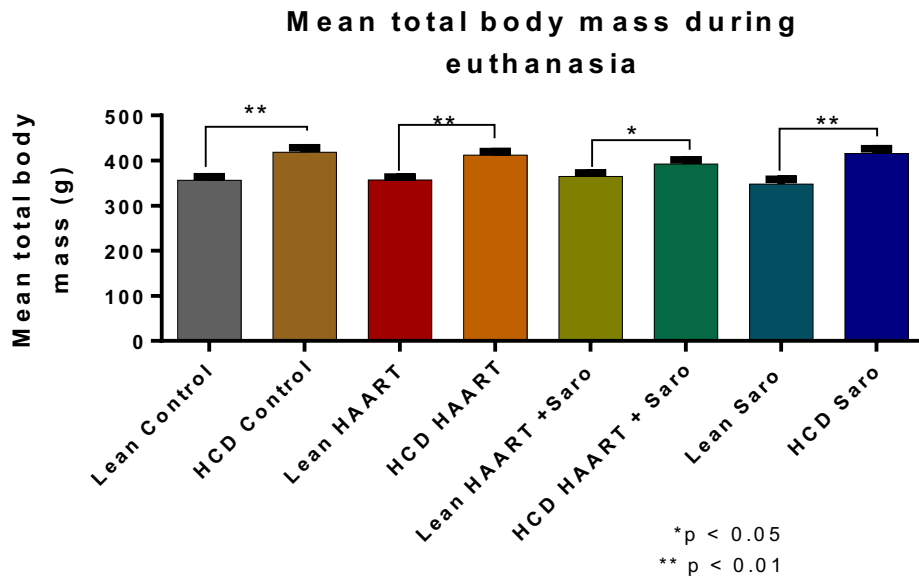


Figure 3.12 Mean total body mass (g) per experimental group during euthanasia.

3.4.2 Visceral / intra-peritoneal (IP) fat mass

The mean visceral fat mass in relation to the total body mass (%) (adiposity index) per group was higher in all the HCD experimental groups compared to the lean groups: HCD control: 6.50 ± 0.40 % vs. lean control: 3.60 ± 0.3 %, $p < 0.0001$; HCD HAART: 5.70 ± 0.40 % vs. lean HAART 3.70 ± 0.30 %, $p < 0.001$; HCD HAART + Saro: 4.30 ± 0.50 % vs. lean HAART + Saro: 2.30 ± 0.2 %, $p < 0.01$; HFD Saro: 5.30 ± 0.41 % vs. lean Saro: 2.70 ± 0.20 %, $p < 0.0001$, $n = 14$ / group.

Furthermore, the HCD HAART (5.70 ± 0.40 %) group registered significantly higher percentage IP fat mass compared to the HCD HAART + Saroglitazar group (4.30 ± 0.50 %, $p < 0.01$). It was also observed that the adiposity index of lean HAART + Saro: 2.30 ± 0.20 % was significantly lower compared to lean HAART group 3.70 ± 0.30 %, $p < 0.01$ (Figure 3.13).

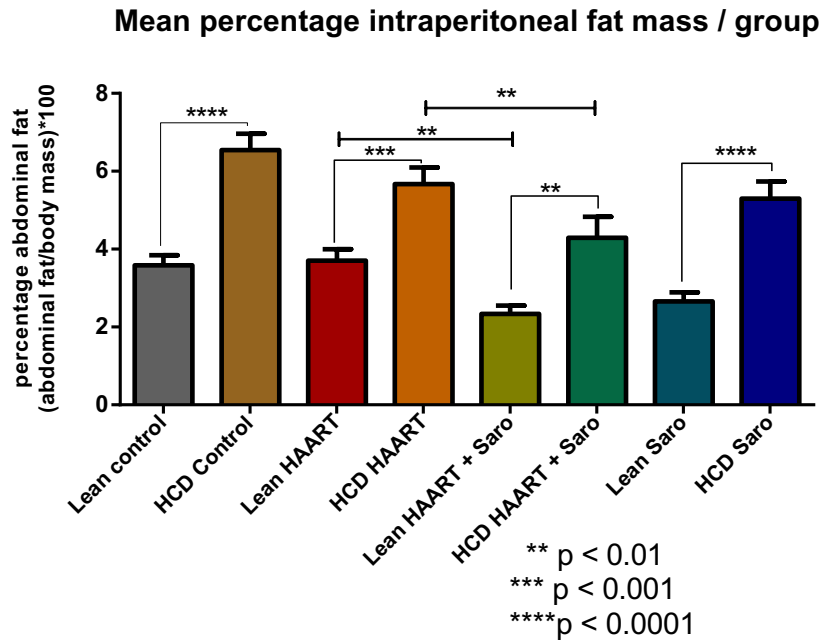


Figure 3.13 Mean percentage intraperitoneal fat (IP) mass / experimental group.

3.4.3 Cardiac mass

3.4.3.1 Absolute cardiac mass

The mean absolute cardiac mass (g) differed significantly between HCD HAART 1.50 ± 0.07 g and Lean HAART 1.33 ± 0.03 g, $p < 0.05$; HCD HAART + Saro 1.34 ± 0.03 g vs. lean HAART + Saro 1.24 ± 0.02 g, $p < 0.05$ and HCD Saro 1.43 ± 0.06 g vs. lean Saro 1.16 ± 0.04 g, $p < 0.05$. Interestingly, HCD HAART group mean absolute cardiac mass (1.50 ± 0.07 g) was significantly higher compared to the HCD HAART + Saro group (1.34 ± 0.03 g), $p < 0.05$, $n = 13-16$ / group. However, no significant differences were observed between the lean control group and the HCD control group mean absolute cardiac mass (Figure 3.14).

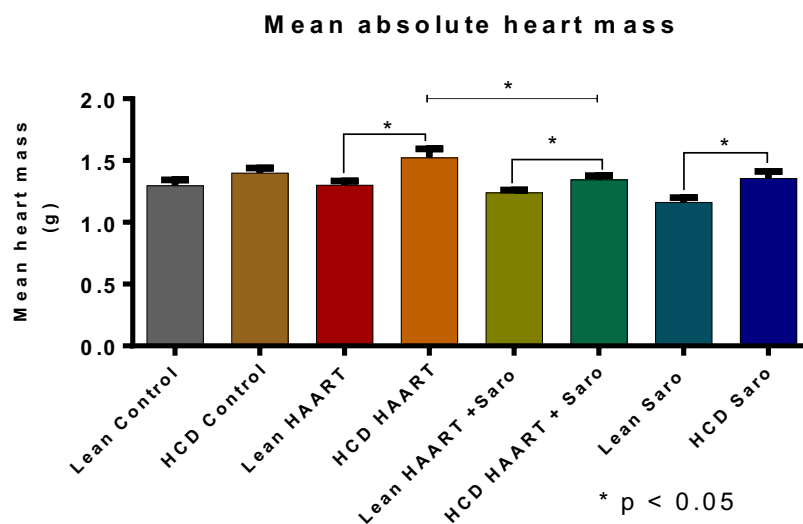


Figure 3.14 Mean absolute cardiac mass (g) / experimental group.

3.4.3.2 Normalised cardiac mass by tibial length

The absolute cardiac mass (mg) of each animal was divided by the length of its tibia (mm) to obtain a normalised cardiac mass index (mg / mm), after which the means of these indices were computed per group. This index has been proposed as a better indicator of cardiac mass changes than relating the cardiac mass to total body weight (Yin et al. 1982). The findings confirmed the mean absolute mass observations i.e., normalised cardiac mass was significantly higher in the HCD HAART group 41.05 ± 1.91 mg / mm compared to lean HAART group 35.18 ± 0.77 mg / mm, $p < 0.05$; HCD HAART + Saro 36.62 ± 0.84 mg / mm higher compared to lean HAART + Saro 33.55 ± 0.72 mg / mm, $p < 0.05$; HCD Saro 36.11 ± 1.49 mg / mm higher compared to lean Saro 31.48 ± 1.04 mg / mm, $p < 0.05$ and HCD HAART 41.05 ± 1.92 mg / mm higher than HCD HAART + Saro 36.62 ± 0.84 mg / mm, $p < 0.05$, $n = 13 - 16$ / group. No differences were observed in the normalised cardiac mass between the HCD and the lean control groups (Figure 3.15).

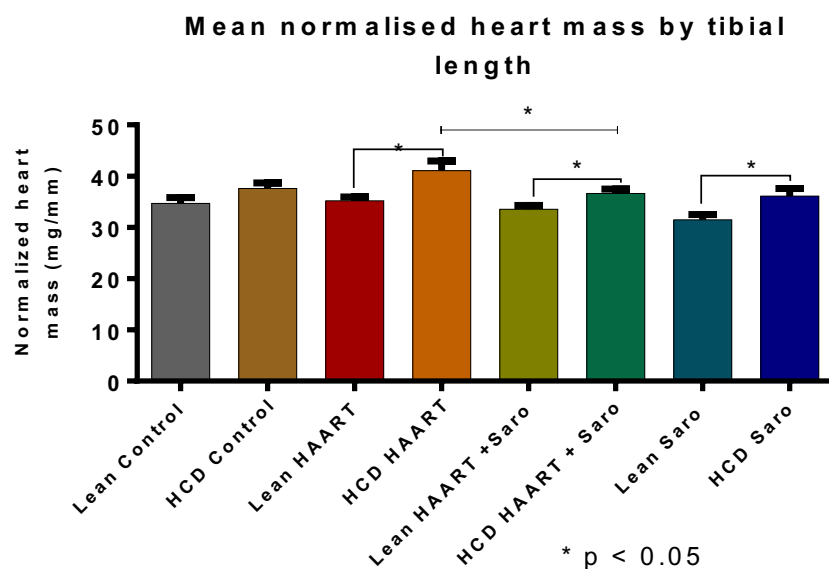


Figure 3.15 Mean normalised heart mass by tibial length (mg / mm) / experimental group.

3.4.4 Liver mass

The mean absolute liver mass (g) and mean normalised liver mass by tibial length (mg / mm) were only significantly increased in the HCD control group compared to the lean control: HCD control (12.04 ± 0.53 g) vs. lean control (10.34 ± 0.28 g), $p < 0.05$, $n = 16$ (Figure 3.16 A). There were no differences observed between any of the other groups. Similarly, after normalisation by tibial length, the differences between the mean HCD control group, 323.00 ± 13.73 mg / mm, was higher than lean control 277.32 ± 7.47 mg / mm, $p < 0.05$, $n = 16$ / group. No differences were observed in the normalised liver mass between the HCD and the lean control groups (Figure 3.16 B).

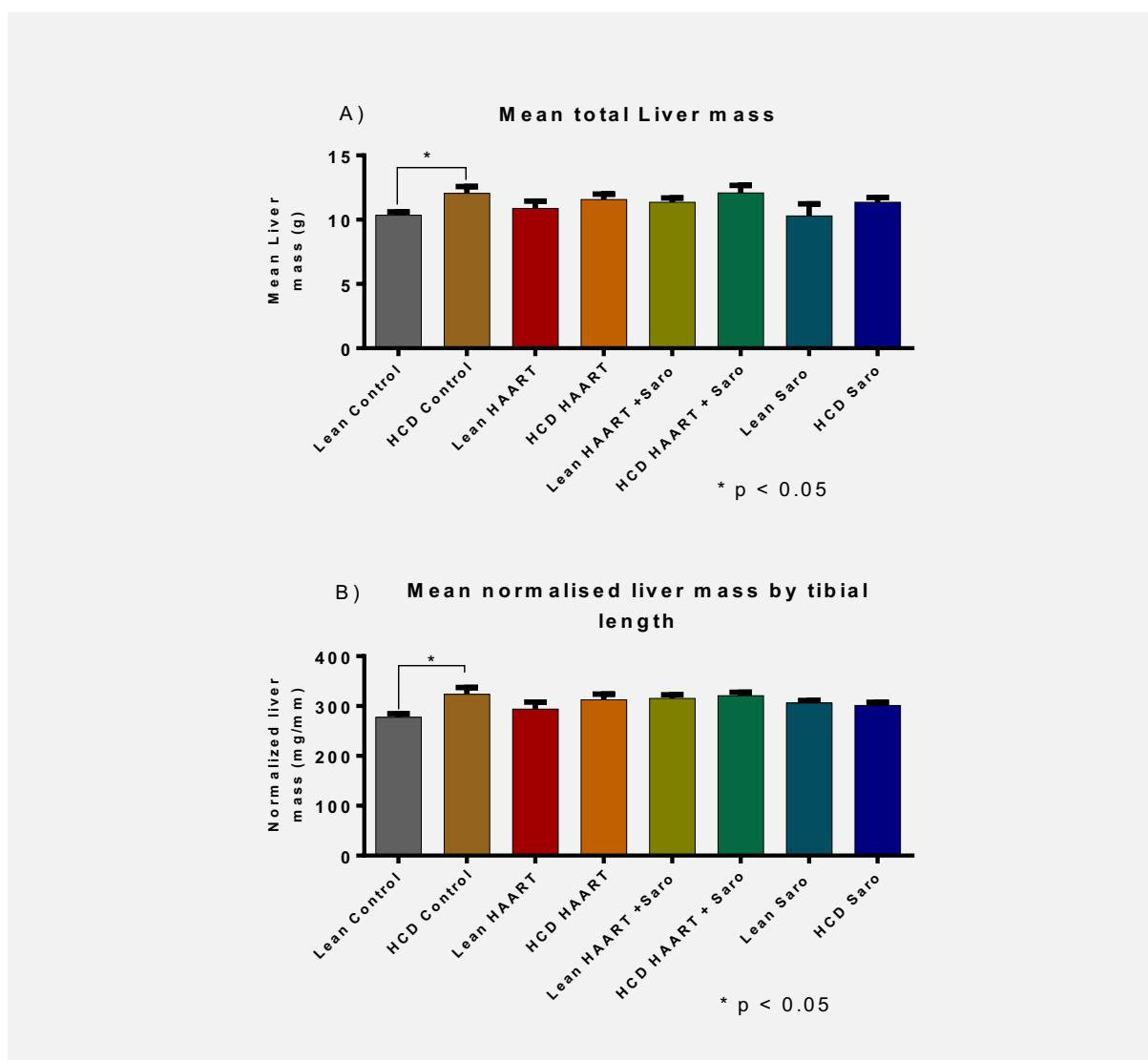


Figure 3.16 A) Mean absolute liver mass (g) / experimental group. B) Mean normalised liver mass by tibial length (mg /mm) / experimental group.

3.5 Blood and serum parameters

3.5.1 Blood glucose levels

Blood glucose was determined for both fasted animals (fasting blood glucose) and non-fasted animals (random blood glucose). No inter-group differences were observed in the mean fasting blood glucose levels, $n = 8$ / group (Figure 3.17).

Similarly, there were no significant differences observed among any of the experimental groups in the mean random blood glucose, $n = 14$ / group (Figure 3.18). However, a comparison of the mean random and fasting blood glucose / group revealed that the mean random blood glucose was significantly higher in all the experimental groups compared to the mean fasting blood glucose: mean random blood glucose 7.19 ± 0.31 mmol/L, $n = 14$ / group vs. mean fasting blood glucose levels 5.19 ± 0.29 mmol/L, $n = 8$ / group; $p < 0.0001$ (Figure 3.19).

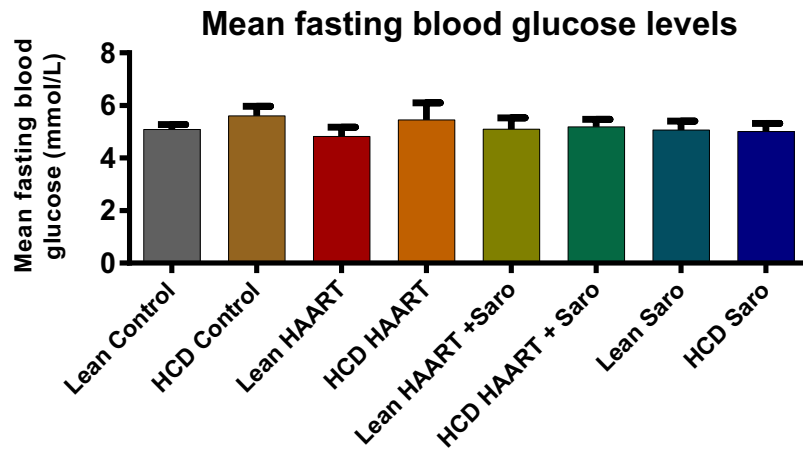


Figure 3.17 Mean fasting blood glucose (mmol/L) / experimental group.

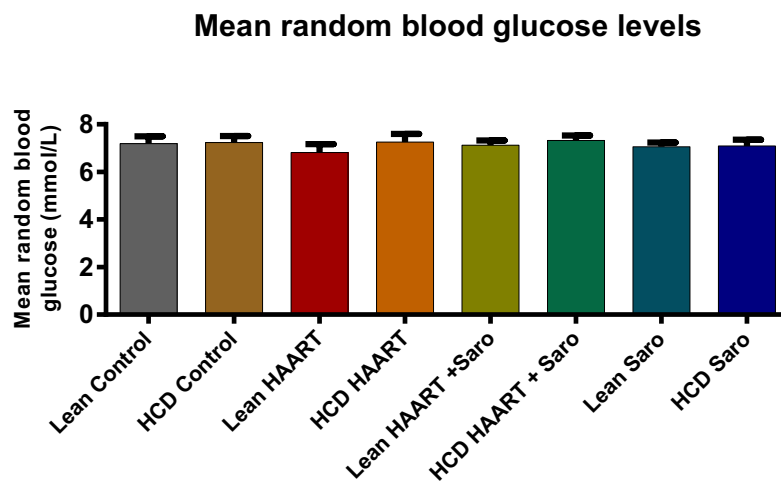


Figure 3.18 Mean random blood glucose (mmol/L) / group.

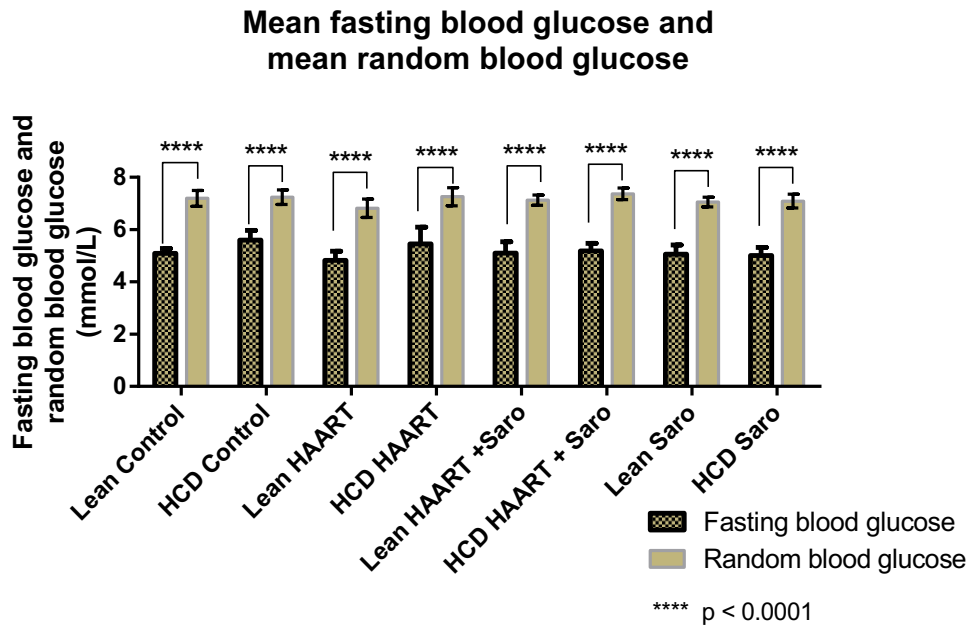


Figure 3.19 Mean fasting blood glucose (mmol/L) and mean random blood glucose (mmol/L) / experimental group.

3.5.2 Lipid profile

3.5.2.1 Serum total cholesterol (TC)

There were no differences noted in the mean serum TC levels between any of the fasted experimental groups. The mean serum TC \pm SEM (mmol / L), n = 7-9 / group are shown below (Figure 3.20).

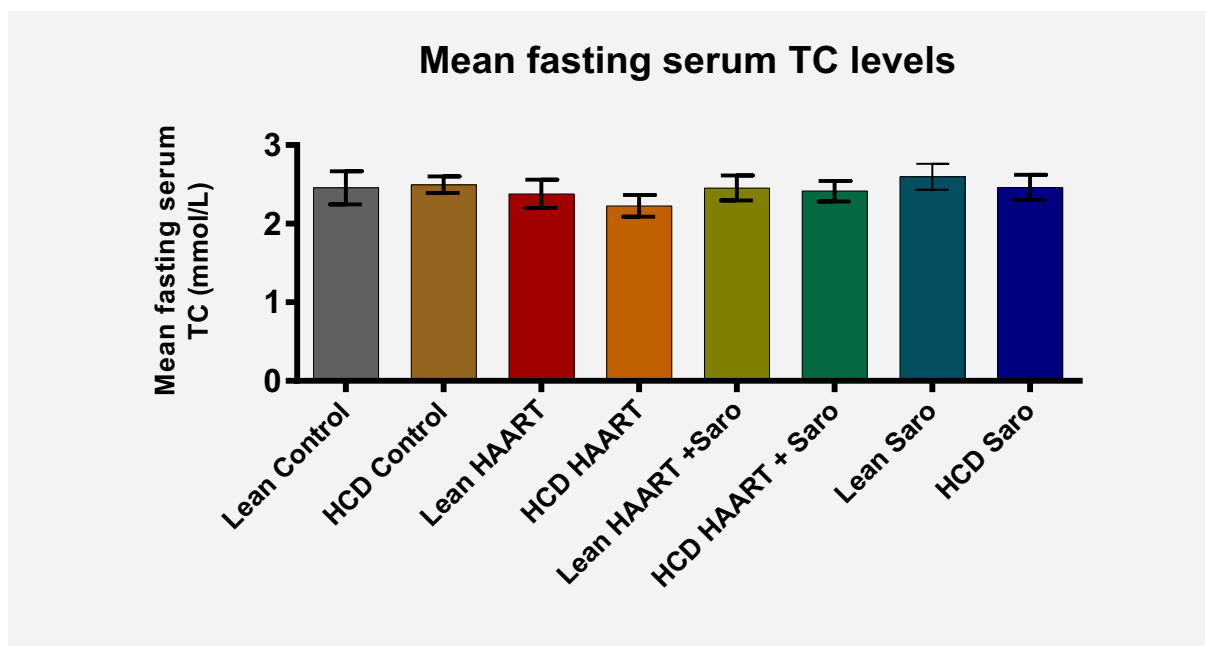


Figure 3.20 Mean fasting serum total cholesterol (TC) (mmol / L) / experimental group.

3.5.2.2 Serum TGs

The mean serum TGs \pm SEM concentrations were significantly elevated in the HCD control group compared to the lean control group (0.95 ± 0.1 mmol / L vs. 0.72 ± 0.08 mmol/L, $p < 0.05$, respectively). However, no other differences were observed among other experimental groups, $n = 7-9$ / group (Figure 3.21).

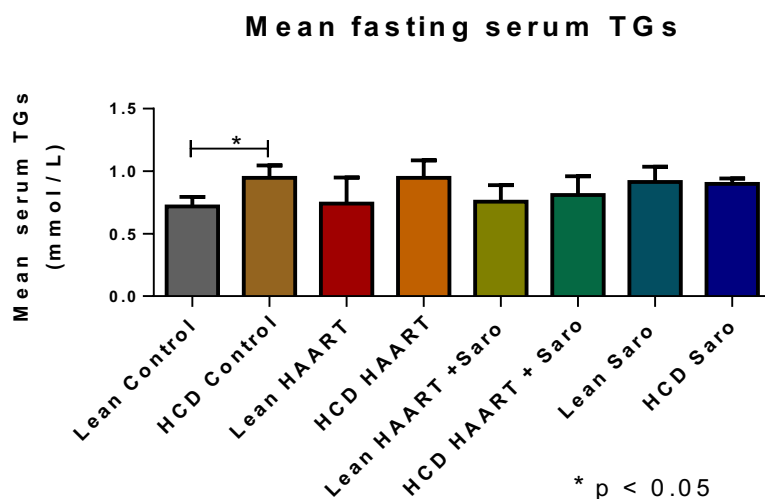


Figure 3.21 Mean fasting serum triglycerides (TGs) (mmol / L) / experimental group.

3.5.2.3 Serum total high-density lipoprotein cholesterol (HDL-C) and low-density lipoprotein cholesterol (LDL-C)

The mean total HDL-C was significantly higher in the HCD control group: 0.49 ± 0.05 mmol / L compared to lean control: 0.37 ± 0.03 , $p < 0.05$, HCD control group: 0.49 ± 0.05 mmol / L compared to HCD Saro group: 0.31 ± 0.02 mmol / L, $p < 0.05$, lean HAART group: 0.44 ± 0.04 mmol / L compared to lean HAART + Saro group: 0.29 ± 0.04 mmol / L, $p < 0.05$, and HCD HAART group: 0.43 ± 0.05 mmol / L compared to HCD HAART + Saroglitazar group: 0.24 ± 0.04 mmol / L, $p < 0.05$, $n = 7 - 9$ / group (Figure 3.22 A).

LDL-C (mmol / L) was calculated using the Friedewald formula: $LDL-C (mmol / L) = TC (mmol / L) - HDL-C (mmol / L) - (TG (mmol / L)/2.17)$. The mean LDL-C was significantly higher in the HCD HAART + Saro group: 2.18 ± 0.12 mmol / L compared to HCD HAART group: 1.80 ± 0.11 mmol / L, $p < 0.05$, $n = 7 - 9$ / group (Figure 3.22 B).

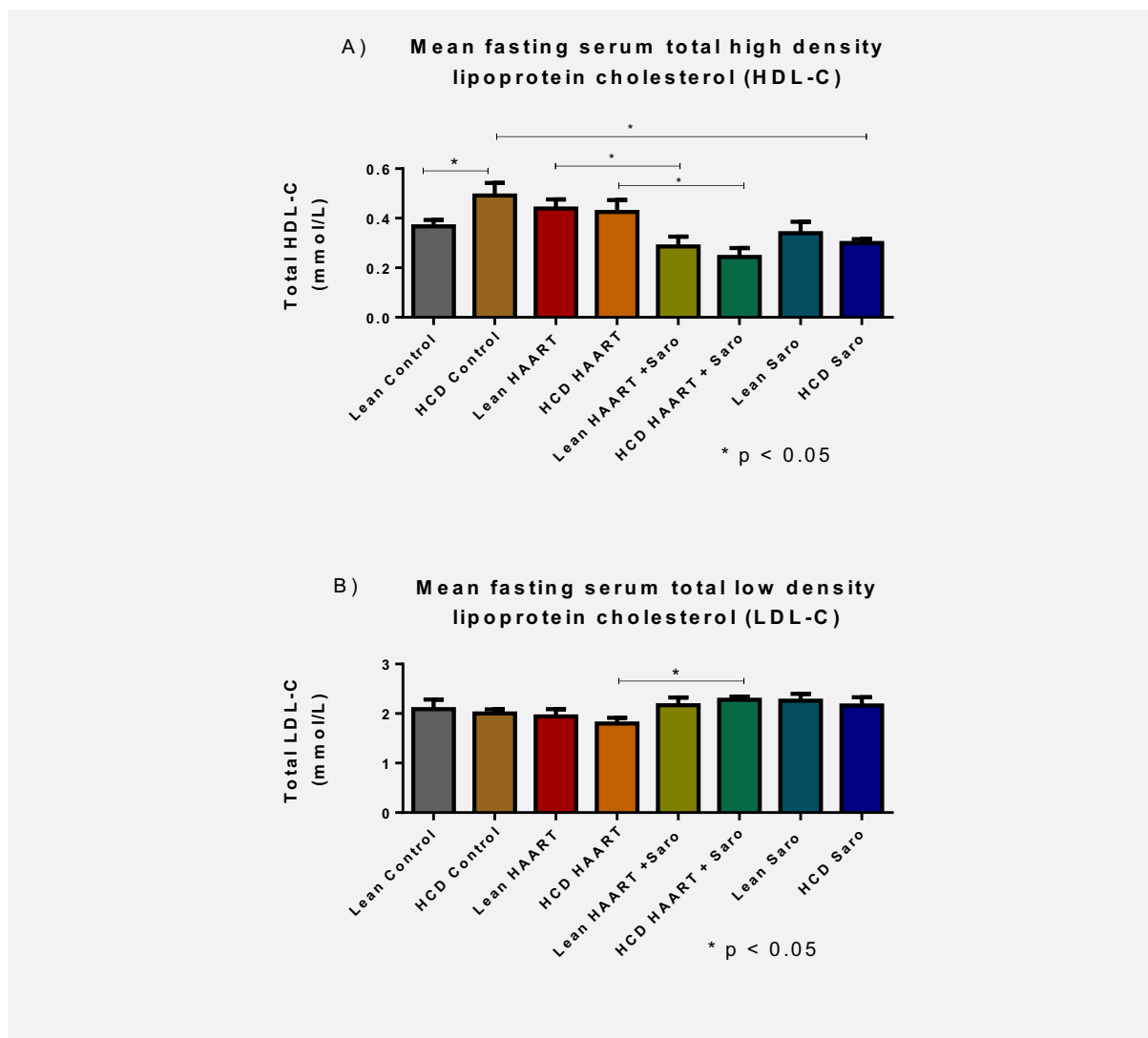


Figure 3.22 A) Mean high-density lipoprotein cholesterol (HDL-C) (mmol / L) / experimental group. B) Mean low-density lipoprotein cholesterol (LDL-C) (mmol / L) / experimental group.

3.5.2.4 Serum phospholipids (PL) + TGs

There were no significant differences in the mean PL + TGs levels in any of the experimental groups as shown on Figure 3.23.

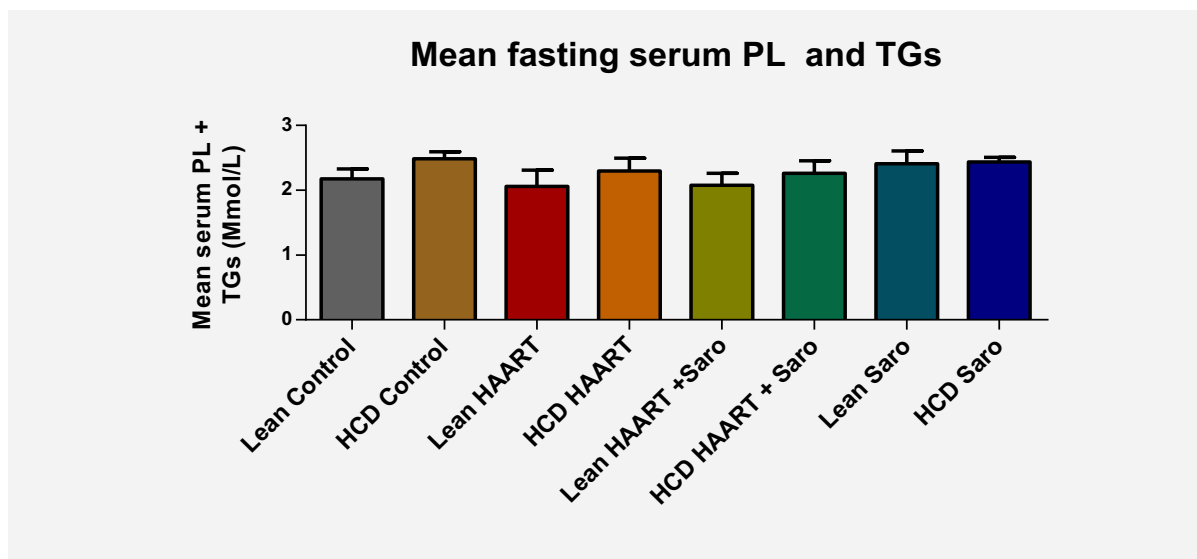


Figure 3.23 Mean fasting serum PL and TGs levels (mmol/L) / experimental group.

3.5.2.5 Serum PL levels

There were no significant differences in the mean serum PL levels among the experimental groups (Figure 3.24).

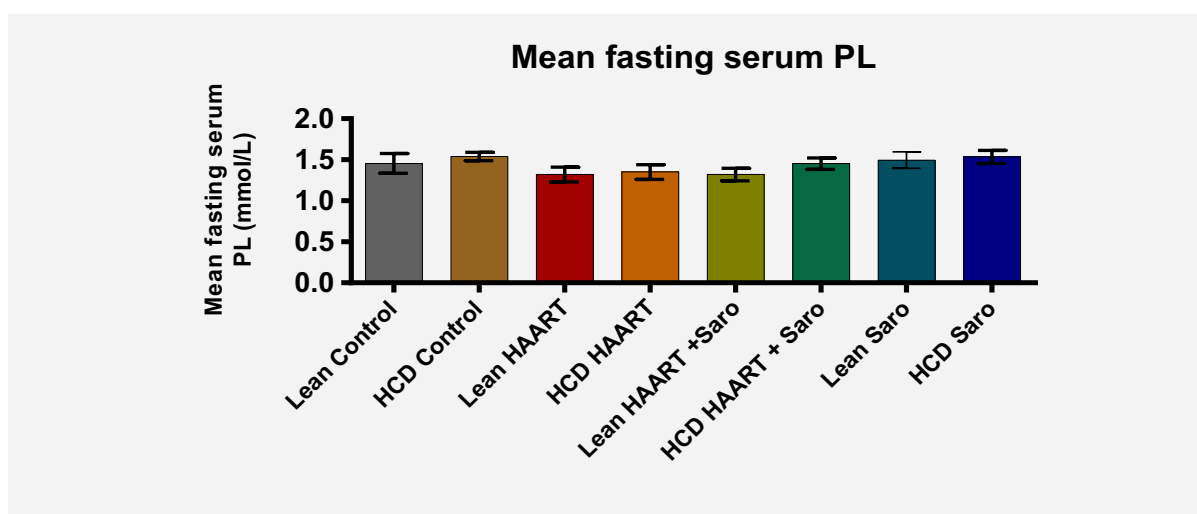


Figure 3.24 Mean fasting serum PL levels (mmol/L) / experimental group.

3.5.2.6 Serum high density lipoprotein subclass 3 (HDL 3)

The mean fasting serum HDL3 levels ($\mu\text{mol} / \text{L}$) were significantly higher in the HCD control group 0.33 ± 0.02 compared to lean control group 0.26 ± 0.03 , $p < 0.05$; HCD control group 0.33 ± 0.02 compared to HCD HAART group 0.23 ± 0.03 , $p < 0.05$; HCD control group 0.33 ± 0.02 compared to HCD Saro group 0.25 ± 0.02 , $p < 0.05$; HCD Saro 0.25 ± 0.02 compared to lean Saro group 0.18 ± 0.02 , $p < 0.05$; HCD HAART group 0.23 ± 0.03 compared to HCD HAART + Saro group 0.17 ± 0.02 , $p < 0.05$ and lean control group 0.26 ± 0.03 compared to lean Saro group 0.18 ± 0.02 , $p < 0.05$ (Figure 3.25).

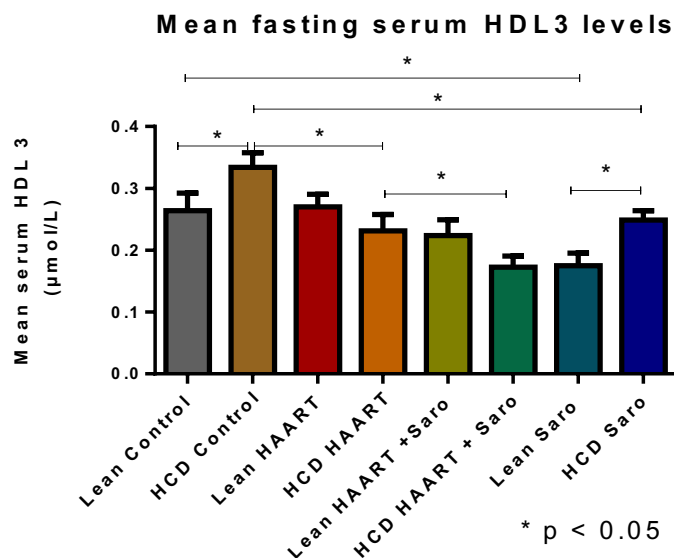


Figure 3.25 Mean fasting serum HDL3 levels ($\mu\text{mol} / \text{L}$) / experimental group.

3.5.2.7 Serum high density lipoprotein subclass 2 (HDL 2)

The mean fasting serum HDL2 levels ($\mu\text{mol} / \text{L}$) were lower in: lean HAART saroglitazar group (0.07 ± 0.03) compared to lean HAART group (0.17 ± 0.04 , $p < 0.05$) and HCD HAART Saroglitazar group (0.07 ± 0.02) compared to HCD HAART group (0.19 ± 0.04 , $P < 0.05$). Similarly, the mean HCD Saroglitazar group HDL2 levels were lower (0.06 ± 0.02) compared to lean Saroglitazar group (0.17 ± 0.05 , $p < 0.05$) (Figure 3.26).

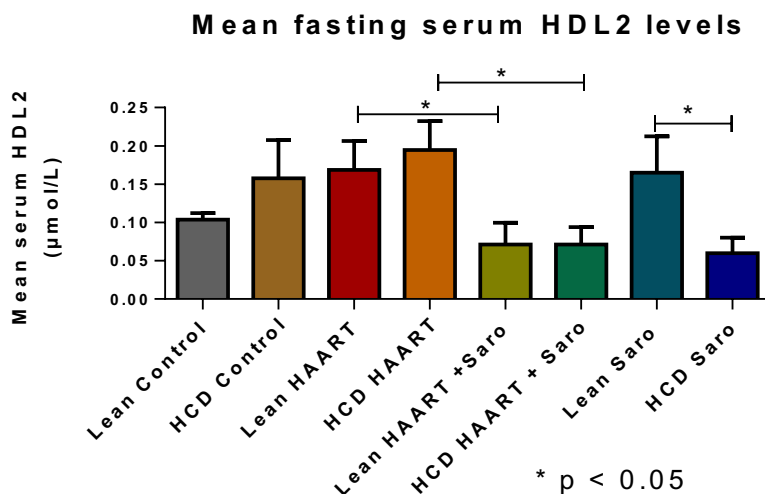


Figure 3.26 Mean fasting serum HDL2 levels (mmol/L) / experimental group.

3.5.3 Serum markers of lipid peroxidation

The total and normalised conjugated dienes (CD) and thiobarbituric acid reactive substances (TBARS) were analysed in all the experimental groups as indicators of lipid peroxidation. The mean absolute concentrations

were expressed as $\mu\text{mol/L}$ and after normalisation with respective fasting serum TGs + PL concentrations, the mean normalised values were expressed as $\mu\text{mol} / \text{mmol}$.

3.5.3.1 Mean fasting serum conjugated dienes (CD)

A comparison of the mean serum CD levels ($\mu\text{mol/L}$) from the experimental groups revealed that treatment of the lean animals with Saroglitazar led to reduced serum CD ($46 \pm 2.23 \mu\text{mol/L}$) compared to the lean control ($76.15 \pm 6.25 \mu\text{mol/L}$), $p < 0.001$. HCD animals treated with Saroglitazar mean serum CD concentrations were significantly lower ($56.6 \pm 5.39 \mu\text{mol/L}$) compared to the HFD control rats, 79.1 ± 6.51 , $p < 0.05$. Additionally, the mean serum CD in the HCD HAART group was significantly higher compared to the HCD HAART group ($63.46 \pm 3.94 \mu\text{mol/L}$ vs. $52.04 \pm 2.44 \mu\text{mol/L}$, $p < 0.05$, respectively, $n = 7-8$, (Figure 3.27).

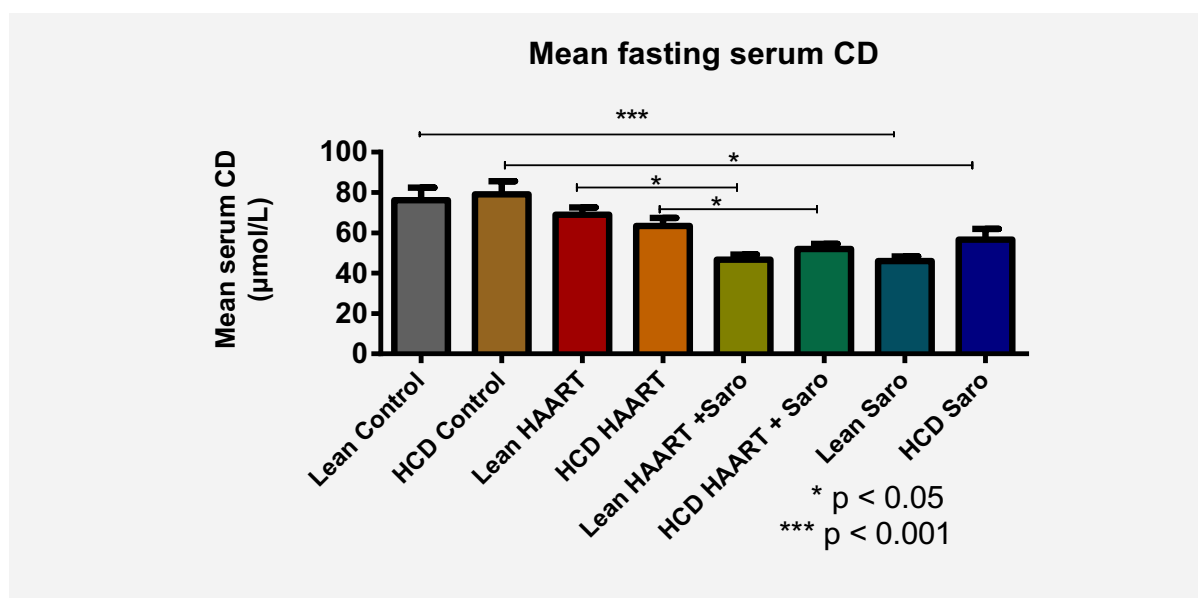


Figure 3.27 Mean fasting serum CD levels ($\mu\text{mol/L}$) / experimental group.

3.5.3.2 Mean normalised serum CD

After normalisation of the serum CD concentrations to PL + TGs, it was observed that, the mean normalised CD was significantly higher in the lean control group compared to the lean Saro group ($35.65 \pm 2.72 \mu\text{mol} / \text{mmol}$ vs. $20.19 \pm 2.10 \mu\text{mol} / \text{mmol}$, $p < 0.01$). The HCD control group mean CD was significantly higher than the HCD Saro group ($32.06 \pm 2.59 \mu\text{mol} / \text{mmol}$ vs. $23.36 \pm 2.45 \mu\text{mol} / \text{mmol}$, $p < 0.01$). Combined treatment of the HCD animals with HAART and Saroglitazar induced significantly lower mean serum CD compared to HAART treatment in the HCD group ($23.91 \pm 2.12 \mu\text{mol} / \text{mmol}$ vs. $29.09 \pm 2.58 \mu\text{mol} / \text{mmol}$, $p < 0.05$, $n = 7-8$) (Figure 3.28).

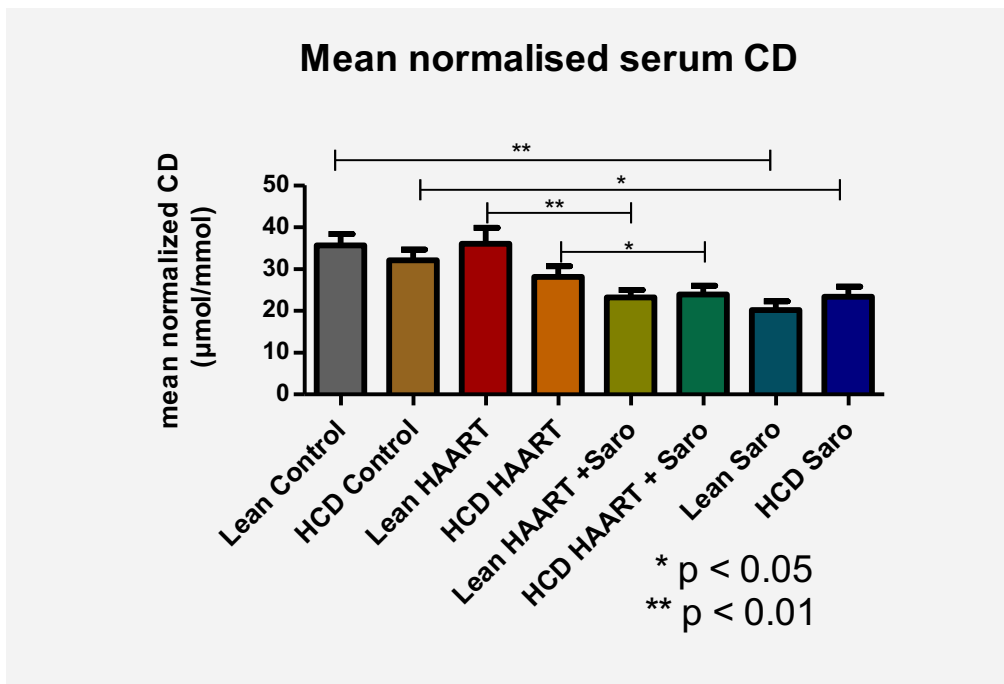


Figure 3.28 Mean normalised serum CD levels ($\mu\text{mol} / \text{mmol}$) / experimental group.

3.5.3.3 Mean fasting serum TBARS

The mean serum TBARS concentrations ($\mu\text{mol/L}$) were also analysed in all the experimental groups and it was observed that the HCD control mean TBARS was higher compared to HCD Saro group ($3.48 \pm 0.20 \mu\text{mol/L}$ vs. $2.76 \pm 0.27 \mu\text{mol/L}$, $p < 0.05$) and the lean Saro group mean serum TBARS was also significantly higher than the HCD Saro group ($4.04 \pm 0.20 \mu\text{mol/L}$ vs. $2.76 \pm 0.27 \mu\text{mol/L}$, $p < 0.05$, respectively, $n = 7-9$) (Figure 3.29).

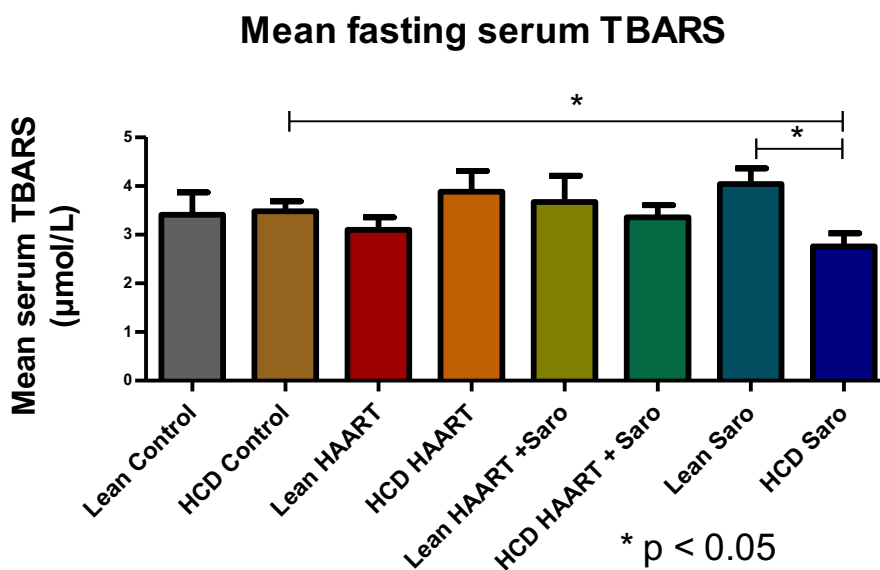


Figure 3.29 Mean fasting serum TBARS levels ($\mu\text{mol/L}$) / experimental group.

3.5.3.4 Mean normalised serum TBARS

After normalisation of the serum TBARS concentrations to fasting serum PL + TGs, the observations made in serum TBARS before normalisation were replicated. The HCD control mean normalised TBARS was higher compared to HCD Saro group (1.55 ± 0.18 vs. 1.13 ± 0.11 $\mu\text{mol} / \text{mmol}$, $p < 0.05$, respectively) and the lean Saro group mean serum TBARS was also significantly higher than the HCD Saro group (1.71 ± 0.14 $\mu\text{mol}/\text{L}$ vs. 1.13 ± 0.11 $\mu\text{mol} / \text{mmol}$, $p < 0.05$, respectively, $n = 7-9$) (Figure 3.30).

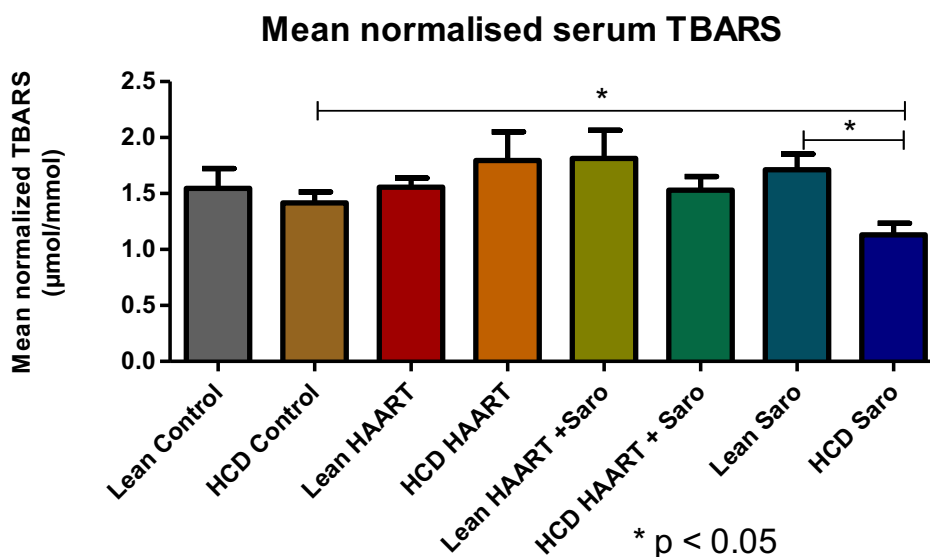


Figure 3.30 Mean normalised serum TBARS levels ($\mu\text{mol} / \text{mmol}$) / experimental group.

3.6 Liver enzymes assays

To assess liver function in the experimental animals, serum alanine aminotransferase (S-ALT), serum aspartate aminotransferase (S-AST), serum alkaline phosphatase (S-ALP), serum lactate dehydrogenase (S-LD) and serum gamma-glutamyltransferase (S-GGT) were analysed in non-fasted serum samples obtained from all the experimental groups, $n = 6 / \text{group}$.

There were no significant differences in the mean S-LD, S-GGT, S-AST and S-ALT among the experimental groups as shown below (Table 3.4).

Table 3.4 Mean serum ALT, AST, LD and GGT enzymes (IU / L) / experimental group.

Experimental group	Lean Control	HCD Control	Lean HAART	HCD HAART	Lean HAART + Saro	HCD HAART + Saro	Lean Saro	HCD Saro
Group Mean \pm SEM (IU/L) Serum assay								
S - ALT	104.8 \pm 28.4	67.2 \pm 22.1	88.3 \pm 20.7	55.2 \pm 10.2	60.3 \pm 14.7	69.67 \pm 11.8	113.8 \pm 34.9	70.7 \pm 16.0
S - AST	212.3 \pm 55.7	129.0 \pm 28.8	161.2 \pm 29.3	113.0 \pm 13.5	111.7 \pm 21.5	118.7 \pm 14.5	198.7 \pm 46.4	139.2 \pm 29.6
S - LD	451.5 \pm 104.4	406.0 \pm 147.7	394.7 \pm 82.7	279.0 \pm 43.3	246 \pm 47.3	268.3 \pm 48.4	460.7 \pm 96.0	356.7 \pm 86.9
S - GGT	< 5	< 5	< 5	< 5	< 5	< 5	< 5	< 5
n	6	6	6	6	6	6	6	6

3.6.1 Serum alkaline phosphatase (S-ALP)

S-ALP concentrations were significantly lower in the HCD HAART + Saroglitazar group compared to HCD Saroglitazar groups (95.0 ± 11.4 IU / L vs. 144.7 ± 23.5 IU / L respectively, $p < 0.05$). Additionally, the mean serum S-ALP was significantly lower in the HCD HAART group compared to the HCD Saro group (88.8 ± 10.9 IU / L vs 144.7 ± 23.5 IU / L, $p < 0.05$ (Figure 3.31). No significant differences were observed in the lean and HCD control and HAART-treated groups, $n = 6$ / group.

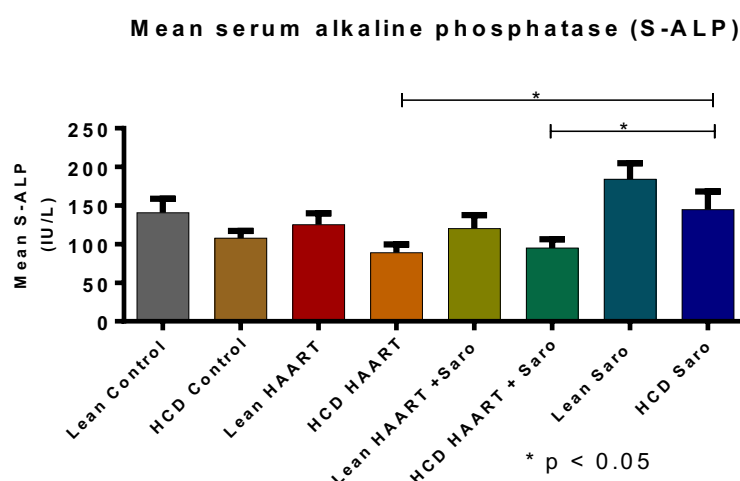


Figure 3.31 Mean serum alkaline phosphatase (S-ALP) levels / experimental group.

3.7 Fasting serum insulin concentrations

The fasting serum insulin concentrations of all the experimental groups were analysed, (n = 7-8 /group) and it was observed that the mean insulin concentrations were higher in the HCD control group compared to the lean control group ($70.2 \pm 11.0 \mu\text{IU} / \text{L}$ vs $20.6 \pm 6.5 \mu\text{IU} / \text{L}$ respectively, $p < 0.05$). HCD HAART insulin concentrations were higher compared to lean HAART and HCD HAART + Saroglitazar ($79.6 \pm 15.8 \mu\text{IU} / \text{L}$ vs. $22.1 \pm 7.4 \mu\text{IU} / \text{L}$ and $32.2 \pm 7.5 \mu\text{IU} / \text{L}$ respectively, $p < 0.05$). The HCD Saro group mean serum insulin was also higher compared to the lean Saro group ($48.8 \pm 11.2 \mu\text{IU} / \text{L}$ vs. $22.3 \pm 3.2 \mu\text{IU} / \text{L}$ respectively, $p < 0.05$), n = 7-8 (Figure 3.32).

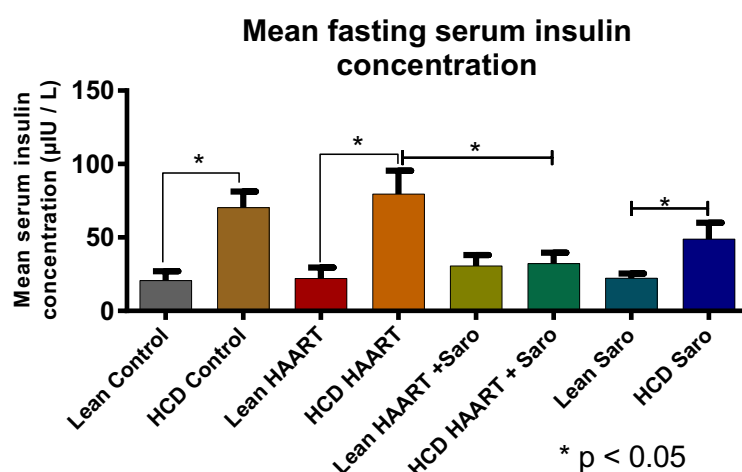


Figure 3.32 Mean fasting serum insulin concentration ($\mu\text{IU} / \text{L}$) / experimental group.

3.8 Homeostasis model assessment for insulin resistance (HOMA-IR)

HOMA-IR is a validated method of assessing insulin resistance and β cell function in Wistar rats (Antunes et al. 2014) and was calculated using the formula: fasting serum insulin concentration ($\mu\text{IU} / \text{L}$) X blood glucose (mg / dl) / 405 (Mathews et al. 1985). The mean HOMA-IR was higher in the HCD control compared to the lean control (17.6 ± 3.4 vs. 4.9 ± 1.8 respectively, $p < 0.05$). Similarly, the HOMA-IR was elevated in the HCD HAART group compared to both lean HAART and HCD HAART + Saroglitazar group (17.1 ± 3.6 vs. 4.7 ± 1.7 and 7.6 ± 2.0 respectively, $p < 0.05$). The mean HOMA-IR was also higher in the HCD Saro group, compared to the lean Saro (11.3 ± 3.1 vs. 4.6 ± 0.5 respectively, $p < 0.05$), n = 7-8 (Figure 3.33).

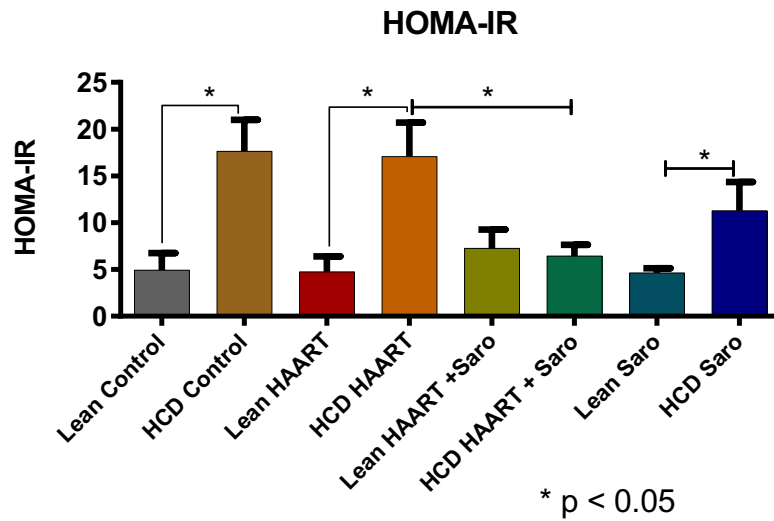


Figure 3.33 Mean HOMA-IR / experimental group.

3.9 Isolated working rat heart perfusion data

The HR (beats per minute), coronary flow rate (Q_e , in mL / min), aortic output (Q_a , in mL / min), total cardiac output, CO (mL / min), systolic pressure, sp (mmHg), diastolic pressure, dp (mmHg), and total work (wt, mW), recorded during the stabilisation phase and reperfusion following regional ischaemia, as well as the percentage recovery for each parameter, are summarised in Table 3.5. Detailed results are shown in the subsequent Figures.

Table 3.5 Mean \pm SEM / experimental group of HR: heart rate (bpm), Qa: aortic outflow (mL / min), Qe: coronary flow rate (mL / min), Wt: work total (mW), sp: systolic pressure (mmHg), dp: diastolic pressure mmHg and percentage (%) recovery of each parameter, * $p < 0.05$ (group comparisons with significant differences are shown in the subsequent Figures). The various parameters are presented from section 3.9.1.

Pre-and post-regional ischaemia-reperfusion working heart data									
Parameter	Perfusion phase & n value	Lean Control	HCD Control	Lean HAART	HCD HAART	Lean HAART +Saro	HCD HAART +Saro	Lean Saro	HCD Saro
HR (bpm) Mean \pm SEM	pre-ischaemia	282.3 \pm 6.7	280.8 \pm 5.6	287.3 \pm 11.1	273.6 \pm 12.9	267.1 \pm 6.0	280.1 \pm 7.6	271.1 \pm 6.9	279.0 \pm 4.9
	n	9	10	8	8	8	7	8	8
	post-ischaemia	271.3 \pm 10.4	280.7 \pm 8.9	282.7 \pm 22.76	278.3 \pm 18.0	266.0 \pm 6.5	281.9 \pm 7.2	267.3 \pm 12.3	265.8 \pm 6.8
	n	9	10	6	7	8	7	8	8
	% HR recovery	96.1	100.0	98.4	101.7	99.6	100.6	98.6	95.3
Qa (mL / min) Mean \pm SEM	pre-ischaemia	37.0 \pm 0.9	37.6 \pm 0.8	40.3 \pm 1.2 *	33.3 \pm 2.4 *	38.8 \pm 2.1	40.9 \pm 2.0 *	40.0 \pm 3.0	42.3 \pm 1.3
	n	10	10	8	8	8	7	8	8
	post-ischaemia	7.5 \pm 2.2	6.5 \pm 1.7	7.4 \pm 2.5	2.3 \pm 1.5 *	5.7 \pm 2.3	7.1 \pm 1.6 *	5.8 \pm 3.0	4.2 \pm 1.0
	n	9	9	8	8	8	7	8	8
	% Qa recovery	16.3	13.6	15.4	5.5 *	12.2	17.0*	12.4	10.0
Qe (mL / min) Mean \pm SEM	pre-ischaemia	16.6 \pm 0.6	16.2 \pm 0.4	16.6 \pm 0.4	15.9 \pm 0.5	15.5 \pm 0.3	16.9 \pm 0.4	16.3 \pm 0.5	16.8 \pm 0.4
	n	10	10	8	8	8	7	8	8
	post-ischaemia	14 \pm 0.9	13.8 \pm 0.8	13.5 \pm 1.5	12.3 \pm 1.4	13 \pm 0.4	13.4 \pm 0.6	13.3 \pm 1.2	14.0 \pm 0.5
	n	9	10	8	8	8	7	8	8
	% Qe recovery	84.3	85.2	80.6	77.1	83.9	79.7	81.5	83.6
CO (mL / min) Mean \pm SEM	pre-ischaemia	53.4 \pm 1.4	53.8 \pm 1.1	57.0 \pm 1.6 *	49.2 \pm 2.3 *	54.3 \pm 2.3	57.7 \pm 2.1 *	56.3 \pm 3.2	59.0 \pm 1.3 *
	n	10	10	8	8	8	7	8	8
	post-ischaemia	20.7 \pm 2.3	19.0 \pm 1.9	20.0 \pm 3.4	14.5 \pm 2.0 *	18.0 \pm 2.2	20.6 \pm 1.7 *	19.0 \pm 2.8	17.3 \pm 1.4
	n	9	10	8	8	8	7	8	8
	% CO recovery	39.0	36.1	34.4	29.6	33.0	35.7	33.4	29.3
Wt (mW) Mean \pm SEM	pre-ischaemia	11.7 \pm 0.5	12.0 \pm 0.4	12.5 \pm 0.5 *	10.5 \pm 0.7 *	12.3 \pm 0.7	12.5 \pm 0.8	12.2 \pm 0.9	12.6 \pm 0.5
	n	10	10	8	8	8	7	8	8
	post-ischaemia	4.0 \pm 0.5	3.7 \pm 0.4	3.3 \pm 0.9	2.5 \pm 0.5 *	3.5 \pm 0.5	4.0 \pm 0.4 *	3.5 \pm 0.6	3.6 \pm 0.4
	n	9	10	8	8	8	7	8	8
	% Wt recovery	35.1	30.8	25.3	23.7	28.5	31.6	28.6	27.9
sp (mmHg) Mean \pm SEM	pre-ischaemia	96.3 \pm 2.5	97.7 \pm 1.6	96.3 \pm 1.8	93.6 \pm 2.3	100.5 \pm 2.2	96.9 \pm 2.5	95.5 \pm 3.1	96.3 \pm 2.4
	n	10	10	8	8	8	7	8	8
	post-ischaemia	85.9 \pm 1.4	87.4 \pm 1.9	66.4 \pm 14.5	71.0 \pm 10.9	87.6 \pm 2.4	85.9 \pm 1.8	79.9 \pm 3.6	86.5 \pm 2.8
	n	9	10	8	8	8	7	8	8
	% sp recovery	89.2	89.5	69.0	75.8	87.2	88.6	83.6	89.9
dp (mmHg) Mean \pm SEM	pre-ischaemia	79.6 \pm 1.3	80.5 \pm 1.6	80.6 \pm 1.5	77.4 \pm 2.3	80.5 \pm 1.6	78.7 \pm 2.0	79.1 \pm 2.5	77.5 \pm 1.9
	n	10	10	8	8	8	7	8	8
	post-ischaemia	75.3 \pm 1.3	74.8 \pm 2.0	57.4 \pm 122.6	60.4 \pm 9.2	76.0 \pm 2.1	72.1 \pm 2.4	66.6 \pm 3.3	73.8 \pm 2.7
	n	9	10	8	8	8	7	8	8
	% dp recovery	94.6	92.9	71.2	78.0	94.4	91.7	84.2	95.2

3.9.1 Heart rate (HR) (beats per minute, bpm)

The HR remained constant during both pre-and post-ischaemic phases in all the groups and there were no significant differences in the mean HR among the experimental groups (Figure 3.34).

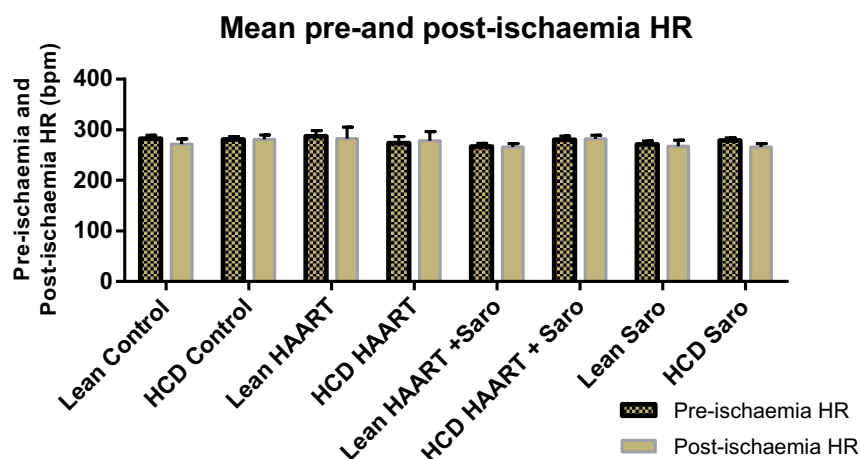


Figure 3.34 Mean pre-and post-ischaeimia heart rate (bpm) / experimental group.

3.9.2 Qa: aortic outflow (mL / min),

Pre-ischaeimia Qa in the HCD HAART group was significantly lower than lean HAART (33.3 ± 2.1 mL/min vs. 40.3 ± 1.2 mL / min respectively, $p < 0.03$). Concomitant treatment with Saroglitazar in the HCD HAART group improved mean Qa compared to HCD HAART treatment only (33.3 ± 2.1 mL/min vs. 40.9 ± 2.0 mL / min respectively, $p < 0.05$). HCD HAART post-ischaeimia Qa recovery was poorer compared to HCD HAART + Saroglitazar (2.3 ± 1.5 mL / min vs. 7.1 ± 1.6 mL / min respectively, $p < 0.04$). Percentage Qa recovery was higher in the HCD HAART + Saroglitazar group compared to HCD HAART group (17.0 ± 3.5 % vs 5.5 ± 3.6 %; $p = 0.04$), $n = 8$ / group (Figure 3.35).

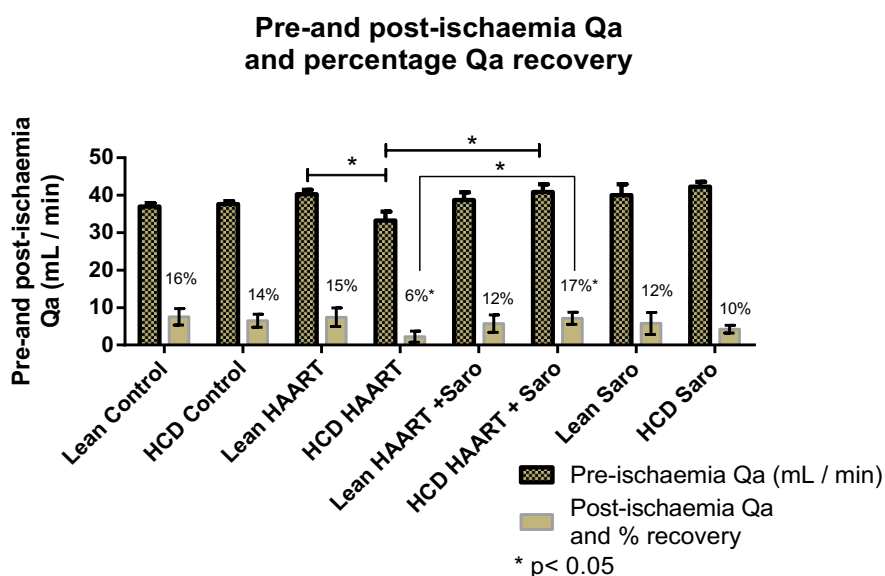


Figure 3.35 Mean pre-and post-ischaeimia aortic outflow (Qa), (mL / min) and percentage Qa recovery.

3.9.3 Q_e: coronary flow rate (mL / min)

There were no differences in the mean pre-ischæmia Q_e in all the groups and similarly, the mean Q_e post ischæmia remained equal in all the experimental groups (Figure 3.36).

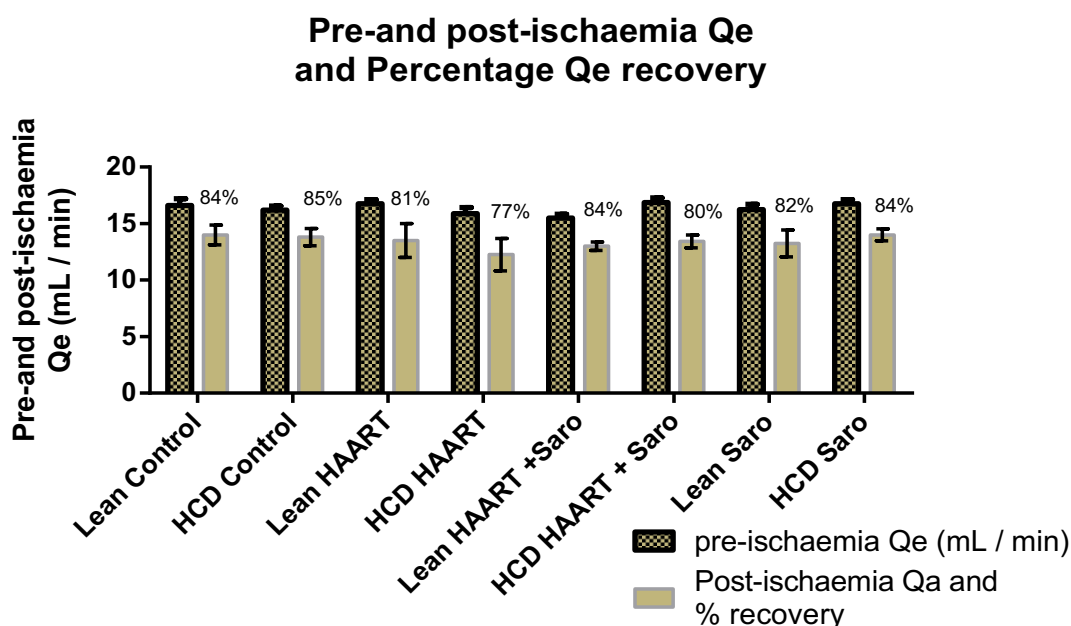


Figure 3.36 Mean pre-and post-ischæmia coronary outflow (Q_e), (mL / min) and percentage Q_e recovery.

3.9.4 Total CO (mL / min)

The pre-ischæmia CO was lower in HCD HAART compared to lean HAART, HCD HAART + Saroglitazar and HCD Saroglitazar groups (49.1 ± 2.3 mL / min vs. 57.0 ± 1.6 mL / min, 57.7 ± 2.1 mL / min and 59.0 ± 1.3 mL / min, respectively; $p < 0.05$). During reperfusion, (post regional ischæmia) the only significant difference was between HCD HAART + Saroglitazar and HCD HAART (20.5 ± 1.67 mL / min (36 %) vs. 14.5 ± 2.0 mL / min (29 %), respectively; $p < 0.05$). No other differences were observed in the percentage CO recovery (Figure 3.37).

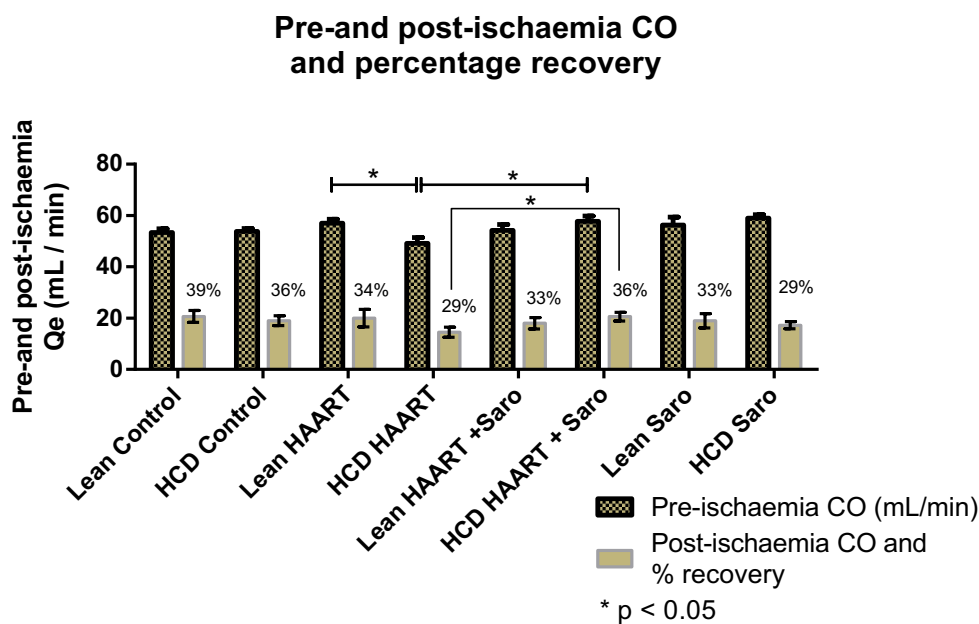


Figure 3.37 Mean pre-and post-ischæmia total cardiac output (CO), (mL / min) and percentage CO recovery / experimental group.

3.9.5 Wt: work total (mW)

Pre-ischæmia Wt was decreased significantly in HCD HAART compared to Lean HAART (10.5 ± 0.7 mW vs. 12.5 ± 0.5 mW, respectively; $p < 0.05$). However, no other differences were observed among the other experimental groups. Post-ischæmia Wt was significantly higher in the HCD HAART + Saroglitazar compared to the HCD HAART (4.0 ± 0.3 mW vs. 2.5 ± 0.5 mW, respectively; $p < 0.05$). Percentage Wt recovery was the same in all the groups (Figure 3.38).

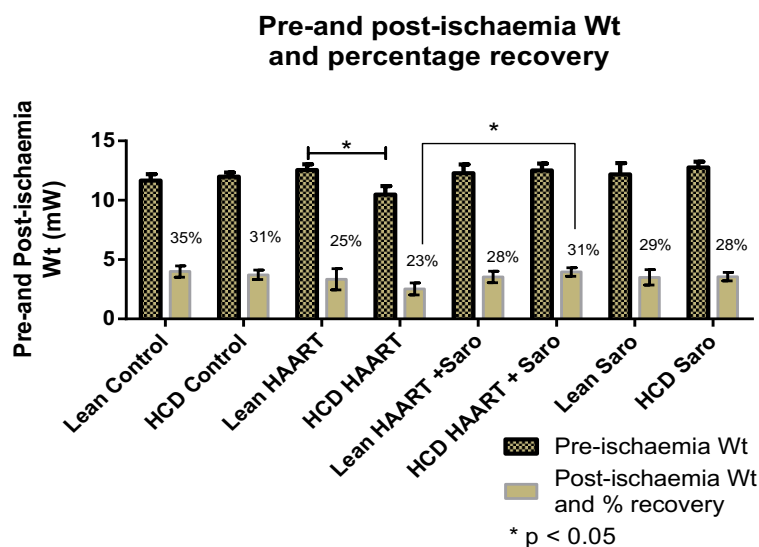


Figure 3.38 Mean pre-and post-ischæmia total work (mW) and percentage Wt recovery.

3.9.6 sp (mmHg) and dp (mmHg)

No differences were observed in the aortic pre-ischæmia and post-ischæmia sp among the experimental groups (Figure 3.39). Similarly, no significant differences were observed in both pre-and post-ischæmia dp (Figure 3.40).

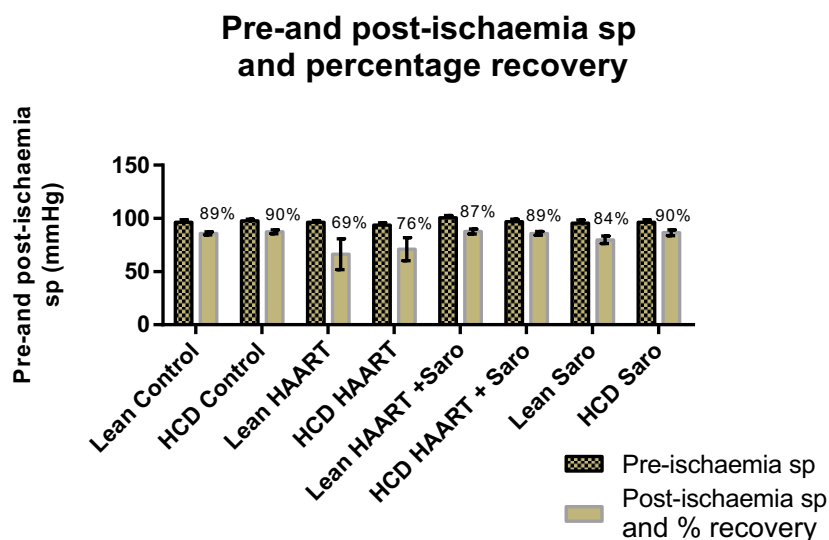


Figure 3.39 Mean pre-and post-ischæmia sp (mmHg) and percentage sp recovery.

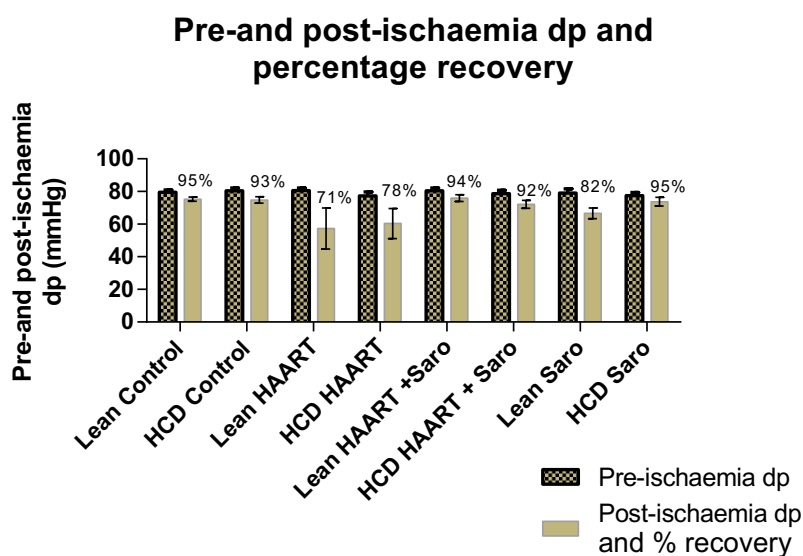


Figure 3.40 Mean pre-and post-ischæmia dp (mmHg) and percentage dp recovery.

3.10 Myocardial infarct size analysis

As described under section 2.5.9, the stained heart tissues were analysed for the left ventricular infarct size following regional ischaemia / reperfusion and results are displayed below (Figure 3.42) as percentage mean

\pm SEM of the infarct area which was calculated using this formula: Infarct size (IS) = infarct area (IA) / (area at risk (AR) + IA) * 100.

The mean percentage infarct size in the lean control group was significantly greater than in the HCD control ($26.1 \pm 2.2\%$ vs $19.1 \pm 1.6\%$ respectively, $p < 0.05$; $n = 7-9$ / group). Similarly, HCD HAART group infarct sizes were significantly smaller compared to the HCD control group ($13.2 \pm 2.1\%$ vs. $19.1 \pm 1.6\%$ respectively, $p < 0.05$, $n = 7-9$ / group). In addition, treatment with HAART led to a significant reduction in the mean infarct size in lean animals compared to their untreated counterparts (lean control, $26.1 \pm 2.2\%$ vs. lean HAART 16.7 ± 1.7 , $p < 0.05$, $n = 7-9$ / group). However, although infarcts were reduced in size in Saroglitazar-treated groups (lean and obese) compared to the lean control group, no differences were noted when compared to HAART-treated groups (lean and obese) as shown below (Figure 3.42). There were no differences noted in the percentage viable area ((viable area / total area of the left ventricle slice) * 100) and percentage area at risk + IA ((AR + IA) * 100) (Table 3.6 and Figure 3.43).

The mean percentage infarct sizes in comparison to mean IA (infarct Area) + AR (area at risk) in all the experimental groups are shown below (Figure 3.43). The mean IA + AR was in the range of $48.4 \pm 1.9\%$ – $52.6 \pm 1.5\%$ and no significant differences were observed among the experimental groups (Table 3.6).

Table 3.6 Mean left ventricular % viable area and % area at risk + infarct area / experimental group.

Group	Lean Control	HCD Control	Lean HAART	HCD HAART	Lean HAART + Saro	HCD HAART + Saro	Lean Saro	HCD Saro
Left ventricular area (Mean + SEM)								
% Viable Area	51.0 ± 2.1	48.4 ± 2.6	48.4 ± 1.8	48.6 ± 2.2	50.8 ± 1.4	50.0 ± 1.9	47.1 ± 2.8	51.3 ± 2.1
% Area at Risk + IA	49.7 ± 1.8	50.1 ± 1.4	51.2 ± 3.0	51.8 ± 2.0	48.4 ± 1.9	49.7 ± 2.8	52.6 ± 1.5	48.9 ± 1.4
n	8	8	7	8	8	7	8	9

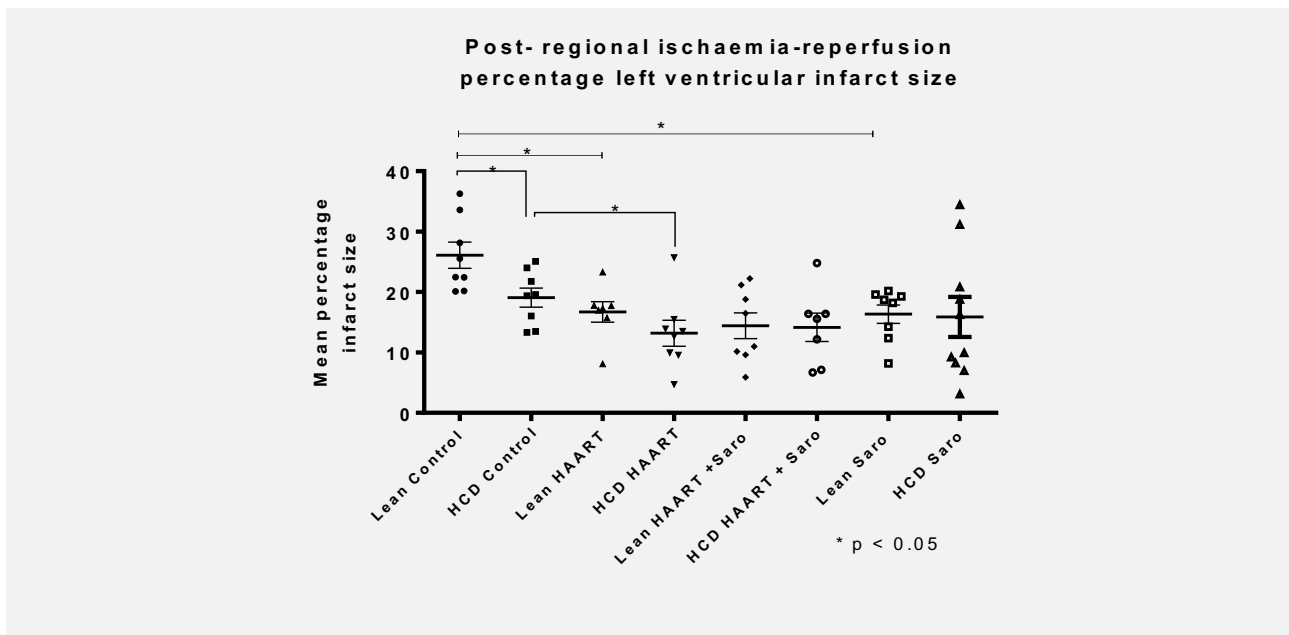


Figure 3.42 Mean left ventricular infarct sizes (%) / experimental group.

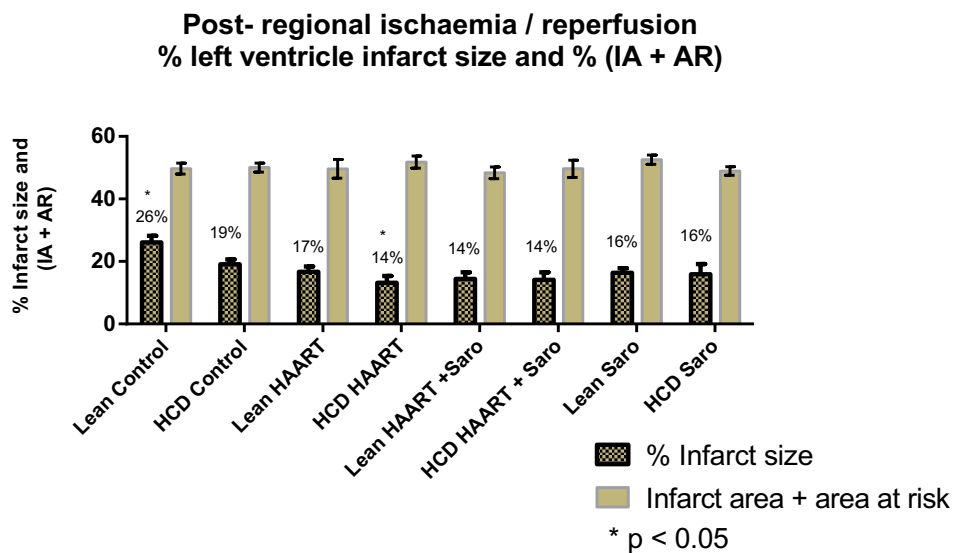


Figure 3.43 Mean percentage infarct size in comparison to IA (infarct Area) + AR (area at risk) / experimental group.

3.11 Liver tissue histology results

As described previously (section 2.5.14.8), the liver tissue samples were analysed histologically and scored based on a validated system described by Kleiner et al. (2005). The results are displayed below (Table 3.7).

Fifty percent of the HCD animals treated with HAART were categorised as having histological features consistent with mild steatosis whereas 16.67 % of the samples in this group had moderate fat infiltration. No samples were categorised as grade three (severe steatosis). On the other hand, HAART co-treatment with Saroglitazar showed that only 16.67 % of the samples presented with mild steatosis, and no samples from this

group displayed features consistent with moderate or severe steatosis. Figures 3.44 and 3.45 show stained liver tissue photo micrographs in various pathological states observed from the different experimental groups.

25.00 % of the HCD HAART liver samples demonstrated features consistent with mild and moderate inflammation, 16.67 % and 8.33 % respectively. Additionally, 8.33 % presented with few balloon cells and another 8.33 % with prominent ballooning indicating varying hepatocyte injury (Figure 3.45). Therefore, the steatotic changes seen in HCD animals treated with HAART were accompanied by mild-moderate inflammation in 25.00 % of the cases.

Liver tissue immunohistochemical studies with anti-placental glutathione S-transferase (GST-P) antibody, did not reveal any GST-P binding (negative for GST-P-positive foci) in any of the experimental groups (Figure 3.44).

Table 3.7 Results of liver tissue histology using a modified scoring criterion for NAFLD, * denotes percentage of animals (liver tissues with fat infiltration (steatosis) and # denotes inflammatory changes (steatohepatitis), @ was an incidental finding of an intrahepatic cyst (6 mm by 4 mm) during laparotomy.

		Percentage of study animals in each experimental group with a particular score							
Histological description									
Steatosis		Lean Control	HCD Control	Lean HAART	HCD HAART	Lean HAART + Saro	HCD HAART + Saro	Lean Saro	HCD Saro
Low-medium –power parenchymal fat infiltration		n = 12	n = 12	n = 12	n = 12	n = 12	n = 12	n = 12	n = 12
Item	Score								
No Steatosis	-	100 %	83.33 %	100 %	33.33 %	100	83.33 %	100 %	91.67 %
<5 %	0	-	16.77 % *	-	50 % *	-	16.77 % *	-	8.36 % *
5 % - 33 %	1	-	-	-	16.77 % *	-	-	-	-
33 % - 66 %	2	-	-	-	-	-	-	-	-
> 66 %	3	-	-	-	-	-	-	-	-
Microvesicular steatosis									
Not present	0	100 %	100 %	100 %	91.77 %	100 %	100 %	100 %	100 %
Present	1	-	-	-	8.33 % *	-	-	-	-
Fibrosis									
None	0	100 %	100 %	100 %	100 %	100 %	100 %	100 %	100 %
Mild-to-moderate	1-2	-	-	-	-	-	-	-	-
Bridging	3	-	-	-	-	-	-	-	-
Inflammation (overall assessment of all inflammatory foci)									
No foci	0	100 %	100 %	100 %	75 %	100 %	100 %	100 %	100 %
< 2 foci/ 200 x field	1	-	-	-	16.67 % #	-	-	-	-
2-4 foci/ 200 x field	2	-	-	-	8.33 % #	-	-	-	-
> 4 foci/ 200 x field	3	-	-	-	-	-	-	-	-
Hepatocyte injury - ballooning									
None	0	100 %	100 %	100 %	91.77 %	100 %	100 %	100 %	100 %
Few balloon cells	1	-	-	-	8.33 % #	-	-	-	-
Prominent ballooning	2	-	-	-	-	-	-	-	-
Other changes (specified)		-	-	-	-	-	-	@	-

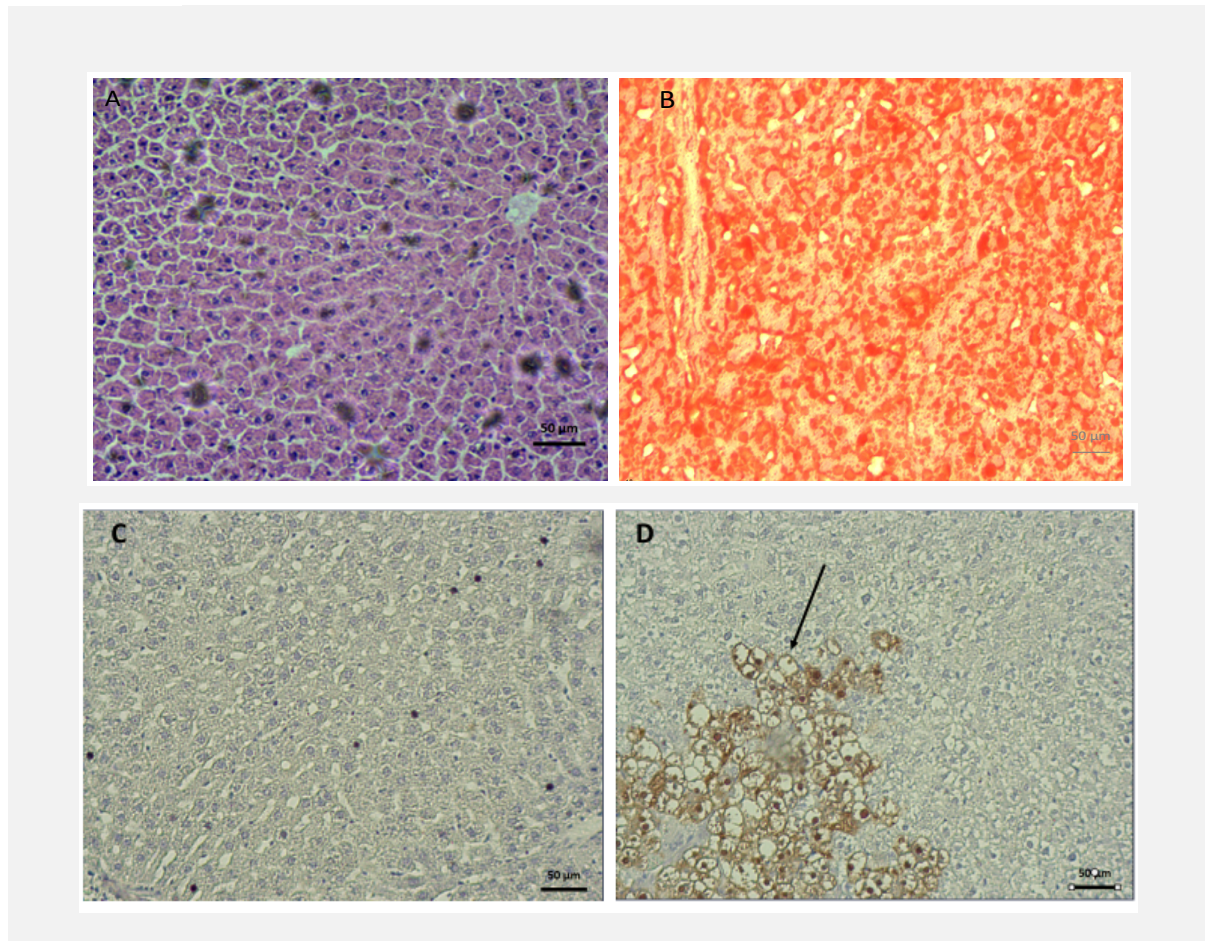


Figure 3.44 Representative liver tissue photomicrographs demonstrating, (A) H & E stain from a lean control liver tissue – no fat infiltration observed, (B) ORO stain from a HCD HAART-treated experimental animal liver tissue with demonstrable fat infiltration, (C) Immunohistochemical stain with anti-(GST-P) antibody (from a HCD control liver tissue, however all the experimental groups showed similar features) – no positive foci and (D) A positive control (not from the experimental groups) - showing a positive GST-P focus. All photomicrographs original magnification, x 100; scale bars shown.

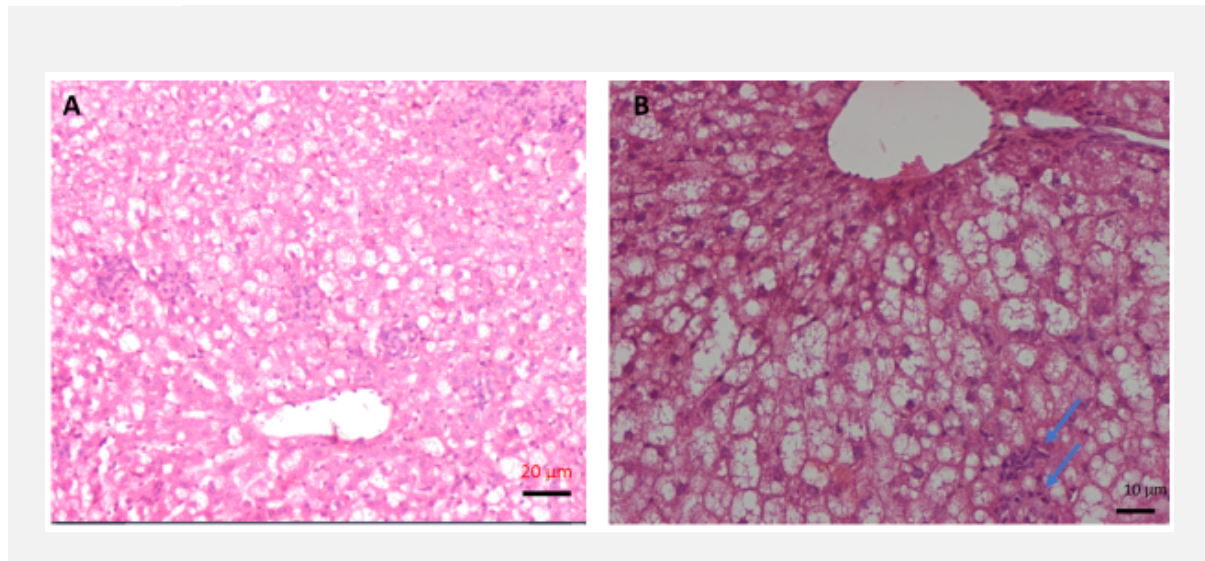


Figure 3.45 Representative liver tissue photomicrographs demonstrating steatosis and steatohepatitis. (A) This field was obtained from HCD HAART-treated liver tissue and shows moderate steatosis but intact hepatocytes. Field (B) was also obtained from the HCD HAART group and demonstrates steatotic cells with foci of inflammation (shown by arrows) and hepatocytes that have undergone ballooning injury. Both photomicrographs: H & E; original magnification, A x 200, B x 400; scale bars shown.

3.12 Vascular reactivity / aortic ring study results

Induction of maximal contractility on aortic rings using cumulative doses of phenylephrine and subsequent stimulation of relaxation using cumulative doses of acetylcholine (described in section 2.5.11) generated results described below.

Table 3.8 below summarises the mean maximal tension (E_{max}) (g) induced by maximal dose of phenylephrine (following successive doses in increasing concentration) and EC_{50} (concentration of the drug inducing half maximal response) determined after log (dose) vs. response transformation. Also, the % maximal relaxation (R_{max}) induced by the maximal dose of acetylcholine and EC_{50} is indicated. Nonlinear regression analysis was performed on the log transformed data using an ‘agonist-dose-response curve’ and results expressed as mean \pm SEM of the EC_{50} .

Table 3.8 Phenylephrine-induced maximal aortic contraction, (E_{max}) (mean \pm SEM (g)) and acetylcholine-induced % maximal aortic relaxation (R_{max}) (Mean \pm SEM (%)). -Log EC_{50} is also indicated per drug in each experimental group. ($p < 0.05$, ** $p < 0.01$, *** $p < 0.001$, † $p = 0.0018$, HCD HAART + Saro vs HCD HAART, ‡ $p = 0.0031$ HCD Control vs HCD HAART, Π $p = 0.0303$ HCD control vs. HCD Saro, Φ $p = 0.024$ HCD HAART + Saro vs. HCD Saro); two-way ANOVA.*

Experimental group	n	Phenylephrine-induced contraction		Acetylcholine-induced relaxation	
		Mean \pm SEM E_{max} Tension (g)	Mean \pm SEM (-Log EC_{50})	Mean \pm SEM R_{max} relaxation (%)	Mean \pm SEM (-Log EC_{50})
Lean Control	9	2.29 \pm 0.17	0.84 \pm 0.75	81.44 \pm 5.26 *	6.91 \pm 0.12
HCD Control	8	2.20 \pm 0.16 **	0.83 \pm 0.60	101.40 \pm 4.75 *	7.10 \pm 0.10 †
Lean HAART	9	2.24 \pm 0.16 **	0.96 \pm 0.71	84.46 \pm 6.88	6.84 \pm 0.15
HCD HAART	9	2.28 \pm 0.17	0.52 \pm 0.38	76.10 \pm 3.58**	6.66 \pm 0.10
Lean HAART + Saro	8	2.24 \pm 0.18	0.68 \pm 0.49	92.77 \pm 6.54	6.87 \pm 0.18
HCD HAART+Saro	8	2.13 \pm 0.15	0.84 \pm 0.45	101.00 \pm 3.12 **	7.09 \pm 0.08 † Φ
Lean Saro	8	2.45 \pm 0.21 ***	0.92 \pm 0.83	91.16 \pm 5.13	6.80 \pm 0.12
HCD Saro	8	2.28 \pm 0.18	0.80 \pm 0.31	92.58 \pm 3.24	6.81 \pm 0.09 Π

3.12.1 Phenylephrine-induced aortic contraction

The aortic response following cumulatively increasing doses of phenylephrine is shown below (Figure 3.46) as mean \pm SEM tension (g) / drug concentration in each group. The curves represent tension generated by the aortic ring from the stabilisation tension (1.5 g) at zero dosage to the maximum tension (plateau, E_{max}) at 1 μ M phenylephrine concentration. The five experimental groups that showed significant differences in the mean E_{max} are also presented separately (Figure 3.47).

phenylephrine-induced a significantly higher maximal mean tension (E_{max}) in the lean Saroglitazar-treated group (2.45 ± 0.21 g) compared to lean HAART, HCD control and HCD HAART + Saro (2.24 ± 0.16 g: $p < 0.01$, 2.20 ± 0.16 g: $p < 0.01$ and 2.13 ± 0.15 g: $p < 0.01$) respectively (Figure 3.47). After log transformation of the phenylephrine aortic-induced contraction, there were no differences noted in the mean \pm SEM of the Log EC_{50} among the experimental groups (Table 3.8 above).

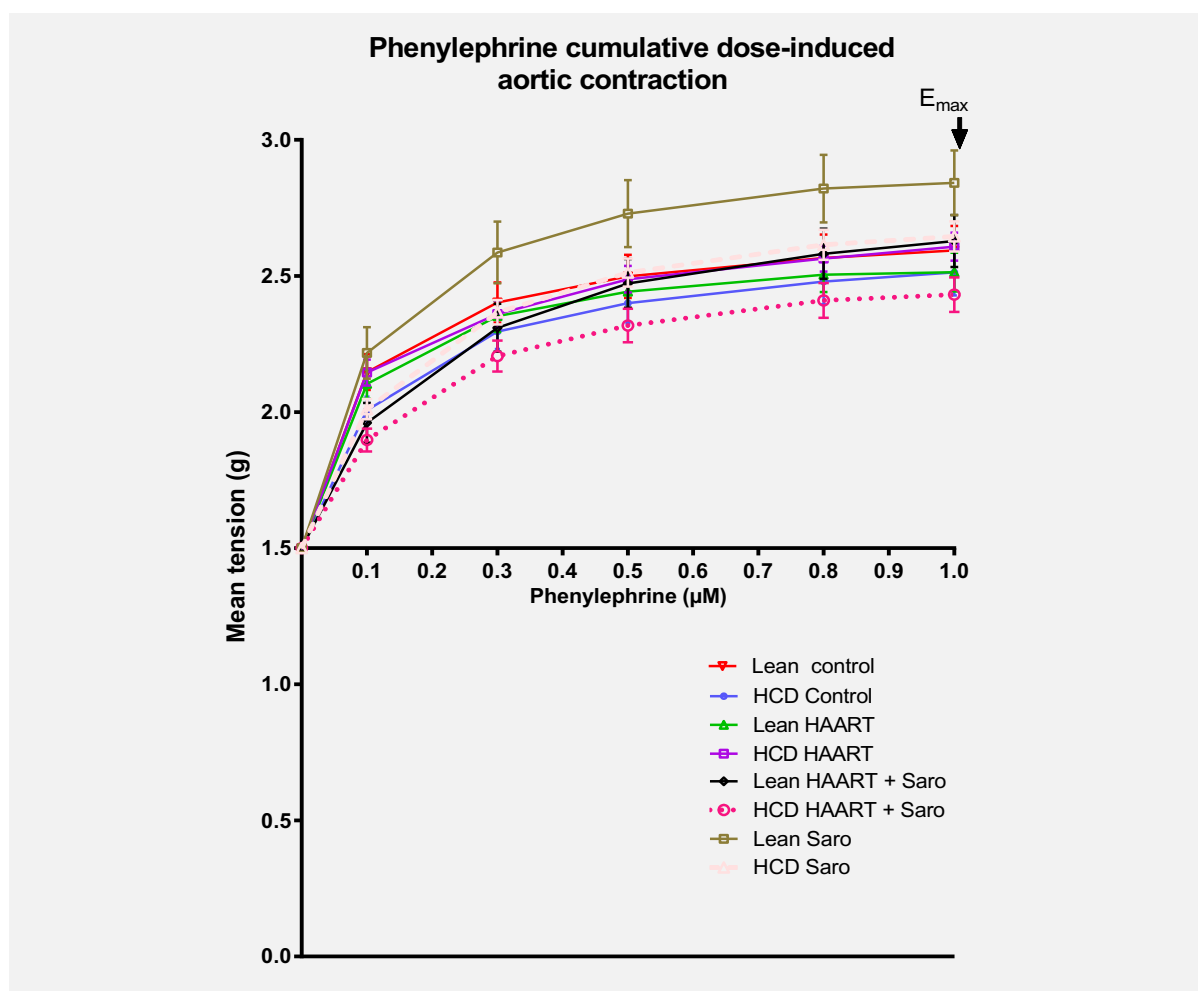


Figure 3.46 Mean phenylephrine cumulative dose-induced aortic tension (g) response curves / experimental group.

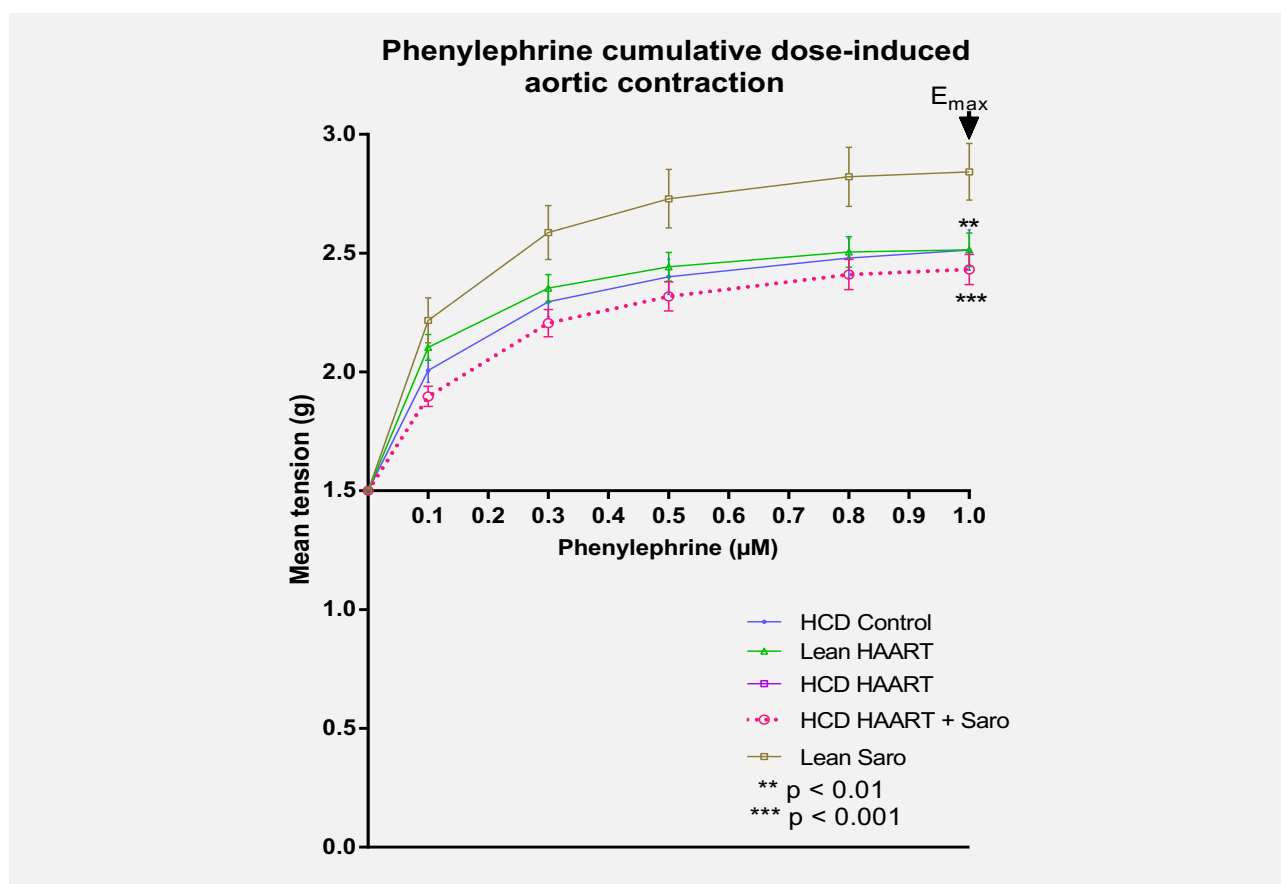


Figure 3.47 Mean phenylephrine cumulative dose-induced aortic tension (g) in the experimental groups with significant differences in the E_{max} (HCD Control, lean HAART, HCD HAART, HCD HAART + Saro and Lean Saro).

3.12.2 Acetylcholine-induced aortic relaxation

Acetylcholine cumulative dose-induced mean aortic relaxation response curves for all eight experimental groups are shown on Figure 3.48 A and the following observations were made: the mean maximal percentage acetylcholine-induced aortic relaxation, R_{max} (%) was significantly higher in the HCD control group (101.40 ± 4.75 %) compared to the lean control (81.44 ± 5.26 %, $p < 0.05$) and HCD HAART (76.10 ± 3.58 %, $p < 0.01$). Similarly, HCD HAART + Saro group mean R_{max} (101.00 ± 3.12 %) was higher compared to HCD HAART group (76.10 ± 3.58 %, $p < 0.001$) and lean control group (81.44 ± 5.26 %, $p < 0.01$) (Figure 3.48 B and Figure 3.49).

The log (X) transformed acetylcholine-induced aortic contraction curve revealed that the mean Log EC_{50} was significantly higher in the HCD HAART + Saro group (7.09 ± 0.08) compared to HCD HAART group (6.66 ± 0.10 , $p < 0.0018$). Similarly, mean Log EC_{50} was also higher in the HCD control group (7.10 ± 0.10) compared to the HCD HAART group (6.66 ± 0.10 , $p < 0.003$) and HCD Saro group (6.81 ± 0.09 , $p < 0.0303$). The nonlinear regression (curve fits) for the acetylcholine-induced aortic relaxation transform are shown in Figures 3.50 and 3.51.

The aortic responses (induced relaxation) following cumulative increasing doses of acetylcholine are shown below as mean \pm SEM (%) / drug concentration in each group (Figure 3.48). The curves represent mean percentage relaxation of the aortic ring (per group) from the maximum tension induced following cumulative doses of phenylephrine (when 30nM acetylcholine was injected) to the maximum relaxation (R_{max}) achieved following cumulative doses of acetylcholine administration.

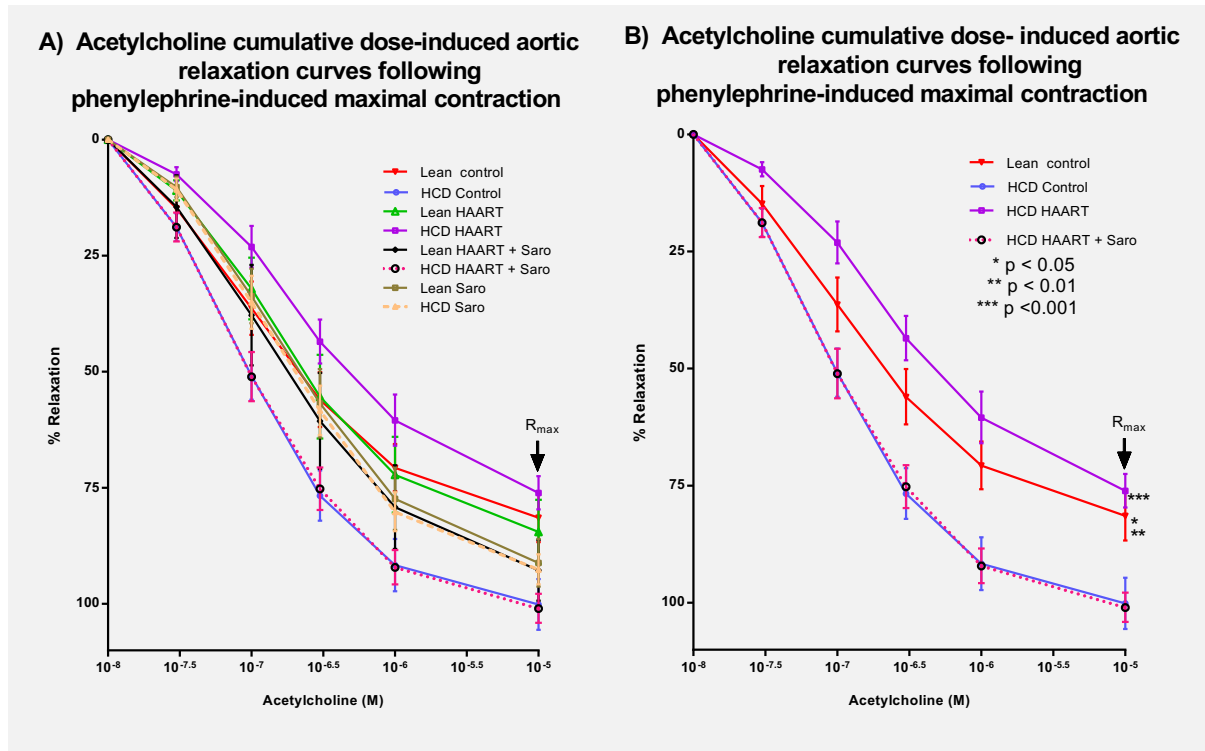


Figure 3.48 (A) Mean acetylcholine cumulative dose-induced aortic relaxation (%) response curves per experimental group. (B) Mean acetylcholine cumulative dose-induced aortic relaxation (%) in the experimental groups with significant differences in the R_{max} (lean control, HCD Control, HCD HAART, HCD HAART + Saro).

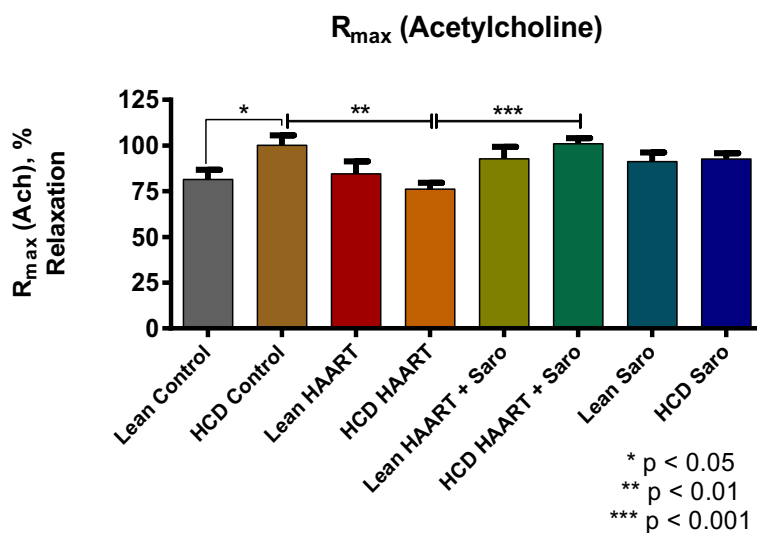


Figure 3.49 Mean acetylcholine-induced maximal aortic relaxation R_{max} (%) / experimental group.

3.12.3 Nonlinear regression for log transformation of acetylcholine dose vs. percentage aortic relaxation

To determine the EC_{50} for acetylcholine, nonlinear regression analysis was performed on the log transformed percentage aortic relaxation data using an 'agonist-dose-response curve' and results expressed as mean of the EC_{50} / group as shown below (Figure 3.50).

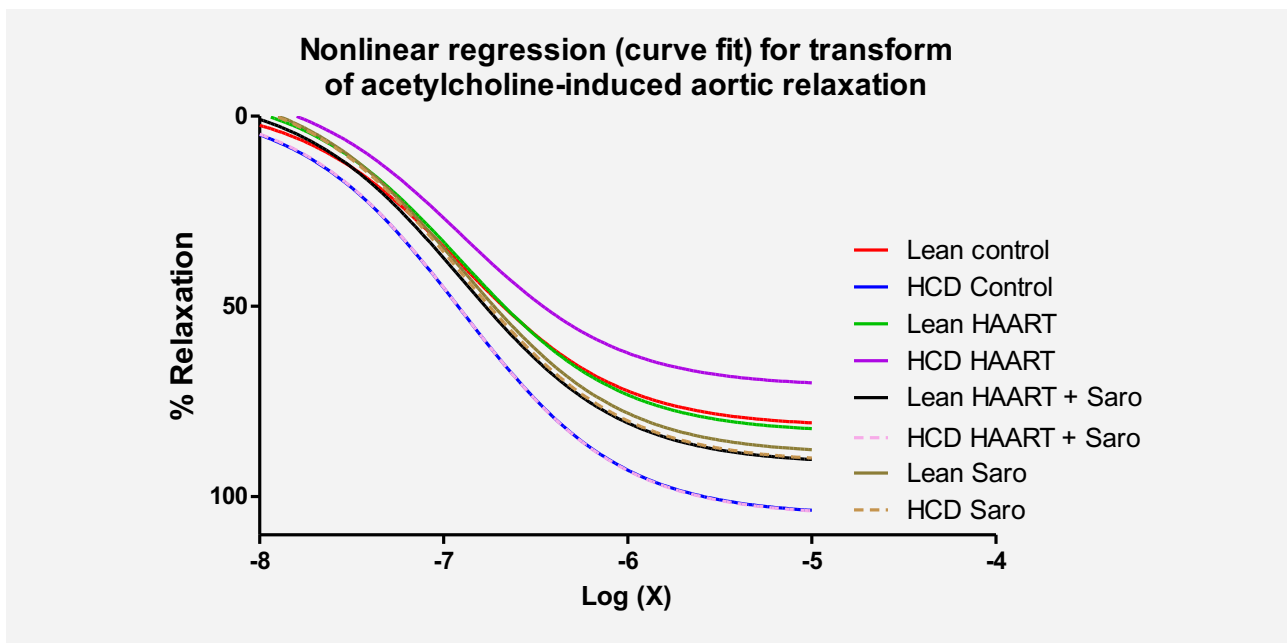


Figure 3.50 Nonlinear regression curves of all the eight experimental groups generated from the log (X) transform of acetylcholine-induced aortic relaxation (%).

After nonlinear regression analysis, it was observed that, the mean \pm SEM of the Log EC_{50} in the HCD HAART group was higher than HCD HAART + Saro group (6.66 ± 0.10 vs. 7.09 ± 0.08 ; $p = 0.0018$), HCD HAART

was higher than HCD control (6.66 ± 0.10 , vs. 7.10 ± 0.10 : $p = 0.0031$), HCD Saro was higher than HCD Control (6.81 ± 0.09 vs. 7.10 ± 0.10 : $p = 0.03$) and HCD Saro was higher than HCD HAART + Saro (6.81 ± 0.09 vs. 7.09 ± 0.08 , $p < 0.024$) (Figure 3.51 A-D).

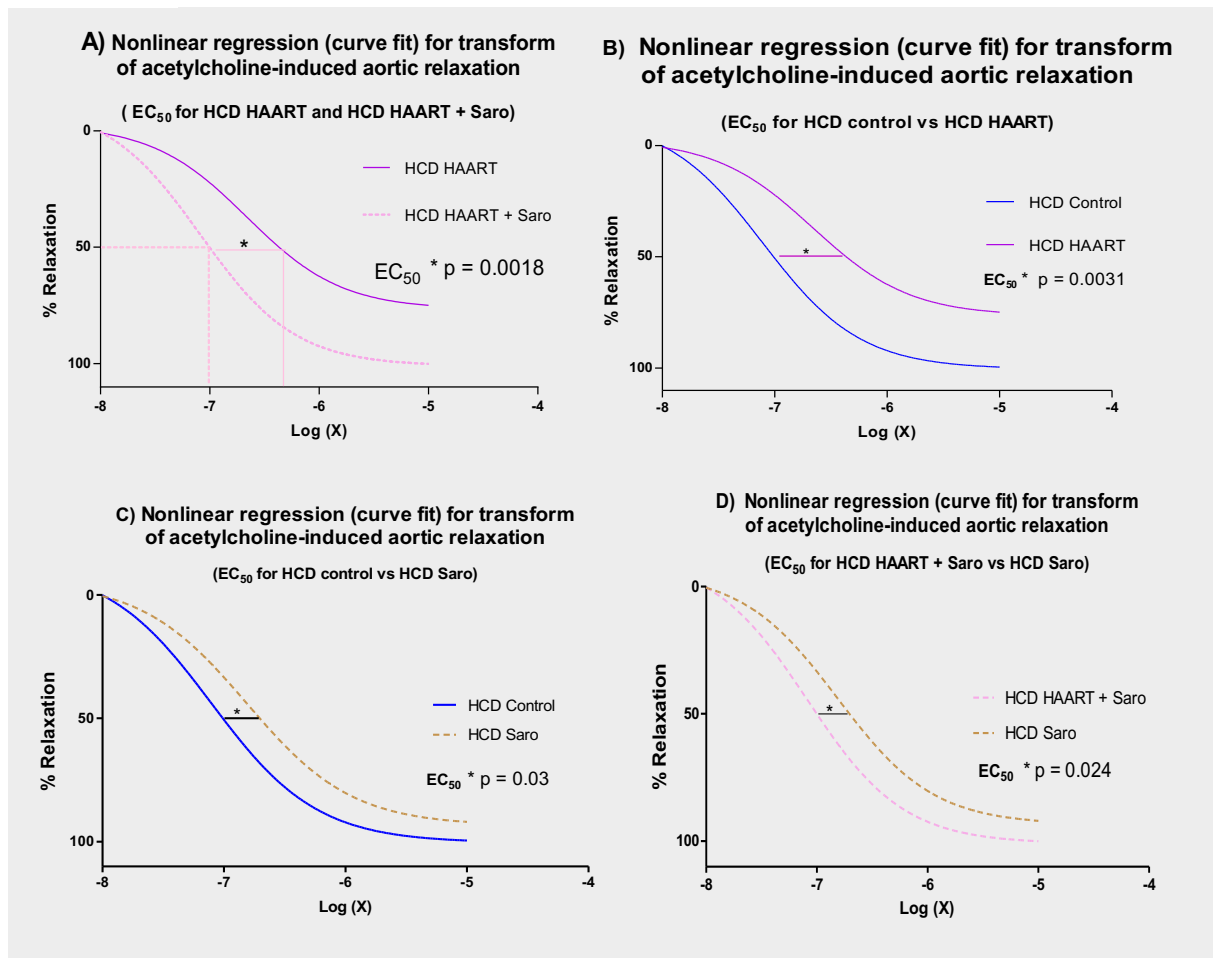


Figure 3.51 Nonlinear regression (curve fit) for log transform of mean acetylcholine-induced aortic relaxation (EC_{50}) (A) HCD HAART vs. HCD HAART + Saro group (B) HCD HAART vs. HCD control, (C) HCD Saro vs. HCD Control and (D) HCD Saro vs. HCD HAART + Saro.

3.13 Protein expression and phosphorylation measurements - Western blot analysis results

The proteins of interest that were analysed in liver, heart (non-perfused heart tissue harvested from fasted animals for baseline (pre-ischaemia) protein determination and snap frozen heart tissue following 20 minutes of global ischaemia and reperfusion), and aortic tissue samples are described in this section. The following proteins were measured: -

- i) Total and phosphorylated AMPK
- ii) Total and phosphorylated eNOS
- iii) Total and phosphorylated PKB/Akt
- iv) Total and phosphorylated Erk 1 / 2
- v) Total and phosphorylated p38
- vi) Expression of I κ B α
- vii) Expression of PGC-1 α
- viii) Expression of PPAR α
- ix) Expression of NADPH, p22-phox
- x) Expression of cleaved caspase 3
- xi) Expression of cleaved PARP

Total and phosphorylated AMPK, eNOS, PKB/Akt, Erk 1 / 2 and p38 were analysed and the ratio of the phosphorylated to total protein (phospho / total ratio) determined to assess activation of the proteins. The results are presented below, categorised per tissue i.e., heart (baseline and post-ischaemia-reperfusion), aorta and liver. For each experimental group, three biological sample replicates (n = 3 / group) were loaded onto the gels and analysed except for the standard control (only one sample loaded) as indicated on the blots displayed. The standard controls were prepared from untreated rats: liver samples were harvested and snap frozen, aorta segments were rinsed in ice cold KHB and snap frozen and hearts were exposed to stabilisation protocol of *ex-vivo* perfusion before snap freezing and subsequent storage at -80° C. The y axis represents arbitrary densitometry units calculated after normalisation of the Chemi-Hi-sensitivity blots to the stain-free-blots which are also displayed for every set of samples analysed.

3.13.1 Heart tissue protein determination

3.13.1.1 AMPK

3.13.1.1.1 AMPK: baseline / pre-ischaemia-reperfusion

No significant differences were observed in the mean total AMPK from the heart tissues analysed in the pre-ischaemic phase. n = 1 / group (standard Control) and n = 3 / group for the experimental groups (Figure 3.52).

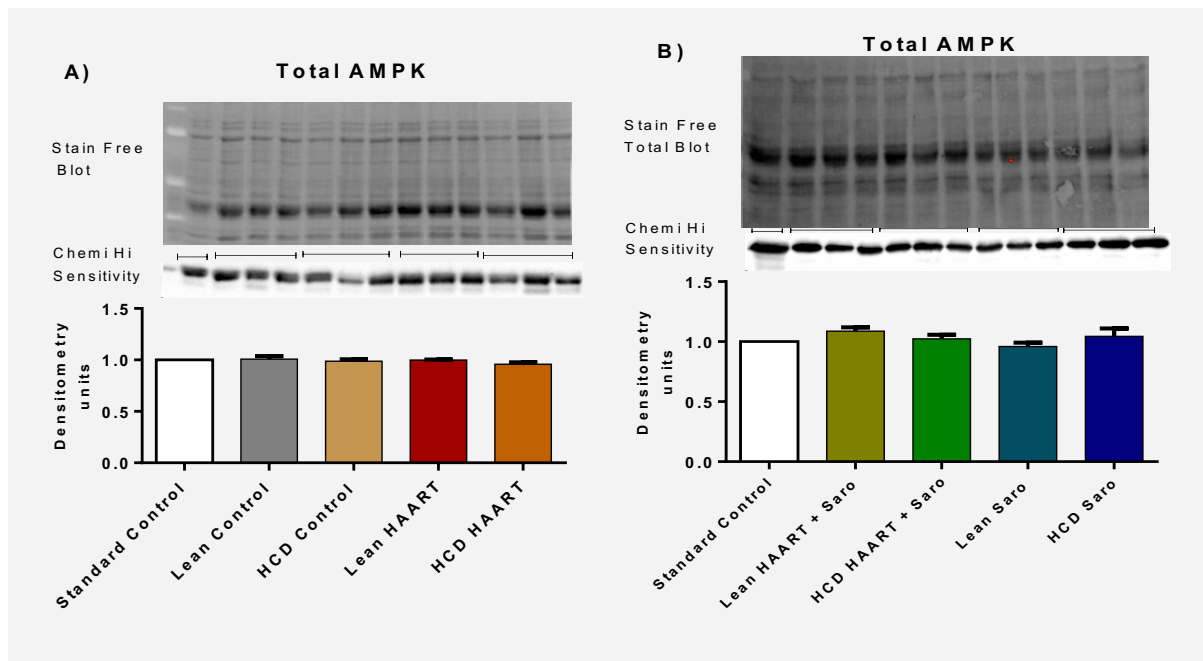


Figure 3.52 A and B- Mean pre-ischæmia cardiac total AMPK / experimental group.

The mean activated AMPK (phospho-AMPK) levels were significantly lower in the HCD control group (0.82 ± 0.05) and HCD HAART group (0.69 ± 0.08) compared to the lean control (1.07 ± 0.10 , $p < 0.05$) and lean HAART (0.94 ± 0.01 , $p < 0.05$ respectively) (Figure 3.53 A). However, the mean phospho-AMPK levels in the Saroglitazar-treated groups did not differ (Figure 3.53 B).

The phospho-AMPK / total AMPK ratios were calculated / group and no significant differences were observed between any experimental groups (Figure 3.54 A).

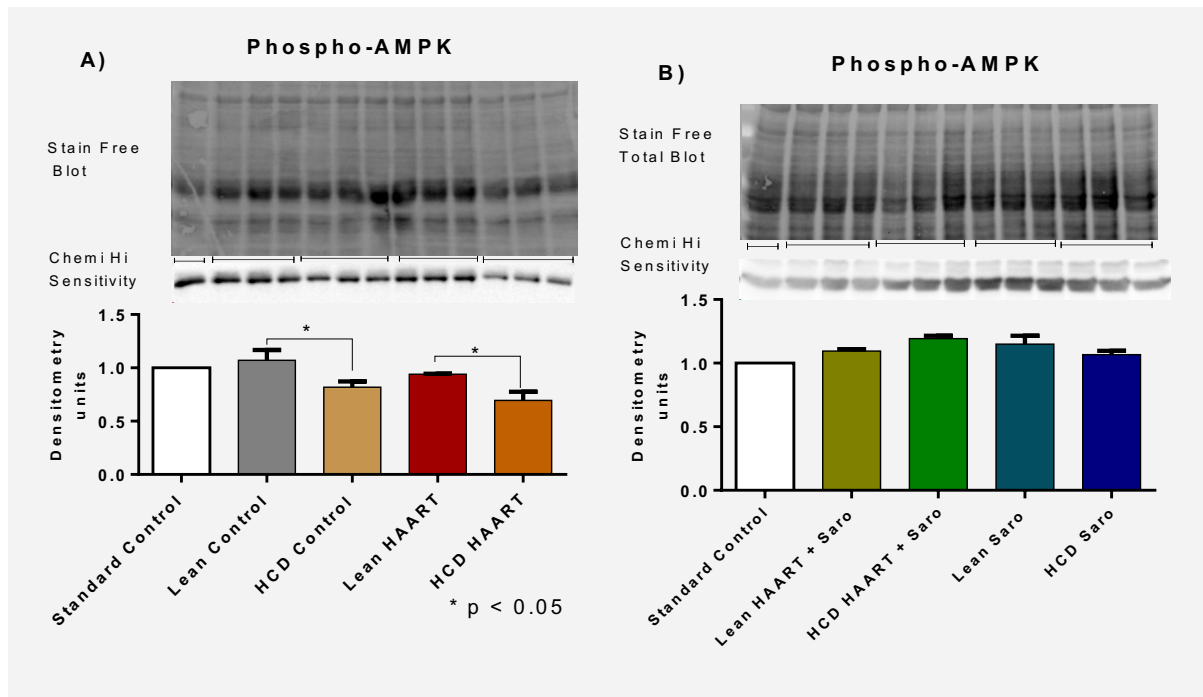


Figure 3.53 A and B. Mean pre-ischæmia phospho-AMPK / experimental group.

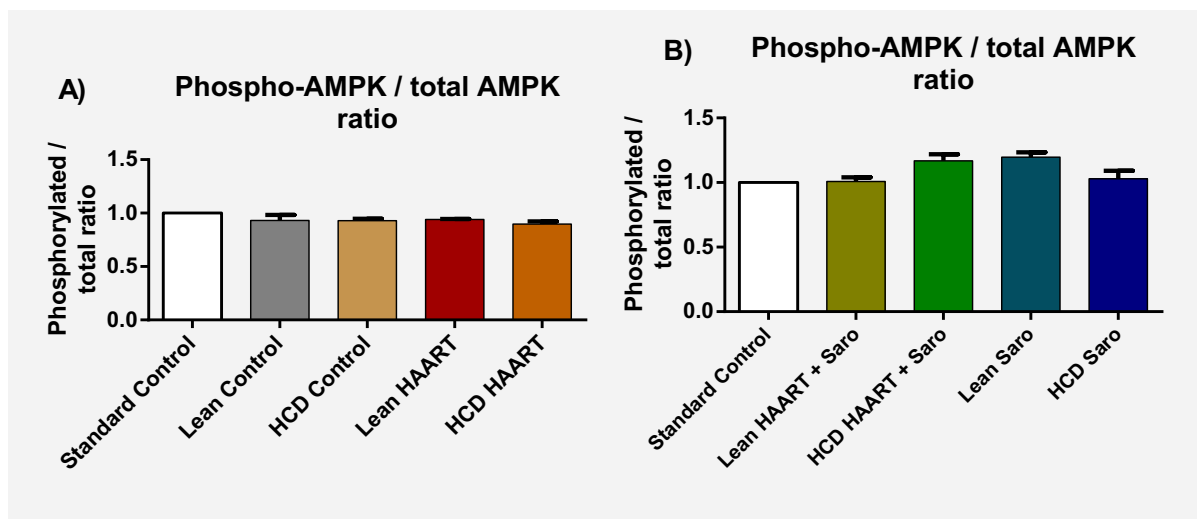


Figure 3.54 A and B. Mean pre-ischæmia phospho-AMPK / total AMPK ratio / experimental group.

3.13.1.1.2 AMPK: post-ischæmia-reperfusion

No differences were observed in the mean post-ischæmia total AMPK / group (blots not displayed). However, the mean phospho-AMPK was significantly higher in the lean Saro group (1.49 ± 0.1) compared to lean HAART + Saro (1.07 ± 0.20 , $p < 0.05$) (Figure 3.55 B). Similarly, the mean phospho-AMPK was significantly higher in the HCD Saro group (1.59 ± 0.10) compared to the HCD HAART + Saro group (1.18 ± 0.10 , $p < 0.01$). No other significant differences were observed (Figure 3.55 B). The mean post-ischæmia phospho-AMPK / total AMPK ratios were higher in the Saroglitazar (only) treated groups: HCD Saro (0.58 ± 0.03) and lean Saro (0.61 ± 0.03) compared to HCD HAART + Saro group (0.49 ± 0.05 , $p < 0.01$) and lean HAART + Saro (0.43 ± 0.03 , $p < 0.05$) respectively. There were no significant differences observed between the lean and HCD control and the HAART-treated groups (Figure 3.56).

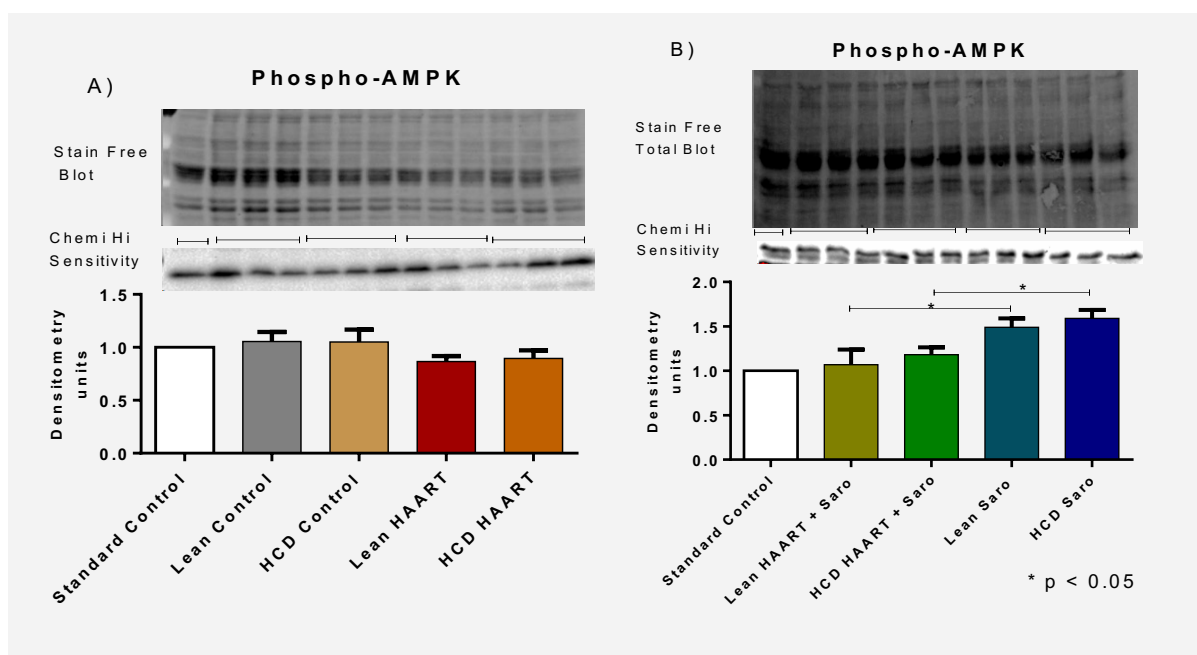


Figure 3.55 A and B. Mean post-ischæmia phospho-AMPK / experimental group.

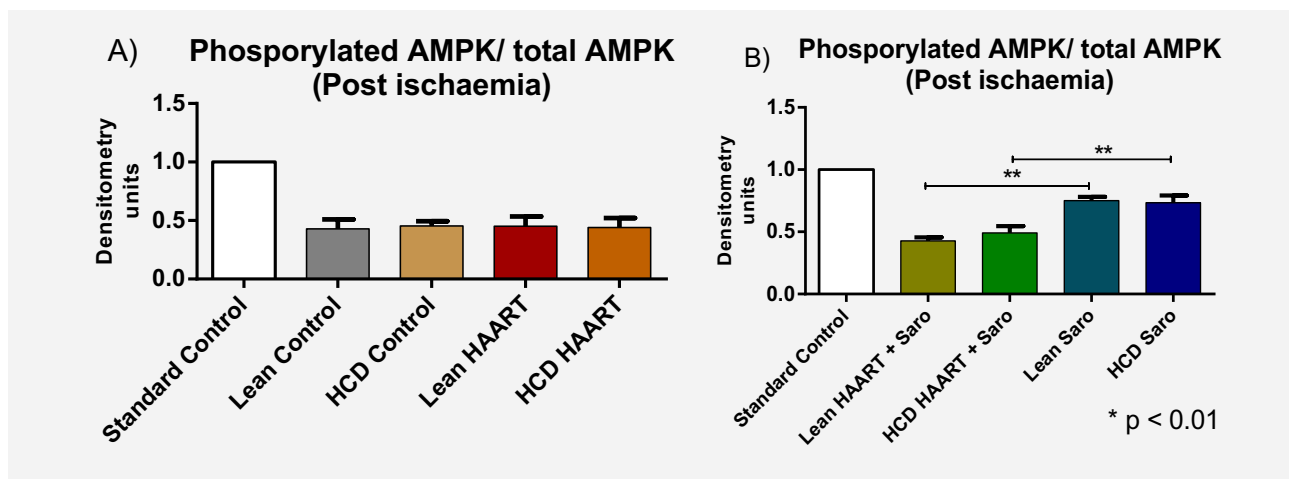


Figure 3.56 A and B Mean post-ischaemia phospho-AMPK / total AMPK ratio / experimental group.

3.13.1.2 eNOS

3.13.1.2.1 Baseline / pre-ischaemia and post-ischaemia-reperfusion

There were no significant differences observed in the total and phosphorylated eNOS levels before induction of ischaemia (results not shown). However, marked differences in the mean phospho-eNOS were observed during the post-ischaemia-reperfusion phase as described below.

3.13.1.2.2 Post-ischaemia-reperfusion

The mean post-ischaemia total and phospho-eNOS / experimental group data are shown below (Figure 3.57 and 3.58). The total expression did not differ significantly among the experimental groups (Figure 3.57).

The mean post-ischaemia phospho-eNOS was significantly lower in the HCD HAART (0.62 ± 0.06) compared to the lean HAART (0.89 ± 0.05 , $p < 0.05$) and HCD control (0.98 ± 0.02 , $p < 0.01$) (Figure 3.58 A).

The mean post-ischaemia phospho-eNOS was higher in the lean HAART + Saro group (1.08 ± 0.08) compared to lean Saro (0.61 ± 0.03 , $p < 0.01$). Similarly, the mean post-ischaemia phospho-eNOS was higher in the HCD HAART + Saro group (0.91 ± 0.03) compared to HCD Saro (0.61 ± 0.05 , $p < 0.01$) (Figure 3.58 B).

The mean ratio of the phosphorylated eNOS to total eNOS was significantly lower in the HCD HAART group (0.56 ± 0.06) compared to HCD control (0.99 ± 0.02 , $p < 0.01$) (Figure 3.59 A). However, the mean ratio was higher in the HCD HAART + Saro group (0.99 ± 0.02) compared to HCD Saro (0.59 ± 0.02 , $p < 0.01$). Similarly, the lean HAART + Saro group mean phospho-eNOS / total eNOS ratio (1.06 ± 0.20) was higher compared to lean Saro (0.76 ± 0.02 , $p < 0.01$) (Figure 3.59 B).

The mean phospho-eNOS was significantly decreased in the HCD HAART group (0.76 ± 0.04) compared to the HCD HAART + Saro group (1.03 ± 0.02 , $p < 0.01$) (Figure 3.59 C). The subsequent mean ratios of the phosphorylated eNOS to total eNOS levels in the HAART-treated groups were significantly lower in the lean HAART group (0.59 ± 0.01) compared to lean HAART + Saroglitazar group (0.85 ± 0.03 , $p < 0.01$). Similarly,

HCD HAART group mean ratio (0.62 ± 0.07) was lower compared to HCD HAART + Saro group (0.84 ± 0.03 , $p < 0.01$) (Figure 3.59 D).

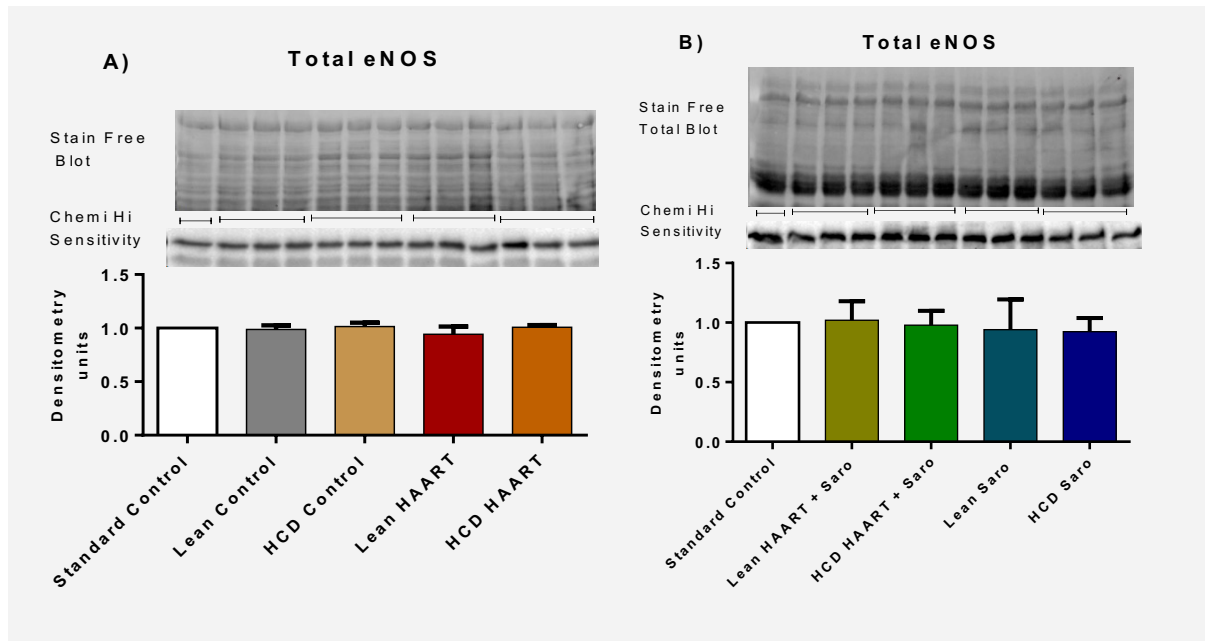


Figure 3.57 A and B. Mean post-ischæmia total eNOS / experimental group.

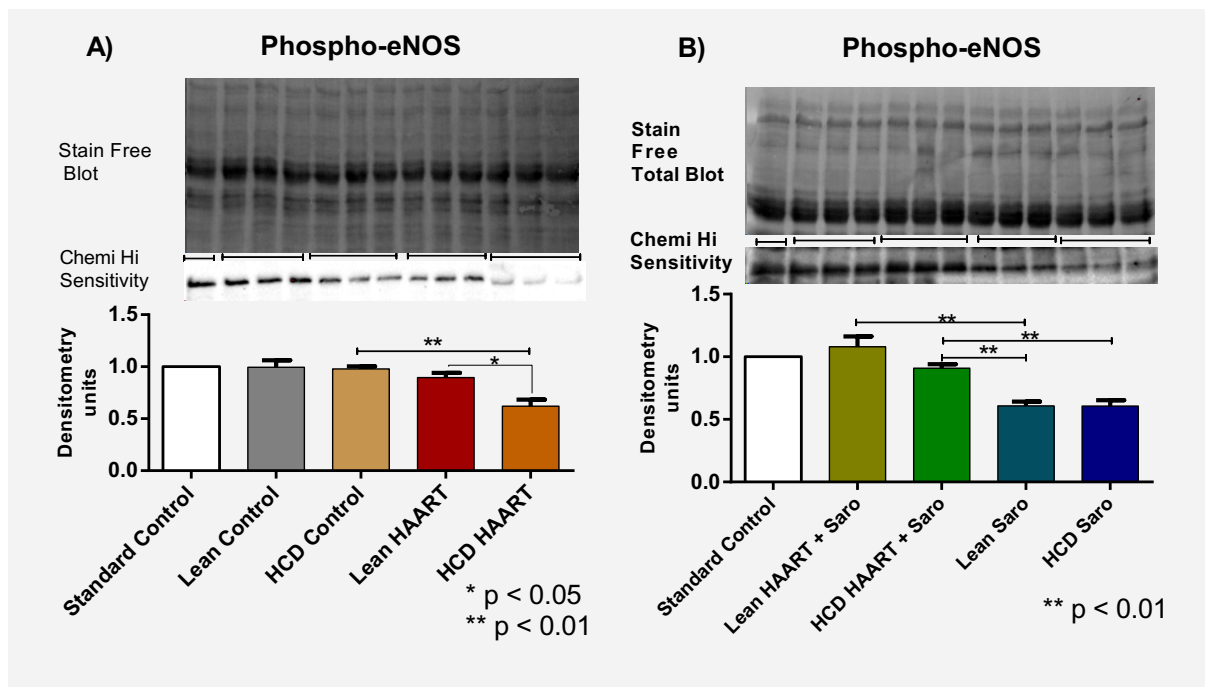


Figure 3.58 A. and B. Mean post-ischæmia phospho-eNOS / experimental group.

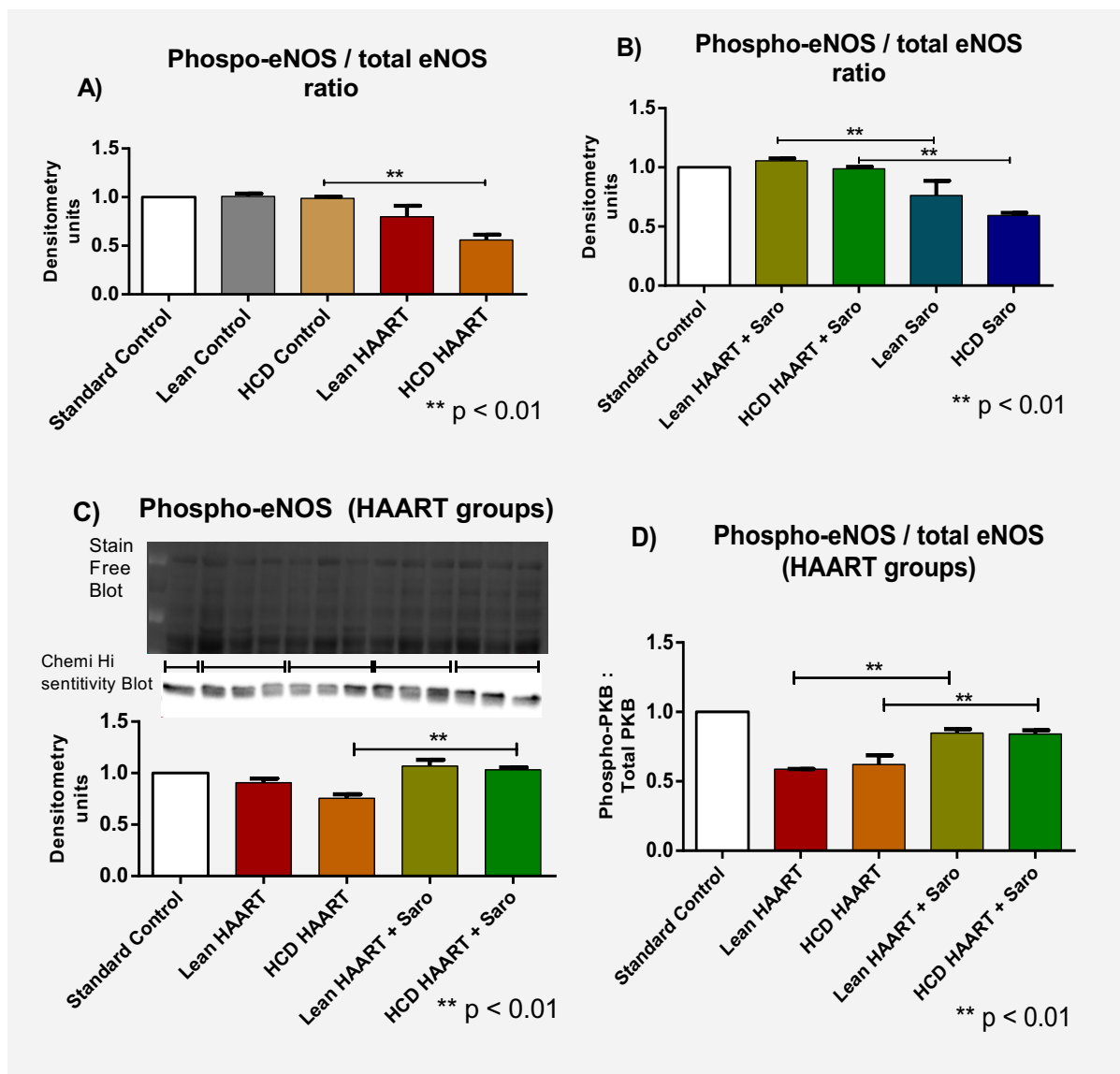


Figure 3.59 A, B and D Mean post-ischaemia phospho-eNOS / total eNOS ratio / experimental group. C. Mean post-ischaemia phospho-eNOS / experimental group.

3.13.1.3 PKB / Akt

3.13.1.3.1 Baseline / before induction of ischaemia

Analysis of the total and phosphorylated PKB /Akt in the heart tissue before induction of ischaemia and reperfusion revealed no significant differences among the experimental groups. However, following induction of ischaemia and subsequent reperfusion, significant differences were observed in PKB /Akt activation as described below.

3.13.1.3.2 Post-ischaemia-reperfusion

The mean post-ischaemia PKB / Akt expression and activation finding are presented below; (Figures 3.60 and Figure 3.61). No significant differences were observed in the mean total PKB expression / experimental group in heart tissues processed after ischaemia-reperfusion (Figure 3.60 A and B).

The mean post-ischaemia phospho-PKB / Akt showed significant decreases in the lean HAART group (0.51 ± 0.05) and HCD HAART group (0.44 ± 0.07) compared to the lean control (0.83 ± 0.1 , $p < 0.05$) and HCD control (0.78 ± 0.15 , $p < 0.05$) respectively (Figure 3.61 A). The mean post-ischaemia phospho-PKB / Akt levels in the Saroglitazar-treated groups did not differ.

A comparison of the post-ischaemia mean values for phospho-PKB / Akt in the HAART-treated groups showed that, the mean phospho-PKB / Akt was higher in the lean HAART + Saro group (1.14 ± 0.02) compared to the lean HAART group (0.90 ± 0.06 , $p < 0.01$) and the mean phospho-PKB / Akt was higher in the HCD HAART + Saro group (1.09 ± 0.03) compared to the HCD HAART group (0.92 ± 0.05 , $p < 0.01$) (Figure 3.61 C).

The mean phospho-PKB / Akt / total PKB / Akt ratios were significantly higher in the HAART + Saro treated groups (lean HAART + Saro 0.85 ± 0.06 , HCD HAART + Saro 0.75 ± 0.04) compared to the HAART (only) treated groups (lean HAART 0.52 ± 0.07 , $p < 0.01$ HCD HAART 0.05 ± 0.02 , $p < 0.01$ respectively (Figure 3.61 D).

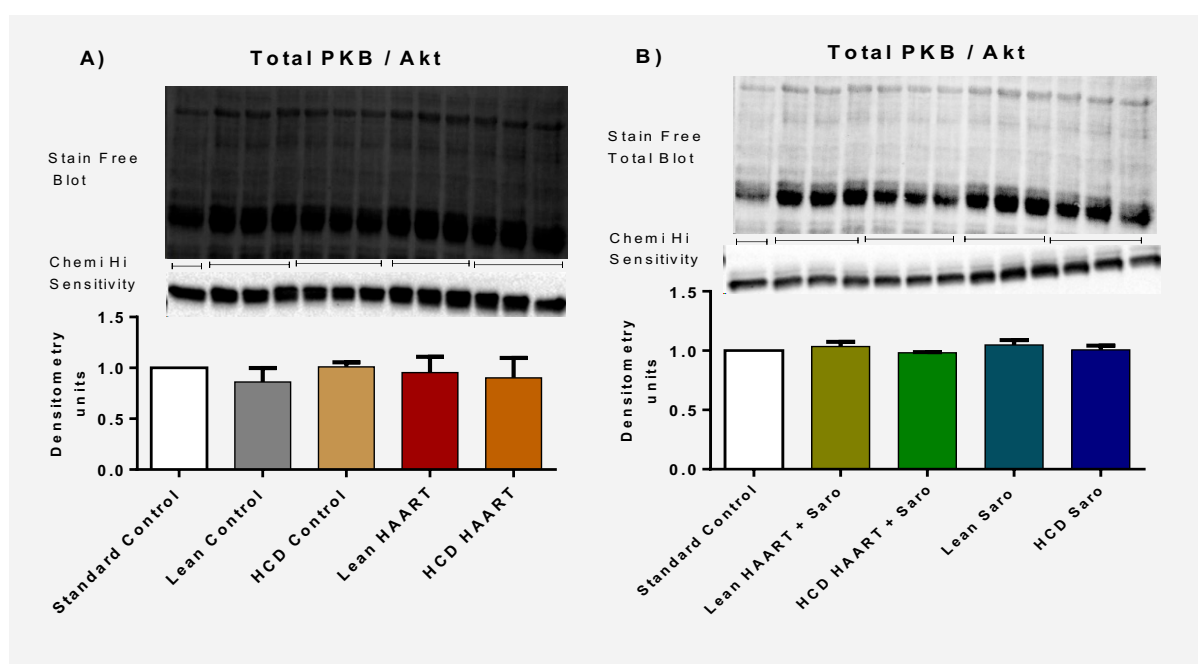


Figure 3.60 A and B. Mean total post ischaemia total PKB / experimental group.

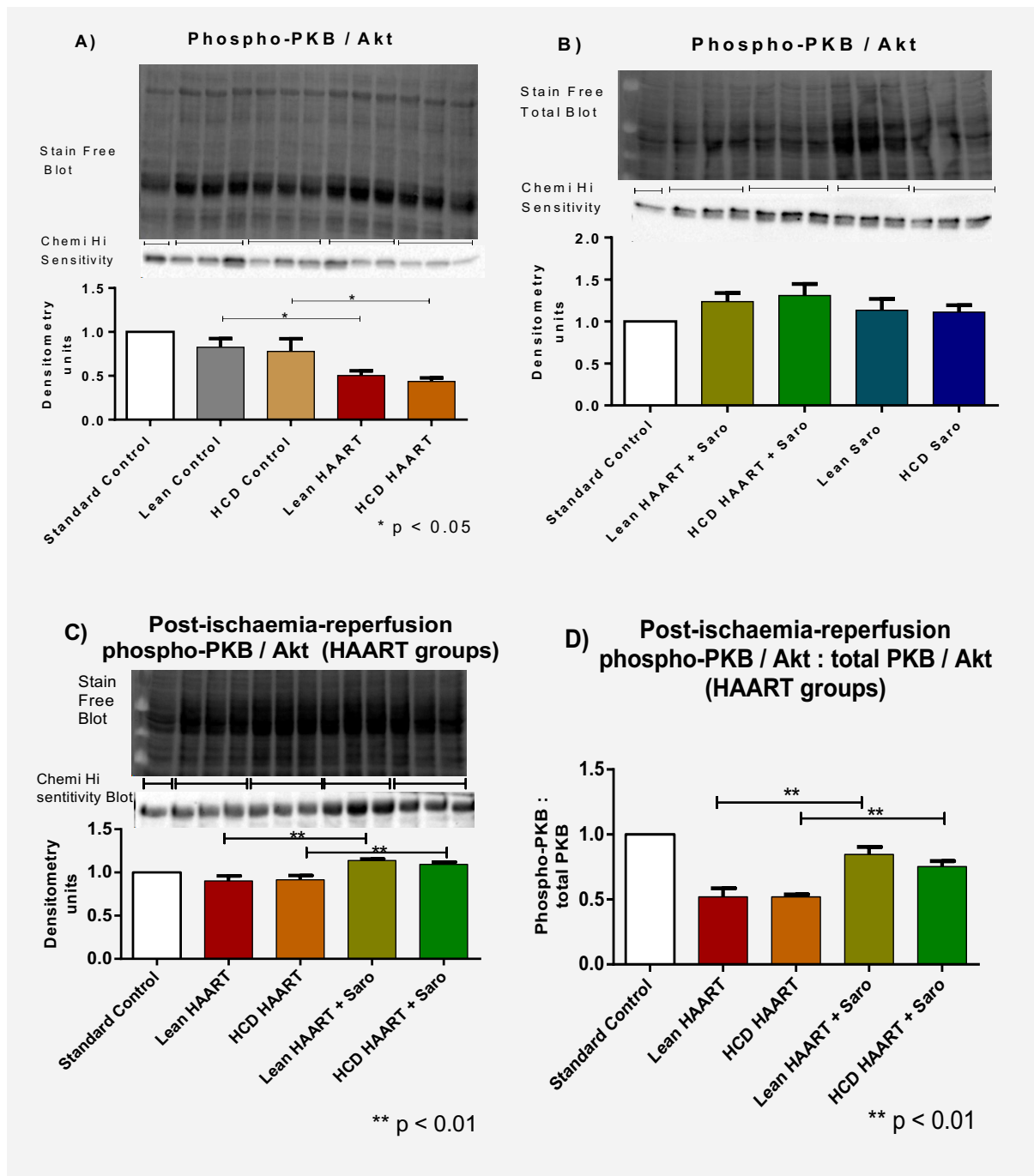


Figure 3.61 A-C Mean post-ischaemia phospho-PKB / experimental group and D mean post-ischaemia phospho-PKB / total PKB ratio / experimental group.

3.13.1.4 Erk 1 / 2

3.13.1.4.1 Baseline / pre-ischaemia-reperfusion

The mean pre-ischaemia total and phosphorylated Erk 1 / 2 levels showed no significant differences between any of the experimental groups. The mean phospho / total Erk ratio / experimental group are shown below (Figure 3.62).

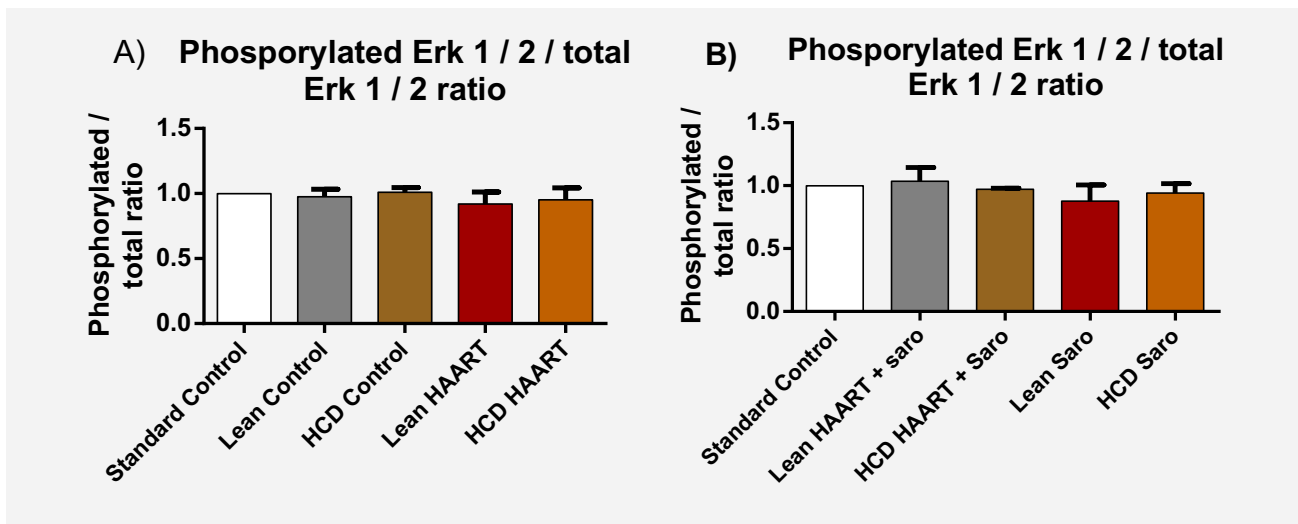


Figure 3.62 A and B. Mean pre-ischæmia phospho-Erk 1 / 2: total Erk 1 / 2 ratio / experimental group.

3.13.1.4.2 Post-ischæmia-reperfusion

Following 35 minutes of regional ischaemia, the total Erk expression remained equal in all the experimental groups (Figure 3.63 A and B).

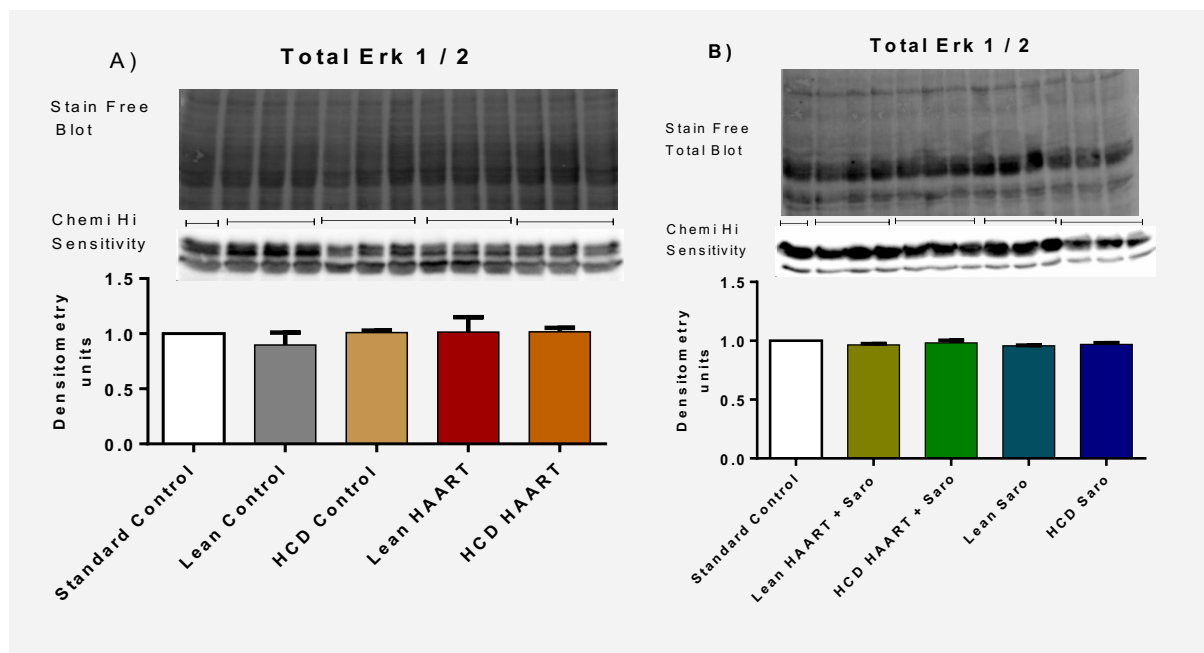


Figure 3.63 Mean post-ischæmia total expression of Erk 1 / 2 / experimental group.

The mean phospho-Erk 1 / 2 expression was higher in the HCD control group compared to the HCD HAART group (Figure 3.64). However, the mean phospho-Erk 1 / 2 : total Erk 1 / 2 ratios were not statistically different following ischaemia-reperfusion.

The mean post-ischæmia phospho-Erk 1 / 2 was higher in the HCD control group compared to the HCD HAART group (1.28 ± 0.04 vs. 0.72 ± 0.01 , $p < 0.01$, respectively) and higher than lean control (1.28 ± 0.04 vs. 0.79 ± 0.01 , $p < 0.01$) (Figure 3.64 A). However, no significant differences were observed among lean

HAART + Saro, HCD HAART + Saro, Lean Saro and HCD Saro groups although the trend indicated an increase in the HCD HAART + Saro group and lean Saro group compared to their respective controls (Figure 3.64 B).

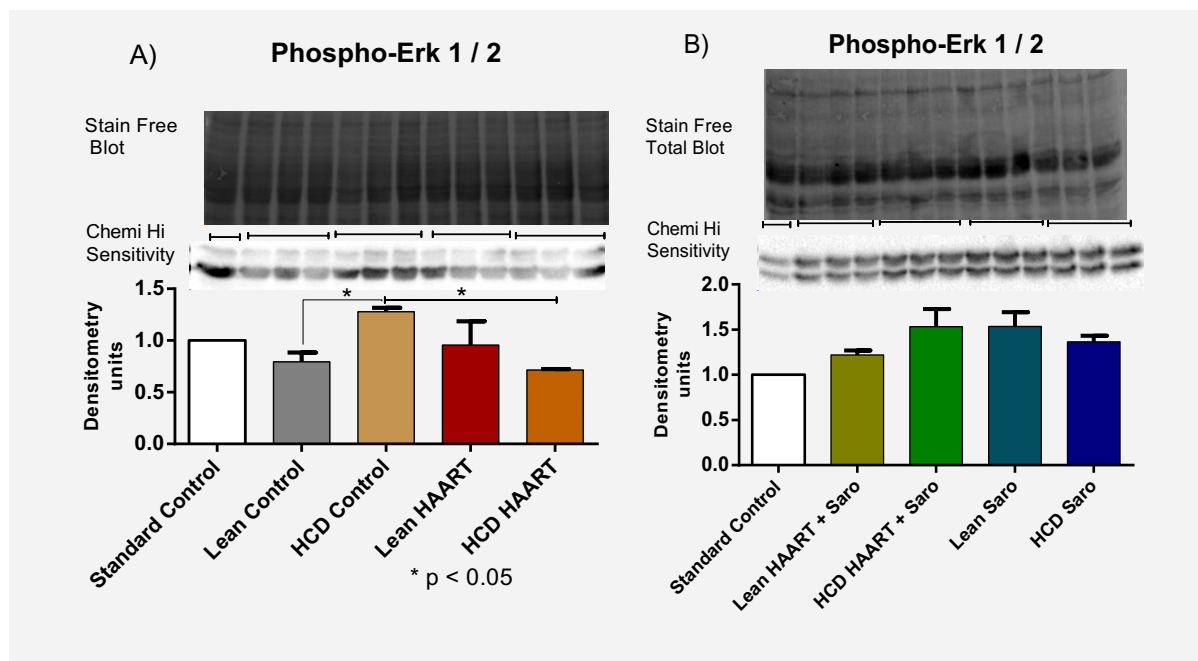


Figure 3.64 A and B-mean post-ischæmia phospho-Erk1 / 2 / experimental group.

3.13.1.5 p38

3.13.1.5.1 Pre-and post-ischæmia-reperfusion

No differences were observed in the expression and activation of p38 in heart tissue lysates before induction of ischaemia and subsequent reperfusion. Similarly, following 20 minutes of global ischaemia and 10 minutes of reperfusion, the total and phosphorylated forms of p38 remained constant in all the experimental groups (Figure 3.65 A and B). Although the trend indicated an increase in the phosphorylated forms in the treated groups, (Figure 3.66 A), there were no significant differences between the HAART-treated groups and the untreated control groups.

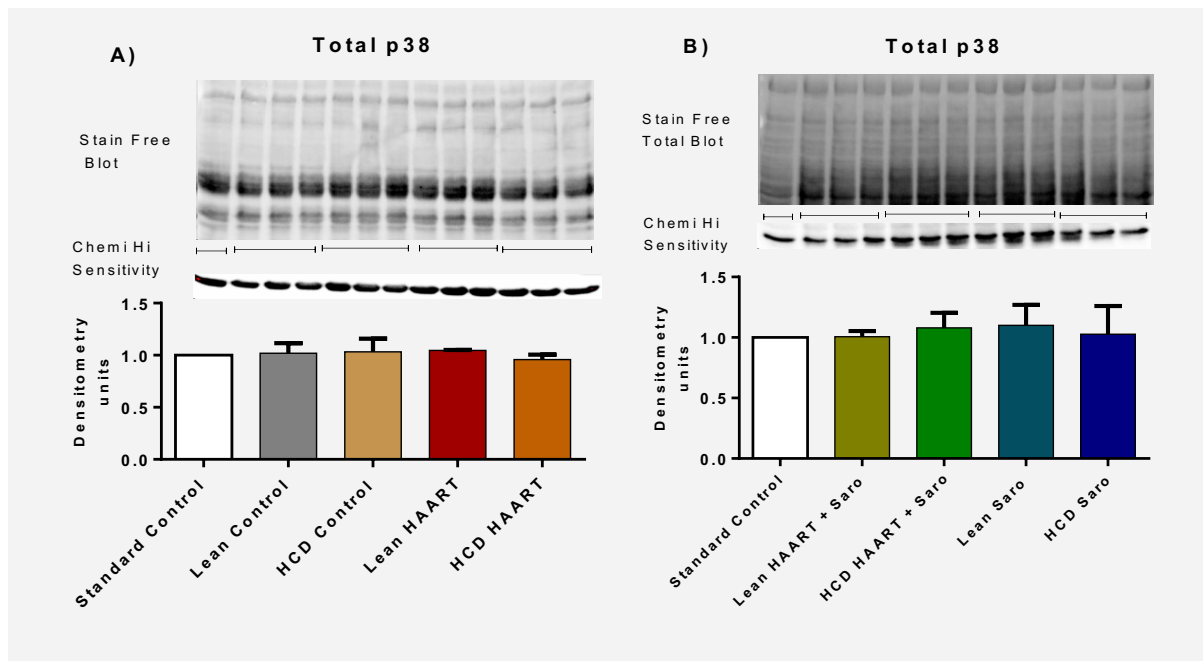


Figure 3.65 A and B Mean post-ischaemia-reperfusion total p38 / experimental group.

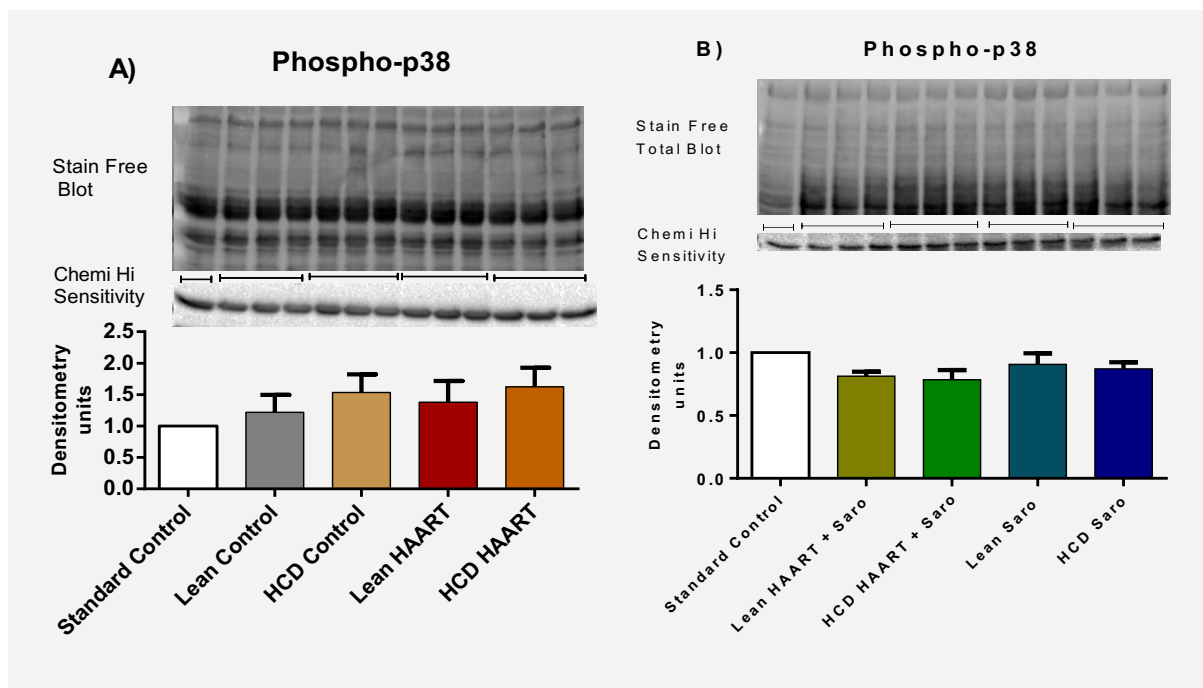


Figure 3.66 A and B Mean post-ischaemia-reperfusion total phospho-p38 / experimental group.

3.13.1.6 Pre-and post-ischaemia I κ B α , PGC-1 α and PPAR α expression

Tissue lysates from non-perfused and post-ischaemia-reperfused hearts did not show any differences in the mean I κ B α , PGC-1 α and PPAR α expression / experimental group. However, all groups had increased mean I κ B α expression following induction of ischaemia compared to the pre-ischaemia I κ B α , expression. This trend was also observed in the PGC-1 α expression but in contrast, PPAR α expression was higher in the non-perfused tissues compared to the post-ischaemia-reperfused PPAR α expression (Table 3.9).

The mean percentage change (increase) in the mean post-ischaemia I κ B α was higher in the HCD HAART + Saro (62.62 \pm 2.62 %) compared to HCD control (34.47 \pm 2.40 %, # p < 0.05); HCD HAART (37.44 \pm 3.13 %, # p < 0.05) and HCD Saro (38.22 \pm 3.24 %, # p < 0.05). Similarly, the mean percentage change (increase) in the mean post-ischaemia PGC-1 α was higher in the HCD HAART (72.35 \pm 4.21 %) compared to HCD control (37.56 \pm 2.31 %, * p < 0.05); HCD HAART + Saro (49.43 \pm 3.20 %, * p < 0.05) and HCD Saro (54.62 \pm 3.51 %, * p < 0.05) (Table 3.9).

The mean percentage change (decrease) in the mean post-ischaemia PPAR α was higher in the HCD control (-40.58 \pm 4.50 %) compared to HCD HAART (-29.24 \pm 3.62 %, ϕ p < 0.05) and HCD HAART + Saro (-23.66 \pm 3.45 %, ϕ p < 0.05). On the other hand, the mean percentage change (decrease) in the mean post-ischaemia PPAR α was lower in the lean Saro group (-10.32 \pm 5.43 %) compared to lean control (30.92 \pm 3.22, ‡ p < 0.05) lean HAART (29.71 \pm 4.62, ‡ p < 0.05) and Lean HAART + Saro (24.34 \pm 2.92, ‡ p < 0.05) (Table 3.9).

*Table 3.9. Mean expression of pre-and post-ischaemia I κ B α , PGC-1 α and PPAR α (mean \pm SEM of normalised volume intensities, densitometry units relative to control) and their mean percentage change in pre-ischaemia expression following ischaemia-reperfusion. Symbols: # p < 0.05, ‡ p < 0.05 and * p < 0.05 (significant group differences are specified above).*

Protein Expression	Lean Control	HCD Control	Lean HAART	HCD HAART	Lean HAART + Saro	HCD HAART + Saro	Lean Saro	HCD Saro
I κ B α , Pre-ischaemia	0.71 \pm 0.06	0.77 \pm 0.02	0.69 \pm 0.07	0.70 \pm 0.02	0.73 \pm 0.04	0.63 \pm 0.05	0.72 \pm 0.04	0.75 \pm 0.03
Post-ischaemia	1.02 \pm 0.05	1.03 \pm 0.02	1.00 \pm 0.05	0.97 \pm 0.05	1.02 \pm 0.05	1.03 \pm 0.06	1.01 \pm 0.02	1.02 \pm 0.03
% change	41.36 \pm 2.23	34.97 \pm 2.40	42.22 \pm 3.62	37.44 \pm 3.13	40.62 \pm 2.13	62.62 \pm 5.62 #	41.66 \pm 3.51	38.22 \pm 3.24
PGC-1 α Pre-ischaemia	0.87 \pm 0.04	0.85 \pm 0.04	0.78 \pm 0.03	0.77 \pm 0.03	0.87 \pm 0.05	0.95 \pm 0.07	0.64 \pm 0.04	0.82 \pm 0.04
Post-ischaemia	1.25 \pm 0.08	1.16 \pm 0.10	1.31 \pm 0.07	1.34 \pm 0.05	1.50 \pm 0.06	1.41 \pm 0.06	1.22 \pm 0.05	1.26 \pm 0.05
% change	42.33 \pm 2.22	37.56 \pm 2.31	65.69 \pm 4.3	72.35 \pm 4.21*	71.23 \pm 3.92	49.43 \pm 3.20	87.34 \pm 3.31	54.62 \pm 3.51
PPAR α Pre-ischaemia	0.97 \pm 0.05	1.01 \pm 0.04	0.92 \pm 0.04	0.95 \pm 0.05	1.03 \pm 0.08	0.97 \pm 0.05	0.87 \pm 0.03	0.94 \pm 0.05
Post-ischaemia	0.67 \pm 0.03	0.59 \pm 0.03	0.67 \pm 0.04	0.68 \pm 0.03	0.77 \pm 0.04	0.76 \pm 0.02	0.79 \pm 0.03	0.61 \pm 0.02
% change	-30.92 \pm 3.22	-40.58 \pm 4.50 ϕ	-29.71 \pm 4.62	-29.24 \pm 3.62	-24.34 \pm 2.92	-23.66 \pm 3.45	-10.32 \pm 5.43 ‡	36.83 \pm 3.74

3.13.1.7 NADPH, p22-phox

3.13.1.7.1 Pre-and post-ischaemia expression of p22-phox

No differences were observed in the mean p22-phox expression among the experimental groups before induction of ischaemia (Figure 3.67 A). However, the mean expression of p22-phox subunit was significantly lower in the HCD HAART + Saroglitazar group (0.75 ± 0.03) compared to the HCD HAART (0.98 ± 0.02 , $p < 0.01$). Similarly, the mean expression was also reduced in the lean HAART Saro group (0.87 ± 0.05) compared to the lean HAART group (1.00 ± 0.02 , $p < 0.01$) (Figure 3.67 B).

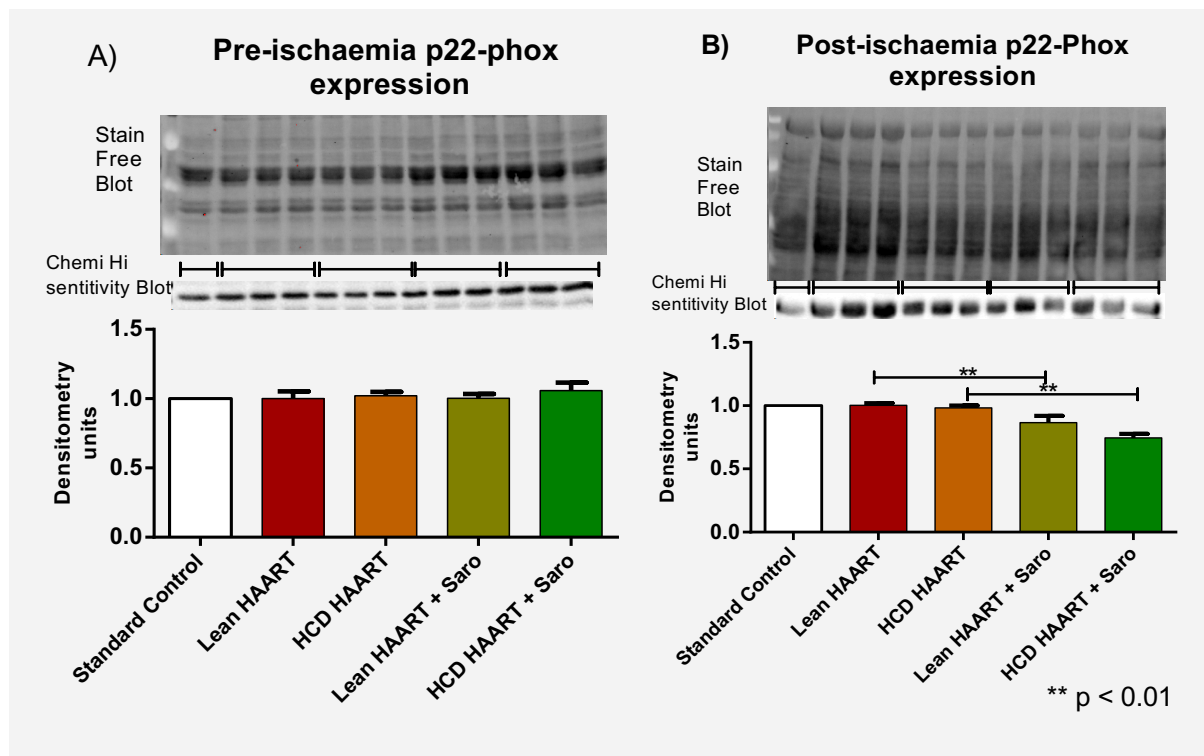


Figure 3.67 A Mean pre-ischaemia p22-phox expression / experimental group and B, mean post-ischaemia expression of p22-phox / experimental group.

3.13.1.8 Cleaved caspase 3

No significant differences were observed in the mean pre-ischaemic expression of caspase 3 / experimental group. However, following ischaemia-reperfusion, the HCD HAART group had significantly higher expression (1.55 ± 0.04) compared to lean HAART (1.17 ± 0.12 , $p < 0.01$) and HCD control group (0.90 ± 0.2 , $p < 0.01$) (Figure 3.68 A). Subsequently, following ischaemia-reperfusion, a comparison of the HAART-treated groups showed that, the mean expression of caspase 3 in the HCD HAART group (1.20 ± 0.11) and lean HAART group (1.06 ± 0.08) were significantly higher compared to HCD HAART + Saroglitazar group (0.35 ± 0.14 , $p < 0.05$) and lean HAART + Saroglitazar group (0.39 ± 0.16 , $p < 0.05$) respectively (Figure 3.68 B).

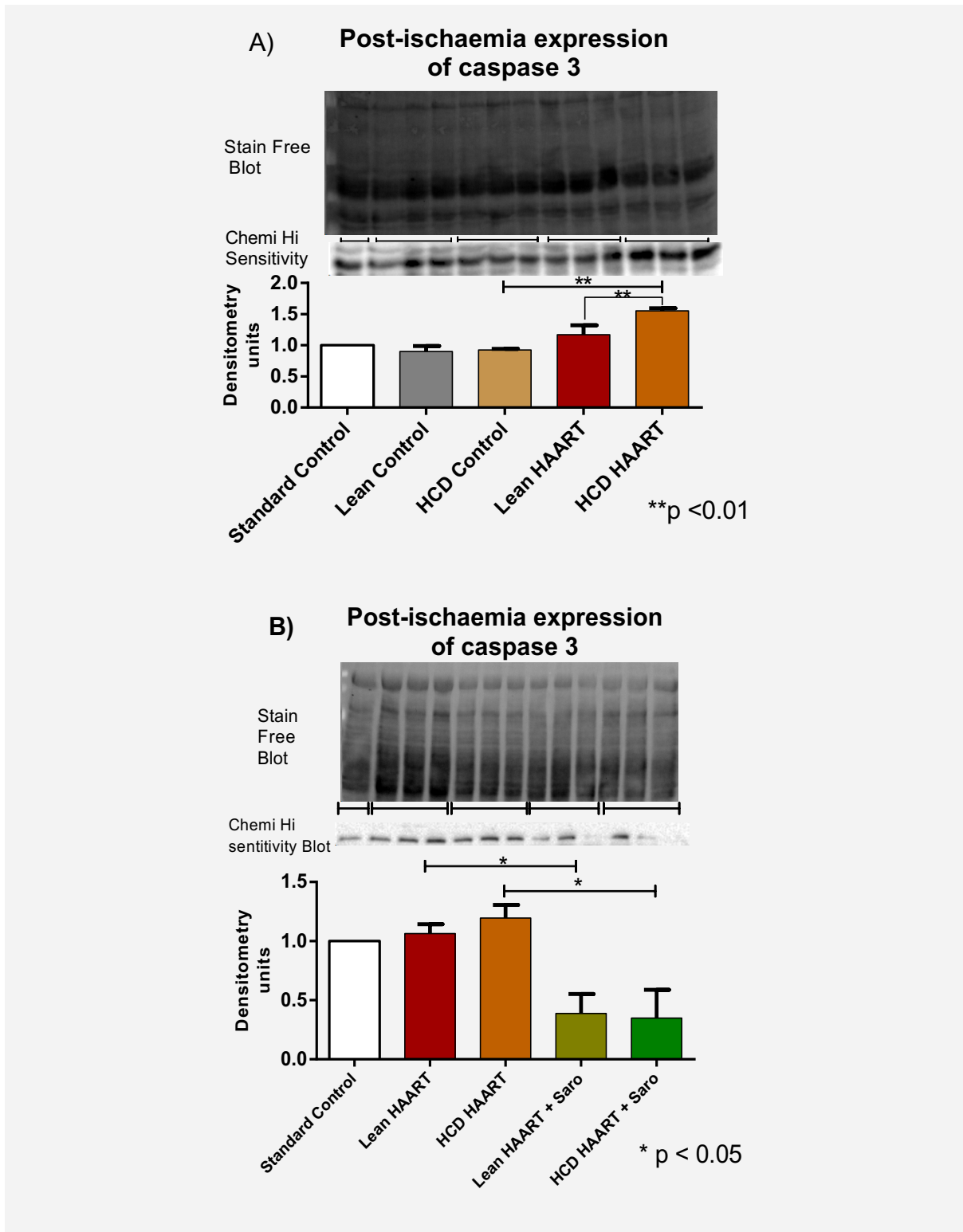


Figure 3.68 A and B. Mean post -ischæmia cleaved caspase 3 expression / experimental group.

3.13.1.9 Cleaved PARP

Although no differences were observed in the expression of cleaved PARP before induction of ischaemia, following ischaemia-reperfusion, the mean cleaved PARP expression was significantly higher in the HCD control (1.68 ± 0.18) compared to the lean control (1.06 ± 0.09 , $p < 0.01$). Also, the mean post-ischaemia expression of cleaved PARP in the HCD HAART group (2.17 ± 0.06) was significantly higher compared to the HCD control group (1.68 ± 0.18 , $p < 0.05$). On the other hand, the lean HAART group mean expression of cleaved PARP (1.73 ± 0.03) was significantly higher than the lean control group (1.06 ± 0.09 , $p < 0.01$) (Figure 3.69 A).

Following induction of ischaemia and reperfusion, the mean cleaved PARP for the HCD HAART + Saro group (1.55 ± 0.11) was significantly lower than lean HAART + Saro group (2.34 ± 0.08 , $p < 0.0001$) and HCD Saro (2.72 ± 0.13 , $p < 0.0001$) (Figure 3.69 B).

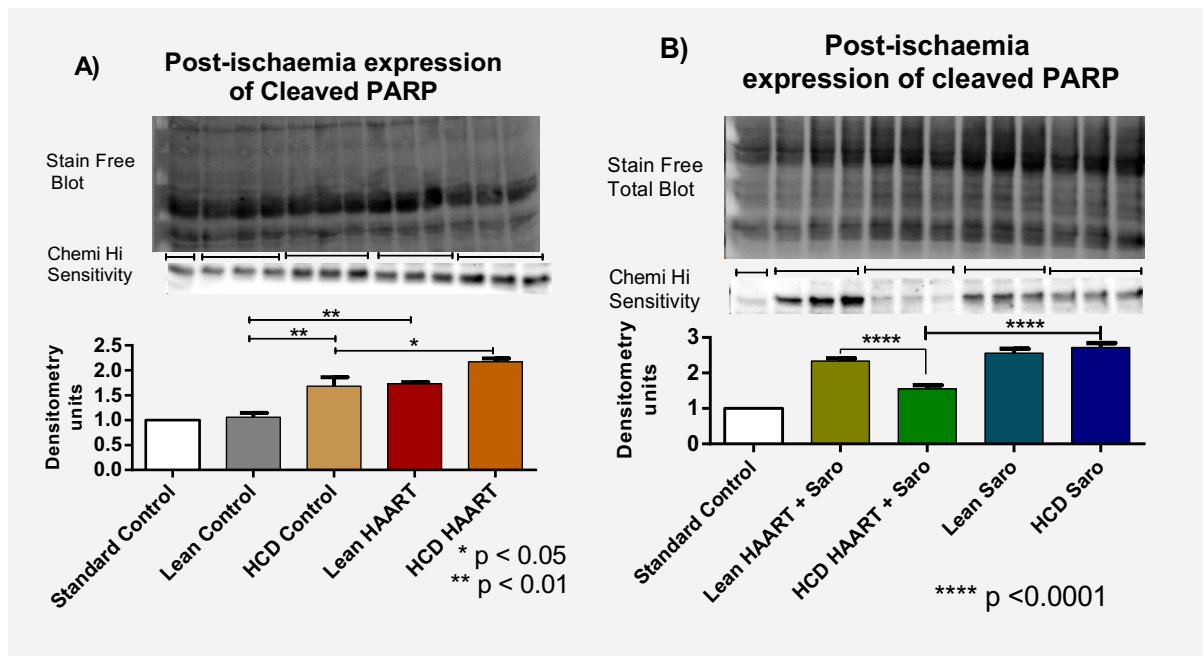


Figure 3.69 A and B. Mean post-ischaemia expression of cleaved PARP / experimental group.

3.13.2 Aortic tissue protein determination

3.13.2.1 eNOS

No significant differences were observed in the mean total eNOS expression / experimental group. However, phosphorylated eNOS levels were significantly higher in the Saroglitazar-treated groups compared to the HAART-treated groups and similar trends were observed with the phospho-eNOS / total eNOS ratios. Subsequently, the mean phospho-eNOS / total eNOS ratios were significantly higher in: the lean control group (0.74 ± 0.02) compared to the lean HAART group (0.52 ± 0.04 , $p < 0.05$), lean HAART + Saroglitazar (0.73 ± 0.02) compared to lean HAART group (0.52 ± 0.04 , $p < 0.05$), HCD control (0.71 ± 0.01) compared to HCD HAART (0.56 ± 0.02 , $p < 0.05$), HCD HAART + Saro (0.75 ± 0.03) compared to HCD HAART (0.56 ± 0.02 ,

$p < 0.05$), lean Saro (0.83 ± 0.09) compared to lean HAART (0.52 ± 0.04 , $p < 0.01$) and HCD Saro (0.85 ± 0.08) compared to HCD HAART (0.56 ± 0.02 , $p < 0.01$) (Figure 3.70).

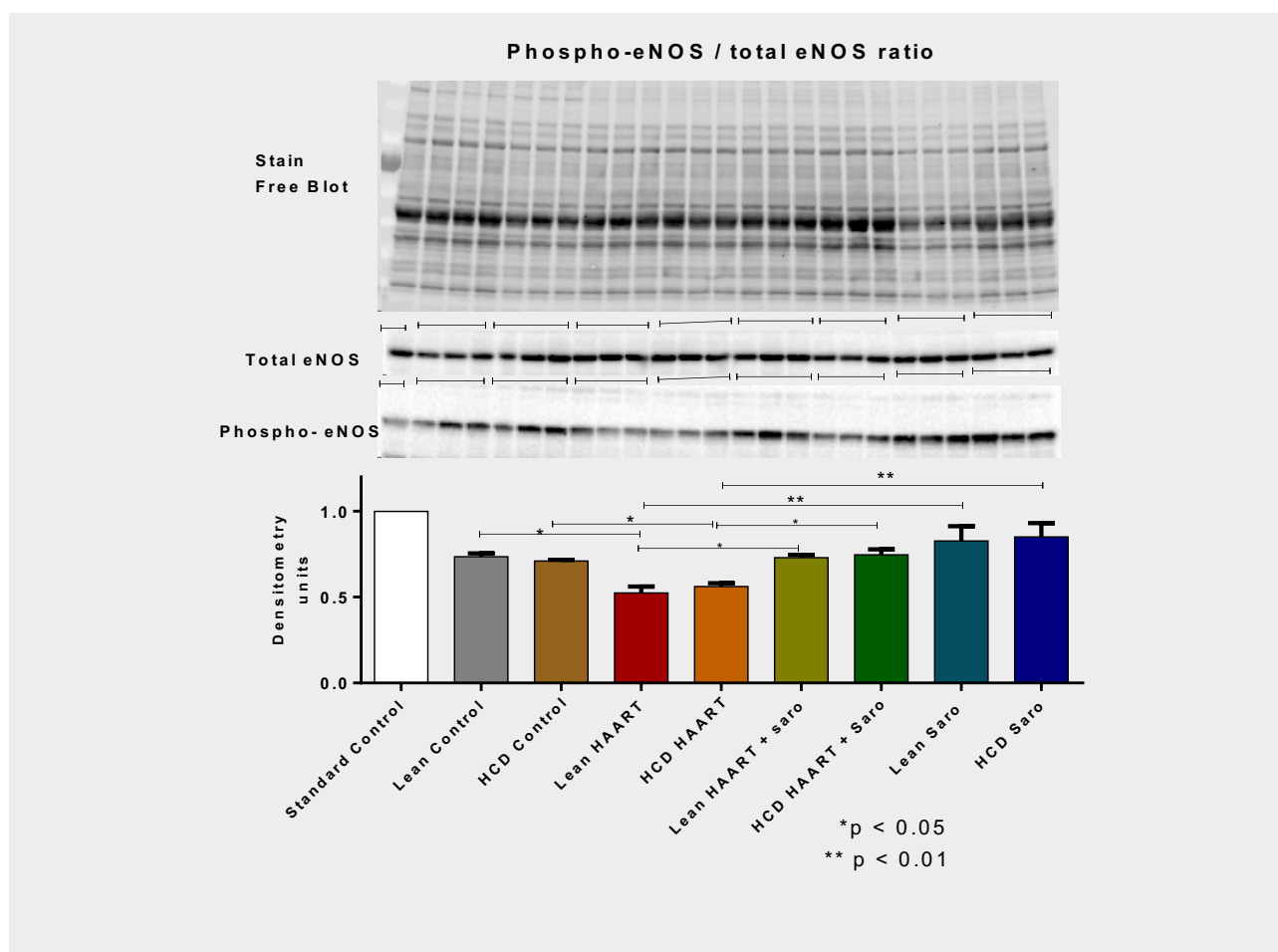


Figure 3.70 Mean aortic phospho-eNOS / total eNOS ratio / experimental group.

3.13.2.2 PKB / Akt

No differences were observed in the mean total PKB / Akt / experimental group (Figure 3.71).

The mean phospho-PKB / Akt was higher in the following groups: - HCD control vs. lean control (1.010 ± 0.001 vs. 0.900 ± 0.010 , $p < 0.01$ respectively), HCD control vs. HCD HAART (1.010 ± 0.001 vs. 0.960 ± 0.010 respectively, $p < 0.01$), lean HAART Saro vs. lean HAART (1.000 ± 0.003 vs. 0.930 ± 0.002 respectively, $p < 0.01$), HCD HAART + Saro vs. HCD HAART (0.990 ± 0.005 vs. 0.960 ± 0.008 respectively, $p < 0.01$) and lean Saro vs. HCD Saro (0.980 ± 0.005 vs. 0.903 ± 0.005 respectively, $p < 0.01$) (Figure 3.72).

The mean phospho-PKB / Akt / total PKB / Akt was significantly higher in the: HCD control group (1.030 ± 0.006) compared to lean control group (0.900 ± 0.150 , $p < 0.001$), HCD HAART + Saro (0.950 ± 0.010) compared to HCD HAART (0.900 ± 0.009 , $p < 0.01$), lean HAART + Saro (0.970 ± 0.004) compared to lean HAART (0.910 ± 0.010 , $p < 0.01$) and lean Saro (0.950 ± 0.011) compared to HCD Saro (0.910 ± 0.006 , $p < 0.01$) (Figure 3.73).

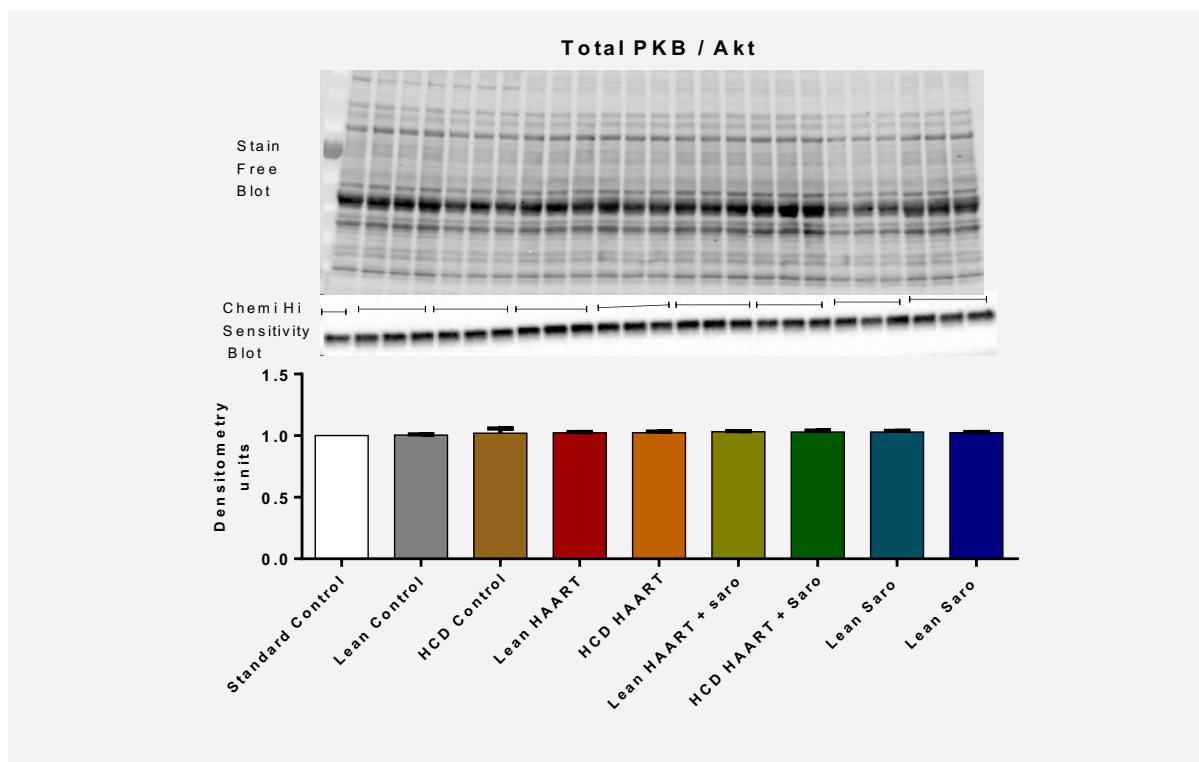


Figure 3.71 Mean aortic total PKB / Akt expression / experimental group.

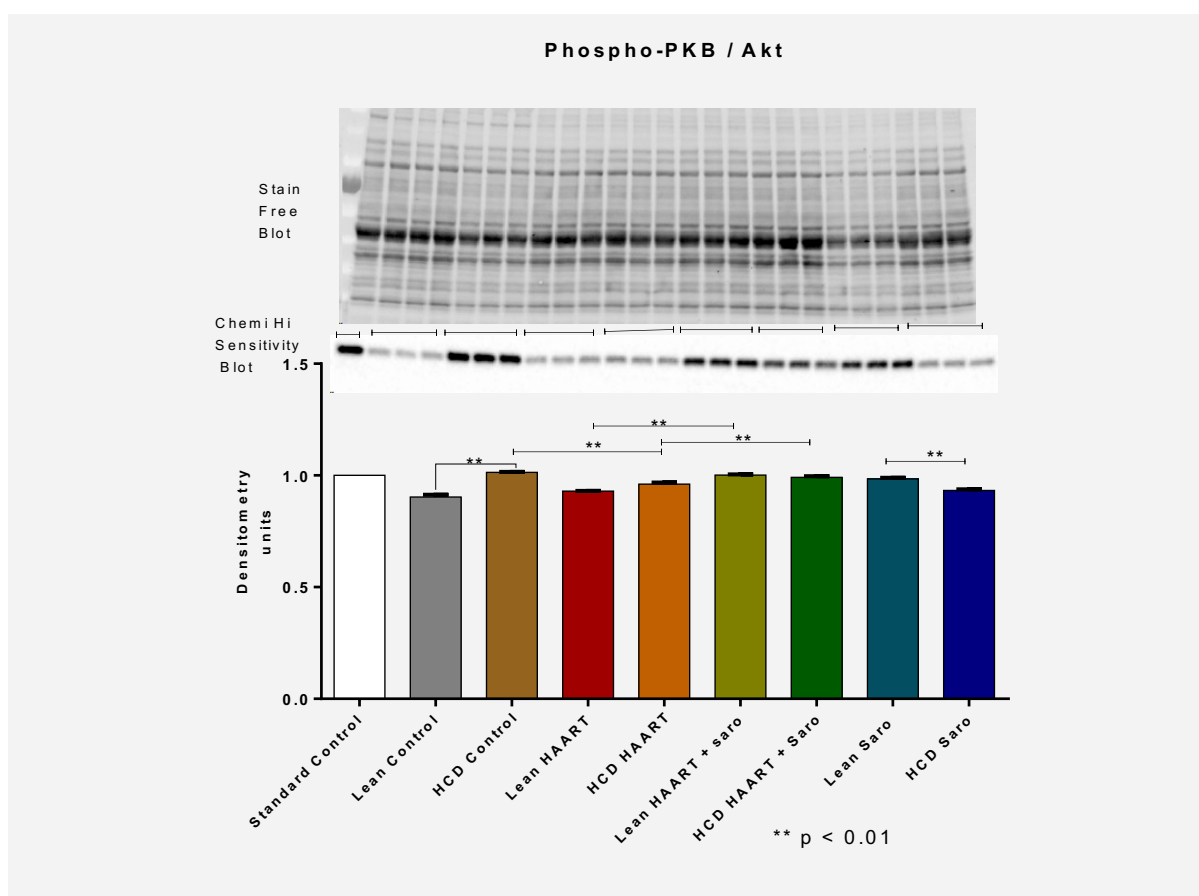


Figure 3.72 Mean aortic phospho-PKB / Akt expression / experimental group.

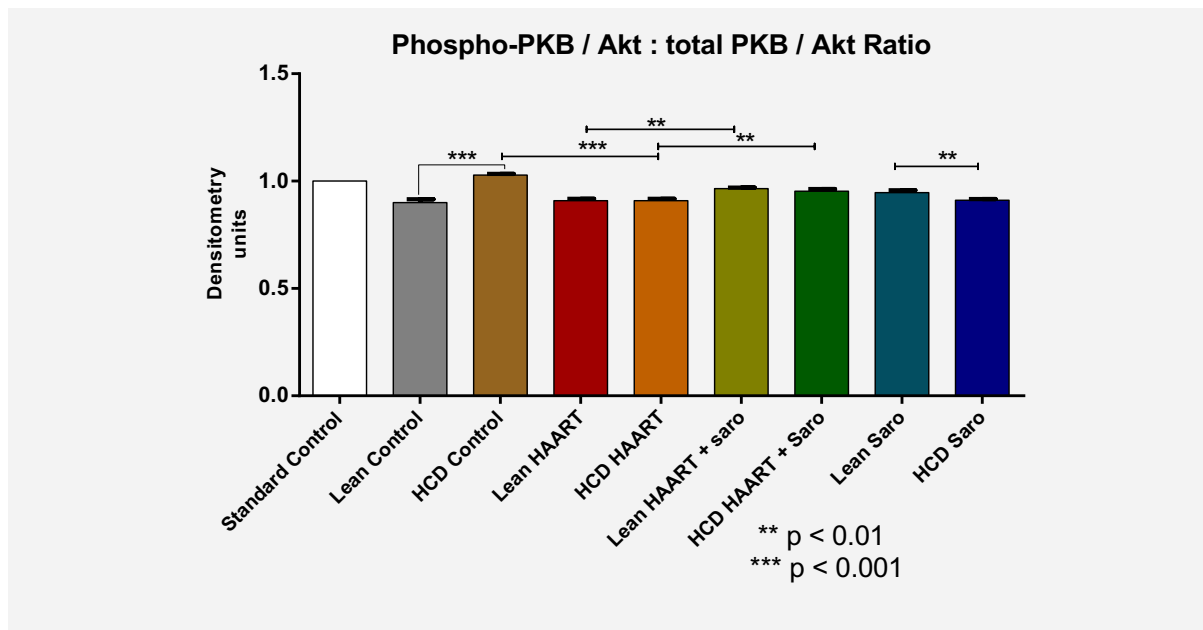


Figure 3.73 Mean aortic phospho-PKB / Akt : total PKB / Akt ratio / experimental group.

3.13.2.3 Erk 1 / 2

The mean aortic total and phospho-Erk 1 / 2 did not differ among the experimental groups (Figure 3.74)

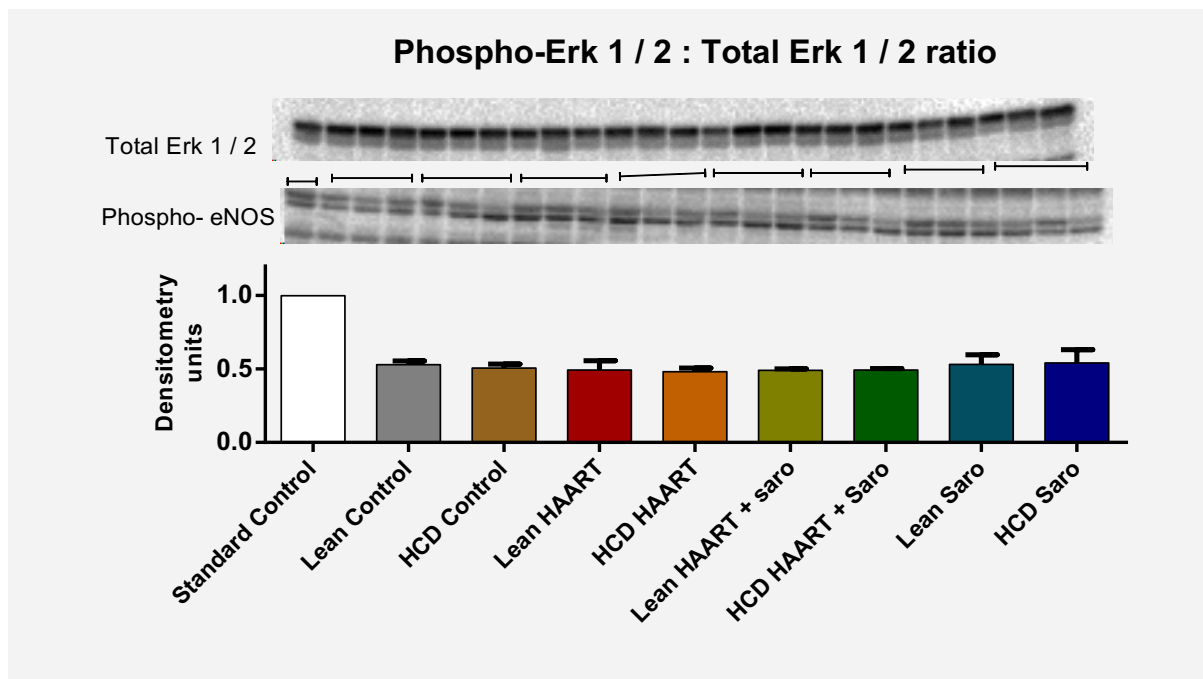


Figure 3.74 Mean aortic phospho-Erk 1 / 2 / total Erk 1 / 2 / experimental group.

3.13.2.4 IκBα

The mean aortic IκBα expression / experimental group was only significantly lower in the lean Saroglitazar-treated group compared to the lean control (0.74 ± 0.03 vs. 1.05 ± 0.04 ; $p < 0.04$) (Figure 3.75).

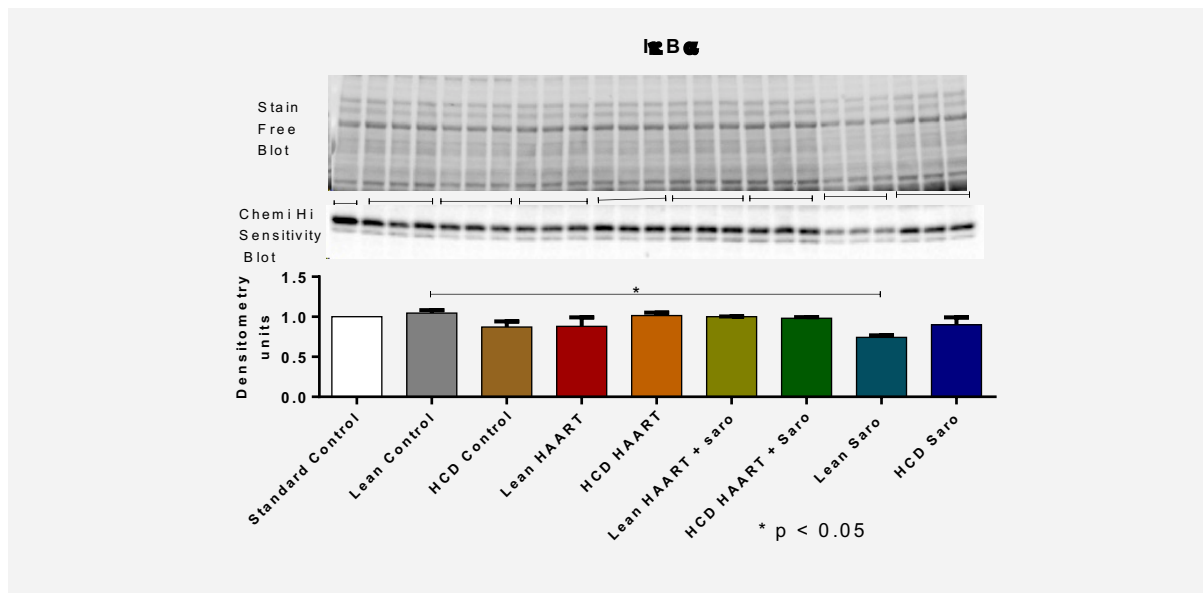


Figure 3.75 Mean aortic *IkBa* / experimental group.

3.13.2.5 PGC-1 α

Mean aortic PGC-1 α was significantly higher in the lean HAART + Saro group (1.16 ± 0.01) compared to the lean HAART group (0.90 ± 0.01 , $p < 0.05$). Also, the mean PGC 1 α expression was higher in the HCD Saroglitazar-treated group compared to the lean Saroglitazar-treated group (1.25 ± 0.09 vs. 0.79 ± 0.05 (39 %), $p < 0.05$). No other significant differences were observed among the other experimental groups (Figure 3.76).

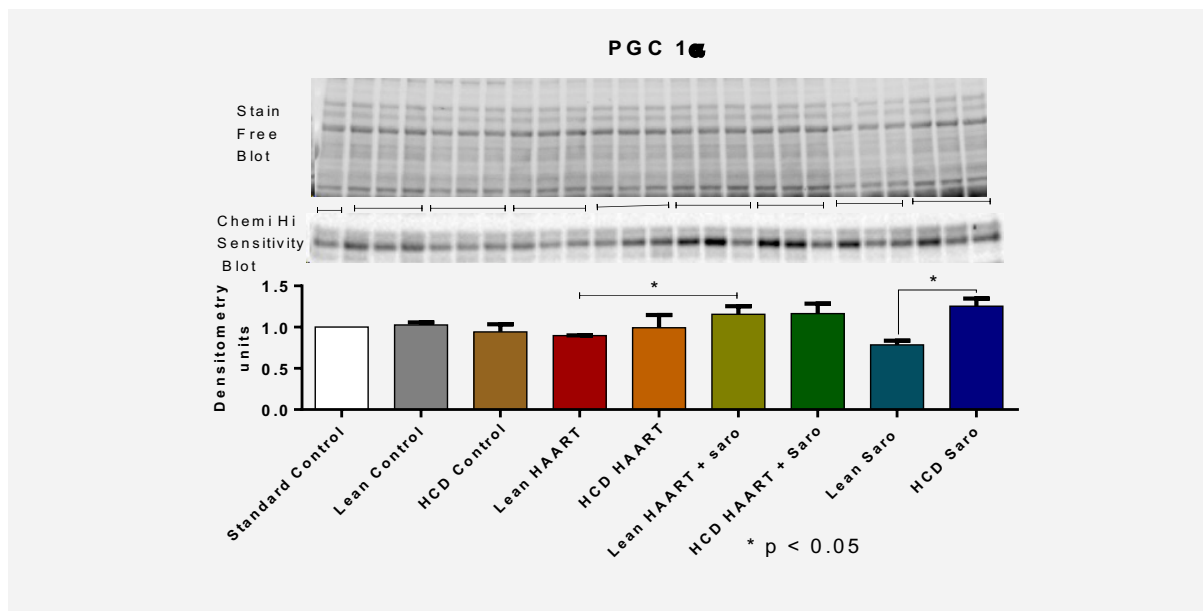


Figure 3.76 Mean aortic PGC 1 α expression / experimental group.

3.13.2.6 p22-phox

The mean aortic p22-phox levels were significantly higher in the HCD and lean HAART-treated groups (3.27 ± 0.19 , 2.92 ± 0.10) compared to the HCD and lean controls (1.6 ± 0.03 , $p < 0.0001$; 1.5 ± 0.05 , $p < 0.0001$), respectively (Figure 3.77 A). The increase in the mean p22-phox of the HCD HAART group represented a 2-fold increase compared to the HCD control group and lean HAART increase represented a 1.8- fold increase compared to the lean control. The mean aortic p22-phox / group in the Saroglitazar-treated groups did not differ significantly with the control (Figure 3.77 B).

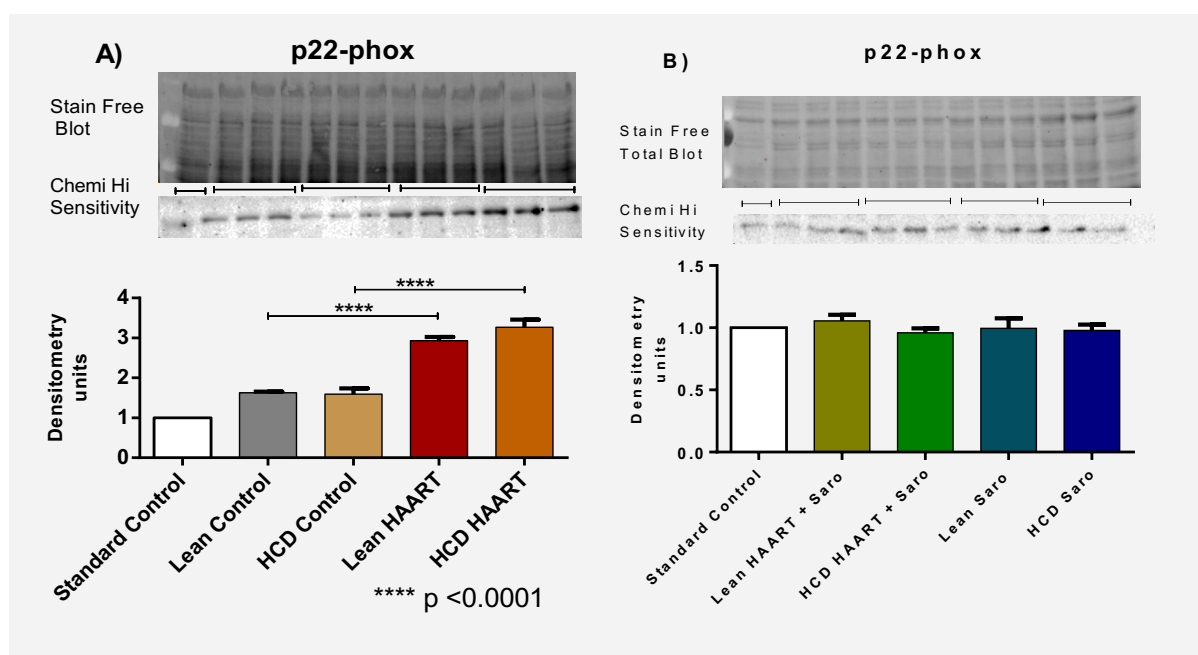


Figure 3.77 Mean aortic p22-phox expression / experimental group.

No significant differences were observed in the mean aortic expression of cleaved caspase 3 and cleaved PARP among the experimental groups. Similarly, the mean total AMPK and phospho-AMPK levels were not statistically different among the experimental groups.

3.13.3 Liver tissue protein determination

The proteins analysed from the experimental animals' liver tissues are presented in this section. The expression of PGC-1 α , I κ B α and PPAR α in the liver did not show any significant differences among the experimental groups and results are tabulated below as mean \pm SEM of the densitometry units per group (Table 3.10).

Table 3.10 Mean hepatic expression of PGC-1 α , I κ B α and PPAR α (mean \pm SEM of normalised volume intensities, densitometry units relative to control) / experimental group.

Protein Expression	Lean Control	HCD Control	Lean HAART	HCD HAART	Lean HAART + Saro	HCD HAART + Saro	Lean Saro	HCD Saro
I κ B α ,	0.53 \pm 0.05	0.55 \pm 0.05	0.50 \pm 0.04	0.60 \pm 0.06	0.54 \pm 0.04	0.53 \pm 0.03	0.48 \pm 0.04	0.55 \pm 0.06
PGC-1 α	0.34 \pm 0.03	0.36 \pm 0.03	0.38 \pm 0.06	0.28 \pm 0.02	0.40 \pm 0.05	0.44 \pm 0.03	0.36 \pm 0.08	0.43 \pm 0.03
PPAR α	0.52 \pm 0.07	0.50 \pm 0.06	0.52 \pm 0.04	0.55 \pm 0.06	0.48 \pm 0.03	0.47 \pm 0.04	0.50 \pm 0.05	0.54 \pm 0.05

3.13.3.1 PKB / Akt

There were no differences observed in the mean hepatic total PKB / Akt among the experimental groups (Figure 3.78 A and B). The mean phospho-PKB / Akt levels were significantly decreased in the HCD control group compared to lean control (0.57 ± 0.02 vs. 0.87 ± 0.03 , $p < 0.01$). Similarly, the HCD HAART-treated group mean phospho-PKB / Akt level was lower compared to the lean HAART group (0.51 ± 0.03 vs. 1.01 ± 0.06 vs. $p < 0.01$) (Figure 3.79 A). No significant differences were observed in the Saroglitazar-treated groups (Figure 3.79 B). Additionally, the mean phospho-PKB/ Akt / total PKB ratios followed similar trend as shown below (Figure 3.79 C and D).

A further comparison of the HAART-treated groups showed that, the mean phospho-PKB/ Akt / total PKB/ Akt ratios were significantly reduced in the HCD HAART (only) treated groups compared to the HAART + Saroglitazar-treated groups: HCD HAART group (0.38 ± 0.03) lower compared to HCD HAART + Saro group (0.65 ± 0.02 , $p < 0.01$) and lean HAART group (0.36 ± 0.03) lower compared to lean HAART + Saro (0.64 ± 0.03 , $p < 0.01$). No other significant differences were observed (Figure 3.80).

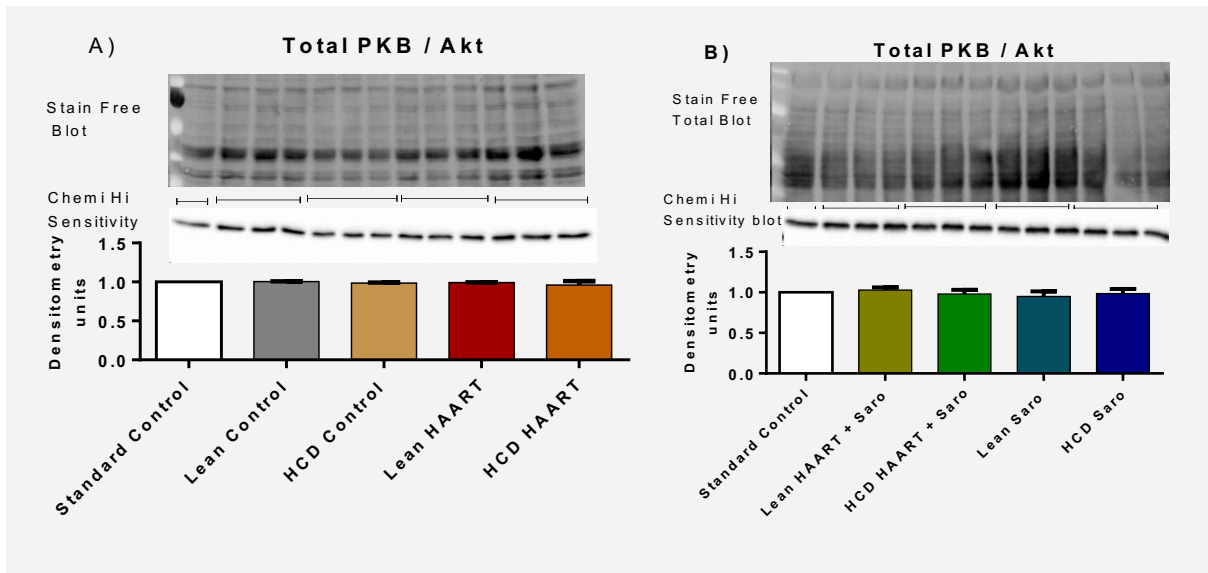


Figure 3.78. A and B Mean hepatic total PKB / Akt / experimental group.

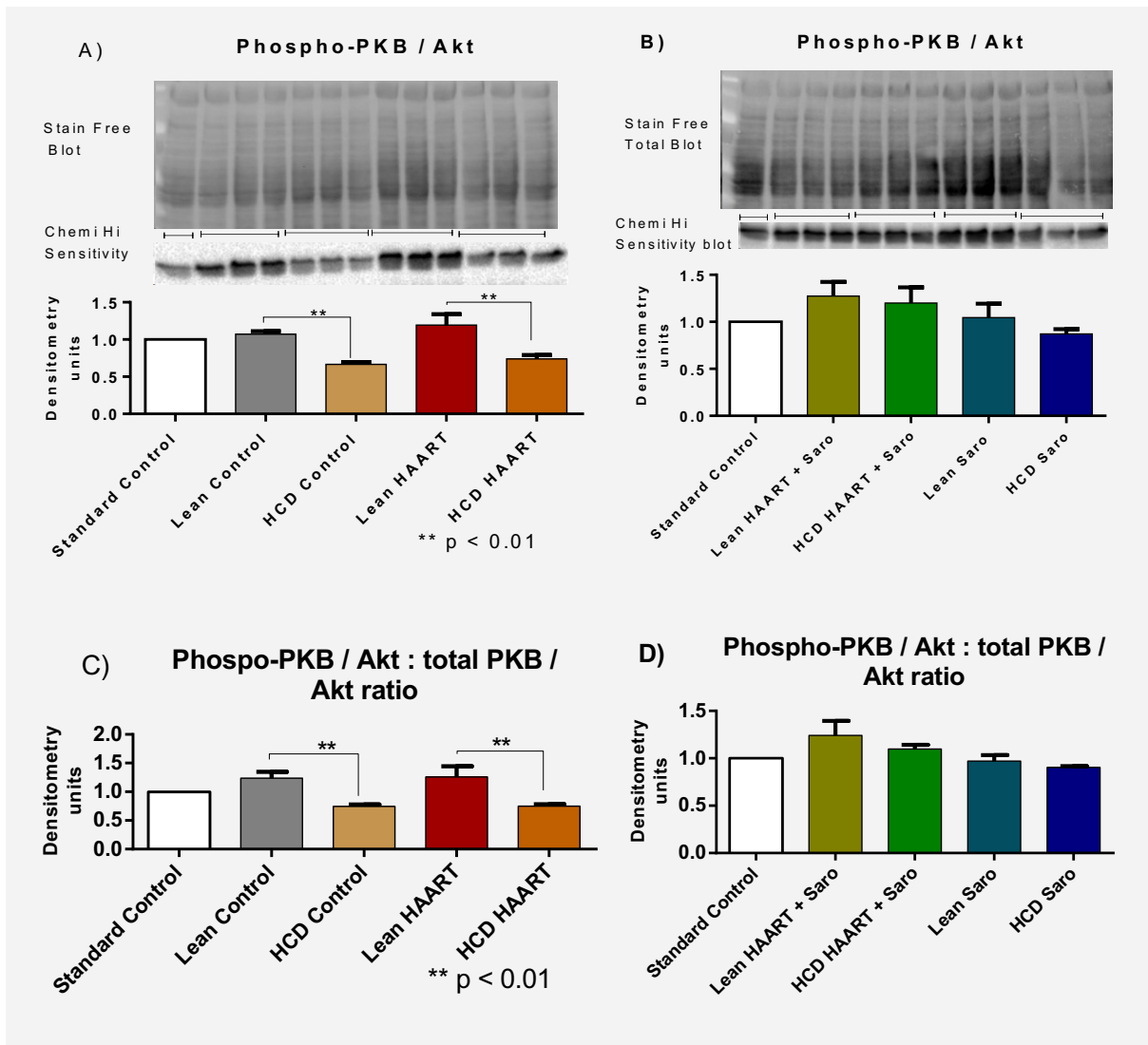


Figure 3.79 A and B. Mean hepatic phospho-PKB / Akt : total PKB / Akt ratio / experimental group.

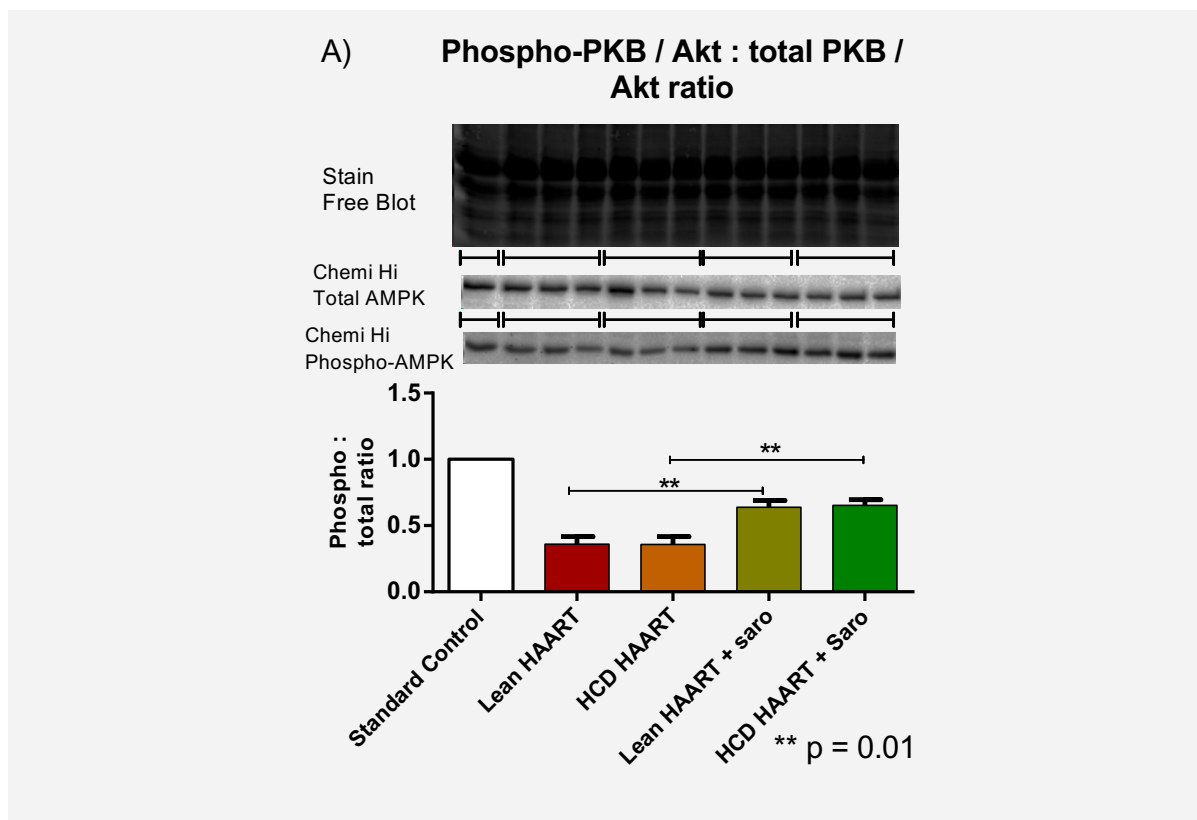


Figure 3.80 Mean hepatic phospho-PKB / Akt : total PKB / Akt ratio / experimental group.

3.13.3.2 Erk 1 / 2

The mean hepatic total Erk 1 / 2 did not differ significantly among the experimental groups. However, the mean phospho-Erk 1 / 2 was higher in the HCD HAART group compared to HCD control (0.97 ± 0.02 vs. 0.73 ± 0.02 respectively, $p < 0.01$). Similarly, the mean hepatic total Erk 1 / 2 in the lean HAART group was significantly higher compared to lean control (0.95 ± 0.01 vs. 0.71 ± 0.06 respectively, $p < 0.01$) (Figure 3.81 A). No significant differences were observed in the Saroglitazar-treated groups (Figure 3.81 B).

The mean phospho-Erk 1 / 2: total Erk 1 / 2 ratios were also significantly higher in the lean and HCD HAART-treated groups (0.62 ± 0.03 , 0.60 ± 0.08) compared to the lean and HCD control groups (0.40 ± 0.01 , 0.36 ± 0.03 , $p < 0.01$) respectively (Figure 3.82 A). No significant differences were observed between any of the Saroglitazar-treated groups (Figure 3.82 B).

Following a further comparison of the HAART-treated groups, it was observed that the mean level of phospho-Erk 1 / 2 in HCD HAART + Saro group (1.17 ± 0.19) was significantly lower compared to the HCD HAART (1.68 ± 0.10 , $p < 0.05$) (Figure 3.83 A). Similarly, the mean phospho-Erk 1 / 2: total Erk 1 / 2 ratio in the HCD HAART + Saro group (1.27 ± 0.25) was significantly lower compared to the HCD HAART (1.84 ± 0.10 , $p < 0.05$) (Figure 3.83 B).

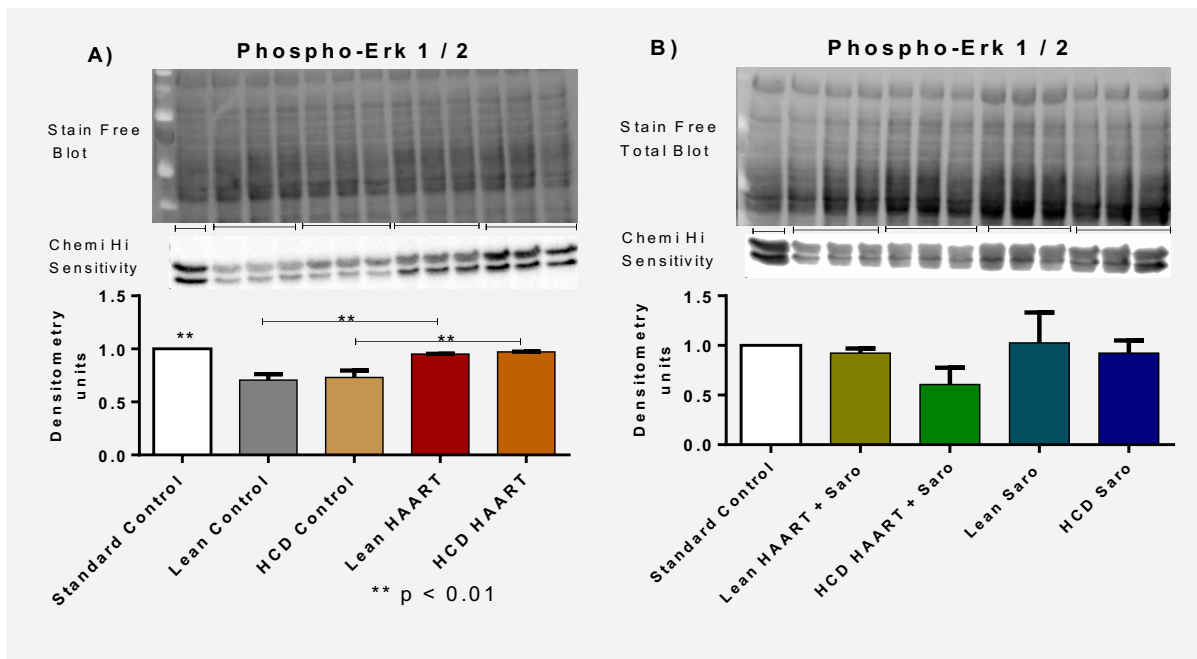


Figure 3.81 A and B. Mean hepatic phospho-Erk1 / 2 / experimental group.

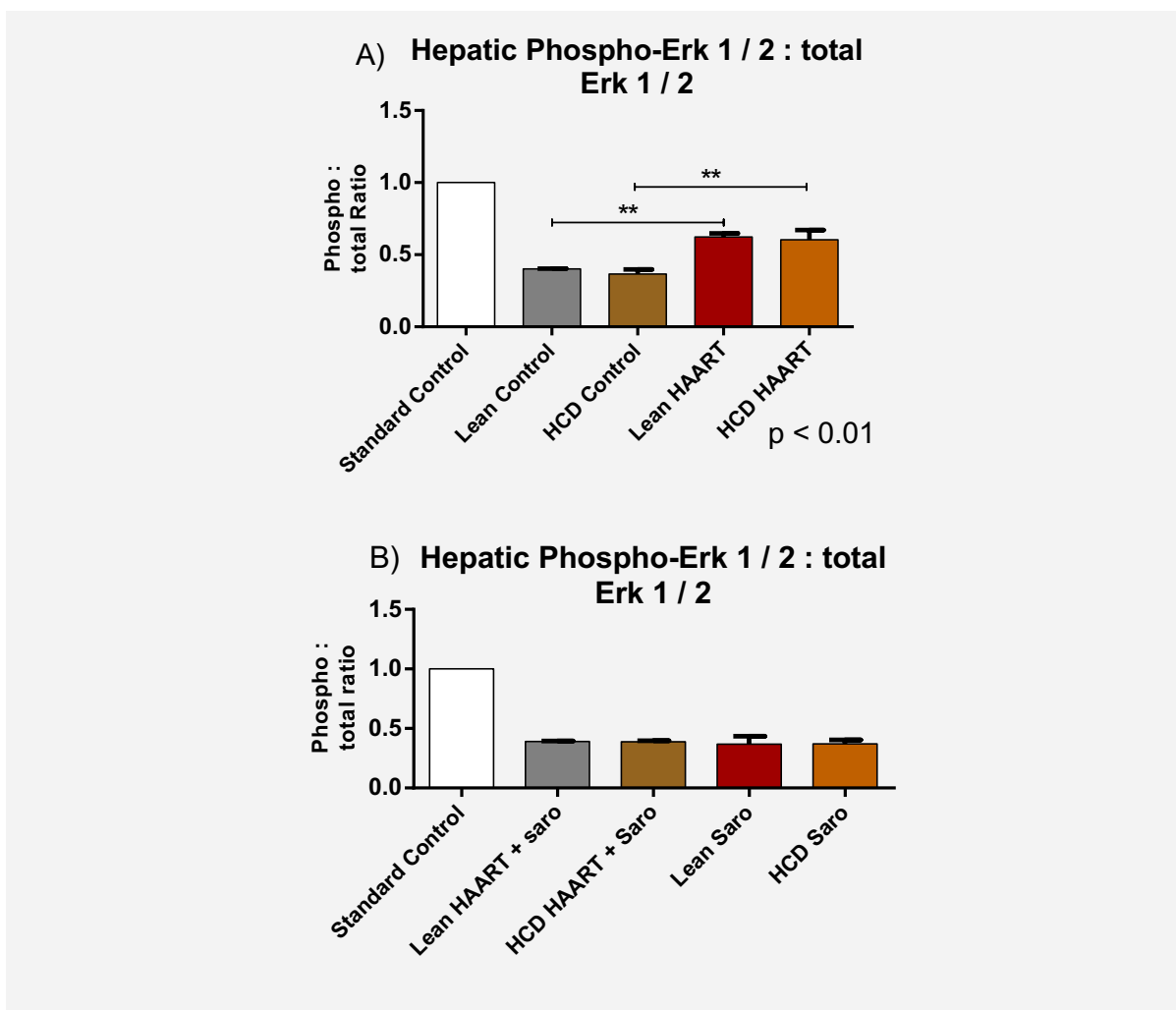


Figure 3.82 A and B Mean phospho-Erk 1 / 2 : total Erk 1 / 2 ratio / experimental groups.

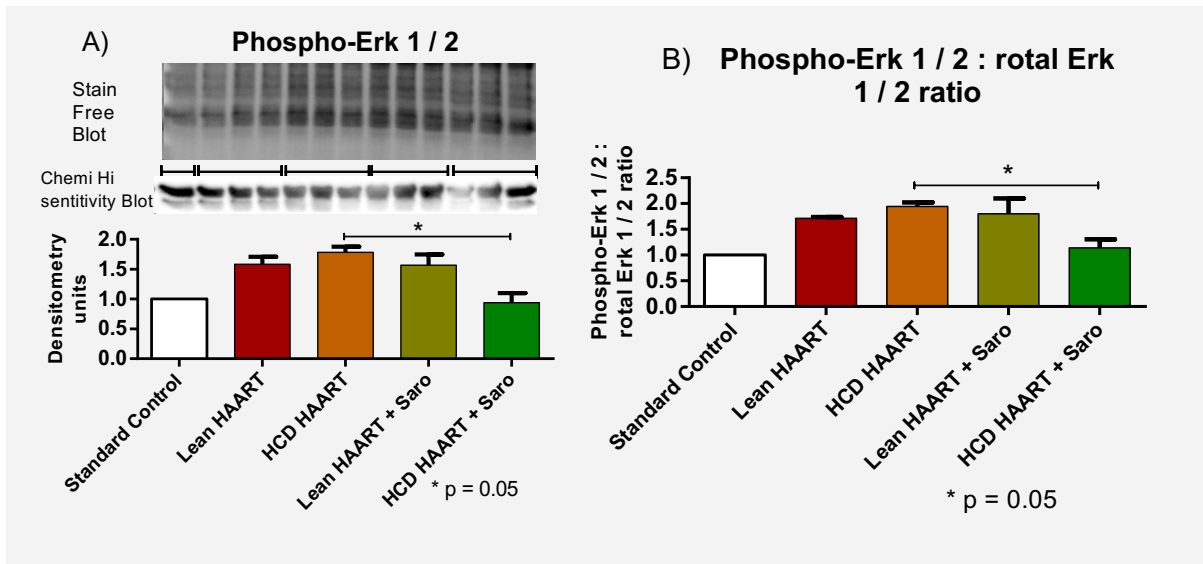


Figure 3.83 Mean phospho-Erk 1 / 2 /experimental group.

3.13.3.3 p22-phox

The mean expression of p22-phox did not show any significant differences among the experimental groups as shown below (Figure 3.84).

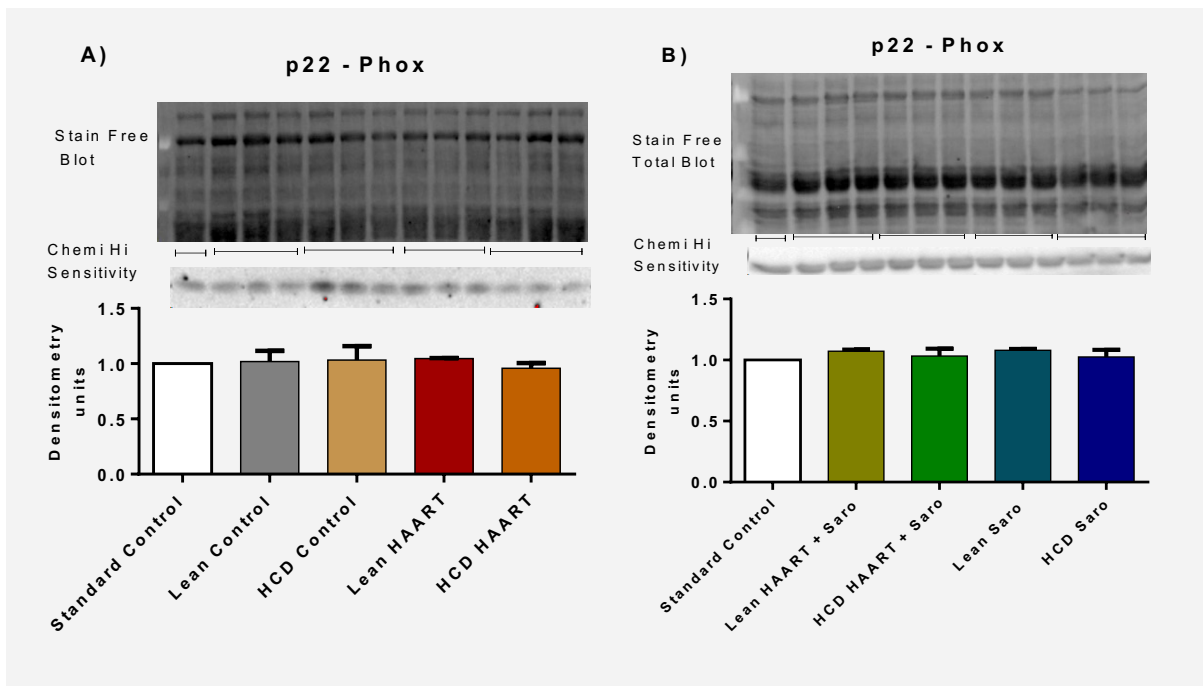


Figure 3.84 Mean hepatic expression of p22-phox / experimental group.

3.13.3.4 Cleaved caspase 3

There were no differences in the mean hepatic expression of caspase 3 among the experimental groups (Figure 3.85).

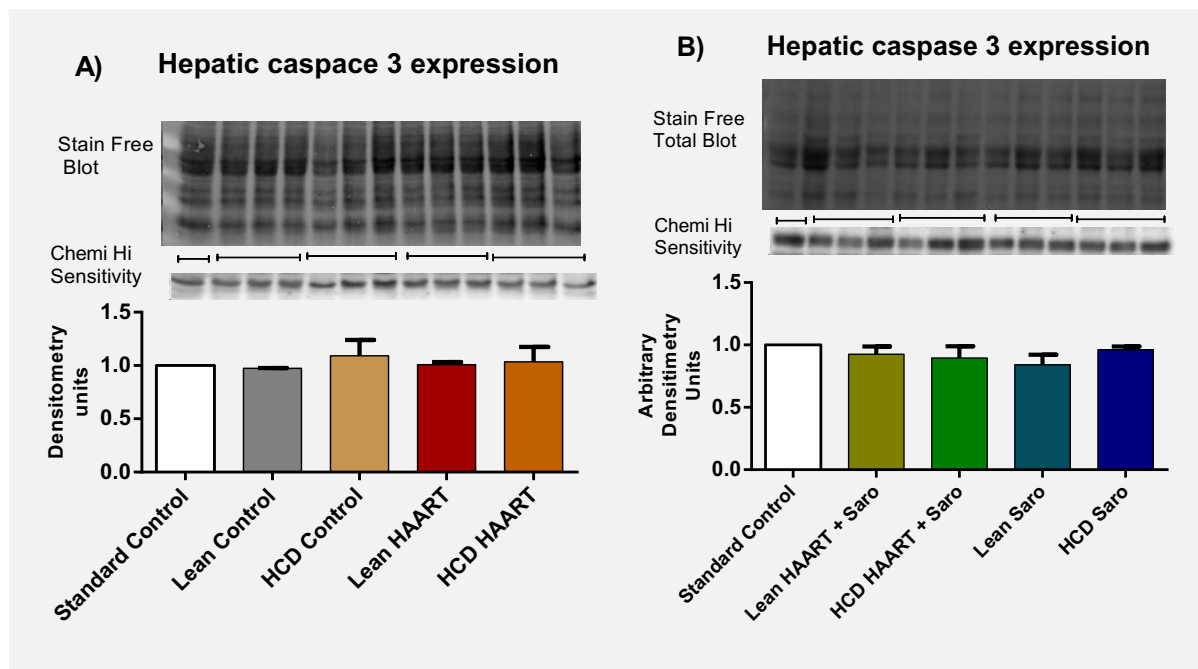


Figure 3.85 A and B. Mean hepatic expression of caspase 3 / experimental group.

3.13.3.5 AMPK

The mean hepatic total AMPK / group showed no significant differences. However, the mean phospho-AMPK level was significantly lower in the HCD HAART group (0.62 ± 0.04) compared to the lean HAART and HCD HAART + Saro group (1.60 ± 0.18 , $p < 0.01$ and 1.64 ± 0.11 , $p < 0.01$ respectively). Subsequently, the mean phospho-AMPK / total AMPK ratio in the HCD HAART group (0.59 ± 0.06) was significantly lower compared to the lean HAART and HCD HAART + Saro group (1.56 ± 0.20 , $p < 0.01$ and 1.56 ± 0.16 , $p < 0.01$ respectively) (Figure 3.86). The reduction in the mean phospho-AMPK / total AMPK ratio in the HCD HAART group represented a 2-fold difference in expression compared to the HCD HAART + Saro group.

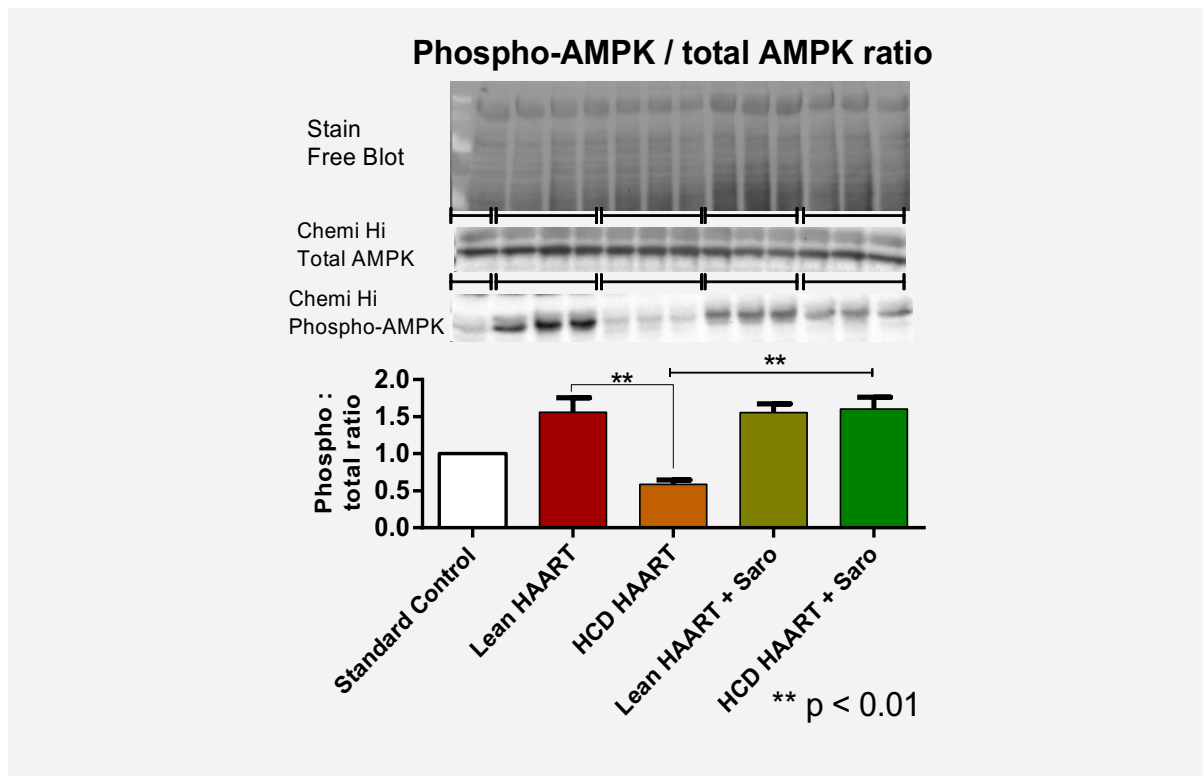


Figure 3.86 Mean hepatic phospho-AMPK / total AMPK ratio / experimental group.

Having presented all the results from the study activities previously highlighted, the subsequent chapter (chapter 4) formulates a discussion, draws conclusions based on the study findings and highlights the study limitations and future directions on this research topic.

Chapter 4 : Discussion

4.1 Introduction

In this chapter, the results previously presented (chapter 3) are discussed focusing on answering the research study questions i.e., whether treatment with HAART (LPV/r + AZT / 3TC) for six weeks led to development of NAFLD with concomitant development of cardiac and vascular dysfunction in lean and obese male Wistar rats compared to their age-matched controls. Furthermore, results obtained from the dual PPAR α / γ agonist, Saroglitazar, treatment for a period of six weeks are discussed hinging on its potential to limit the metabolic derangements associated with use of ARVs.

4.2 Feeding programme

The present study conducted an evaluation of two diets (normal rat chow and high calorie diet) that were supplied *ad libitum* for a period of 16 weeks to male Wistar rats from the age of eight weeks based on previously published diet models (Webster et al. 2017; Salie et al. 2014; Pickavance et al. 1999). We have presented data based on both food and water consumption monitoring and below are the inferences drawn.

4.2.1 Food intake

The vast majority of overweight and obesity cases in humans are associated with Westernized lifestyle where people not only consume readily available highly palatable food, but also consume it in large quantity. Dietary practices have been implicated greatly in causation and prevention of various diseases to name a few, cancer, T2DM and CVD (Willett 1994). Therefore, dietary monitoring was essential in this present study due to the implication in metabolic syndrome and CVD.

Before onset of drug treatment, animals that were fed the HCD and normal rat chow combination preferred the highly palatable HCD and barely consumed the rat chow (see Figure 3.1 and Figure 3.4). This trend persisted after the onset of drug treatment in all the groups (HCD HAART, HCD HAART + Saro, HCD Saro and the HCD Control) throughout the programme (Figure 3.5). There were no differences noted in the mass of food consumed in the various experimental groups among the HCD-fed animals. Similarly, consumption of normal rat chow was fairly constant in all the diet control experimental groups.

Furthermore, perhaps the most intriguing finding in the feeding behaviours of the two groups (chow-fed and HCD-fed) was that the HCD group not only had preference for the sweeter diet but consumed more compared to the mass ingested by the chow-fed group (Figure 3.2 and Figure 3.4). The mass ingested per rat per day by the HCD groups was more than double that consumed by the chow group.

The present study findings are consistent with previous studies, since it has been established that Wistar rats and other rodents prefer the more palatable diet than chow (Pickavance et al. 1999; Avena et al. 2008; La Fleur

et al. 2014). Using a high fat diet (45 % energy from fat), Hafizur et al. (2015) demonstrated an increase in the mass of food consumed by young Wistar rats compared to the standard rat chow fed control rats. The diet programme was extended for a period of six months and resulted in weight gain, insulin resistance (as evidenced by elevated serum insulin) and pancreatic islet hypertrophy features consistent with rodent pre-diabetes. Therefore, the diet model in the present study fits the criterion of hyperphagia inducing diet model (Corbit et al. 1964) and forms the basis of translatable findings to some human conditions as discussed in subsequent sections.

Treatment with HAART or Saroglitazar or combined treatment did not alter the mass of HCD or normal rat chow intake. However, it was observed that when the rats were initiated on the oral gavage procedure, their average food intake (in all groups including the vehicle – control group) dropped temporarily, and we ascribe this to the initial discomfort of the procedure since after three to five days of continued oral gavage, their food intake resumed to the pre-gavage mass.

4.2.2 Water consumption

Water consumption in the normal chow fed groups before and during treatment was significantly higher compared to the HCD group (Figure 3.8). On average, water intake for the chow-fed animals was double that of the HCD-fed animals. There is paucity in the literature of reports on water consumption in this diet model, but the findings in this present study suggest that the intake was lower in the HCD groups because their food was prepared by mixing the different components in water and therefore the moisture content was higher than that present in commercially available chow pellets. However, this difference could not be ignored because increased water consumption has been associated with several factors in humans. For example, a study by Kant et al. (2009) in a USA population reported that higher water intake is directly associated with diet quality (a key factor being dietary fibre), and inversely related to energy from fat and energy dense foods supporting the findings in the Wistar rat HCD model.

Treatment with HAART, Saroglitazar or combination of HAART and Saroglitazar had no effect on volume of water consumed in either the chow-fed or HCD-fed rats. Although both water and food intake alterations are observed in patients treated with PIs + NRTIs, the effects are attributed to direct gastrointestinal adverse effects like nausea vomiting and diarrhoea (Hill et al. 2009). However, neither lean nor HCD rats suffered from such effects and no features of dehydration were observed.

4.3 Body mass monitoring

Monitoring of body weight is a simple but effective tool in assessing the general status of health in humans and experimental animals. Since a relationship exists between dietary energy (fat) intake, metabolic syndrome and body weight (Melanson et al. 2009), it was imperative for us to monitor animal weight gain / changes in the various experimental groups. After randomly assigning the rats into two groups and introducing two different diets, it was clear that by the sixth week, the HCD group had started to gain more weight than the

chow-fed control group (Figure 3.10). This trend was maintained and by the tenth week when the treatment was commenced, the difference was even more pronounced as indicated by the fact that the HCD group had on average gained over 30 g / rat (12 %) more compared to the chow control group (Table 3.3).

After drug treatment was commenced, the difference in total body mass between HCD and lean treated groups persisted. However, the various treatment regimens exerted no additional effects, since the mean body mass for all HCD groups remained unaltered and similarly for the lean treated groups. Perhaps, continued treatment beyond 16 weeks would have produced different results since the trend as shown on Figure 3.11 indicated that the HCD control group rate of mean body mass increase was higher (although not statistically significant) in comparison to the other HCD-treated groups. On the day the animals were sacrificed, the HCD control group registered 15.6 % greater total body weight compared to the control and this finding was observed in all the experimental groups (Figure 3.12).

At this point, the present study has demonstrated that the HCD led to increased weight gain compared to the normal chow diet. Consequently, the findings corroborate those of previous studies (Salie et al. 2014; Webster et al. 2017; Pickavance et al. 1999) exploring body mass changes in Wistar rats using a similar diet, although some of these studies reported greater weight gains (30 % more) compared to the lean controls. The increase in body mass has been reported to be as high as 60 % in HFD (45 % dietary fat) in a period of nine weeks. (Hafizur et al. 2015). Unfortunately, literature on rat body mass with ART is limited.

Perhaps, what was expected was that the different drugs would induce body mass changes. Use of a thiazolidinedione (TZD, (PPAR γ agonist)), rosiglitazone did not show any weight alterations in dietary obese rats (Pickavance et al. 1999) a similar finding to the present study where Saroglitazar did not induce any weight changes. However, TZDs are known to induce weight gain despite improving insulin sensitivity in diabetic human subjects (Fonseca 2003). The mechanisms leading to PPAR γ mediated weight gain remain incompletely understood but is postulated to be as a result of enhanced adipocyte fat storage in the subcutaneous tissue because of the associated reduction in visceral fat accumulation (Kelly et al. 1999). In the present study, the serum drug concentrations were not assessed. Because the rate of metabolism is high in rodents, future studies should consider evaluation of serum drug concentrations to correlate with body mass changes. Perhaps higher serum Saroglitazar concentrations are required.

Studies on body mass in HAART often produce contradictory findings. However, there is adequate evidence suggesting that when the initiation of HAART is coupled with proper nutritional supplementation, the net result is an increase in total body mass. This finding was clearly illustrated by Banerjee and colleagues (2013) who evaluated over 180 children from a resource-constrained Indian population and found significant weight gain following HAART initiation and nutritional supplementation. To date, the situation has changed because, as demonstrated earlier (section 1.3.8), the onset of HAART has been revised and introduction of these drugs in patients who are already in the overweight / obese category has been referred to as “the latest epidemic” (Crum-Cianflone et al. 2008). Furthermore, it is now emerging that weight gain in HIV patients on HAART is

becoming more prevalent and is often associated with other cardiovascular risk factors such as hypertension and dyslipidaemia (Leite et al. 2010).

Riddle et al. (2001), using ritonavir on male C57BL/6 mice that were fed HFD, reported significant weight gains in the treated animals compared to the control, and the increase in body mass was also associated with dyslipidaemia as discussed below.

4.4 Visceral fat

Weight gain *per se* may not indicate accurately the risk it poses on health in general and therefore better indicators of body fat have been devised. Although the use of BMI remains a useful indicator for assessing body fat, its usefulness is of limited accuracy in adults. Other indicators of body fat like body adiposity index (BAI) (Bergman et al. 2011) and waist: hip circumference ratio have been suggested as more accurate indices. However, in our experimental study although we monitored only the total body mass during the treatment and feeding programme, after the animals were sacrificed, IP fat was harvested, weighed and expressed as a percentage to total body mass. The results are shown in Figure 3.13. The HCD control group had a significantly higher percentage IP fat mass compared to lean control. Additionally, the percentage IP fat mass of all the treated HCD groups was significantly higher than their lean control counterparts.

Intriguingly, co-treatment with HAART + Saro led to significant reduction in percentage IP fat mass in both lean and HCD groups. Although stimulation of the PPAR γ has been documented to lead to increased body mass (Fonseca 2003) the present study shows that dual PPAR α / γ stimulation *in vivo* led to a significant reduction in percentage IP mass in both chow-fed and HCD-fed Wistar rats. There were no differences observed between lean HAART vs. lean control and HCD HAART vs. HCD control.

There is supporting evidence that PIs predispose individuals to development of lipodystrophy which is characterised by changes in body fat distribution with peripheral wasting and central obesity (Williamson et al. 1999; Carr et al. 1998). However, this has not been demonstrated in rats. A combination of PIs with NRTIs has also been shown to increase the risk to development of peripheral lipodystrophy as described by Van der Valk et al. (2001). The present study did not demonstrate any changes in fat deposition within the peritoneum between the LPV / r + AZT / 3TC-treated lean and obese groups and therefore future studies ought to evaluate the entire fat profile including peripheral fat depots (subcutaneous).

Dietary factors also play a critical role in both deposition and distribution of body fat. In HIV patients on HAART, it has been reported that those who consume lipids excessively are at an increased risk of developing central obesity (odds ratio: 1.28) (Jaime et al. 2006). On the other hand, in a nested case-control study, HIV patients who consumed more fibre and proteins in their diet presented with less fat deposition compared to those who ingested less fibre and more fat (Hendricks et al. 2003).

From the foregoing discussion, it is clear that the first objective of the present study has been successfully achieved because by using these two markers of obesity / adiposity, the HCD was shown to induce an increase in net total body mass and percentage IP fat mass compared to the chow diet group. This finding can be

attributed to hyperphagia and high calorie intake because, the HCD contained more fat, carbohydrates and sucrose compared to chow (6 g / 100 g fat, 10.8 mg / 100 g cholesterol, 7.4 % carbohydrate and 18 % sucrose) respectively. However, the HCD did not differ significantly in the composition of micronutrients as shown on Addenda A 1 and A 2.

Furthermore, addition of Saroglitazar to the HAART regimen (LPV / r + AZT / 3TC) led to a significant reduction in the percentage IP fat compared to the lean HAART and HCD groups. Since visceral obesity has been implicated in various types of organ damage and dysfunction (Tchernof and Després 2013), we evaluated the liver and heart mass changes.

4.5 Organ mass

Determination of organ mass, especially the liver and the heart, is essential in experimental diet and treatment programmes because this provides an indication of the drug and dietary effects on tissues and organs. Although an ideal monitoring method would be to track changes in organ and tissue mass during the programme for example through use of high-resolution magnetic resonance imaging techniques (Tang et al. 2002), these techniques are expensive, not readily available and therefore in the present study, organs were harvested and weighed at the end of the programme after the animals were sacrificed.

4.5.1 Heart mass

Heart mass assessment is important because an increase, not only portends cardiomegaly resulting from cardiac hypertrophy but could also indicate abnormal fat deposition. The absolute (total) cardiac mass and normalised cardiac mass to tibial length were not significantly different between the HCD control and lean control groups. However, significant differences were observed among HAART, HAART + Saro and Saro treated groups compared to their respective lean controls (see Figure 3.14 and Figure 3.15).

Various HFD compositions have been shown to exert different effects on heart mass. Although the specific diet composition investigated in this study has not been reported to induce an increase in heart mass, (Pancani et al. 2013; Salie et al 2014), a HFD containing 25 % fat, 32 % protein and 25 % carbohydrate, as well as more palmitate (91.12 g/kg) and oleate (100.24 g/kg) was reported to induce an increase in cardiac mass compared to lean control animals, and the increase in mass was associated with an increase in the TG content within the heart tissue (Ouwens et al. 2005).

Tibial length has been proposed to be a good normalizing parameter for quantifying cardiac hypertrophy (Yin et al. 1982). Although the HCD control rats did not show any difference compared to the lean control rats, the cardiac mass normalised by tibial length was significantly greater in HCD treated groups compared to their respective lean control groups. Since this has not been reported before, we consider it a novel finding in this study.

Clinical studies have reported on the existence of cardiomegaly and dilated cardiomyopathy in patients on HAART especially those on NRTIs. Tanuma and colleagues (2003) described a case of a middle-aged woman

who developed cardiomegaly following 20 months of treatment for HIV with nelfinavir, 3TC and AZT. The cardiomyopathy was associated with histological features of hypertrophied cardiomyocytes and intra-mitochondrial myelin-like figures. These are features associated with AZT mitochondrial damage and following withdrawal of AZT from the HAART regimen, the clinical features of cardiomyopathy-induced heart failure all but disappeared. Other clinical studies have reported similar findings (Akinbami et al. 2012; Oberdorfer et al. 2008).

Metabolic derangements associated with both NRTIs and PIs that lead to lipodystrophy and dyslipidaemia also explain the high incidences of elevated heart mass in HIV / AIDS patients as a result of ectopic fat deposition in the heart tissue (Leite et al. 2008; Lake et al. 2010). Since the lean HAART group did not show any significant difference compared to the lean untreated group, we therefore ascribe the increase in heart mass to the combined effects of both diet and PIs + NRTIs treatment and therefore emphasizing the importance of diet in body fat distribution as previously reported (Hendricks et al. 2011; Jaime et al. 2006).

In the HCD HAART + Saro group, both the absolute and normalised mean cardiac mass were lower compared to the HCD HAART. Since this has not been reported before, it is a novel finding and we ascribe this to dual PPAR α / γ stimulation leading to not only a reduction in the % IP fat (in obese rats on HAART) but also possibly to improved fat distribution with reduced ectopic cardiac lipid deposition.

Treatment with Saroglitazar did not alter heart mass when compared to HAART treatment in both lean and HCD groups, a finding that is consistent with other TZDs. Gavrilova and colleagues (2003) demonstrated that PPAR γ stimulation with rosiglitazone protected other tissues from TG accumulation although it was associated with increased TGs in the liver. However, no significant differences in heart mass were observed. Future studies should consider evaluating the heart tissue histology since the present study did not.

4.5.2 Liver mass

Liver mass was only significantly elevated in the HCD compared to the lean control and no other differences were observed. Treatment with a combination of LPV/r and AZT + 3TC did not significantly increase liver mass and neither did combination with Saroglitazar or Saroglitazar monotherapy (Figure 3.16). Although there are no previous studies we can cite that have demonstrated increased liver mass using this specific diet composition, it is already established that HFD induces increased liver mass through deposition of lipids and also by inducing varying degrees of liver damage. For example, a high fat emulsion administered via oral gavage to male Sprague-Dawley was used to establish a model of NASH that was characterised by elevated aminotransferase, hyperglycaemia, hyperlipidaemia and overt obesity (Zou et al. 2016).

The finding that combined LPV/r and AZT + 3TC therapy did not alter liver mass was unexpected since there is ample evidence that PIs are associated with the development of lipodystrophy, hepatic steatosis and hepatomegaly (Riddle et al. 2001; Williamson et al. 1999; Carr et al. 1998). However, since no experimental studies using combined PIs and NRTIs have evaluated liver mass in this context, we suggest that NRTIs may

offer an antagonistic effect to the PI-induced liver enlargement. Another possible explanation is that six weeks of therapy were not long enough to induce demonstrable liver mass changes.

Additionally, the failure of Saroglitazar treatment to impact liver mass was unexpected since as already alluded to, TZDs have previously been implicated in hepatic steatosis due to increased TG deposition (Gavrilova et al. 2003). However, since Saroglitazar not only stimulates PPAR γ but also PPAR α , this may mediate the protection since a rat HFD-induced NASH model was shown to have diminished expression of PPAR α activity (Zou et al. 2006). We therefore propose that a longer HCD follow-up and treatment with PI and NRTIs beyond 16 weeks, may produce obvious changes in liver mass.

4.6 Food intake, body mass and IP mass

Intake of excessive amounts of unhealthy foods (high fat diet) leads to excess energy in the body and if this excess energy is not utilised, an imbalance occurs leading to storage of the extra energy in the body in form of fat by the adipocytes. This results in the clinical syndrome referred to as obesity. Although adipocytes are present in the subcutaneous tissues and in the viscera, the most significant partition of adipose tissue is present within the viscera and particularly within the abdominal cavity. In the present study, we have shown that HCD intake led to increased percentage IP fat mass compared to standard chow. Therefore, since both groups engaged in equal level of activity (energy expenditure was the same, although this was not analysed, it is an assumption that stands since these animals were housed under similar conditions and daily observations did not reveal any altered level of activity in both groups), we infer that excess energy contained in the HCD was stored within the IP fat compartment in the HCD animals.

In order to handle the excess fat in the body, the adipocytes undergo both hypertrophy (enlargement) and hyperplasia (multiply in number) (Goedecke et al. 2006). These adipocytes show both structural and functional impairments affecting their secretory and humoral properties. It has been established that hypertrophied adipocytes secrete several inflammatory mediators (Virtue 2010) which are associated with the chronic low-grade inflammation that characterises obesity. Unfortunately, the present study did not evaluate this effect.

Increased visceral fat has been associated with several deleterious health effects. For example, fat laden adipocytes have been shown to respond poorly to insulin stimulation through mechanisms that have already been discussed (section 1.4.3) (Hirani 2013). This leads to increased concentrations of insulin in the circulation (insulin resistance) as clearly demonstrated in the present study (Figure 3.32 and Figure 3.33) and high glucose levels in blood (not observed in the present study). The impaired insulin response does not only occur in the adipocytes, but has also been shown to occur in other tissues such as the skeletal muscle tissues and liver (Gaggini et al. 2013; An & Rodrigues 2006), thus aggravating glucose homeostasis. Another pathology associated with visceral obesity is excess release of FFAs into the circulation and alteration of serum lipid profile as described in the subsequent section.

4.7 Biochemical Analyses

Assessment of blood and serum biochemistry is vital in the evaluation of drug and dietary effects. This is because altered levels of biochemical markers not only offer insight into the organ function / dysfunction, but also to a greater degree determine how the organs respond to both the exogenously administered compounds and secreted circulating compounds. This section discusses the implications of the findings from the biochemical analyses performed on blood and serum from the experimental animals.

4.7.1 Blood glucose levels

The present study analysed both fasting and random blood glucose levels and as shown on Figures 3.17 and 3.18; no differences were observed between lean and obese animals. However, as expected, fasting blood glucose levels were lower compared to the random glucose levels (Figure 3.19). These results have been replicated in previous studies using similar diet (Ouwens et al. 2011; Nduhirabandi et al. 2011 and Pickavance et al. 1999). Although higher dietary fat composition has been shown to induce hyperglycaemia in both rats and mice (Zou et al. 2006, Riddle et al. 2001, Hafizur et al. 2015), a HCD composed of 11.5 g / 100 g (fat), 7.6 g / 100 g (saturated fats) and 13 mg / 100 g cholesterol diet for 16 weeks consistently showed no effect on blood glucose. Perhaps regular monitoring of glucose levels (for example every two weeks) or oral glucose tolerance testing would have provided greater insights, since the present study only evaluated glucose levels on the last day during euthanasia.

Unexpectedly, treatment with HAART, HAART + Saro or Saroglitazar did not produce any differences in either fasting or random blood glucose levels. PIs have been shown to induce hyperglycaemia in both experimental and clinical studies. A five-year cohort study on 221 HIV patients on PI therapy reported a strong association between use of PIs and development of hyperglycaemia with an adjusted incidence rate ratio of 5.0. In the said study, 11 % of the patients registered > 7.8 mmol / L of fasting blood glucose and 5 % of the patients were diagnosed with new-onset hyperglycaemia (Tsiodras et al. 2000). Similar findings were reported by Riddle et al. (2001) while evaluating ritonavir in mice. The degree of hyperglycaemia was even greater when ritonavir was combined with Western type HFD. It is possible that since the present study evaluated the combined effect of LPV / r and AZT + 3TC, no hyperglycaemic effects were elucidated.

In vivo PPAR α / γ stimulation did not significantly decrease blood glucose levels when administered alone or in combination with antiretroviral drugs. Saroglitazar has been reported to reduce serum glucose in both mice (12 days treatment) and rats (14 days treatment) although these animals were not on a HFD programme (Jain et al. 2015). Pickavance et al. (1999), also observed similar declines in blood glucose levels following 21 days of treatment with rosiglitazone in HFD-fed Wistar rats for eleven weeks. These findings have been replicated in clinical studies using Saroglitazar (Jani et al. 2014). However, in the present study, even the lean rats treated with Saroglitazar did not show any significant differences in either fasting or random blood glucose levels. Serial blood glucose measurements could have offered a better insight. However, this was out of the scope of

the present study and we also did not want to introduce confounding factors (such as frequent bleeding) to the cardiovascular system (Teilmann et al. 2014).

4.7.2 Fasting serum insulin and HOMA-IR

Fasting serum insulin concentrations and HOMA-IR are shown in Figures 3.32 and 3.33. HCD groups had significantly higher fasting insulin concentrations and HOMA-IR compared to their respective lean controls. An increase in fasting insulin in HCD has been previously reported (Nduhirabandi et al. 2011; Pickavance et al. 1999; Salie et al. 2014). The increase in fasting insulin concentration was as a result of diet-induced insulin resistance as confirmed by an increase in HOMA-IR. HOMA-IR is a method of assessing both insulin resistance and β cell function and has been validated for assessment in the Wistar rat model (Antunes et al. 2014). Therefore, the diet used in the present study successfully induced insulin resistance in the HCD control, HCD HAART and HCD Saro experimental groups. However, no differences were noted between the HCD HAART group and the HCD control group.

HAART, and in particular, PIs, have been associated with the development of insulin resistance which is characterised by hyperglycaemia and hyperinsulinaemia (Walli et al. 1998; Carr et al. 1998; Riddle et al. 2001). PIs bind to the hepatic lipoprotein-receptor-related protein (LRP) and interfere with PPAR γ activity, thus impairing lipid (TG) clearance leading to central fat deposition and insulin resistance (Carr et al. 1998). Furthermore, PIs also impair peripheral adipocyte differentiation and stimulate apoptosis thereby facilitating lipodystrophy as illustrated below (Figure 4.1).

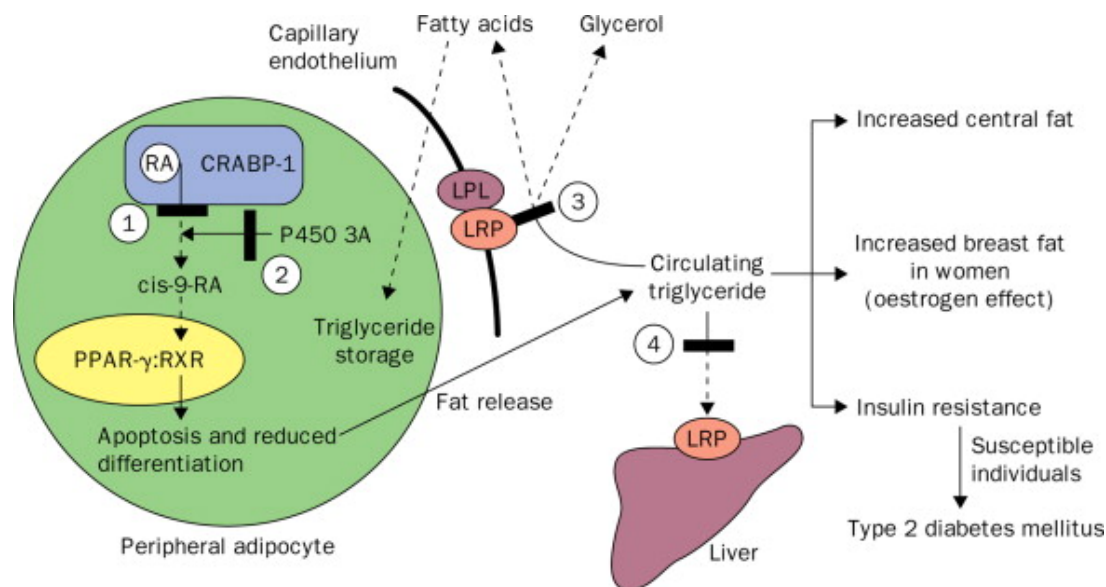


Figure 4.1 Mechanisms of HIV-1 protease inhibitor-induced insulin resistance and other lipodystrophies. Abbreviations: CRABP-1 – cytoplasmic retinoic-acid binding protein 1, RA - retinoic acid, RXR – retinoid x receptor, PPAR γ – peroxisome proliferator-activated receptor type gamma, LPR – lipoprotein receptor-related protein, LPL – lipoprotein lipase. (Adapted with permission from Carr et al. 1998).

NRTIs have also been associated with the development of insulin resistance and subsequently disturbed insulin-mediated glucose disposal. Although the actual mechanisms responsible for this dysregulation have not been elucidated, there is evidence that insulin resistance is accompanied by disturbances in lipid metabolism and changes in body composition. In a randomised clinical trial investigating the metabolic effects of 3TC + AZT and LPV / r, Blümer and colleagues (2008) demonstrated that although glucose levels were not altered in these 50 HIV 1-infected men followed up over a period of three months, their fasting insulin concentrations were elevated and there was a marked increase in lipolysis and suppressed glycerol turnover. These patients, however, did not present with any features of limb lipoatrophy or truncal obesity. In the study by Blümer et al. (2008), patients on LPV / r + NRTI-sparing ART, (nevirapine) did not present with features of insulin resistance or disturbances in insulin-mediated glucose disposal. These findings have also been reported in similar clinical studies (Meininger et al. 2002; Brown et al. 2005).

HCD HAART + Saro treated animals demonstrated lower insulin levels and a lower HOMA-IR index compared to the HCD HAART animals. Experimental studies have demonstrated that stimulation of PPAR γ not only improves serum glucose levels, but also improves insulin sensitivity and consequently the HOMA-IR index (Pickavance et al. 1999). Saroglitazar has been shown to exert modest reductions in glucose and insulin concentrations in both mice and rats at 3 mg / kg / day (Jain et al. 2015). The mechanisms of PPAR regulation of lipid, glucose and insulin homeostasis are discussed below and illustrated on Figure 4.2. A clinical study evaluating the efficacy and safety of Saroglitazar in HIV-associated lipodystrophy, however, reported an increase in fasting serum insulin levels compared to the control group (Deshpande et al. 2016).

The present study therefore provides new evidence that co-administration of Saroglitazar with HAART reduces serum insulin concentration and thereby improves insulin sensitivity as evidenced by a reduction in the HOMA-IR index.

4.7.3 Mechanisms of PPAR α and PPAR γ that mediate their biological effects

The mechanisms that mediate the biological effects of PPAR α and PPAR γ are as a result of gene transcription. PPAR binds to its retinoid X receptor and dimerizes to bind to the peroxisome proliferator response element (PPRE) and subsequently activates genes that mediate their various biological effects as shown below (Figure 4.2) (Ijpenberg et al. 1997; Kota et al. 2005).

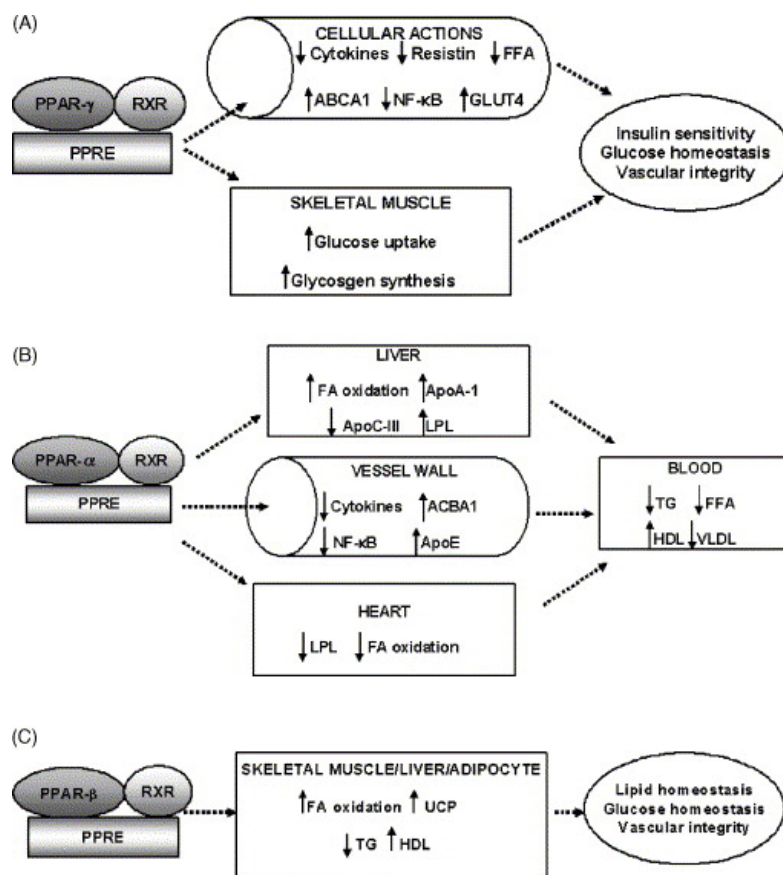


Figure 4.2 showing biological effects of (A) PPAR γ , (B) PPAR α and (C) PPAR β stimulation leading to insulin sensitization, serum glucose concentration reduction and anti-atherosclerosis through reduction in VLDL and increased HDL. Abbreviations: PPAR (peroxisome proliferator-activated receptors, PPRE (peroxisome-proliferator response element), RXR (retinoid X receptors), FFA (free fatty acids), TG (triglyceride) HDL (high-density lipoprotein), VLDL (very low-density Lipoprotein), NF κ B (Nuclear factor kappa B), UCP (uncoupling protein), ApoC (apolipoprotein C), LPL (lipoprotein lipase), ABCA1(ATP-binding cassette transporter 1). \uparrow indicates an increase and \downarrow indicates a decline. (Adapted with permission from Kota et al. 2005).

4.8 Serum lipid profile

The effects of a high calorie / fat diet on the serum lipid profile are well documented and the clinical condition that is characterised by the excess weight gain and deranged serum lipid parameters (obesity) remains a major health concern due to its high prevalence, high economic burden and associated cardiovascular risk and mortality (Wolf et al. 1998; James et al. 2001; Wilson et al. 2002). Excess intake of dietary lipids not only leads to fat deposition within the adipocytes, but also is associated with fat accumulation and damage to the liver that is accompanied by insulin resistance and excess circulating LDL, TC, TGs, FFAs and reduced HDL (Grundy and Denke 1990; Pelkonen et al. 1977). Therefore, it was of vital importance to assess the serum lipid profile of the experimental animals in the present study.

4.8.1 Serum total cholesterol, TC

Total serum cholesterol refers to the sum all the cholesterol in circulation that is carried by the three major lipoproteins, namely: - very low-density lipoprotein (VLDL-C), low-density lipoprotein (LDL) and high-density lipoprotein (HDL) (Kwiterovich 2000). Therefore, measurement of TC offers an insight into the overall load of cholesterol in a biological system.

The HCD did not induce any significant differences compared to the standard diet and similarly, no changes were observed among the treated groups compared to their respective lean controls (Figure 3.20). This finding is supported by similar studies (Nduhirabandi et al. 2011; Salie et al. 2014). Clinical studies have consistently demonstrated elevated total serum cholesterol in visceral obesity (Fujioka et al. 1987). Excess visceral fat accumulation (omental and mesenteric fat) has been associated with greater glucose and lipid metabolism alterations compared to subcutaneous obesity.

Although the present study did not find any changes in TC, PIs and NRTIs are known to increase serum TC in lipodystrophy (Carr et al. 1998; Bogner et al. 2001). Although this particular combination of ART has not been studied before in experimental animals, six weeks of treatment did not impact negatively on visceral fat mass, liver mass and TC and therefore future studies should consider extending the treatment period or introducing the drugs at the onset of diet programme.

4.8.2 HDL-C

One of the major carriers of cholesterol is the high-density lipoprotein. It has several subtypes that have different associations with CAD, namely: -

- i) HDL2- C with several subclasses H5, H4 and H3.
- ii) HDL3- C with subclass H2 and H1.

HDL2- C was previously referred to as a cardioprotective lipoprotein (Salonen et al. 1991) because it is involved in reverse cholesterol transport (Ramaley et al. 1999) (transportation of cholesterol from peripheral tissues and cells such as macrophages back to plasma). Furthermore, it was thought to play an important role in mediating against factors which aggravate atherosclerosis and thrombosis by the inhibition of LDL-C oxidation in atherosclerotic plaques, reduction in the levels of vascular endothelial cell adhesion molecule (VCAM) and degradation of fibrin clots (Kwiterovich 2000). However, recent studies propose that HDL3-C is the cardioprotective subtype (Woudberg et al. 2016) due to its association with antioxidant enzymes and the cardioprotective lipid, sphingosine-1-phosphate.

The HDL-C concentrations were higher in the HCD group compared to the lean control (Figure 3.22 A). This finding has been replicated in previous studies in our laboratory using a similar diet programme (Nduhirabandi et al. 2011). The reason why the HCD diet led to elevated levels of HDL- C has not been explained since Zou and colleagues (2006) using a high fat emulsion diet reported a reduction in HDL in their diet model compared to the control. However, we went further and analysed the two subtypes (HDL3- C and HDL2- C) and the

present study presents new evidence that HCD led to increased HDL3- C, but not HDL2- C, in the diet group compared to the lean control (Figures 3.25 and 3.26).

There were no changes noted in the HAART-treated groups compared to the controls (both lean and HCD). Although the combination of LPV / r and AZT + 3TC has not been investigated using experimental animals (to the best of our knowledge), Riddle and colleagues (2001) using Ritonavir in HFD mice demonstrated increased concentrations of serum HDL compared to the control. Clinical studies have reported reduced serum concentrations of HDL in patients on PI-based HAART regimen (Carpentier et al. 2005; Asztalos et al. 2006). Serum HDL3- C concentrations in the HCD HAART group were significantly lower compared to HCD control group, however, no differences were observed in lean HAART treatment group. No differences were observed in the serum HDL2- C concentrations in the HAART-treated groups compared to the controls.

Both lean and HCD HAART + Saro groups had reduced serum HDL- C levels compared to the HAART-treated groups (Figure 3.22 A), a finding that was also observed in the serum HDL3- C and HDL2- C concentrations. Serum HDL- C and HDL3- C concentrations were also lower in the HCD Saroglitazar group compared to the HCD control group. Serum HDL3- C concentrations were higher in HCD rats compared to lean Saroglitazar-treated animals and serum HDL2- C concentrations were higher in lean Saro group compared to the HCD Saro group. These findings are difficult to explain since studies for comparison are limited but the mechanisms via which PPAR α and PPAR γ mediate their actions are illustrated above (section 4.7.3).

4.8.3 LDL-C

Serum LDL-C concentrations were elevated in the HCD HAART + Saro group compared to the HCD HAART group and no other differences were observed (Figure 3.22 B). We do not know the mechanism behind this observation because this finding is in contrast with previous studies that have investigated the effects of PIs on LDL and reported higher concentrations in the PI-treated obese groups compared to the lean controls (Riddle et al. 2001). Furthermore, clinical studies have reported elevations in LDL levels in various HAART regimens (Carpentier et al. 2005). Deshpande et al. (2016) demonstrated a significant reduction in serum LDL concentrations in HIV / AIDS patients on HAART co-treated with Saroglitazar for a period of 12 weeks. However, these patients had features of lipodystrophy with marked hypertriglyceridaemia at the onset of therapy.

4.8.4 Serum phospholipids

The present study did not observe any significant differences in serum phospholipids, either in HCD or treated animals compared to their respective controls. However, lipodystrophic changes associated with HAART (especially PI-based regimen) have been linked to increased concentrations of serum phospholipids in lipodystrophic syndrome (McComsey et al. 2016). We suggest that the treatment period of the present study (six weeks) was not long enough to induce significant changes in serum phospholipids.

4.8.5 TGs

High concentrations of serum TGs have been positively correlated with both a high incidence and severity of atherosclerosis, a major risk factor for CAD (Patsch et al. 1992). Serum TG concentrations were significantly increased in the HCD group compared to the lean control (Figure 3.21). Studies in rodent models of DIO have reported similar findings (Pickavance et al. 1999; Riddle et al. 2001; Salie et al. 2014; Nduhirabandi et al. 2011). Sources of serum TGs are from both exogenous intake (excess dietary intake of highly saturated fats) and endogenous secretion from the liver (Kwitervonich 2000).

Both HAART and Saroglitazar failed to significantly alter the serum TG concentrations. This was unexpected, because PIs and NRTIs have previously been shown to induce lipodystrophy that is accompanied by steatosis and excess release of both FFAs and TGs into the circulation (Carpentier et al. 2005). On the other hand, use of PPAR α / γ stimulants in reduction of serum TGs has been established (Deshpande et al. 2016; Pickavance et al. 1999). It is possible that prolonged exposure to these two treatments would have produced different effects.

Although the present study did not evaluate organ TG quantities, previous studies have associated high concentrations of circulating TGs to increased ectopic deposition into the heart, blood vessels and the kidneys (Kopelman 2007). This correlates with the liver mass assessment findings in this study where HCD animals recorded higher liver mass compared to the lean controls. Furthermore, increased heart mass in the HCD-treated groups (HCD HAART, HCD HAART + Saro and HCD SARO) compared to the lean control groups could partly be explained by this alteration.

4.8.6 Serum lipids and atherosclerosis

High serum concentrations of VLDL, LDL and IDL have been associated with proatherogenicity. When the endothelium is dysfunctional and lipoproteins cross the barrier into the vessel wall, they are oxidised and are ingested by macrophages to form foam cells. Together with activated endothelial cells, they secrete growth factors that drive smooth muscle migration and proliferation leading to atherosclerosis as shown in the Figure 4.3 below (Price & Loscalzo 1999; Kwitervonich 2000).

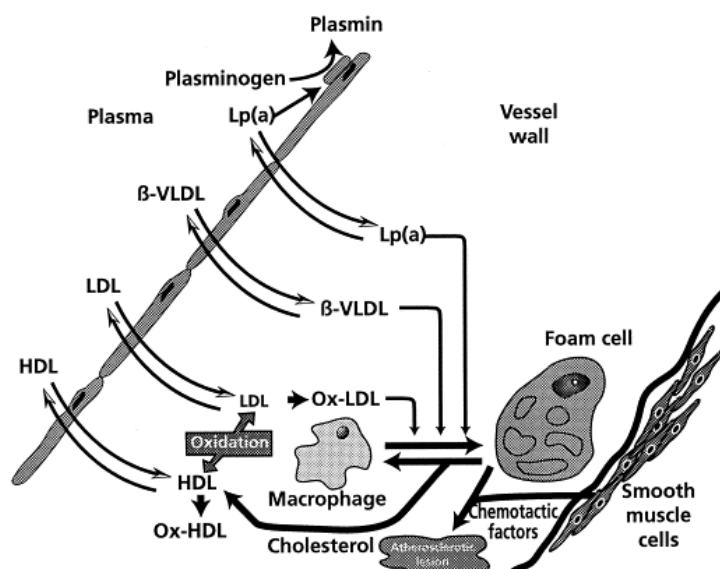


Figure 4.3 Mechanisms of atherosclerosis as a result of LDL deposition and oxidation. Also showing how HDL inhibits LDL oxidation and promotes reverse cholesterol transport. Abbreviations: HDL (high-density lipoprotein), LDL (low-density lipoprotein), VLDL (very low-density lipoprotein) LP (a), (lipoprotein a) (Kwiterovich 2000).

4.9 Serum markers of lipid peroxidation

4.9.1 CD and TBARS

Results of the CD analyses are presented on section 3.5.3. Lipid peroxidation is the process via which oxidants attack unsaturated FA and lipids. Early stages of FFA, TG and PL oxidation are detected using serum analyses of CDs and serve as a marker of lipid and FA metabolism. However, TBARS assay is a useful marker of final products of decomposition of larger polyunsaturated fatty acids (PUFA) (Ayala et al. 2014). There were no differences observed between the HCD and the lean control rats contrary to reports in the literature that DIO contributes to increased FA oxidation (Logani & Davies 1980; Clarkson & Thompson 2000). However, both mean absolute and normalised CD levels were higher in both lean and HCD HAART-treated animals compared to the lean and HCD HAART and Saroglitazar-treated animals. This finding supports literature (Section 1.4) that PIs and NRTIs alter the lipid and FA metabolism (Matthews et al. 2011; Day and James 1998) that eventually results not only in serum lipid profile changes but also hepatic steatosis which is attended by both local and systemic inflammation.

Although adipose tissue histology was not performed, it would have shed light on structural changes that occur in excess fat intake (DIO) and aggravated by PIs and NRTIs. Use of a dual PPAR α , γ agonist effectively reduced the CD in all the groups that received Saroglitazar i.e., lean Saro, HCD Saro, lean HAART + Saro and HCD HAART + Saro. We consider this a novel finding because, although Saroglitazar has been shown to reduce serum TGs and cholesterol in patients on HAART (Deshpande et al. 2016), CD concentrations have not been evaluated especially in the context of HAART use in HCD / DIO. TBARS were only significantly

reduced in the HCD Saroglitazar-treated group compared to the lean Saroglitazar-treated group (Figure 3.30). There were no differences noted between the HCD and lean control and the HAART-treated groups. This finding was unexpected because we have elaborated on the role played by both diet and PIs and NRTIs in mediating lipid metabolic changes that are accompanied by lipid peroxidation (Section 1.4). TBARS as a by-product of peroxidation of lipids has been used as a biomarker of both lipid peroxidation and oxidative stress (Trevisan et al. 2001). Although we cannot dismiss oxidative stress mediated role in the HCD HAART cardiac dysfunction during ischaemia-reperfusion based on reduced Qa, CO and Qt, and HCD HAART poor aortic relaxation, the biomarker we targeted in the present study (TBARS), did not reveal such changes in this group. However, Schisterman et al. (2001) having assessed TBARS in a cross-sectional study showed that even with elevated serum TBARS concentrations, association with increased risk of CVD prevalence was lost after adjusting for blood glucose variations. Therefore, better indicators of oxidative stress would provide clearer answers.

In summary, we have demonstrated that in support of the clinical studies that have shown a reduction in cholesterol and TG with use of Saroglitazar in patients on HAART, the human equivalent Saroglitazar dose of 4 mg/ 70 kg/ day administered orally for six weeks to obese Wistar rats, reduced serum CD significantly compared to obese rats on HAART without Saroglitazar. Although Saroglitazar is well known to impact substantially on blood glucose levels, cholesterol and TG levels (Agrawal 2014), it has a relatively short serum terminal half-life 5.6 hours and its maximum plasma concentration is in the range of 3.98 to 7,461 ng / mL (achieved in less than one hour) in humans (Jani et al. 2013). Considering the high rate of metabolism in rodents, it is possible that the drug bioavailability was low and may have limited its effectiveness in the present study as evidenced by lack of change in TC and blood glucose. As previously stated, evaluation of the serum drug concentrations during the treatment period should be considered in future studies in the context of HAART.

4.10 Working heart perfusion studies

4.10.1 HR

There were no differences noted in the baseline HR among the experimental groups (Table 3.5). Therefore, there were no dietary or drug effects that led to HR variation prior to ischaemia. Similarly, following 35 minutes of regional ischaemia and one hour of reperfusion, no HR changes were observed. These findings have been reported in previous studies evaluating cardiac performance using the same diet composition (n = 5–6) (Salie et al. 2014; Webster et al. 2017). Therefore, HAART with or without Saroglitazar treatment in obese and lean Wistar rats has no effect on cardiac rate of contraction in the pre-and post-ischaemic phase.

4.10.2 Coronary flow rate (Qe) and aortic diastolic / systolic pressure

There were no significant differences noted in the Qe pre-and post-ischaemia in any of the experimental groups (Table 3.5). Although studies have not been conducted on HAART (LPV / r and AZT/3TC), Reyskens et al.

(2013) using LPV/r did not observe any alterations in Q_e despite attenuation of the cardiac performance. No changes have been reported on Q_e in obese rats following ischaemia-reperfusion without preconditioning (Salie et al. 2014; Mazumder et al. 2004). Furthermore, no changes were observed in pre-and post-ischaemia systolic pressure (sp) and diastolic pressure (dp) among the experimental groups (Figures 3.39 and 3.40). Although no studies (to the best of our knowledge) have been performed on DIO rats treated with Saroglitazar and HAART, we report no observable differences in comparison to the lean treated and untreated Wistar rats.

4.10.3 Aortic output (Qa), total cardiac output (CO) and total work (Wt)

There were no significant differences in Q_a between the lean and HCD animals before induction of ischaemia, and similarly, no significant differences in post-ischaemia Q_a recovery were observed between the two groups (Table 3.5 and Figure 3.35). Salie and colleagues (2014) did not observe any significant differences (pre-ischaemia) between the lean control and the obese animals ($n = 4-6$ / group), although the post-ischaemia reduction in Q_a was significantly higher in the obese group compared to the control group. Other studies have reported similar findings to the present study using an insulin resistant obese mouse model (Buchanan et al. 2005).

The HCD HAART group had lower baseline Q_a compared to the lean HAART and HCD HAART + Saroglitazar groups. Following induction of ischaemia, the percentage recovery in Q_a and W_t was improved in the HCD HAART + Saro group compared to the HCD HAART group. Similarly, the CO was improved in the HCD HAART + Saro group. We consider this finding novel because the HAART combination (LPV / r + AZT / 3TC) that we investigated has not been evaluated previously in this context. However, the reduction in Q_a in the HCD HAART group may be attributable to the known mitochondrial damage and oxidative stress induced by NRTIs and PIs (Friis-Moller et al. 2007). These factors have been shown to contribute to impaired myocardial function in non-ischaemic heart and are aggravated in ischaemia-reperfusion (Doenst et al. 2013; Ferdinandy et al. 2007). Although Pickavance et al. (1999) using a highly palatable diet noted improvement in insulin resistance with rosiglitazone (a TZD) treatment, this improvement has not been demonstrated to translate in improved cardiac performance in obese rats.

The present study has also presented evidence (section 4.13.2.1) that HCD HAART cardiac tissues showed reduced activation of PKB / Akt, a major component of the RISK pathway (Hausenloy and Yellon 2007; Hausenloy and Yellon 2004), that partly explains the reduction in post-ischaemia Q_a and general cardiac performance. Activation of this pathway mediated by (PI3K - PKB / Akt and Erk 1 / 2) improves survival through activation of anti-apoptotic mechanisms following ischaemia-reperfusion. Other protective signalling proteins whose levels were reduced in the HCD HAART group include phospho-AMPK and phospho-eNOS. All these proteins were however, upregulated when HAART was co-administered with dual PPAR α/γ agonist, Saroglitazar, suggesting that the mechanism of the improved Q_a , CO and cardiac performance (W_t) was mediated by activation of these protective / survival signalling pathways. Work in this research area is currently ongoing in our laboratory where cardio-protection in ischaemia-reperfusion is being investigated, targeting the PPAR α/γ stimulation in pre-and post-conditioned hearts.

Poor post-ischaemia functional recovery in HCD HAART (reduced Qa, CO and Wt) could also be indicative of the effects of impaired lipid and insulin metabolism in MI, having demonstrated increased CD and hyperinsulinaemia in this experimental group. We have also demonstrated that these animals were insulin resistant based on an increased HOMA-IR index (despite normal blood glucose levels) and had increased visceral fat (IP). Buchanan and colleagues (2005), using a mouse model of insulin resistance and obesity, demonstrated that cardiomyocytes show altered substrate metabolism before the onset of increased blood glucose levels and impaired myocardial contractility. Therefore, the role of altered cardiac metabolism is critical in both pre-and post-ischaemia performance. Other studies have implicated fatty acid oxidation disruptions in poor cardiac performance (contractility) (Wilson et al. 2007). Therefore, PIs and NRTIs alterations in both metabolic disturbances (fatty acids, glucose / insulin metabolism) and mitochondrial function aggravate the ischaemic insult resulting in poor recovery post-MI. In addition, Reyskens et al. (2013) described disruption of the cardiac ubiquitin proteasome system leading to accumulation of calcineurin and impaired myocardial contractility in rats treated with LPV / r. This further supports the findings of the present study and suggests that the mechanisms involved in HAART-induced cardiac dysfunction are diverse.

Therefore, although the HCD was not associated with obvious alterations in cardiac contractile function before and after ischaemia, treatment with HAART reduced both baseline performance and post ischaemia recovery as evidenced by reduction in Qa, CO and Wt. All these parameters were, however, improved upon administration of a PPAR α , γ agonist together with HAART in the HCD group. This demonstrates that treatment with Saroglitazar has potential to limit HAART-induced cardiac dysfunction. In retrospect, perhaps use of a global ischaemia-reperfusion model for assessment of cardiac performance would have shown obvious alterations in the HCD animals and various treatment groups because of a larger area of the left ventricle undergoing ischaemic changes. Unfortunately, induction of global ischaemia does not reflect the true clinical picture and therefore the findings are not as translatable as those of regional ischaemia model.

4.10.4 Left ventricular infarct size analysis

Section 3.10 outlines findings on the infarct size analyses shown in Figure 3.42. The HCD control animals showed a reduction in the left ventricular infarct size compared to the untreated lean control animals. Additionally, the infarct sizes in the HCD HAART group were smaller compared to the HCD control. No other differences were observed.

Previous studies have observed a reduction in infarct sizes in diet-induced obese insulin resistant rats compared to control rats (Salie et al. 2014; Webster et al. 2017). Although the exact mechanisms mediating this protection are not completely understood, hyperinsulinaemia in insulin resistance could confer a possible preconditioning state as described by (Hausenloy and Yellon 2007; Hausenloy and Yellon 2004). This observation is supported by du Toit and colleagues (2008) who observed that in the absence of insulin, (the pre-diabetic model of DIO) the myocardium was more susceptible to both poor contractility and myocardial ischaemia. However, the finding that the HCD HAART group infarct sizes were smaller compared to the control and HCD HAART + Saro groups has not been described before (to the best of our knowledge). Although it has been reported that

infarct sizes are not correlated to post-ischaemia mechanical / haemodynamic performance in the working heart perfusion model (Lochner et al. 2003), it is startling to find that the experimental animals (HCD HAART group) that showed poor percentage post-ischaemia recovery (reduced Qa, CO and Wt) and downregulation of phosphorylated PKB/Akt and eNOS, were not at increased risk of developing larger myocardial infarcts.

We ascribe this finding to a possible stunning effect, which is one of the factors that complicate this model of *ex vivo* working heart perfusion studies. Furthermore, since the perfusion buffer only supplied the cardiomyocytes with glucose (no fatty acids were added), it is possible that there was an alteration in the main fuel supply and consequently hearts would have increased the breakdown of glycogen and TG stores to compensate. This compensatory mechanism we speculate is altered (during perfusion) especially in the lean untreated rats. However, as already explained, increased concentrations of serum insulin (insulin resistance) is a plausible mechanism explaining the permanent preconditioning state in the cardiac tissue resulting in reduced infarct sizes.

4.11 Aortic ring isometric tension studies

Aortic ring isometric studies have been extensively employed in experimental studies to investigate vascular reactivity to various compounds administered either *in vivo* or *ex vivo* (Durante et al. 1988; Razali et al. 2013). The aortic contraction studies are studied through use of a contractile agonist (phenylephrine) while endothelial dependent relaxation properties are evaluated through administration of a pro-relaxant agent (acetylcholine) (Furchgott 1983; Furchgott & Zawadzki 1980). However, relaxing substances / agents can also mediate vascular relaxation through endothelial-independent mechanisms such as nitroprusside and adenosine by directly acting on vascular smooth muscles (Durante et al. 1988; Furchgott 1955). Phenylephrine mediates its pro-contractile properties to the rat thoracic aorta through the agonistic effect of α_1 adrenoceptors (Hussain and Marshal 1997). The present study investigated the aortic relaxation response to endothelial-dependent acetylcholine stimulation following phenylephrine cumulative dose induced maximal contraction and the discussion below is based on the findings from the eight experimental groups.

4.11.1 Phenylephrine-induced aortic contraction

Phenylephrine-induced maximal aortic contraction (E_{max}) and $\log EC_{50}$ findings are shown in Table 3.8. There were no significant differences observed in (E_{max}) and $\log EC_{50}$ between the HCD and lean control groups in the present study. Vascular reactivity studies in obese experimental animal models have produced contradicting results where some studies have demonstrated that aortic rings from obese animals contract sub-maximally compared to lean controls. For example, Tesfamariam and colleagues (1989), using a rabbit obese model demonstrated that, aortas extracted from obese rabbits had poorer contractility compared to normal control rabbits. Similarly, diabetic rabbits also demonstrated submaximal phenylephrine contractility compared to controls. Phenylephrine-induced aortic contractility studies on obese Zucker rat models reported similar findings where endothelial intact aortas did not differ in contractility (tension per aorta tissue weight) compared to the controls (Auouet et al. 1989).

On the other hand, some researchers have demonstrated and argued that obesity promotes both vascular smooth muscle and endothelial dependent contractility through stimulatory effects of various pressor agents. Troupe et al. (2002) demonstrated this using C57BL/6J mice (obese model) ascribing the effect to increased prostanoid-mediated vasoconstriction. The pro-contractility properties of the obese and diabetic vessels mediated by pressor agents have been postulated as some of the causes of hypertension (Scarborough and Carrier 1983). Clinical studies however, show clear association between obesity and hypertension (Rahmouni et al. 2005).

Although our HCD control animals were not diabetic, it seems that the findings from phenylephrine-mediated aortic contractility compares with other studies that have evaluated this property using diabetic models. Chang et al. (1992) using a streptozotocin diabetic rat model aorta observed that 12 weeks after induction of diabetes did not produce any demonstrable changes in phenylephrine sensitivity and contractility to rings with intact endothelium. However, in long term metabolic studies (52 weeks), the rings demonstrated both increased sensitivity and contractility induced by phenylephrine. We therefore base our finding to the duration of exposure to the dietary effects and suggest that future studies should evaluate longer term effects (beyond the present study duration of 16 weeks).

It is worth mentioning that since our HCD (obese) model induced insulin resistance compared to the lean controls, previous studies have reported enhanced response to phenylephrine in Zucker obese and insulin resistant rats compared to controls (Ouchi et al. 1996). However, this finding was not reproduced in our model.

Among the treated groups, the lean Saroglitazar animals had a significantly higher E_{max} compared to lean HAART, HCD control and HCD HAART + Saro groups. There are limited studies to compare this finding to. However, Chakrabarti et al. (2014) using DRF 2519 (a compound with dual PPAR α and γ agonist activity similar to Saroglitazar) did not report any significant differences in phenylephrine-mediated pro-contractile effects in lean treated animals compared to the obese. The response of the obese treated animals was a reduction in maximal contractility by 70 % compared to the controls. However, the diet model was different from the one used in the present study. They used a hyperlipidaemic male Sprague–Dawley rat model fed on a high-fat diet containing 2% cholesterol and 1% sodium cholate.

Although the relaxation of the lean Saroglitazar-treated animals was not altered, (discussed below section 4.11.2) we suggest that stimulation of PPAR α and γ in lean animals may have detrimental effects not only on the vasculature but also on other tissues, for example elevation of TBARS (shown on Figure 3.30) could suggest increased oxidative stress. Furthermore, the lean Saroglitazar-treated group also had significantly elevated serum ALP (Figure 3.31). It is possible that treatment with a dual PPAR α and γ agonist in the lean animals could enhance vascular contractile response to vasopressor agents (such as phenylephrine) as shown on Figure 3.47 resulting from voltage gated dependent Ca^{2+} channels in vascular smooth muscles and therefore predispose to hypertension. This area needs to be investigated further.

Treatment with HAART did not show any significant differences in phenylephrine log EC_{50} between HCD and lean controls or HCD HAART + Saro and HCD HAART. Although there are no vascular reactivity studies

(to the best of our knowledge) to compare this finding to, it was unexpected since use of PIs and NRTIs has previously been associated with metabolic disturbances therefore increasing the risk of atherosclerosis (Friis-Møller et al. 2007; Durand et al. 2011). Additionally, the endothelial dysfunction in PI and NRTI use is well documented in both clinical and experimental studies (Zhou et al. 2005; Lipshultz et al. 2012; Reyskens & Essop 2014). Possibly, the duration of therapy in the present study was not long enough to induce demonstrable altered contractility, but we also suggest that HI-viral effects cannot be overlooked especially when relating clinical studies (HIV patients on HAART) with experimental animals where effects are studied in non-HIV models.

4.11.2 Acetylcholine-induced aortic relaxation

Investigation of acetylcholine-induced aortic relaxation generated interesting findings. As shown in Figures 3.48 A and B, and 3.51 A – D, the maximal relaxation (R_{max}) was significantly higher in the HCD control group compared to lean control group. Similarly, the R_{max} was also significantly higher in the HCD HAART + Saroglitazar group compared to the HCD HAART group.

The log EC_{50} (Figure 3.51) was lower for the HCD HAART + Saro group compared to HCD HAART; HCD control group lower compared to HCD HAART group; HCD control group lower compared to HCD Saro group and HCD HAART + Saro group was lower compared to HCD Saro group.

From the above findings, the HCD control group clearly demonstrated enhanced endothelium-dependent acetylcholine-induced aortic relaxation compared to the lean controls. From the principles described by Furchgott and Zawadzki (1980) on “The obligatory role of endothelial cells in the relaxation of arterial smooth muscle by acetylcholine” we can state that the HCD induced improved endothelial-dependent vascular relaxation since use of the NOS-inhibitor, L-NAME, abolished the acetylcholine relaxation in the present study. This advances the “obesity paradox” reported by researchers who have reported improved cardiovascular performance in our HCD formula compared to the lean control animals (Salie et al. 2014; Webster et al. 2017). This finding from experimental studies is supported by many clinical studies that have reported improved cardiovascular outcomes in either obese patients or those categorised as overweight based on their BMI.

For example, a longitudinal clinical study (61,835 patient years) over 24 months by Uretsky et al. (2007) reported that hypertensive patients with a history of CAD diagnosed as having obesity class 1 (BMI 30-35 kg / m²), showed improved outcomes (reduced mortality rate, reduced incidence of non-fatal MIs and non-fatal strokes) compared to those with normal weight (BMI 20 – 25 kg / m²). Since hypertension, MI and stroke are all vascular related pathologies (aetiologically), it follows that obesity seems to offer some protection against vasculopathies. Other studies have supported these findings (Fonarow et al. 2007; Lavie et al. 2003).

However, some experimental studies have reported on the contrary pertaining to the effect of HFD on aortic response to acetylcholine compared to lean controls. For example, Jayakody et al. (1985) reported significant reduction in endothelial-dependent acetylcholine relaxation in aorta rings harvested from New Zealand white

rabbits that were fed on 2 % cholesterol for four to eight weeks. Verbeuren et al. (1986), using a 0.3 % cholesterol diet for 16 weeks, described reduced endothelial-dependent acetylcholine-induced relaxation in rabbits and further described an increased risk of aortic atherosclerotic lesions. Therefore, the diet composition and duration of diet administration produce varying degrees of both functional and structural aortic damage.

Our diet model did not induce overt DM, but resulted in marginal induction of insulin resistance. Although we still support the paradoxical vascular / endothelial protection by obesity, it is important to note that the obese animals in the present study had normal blood glucose levels, were only approximately 15 % heavier than controls and did not present with elevated total serum cholesterol and LDL levels. We therefore agree with the findings by other researchers investigating vascular response in obese / diabetic models, such as Tesfamariam et al. (1989); Durante et al. (1988) who demonstrated that diabetic / obese endothelial-dependent relaxation via acetylcholine is depressed in rats and rabbits.

Treatment of HCD rats with HAART was associated with an increased EC_{50} compared to the HCD control. This further supports findings from clinical studies that have linked the use of PI and AZT / 3TC with the development of endothelial dysfunction and vasculopathies (Reyskens & Essop 2014; Lipshultz et al. 2012). Although the HCD HAART-exposed animals did not show classic features of metabolic syndrome (no definite dyslipidaemia), we have demonstrated that this group of experimental animals developed insulin resistance, had increased % IP fat, increased normalised heart mass, and presented with features consistent with hepatic steatosis / steatohepatitis and therefore, this milieu may explain the poor vascular response. It has been shown that these factors contribute to a reduction in endothelium-derived NO, impaired diffusion of the NO from the endothelial cells to smooth muscles, and disturbed acetylcholine receptor density and transduction mechanism (Durante et al. 1988), thereby resulting in poor endothelial-dependent acetylcholine-mediated relaxation (Chen et al. 2005). Perhaps the observation by Scarborough & Carrier (1983) that in diabetes these alterations lead to hypertension may explain the higher incidences of hypertension in PI and NRTI therapy (Zhou & Gurley 2006).

When HCD HAART animals were co-treated with Saroglitazar (HCD HAART + Saro), both the EC_{50} and R_{max} were significantly improved (Figure 3.48 B and 3.51 A) This finding, to the best of our knowledge, is novel since no studies have investigated this in the context of LPV/r + AZT/3TC in combination with dual PPAR α and γ stimulation. Section 4.7.3 above describes the various mechanisms via which PPAR α and γ stimulation mediate their biological effects. In reference to the vascular / endothelial physiology, the present study provides new evidence that, apart from improved insulin sensitivity (Figure 3.33) in HCD rats treated with HAART + Saroglitazar, Saroglitazar also improved endothelial-dependent acetylcholine-induced relaxation compared to the HCD HAART group. In contrast, Saroglitazar co-treatment with HAART in obese animals showed a reduction in serum HDL3 and HDL2 compared to the HCD HAART-exposed animals (Figures 3.25 and 3.26, respectively).

The HCD Saro-treated group showed mixed results: there were no significant differences in the R_{max} in comparison to the lean Saro and lean control group. However, the EC_{50} was significantly increased compared

to the HCD control and HCD HAART + Saro groups. This finding is intriguing since dual PPAR α and γ stimulation has been shown to induce improved relaxation in obese rats compared to controls (Chakrabarti et al. 2014). However, the said study investigated aortic smooth muscle response to insulin-induced relaxation and therefore comparing these findings with the present study would be misleading. Since Saroglitazar has been shown to mediate an improved lipid profile in clinical studies compared to untreated dyslipidaemic patients, it was expected that these improvements will manifest with improved endothelial-dependent acetylcholine-induced aortic relaxation, which was not observed. This warrants further investigations.

In summary, from the aortic ring isometric tension studies we infer that treatment of lean animals with Saroglitazar results in enhanced phenylephrine-induced vascular smooth muscle contraction compared to HCD control, lean HAART and HCD HAART (Saro) treated groups and this observation is consistent with the elevation of serum TBARS (i.e. development of oxidative stress) in these animals. Additionally, HCD induced increased relaxation in the untreated animals compared to the lean control animals, which is an observation consistent with the obesity paradox as reported by other researchers. Lastly, addition of Saroglitazar to HAART therapy in HCD significantly improved endothelium-dependent aortic relaxation induced by acetylcholine, an observation that the present study considers to be of potential therapeutic value in HAART-induced endothelial dysfunction in obese patients.

4.12 Liver tissue histology

The gold standard technique for liver assessment in the diagnosis of structurally related pathology is tissue biopsy followed by histological assessment. This is widely used in both clinical and experimental studies. Section 1.4 of this treatise has already supplied a concrete background on NAFLD and how HAART is associated with both the induction and aggravation of liver fatty changes and its sequelae.

Results from the present study (Table 3.7) demonstrate clearly that six weeks of treatment with a combination of LPV / r and 3TC + AZT led to the development of mild-moderate hepatic steatosis in over 66 % of the HCD animals (50 % grade (score) 1 and 16.7 % grade 2). Furthermore, 25 % of the HCD HAART-treated animals showed features consistent with mild to moderate inflammation (16.7 % mild steatohepatitis, 8.3 % moderate steatohepatitis) and 17 % with hepatocyte injury. This contrasted with the lean HAART-treated animals that did not show any features of steatosis or hepatic inflammation (100 %, score 0). Only 16.7 % of untreated HCD animals developed mild steatosis. Combined therapy Saroglitazar with HAART significantly reduced the incidence of steatosis, with only 16.7 % of the animals scoring grade 1 without any features of inflammation or hepatocyte damage. Only 8.3 % of HCD Saroglitazar-treated animals developed mild steatosis, and no features of inflammation or hepatocyte damage were observed.

Development of fatty liver in the HCD HAART animals was accompanied by metabolic derangements as demonstrated by hyperinsulinaemia, insulin resistance and visceral obesity. In addition, these animals demonstrated features of dysregulated intracellular signalling protein cascades (discussed on section 4.13), not only in the liver, but also in the heart and aortic tissue. Co-administration of Saroglitazar with HAART

improved the hepatic fat accumulation in the HCD animals and this protection was accompanied by improvement in insulin levels and intracellular signalling as discussed in the subsequent sections. We therefore present this as another milestone in the present study because this is new evidence that dual stimulation of PPAR α / γ receptors improve HAART-induced hepatic steatosis and insulin resistance.

4.12.1 Diet and NAFLD

As already stated (section 1.4.2.2), unhealthy dietary practices have been greatly implicated in the development of liver steatosis and in fact, DIO in humans has been classified in the high-risk category for both simple steatosis and steatosis-induced liver complications such as steatohepatitis and cirrhosis (Boza et al. 2005; Machado et al. 2006). Experimental studies have shown similar results where rats or mice fed with a Western type diet develop hepatic fat infiltration and ultimately steatohepatitis (Riddle et al. 2001; Zou et al. 2006; Oakes et al. 1997; Aragno et al. 2009). Excessive dietary intake of fat results in hepatic accumulation of TGs and stimulates hepatic lipogenesis culminating in the ‘first hit’ as described by Day & James (1998) as a result of insulin resistance. Following this, the second hit comes into play when the lipid laden hepatocytes show increased lipid peroxidation, and this is coupled with the generation of pro-inflammatory mediators (TNF- α , IL-6) and mitochondrial dysfunction (ROS generation) resulting in hepatocyte damage. Additionally, FFAs and TNF- α through JNK stimulation inhibit IRS-1, and this is associated with impaired insulin mediated glucose homeostasis and insulin resistance (Hirosumi et al. 2002).

Although the present study did not report any evidence of hepatic fibrosis (cirrhosis), steatohepatitis has previously been implicated in the induction of stellate cell proliferation and fibrogenesis (Lemoine et al. 2006). We suggest that perhaps a longer treatment duration could produce similar findings.

4.12.2 HAART and NAFLD

A combination of PIs and NRTIs has been implicated in development of body fat composition changes i.e., lipodystrophy, and visceral obesity which are associated with hypertriglyceridaemia, hyperinsulinaemia and low HDL (Crum-Cianflone et al. 2009; Crum-Cianflone et al. 2008). These are known triggers of NAFLD. Although the HI-virus is also implicated in viral-induced hepatic changes, treatment with PIs and NRTIs has not only led to an increased prevalence of steatohepatitis, but also fibrosis (Bhatia et al. 2012). The risk of excessive lipid deposition within the liver is greater in this combination because PIs cause dyslipidaemia, increased lipolysis and insulin resistance, and on the other hand, NRTIs lead to hepatic mitochondria toxicity as a result of mitochondrial RNA depletion (Matthews et al. 2011; Lai et al. 1999; Olano et al. 1995).

These findings have been replicated in previous experimental studies using ARVs. For example, Riddle et al. (2001) reported excess fat deposition in the liver tissue of mice treated with ritonavir (10 days) and fed on a HFD (21 % (w/w) anhydrous milk, 0.15 % (w/w) cholesterol, n = 4/ group. However, to the best of our knowledge, there are no previous reports of combined LPV/r and AZT / 3TC therapy (6 weeks) on rats fed on HFD / HCD (4 months) and therefore, the present study supports these findings and provides new evidence

that PIs and NRTIS combined with HFD result in the development of both steatosis and steatohepatitis in Wistar rats.

Co-administration of a PPAR α / γ agonist with HAART resulted in reduction in the number of rats that developed steatosis compared to the HAART only-treated animals. PIs have previously been implicated in decreased expression of transcription factors that regulate lipid metabolism (PPAR γ) (Lemoine et al. 2006). PPAR γ is also involved in the inhibition of activated stellate cells and therefore reducing fibrogenesis (Hezra et al. 2004). Furthermore, impaired PPAR α activity in dyslipidaemia and lipodystrophy associated with PIs and other metabolic conditions (obesity and DM) may explain the higher prevalence of NAFLD in these conditions. Therefore, by combining PPAR α and γ stimulation in HAART, our findings show a successful reduction of lipid deposition in the liver, which subsequently protected the hepatocytes from inflammatory and cytotoxic effects. Although a previous study has established that overexpression of PGC-1 α protected cardiomyocytes from NRTI-induced toxicity (Liu et al. 2015), to the best of our knowledge, no other studies have evaluated the effects of dual PPAR α and γ stimulation in the setting of a combined PI + NRTI-HAART regimen. Therefore, we consider this finding novel. Treatment of HCD rats with Saroglitazar similarly showed protection from steatosis and inflammation.

Liver immunohistochemical studies with anti-glutathione S-transferase placental form (GST-P) antibody did not show any positive GST-P foci in any of the experimental groups. HAART has altered the natural history of HIV / AIDS and has led to chronicity that is now associated with rising prevalence of hepatic neoplasia, among other malignancies (Maso et al. 2009). We therefore included this marker in the present study with the aim to detect any drug-induced liver hyperplastic nodules, pre-neoplasia or even hepatic carcinoma. GST-P has been used as a reliable marker for pre-neoplasia in rat chemical hepatic neoplasia (Sato et al. 1984; Sugioka et al. 1985). The detoxification enzyme is hardly detectable in normal liver and therefore, since the present study did not detect any foci suggestive of hyperplasia or neoplasia, we can conclude that neither the HCD nor the treatment with HAART with / without Saroglitazar induced detectable hepatic neoplasia. This finding is congruent with our previous findings since no fibrosis was detected as a sequel to steatosis.

4.13 Signalling proteins

In this section, results from proteins of interest that were analysed in the cardiac, aortic and liver tissues are discussed.

4.13.1 AMPK

As a master regulator of cellular energy homeostasis, AMPK senses the energy status in the cells and responds by stimulating or upregulating energy generating processes and at the same time switching off or negatively controlling energy consuming processes (Hardie 2011) (See section 1.5.5). The expression of total AMPK and its activated form, phosphorylated AMPK (Phospho-AMPK), were analysed in the heart (before and after ischaemia-reperfusion), aorta and liver tissues.

4.13.1.1 Cardiac AMPK

The baseline (pre-ischaemia) analysis of AMPK showed no changes in the total AMPK expression, but the phospho-AMPK levels were significantly lower in the HCD control group compared to the lean control and similarly, lower in the HCD HAART group compared to the lean HAART group. Treatment with Saroglitazar was not accompanied by any significant changes in AMPK expression or activation (Figures 3.52 and 3.53). However, following 10 minutes of reperfusion after 20 minutes of global ischaemia, activation of AMPK was enhanced in both lean and HCD Saroglitazar-treated groups as evidenced by significantly higher levels of both phospho-AMPK and phospho/total ratios in these two groups compared to combined HAART and Saroglitazar treatment in lean and obese experimental animals (Figure 3.55 and Figure 3.56).

Studies on the activity of AMPK in HC/FD have generated contradicting findings with some reporting a reduction in obesity (Pang et al. 2008; Liu et al. 2006) and others an increase (Cao et al. 2011). In the present study, no differences were observed between untreated HCD animals and lean control animals. We ascribe this finding to the fact that, our obese model did not present with overt dyslipidaemia, while the percentage visceral (IP) fat was only 3 % higher compared to the control. The control animals also presented with substantial IP fat of 3.6 % / total body mass and therefore the difference in AMPK activation in the heart tissue may not have differed. Altered expression of AMPK activity (reduced activation) has previously been associated with several deleterious outcomes, such as impaired fatty acid oxidation leading to deranged serum lipid profile that is characterised by hypertriglyceridaemia and organs / tissue lipid accumulation (Liu et al. 2006; Sriwijitkamol et al. 2006). In fact, some researchers have argued that although AMPK activity suppression is not the primary abnormality preceding T2DM and metabolic syndrome, it plays a critical role in exacerbating these pathologies (Zhang et al. 2009).

Before ischaemia, no upregulation of AMPK was observed in the Saroglitazar lean and HCD groups, which was unexpected since previous studies have demonstrated activation of AMPK by compounds that stimulate PPARs and PGC 1 α (Tu et al. 2013; Leopardine et al. 2010; Hardie 2008). However, upon induction of ischaemia and reperfusion, Saroglitazar monotherapy in both lean and HCD was associated with significantly higher phosphorylated AMPK levels compared to other treatment groups. This finding is in concurrence with previous studies that have shown improved insulin sensitivity via upregulation of AMPK activity (Figure 4.4) in overweight and obesity by drugs such as metformin and TZDs (Liu et al. 2006; Leonardini et al. 2009). Although we anticipated that combining HAART with Saroglitazar would induce cardiac AMPK activation before ischaemia, this was neither observed in lean nor obese animals.

The finding that obese animals treated with HAART had reduced activation of AMPK was anticipated since it has previously been established that NRTI-induced mitochondrial toxicity and PI-induced lipid metabolism dysregulation lead to altered cellular energy production with subsequent tissue steatosis and insulin resistance (Videla et al. 2004; Lewis et al. 2001). Since a reduction in AMPK activity has also been associated with myocardial lipid accumulation / cardiac lipotoxicity which leads to cardiomyopathy in obese rodents (An & Rodrigues 2006; Wang and Unger 2005), the present study's finding that the normalised heart masses were

significantly elevated in all HCD HAART-treated animals (compared to the respective lean controls) is another pointer to a probable link to the reduction in AMPK activity. Interestingly, the HOMA-IR index reflected the same observation that the HCD control and HCD HAART groups developed insulin resistance with a reduction in AMPK activity. The increase in cardiac mass and HOMA-IR were significantly reduced in the HCD HAART + Saroglitazar-treated animals compared to the HCD HAART-treated animals, and similarly this combination therapy with Saroglitazar resulted in improved AMPK activity.

Although it was expected that the addition of Saroglitazar to the HAART regimen would improve the AMPK activity following the ischaemic-reperfusion insult, the present study did not observe such improvement. Interestingly, both lean and obese Saroglitazar-treated animals demonstrated significantly higher activation of AMPK compared to the respective HAART + Saroglitazar-treated groups. Of importance to note is that all the Saroglitazar-treated groups had improved HOMA-IR indices, which has previously been linked to both PPAR α and γ activation leading to PGC-1 α and AMPK activation and subsequent increased FA oxidation as shown below (Figure 4.4). These observations support findings by Qi & Young (2015) and Russell et al. (2004), who suggested that pharmacological interventions that upregulate AMPK activity may offer therapeutic benefit in metabolic syndrome.

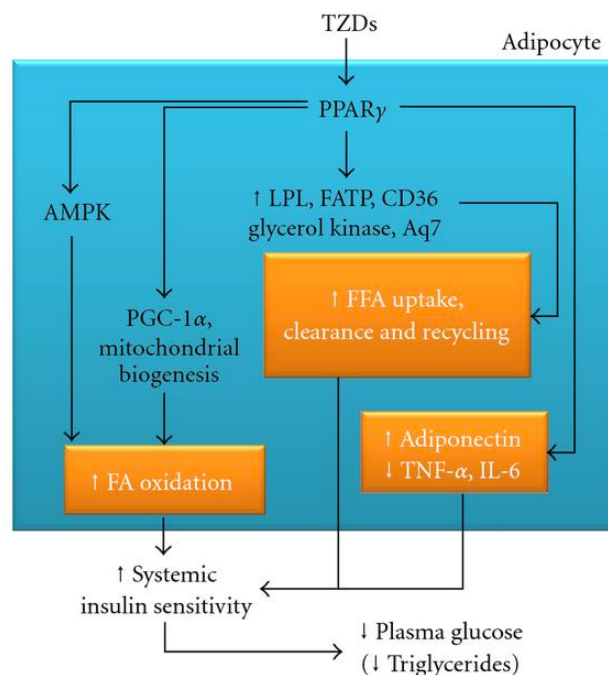


Figure 4.4 Mechanisms via which PPAR γ activation by thiazolidinediones (TZDs) lead to improved systemic insulin sensitivity through AMPK mediated signalling. Abbreviations: TNF- α (tumour necrosis factor), FFA (free fatty acids), IL-6 (interleukin 6) PPAR γ (peroxisome proliferator-activated receptor gamma), LPL (lipoprotein lipase) CD36 (cluster of differentiation 36), PGC-1 α (peroxisome proliferator-activated receptor gamma co-activator alpha), FATP (long-chain fatty acid transport protein), \uparrow (increase), \downarrow (decrease). Adapted from Leonardini et al. (2009). (Creative commons attribution license _unrestricted use).

4.13.1.2 Aortic AMPK

Although impaired activity of endothelial AMPK has been implicated in endothelial dysfunction (Russell et al. 2004; Qi & Young 2015), the present study did not observe any significant changes in AMPK activation among the various treatment groups. This was unexpected because, as already discussed (section 4.11), HCD HAART animals showed marked impaired relaxation and the lean Saroglitazar-treated animals also demonstrated marked hypercontractility. All these changes were expected to have an association with endothelial AMPK-mediated energy regulation and subsequently changes in AMPK expression. However, since we only conducted baseline AMPK analyses and no analyses were performed following the aortic isometric tension studies, this is an area that should be further investigated. In addition, we only evaluated vascular AMPK activity (i.e. including smooth muscle and connective tissue AMPK) and therefore measurement of the specific endothelial AMPK should be considered in future vascular studies.

Chronic use of PIs and NRTIs has been associated with endothelial dysfunction as a result of increased generation of ROS, increased endothelial inflammation and dyslipidaemia leading to atherosclerosis (Dressman et al. 2003; Stein et al. 2001). Although the exact mechanisms have not been clearly elucidated, Dressman and colleagues (2003), established that ritonavir administered to mice for a period of eight weeks led to development of atherosclerotic lesions in the ascending and descending thoracic aortic segments and subsequent *in vitro* studies confirmed upregulation of CD36 (sterol scavenger receptor), leading to increased sterol uptake by macrophages. Li et al. (2011) further reported that AMPK activation, through the inhibition of the SREBP, ameliorates liver fat accumulation and atherosclerosis in diet-induced insulin resistance. Therefore, AMPK has been suggested to be a therapeutic target for anti-atherosclerosis treatment, malignancies and hepatic steatosis (Motoshima et al. 2006). The present study therefore, did not observe any effects of dual PPAR α and γ stimulation using Saroglitazar on aortic tissue expression and activation of AMPK in either lean or obese Wistar rats treated with PIs and NRTIs, despite improved aortic relaxation in the HCD HAART + Saroglitazar group.

4.13.1.3 Hepatic AMPK

The role of AMPK in both normal liver physiology and liver pathology has been reviewed (Section 1.5.6) and it is well established that AMPK activity plays a critical role in the regulation of hepatocyte lipid homeostasis. Results from the AMPK measurements in the experimental animals are presented in section 3.13.3.5. Although no changes were observed in AMPK expression and activation in the lean and HCD control groups (results not displayed), there was a clear reduction in AMPK activation in the HCD HAART group compared to lean HAART group and HCD HAART + Saro group (Figure 3.86). Additionally, the lean and HCD HAART + Saroglitazar-treated groups showed marked increase (2-fold increase) in the activation of AMPK compared to the HCD HAART.

Obese rats treated with PIs and NRTIs presented with features of steatosis and steatohepatitis (section 4.12) and with a marked reduction in AMPK activation contrary to the observations made in the HCD rats treated

with both HAART and PPAR α and γ agonist. Therefore, we have demonstrated that the hepatic effects of HCD and LPV / r in combination with AZT / 3TC are marked by both structural and signalling abnormalities. To the best of our knowledge, this is new evidence because no studies have described the above findings in the context of PIs and NRTIs with concomitant PPAR α , γ agonist therapy, even though previous studies have been conducted on PIs (ritonavir) (Li et al. 2001; Dressman et al. 2003). Use of Saroglitazar in HIV patients on HAART has been reported to improve the lipid profile (reduction in serum cholesterol and TGs) (Deshpande et al. 2016). Although these findings were not reflected in the present study, there is now evidence that at signalling level, AMPK plays a major role in ameliorating the hepatic HAART and diet-induced steatosis.

4.13.2 PKB/Akt

PKB /Akt (from diverse stimuli such as, IGF-1, bFGF, EGF and platelet-derived growth factor receptor (PDGF-R) regulates a variety of cellular responses ranging from metabolism, growth, cell survival and intracellular signal transduction (Barnett et al. 2005; Kitamura et al. 1999). The metabolic derangements observed in the HCD and HAART are known to interfere with cardiac, aortic and hepatic PKB/Akt activity and below are the inferences we make from this study.

4.13.2.1 Cardiac PKB/Akt

Implications of PKB/Akt pathway disturbances in cardiac pathology have been reviewed (section 1.5.4.2). PKB/Akt activation is critical in cardioprotection in both pre-and post-ischaemic conditioned heart perfusion (Hausenloy et al. 2005). Before induction of ischaemia (baseline), the present did not observe any significant differences in either the expression (total PKB/Akt) or phosphorylation of PKB/Akt (phospho-PKB/Akt) (section 3.13.1.3.1). Although previous studies have reported on a reduction in the phosphorylation of PKB/Akt in HFD compared to lean controls, the expression of total PKB/Akt remained the same (Ouwens et al. 2005). The changes observed in PKB/Akt phosphorylation by Ouwens et al. (2005), are explained by the differences in diet composition. The diet model they employed contained palmitate (91.12 g/kg) and oleate (100.24 g/kg); furthermore, the rats were heavier (302 g) at the onset of the programme, indicating that they were older (age not indicated), n = 34 / group. Furthermore, the diet-induced hyperglycaemia and insulin resistance (T2DM) model resulted in overt hyperglycaemia and cardiac ultrastructural changes marked with degenerative changes (mitochondriopathic changes) and dilated cardiomyopathy. In the present study, systolic / diastolic pressures and HR did not differ significantly among the experimental animals and therefore a possible explanation for the unaltered PKB/Akt levels.

Following the induction of ischaemia and subsequent reperfusion, the total expression of PKB/Akt did not differ significantly among the different experimental groups. However, the PKB/Akt phosphorylation was markedly reduced in the HAART-treated groups (lean and HCD) compared to untreated control and Saroglitazar combined with HAART groups (lean and HCD) (Figure 3.61 A-C). Similarly, the ratio of phospho-PKB/Akt / total PKB/Akt was also significantly reduced in the HCD and lean HAART groups

compared to the lean and HCD HAART + Saroglitazar groups (Figure 3.61 D). From these findings, it appears that the effect of diet was not reflected in the expression and phosphorylation of PKB/Akt as previously stated and we ascribe this observation to the fact that, although the HCD induced insulin resistance in the HCD groups compared to the controls, there were no significant differences in the circulating blood glucose.

Previous studies that have reported reduced PKB/Akt phosphorylation in HCD animals, did demonstrate hyperglycaemia and hypertrophic-like changes in the heart tissue (Ouwens et al. 2005; Coa et al. 2011). Although Salie and colleagues (2014) reported cardiac protection against ischaemia-reperfusion using a similar DIO model, the present study did not observe a correlation between reduced infarct sizes and PKB/Akt activation. In fact, phosphorylation of PKB/Akt was not increased following preconditioning with the β_2 adrenergic receptor stimulating drug, formoterol, which supports the findings of the present study. Therefore, the diet was not associated with alterations sufficient to induce cardiac PKB/Akt expression and activation. However, following administration of PIs and NRTIs, it was evident that phosphorylation of PKB/Akt was decreased during the 20 minutes of global ischaemia and 10 minutes of reperfusion.

As previously discussed, ritonavir is associated with the induction of lipodystrophies that also manifest with an accumulation of tissue lipids, which is further compounded by AZT / 3TC-induced mitochondrial damage. Although the present study did not evaluate cardiac lipid / glycogen load, we deduce from the above findings that hearts from HAART-treated animals subjected to an ischaemic insult are unable to competently activate protective/ survival mechanisms as observed in the animals treated with Saroglitazar and HAART. Poor phosphorylation of PKB/Akt was observed in both lean and HCD animals treated with LPV / r and AZT / 3TC. It is well documented that PKB/Akt activation following ischaemia mediates cardioprotection through activation of anti-apoptotic pathways, such as the RISK pathway (Hausenloy et al. 2005; Hausenloy & Yellon 2007; Tsang et al. 2004). However, the mechanisms underlying PI and NRTI-mediated cardiac damage remain incompletely understood. Therefore, the present study contributes new knowledge in this area since we have demonstrated that treatment with a dual PPAR α , γ agonist, improves PKB/Akt activation in both lean and HCD Wistar rats, treated with LPV / r and AZT / 3TC. This discussion is advanced in the subsequent sections on the role played by PKB/Akt in eNOS signalling.

4.13.2.2 Aortic PKB/Akt

Activation of PKB/Akt in vascular tissue plays a critical role in the maintenance of homeostasis and angiogenesis (Shiojima & Walsh 2002). PKB/Akt mediates many vascular processes such as cell migration, glucose metabolism, protein synthesis, cell attachment, survival and NO production. The function that will be highlighted in the present study is the PKB/Akt-mediated eNOS phosphorylation leading to increased NO production through vascular endothelial growth factors (VEGF) activation of PKB/Akt. PI3K and PKB/Akt-mediated vascular effects are summarised below (Figure 4.5).

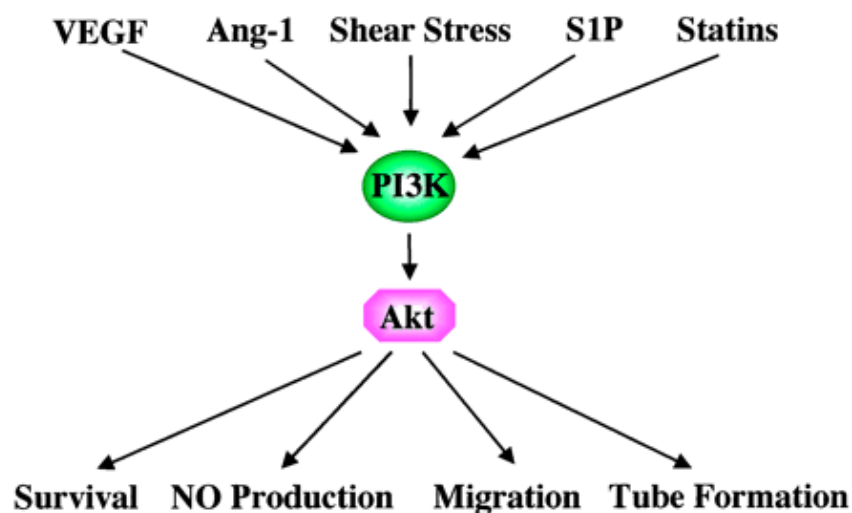


Figure 4.5 PI3K and PKB/Akt mediated vascular effects. Abbreviations (NO - nitric oxide, PI3K- 3-phosphoinositide kinase, Ang-1 angiotensin 1, S1P - sphingosine-1-phosphate, VEGF - vascular endothelial growth factors. Adapted with permission (Shiojima & Walsh 2002).

The findings from the present study (Figure 3.71) indicate that, the total PKB/Akt was not altered in any of the experimental groups; however, phosphorylation of PKB/Akt was higher in the HCD group compared to the lean control and the HCD HAART groups (Figure 3.72). Therefore, HAART appeared to downregulate PKB/Akt activation in both obese and lean animals. A very interesting finding was that this downregulation was limited when Saroglitazar was co-administered with HAART to both lean and obese animals.

We have already shown that the HCD control aortic rings demonstrated improved endothelial-mediated acetylcholine-induced aortic relaxation and this may be explained by the activation of PKB/Akt in the HCD group. Phosphorylation of PKB/Akt has previously been shown to increase phosphorylation of eNOS and therefore increased production of NO that explains the improved relaxation following acetylcholine stimulation (Figure 4.5). The factors that lead to improved modulation of the endothelium in the HCD remain incompletely understood, but the role of VEGF has been shown to play a major role in PKB/Akt-mediated endothelial /vascular survival (Fujio & Walsh 1999; Gerber et al. 1998).

PIs and NRTIs are implicated in endothelial damage and vasculopathies. eNOS down-regulation and increased oxidative stress have been suggested as some of the underlying causes (Wang et al. 2009). Since PKB/Akt is intricately involved in vascular endothelial survival, the present study investigated the activation of PKB/Akt in LPV / r and 3TC / AZT and the role played by dual PPAR α , γ stimulation. The findings were intriguing because the down-regulation of phospho- PKB/Akt and phospho- PKB/Akt / total ratio observed in both lean and obese HAART-treated animals were upregulated upon combining Saroglitazar with HAART (Figure 3.72). Additionally, this was reflected in the isometric aortic tension studies where the HCD HAART + Saroglitazar-treated group had significantly improved endothelial-mediated acetylcholine-induced aortic relaxation compared to the HCD HAART-treated animals. This is a novel finding because a combination of PIs and NRTIs with dual PPAR α , γ stimulation has not been investigated before. Our experimental model of HCD-

induced obesity in male Wistar rats has demonstrated clear improvements in both functional (relaxation) and signalling (PKB/Akt) upon combining PPAR α , γ agonist (Saroglitazar) with a PI-based regimen (LPV / r + AZT / 3TC).

4.13.2.3 Hepatic PKB/Akt

PKB/Akt plays a central role in both hepatocyte survival and regulation of hepatocyte insulin / glucose and protein synthesis (Cichy et al. 1998). Therefore, metabolic derangement in disease states or in drug therapy impact greatly on PKB/Akt activity. PKB/Akt pathway dysregulation has been implicated in impaired insulin signalling and subsequent glucose metabolism (Leclercq et al. 2007; Hanada et al. 2004). Figure 4.6 below illustrates how downstream PKB/Akt signalling mediates insulin receptor stimulation via PI3K and PDK1,2 pathway (see section 1.5.4.1 for more details).

Following the binding of insulin to its receptor, a conformational change is triggered which leads to the phosphorylation of three intracellular pathways, namely: -

- i) PI3K pathway: PI3K activation in-turn activates PDK1, 2 which phosphorylates PKB/Akt at Thr 308 leading to its protein and glucose metabolism mediated regulation.
- ii) MAPK: Mediates insulin-induced mitogenic, growth and cell differentiation processes.
- iii) CAP/Cbl/TC10 pathway: Mediates GLUT 4 translocation to the membrane (in GLUT 4 expressing tissues such as adipose and skeletal / cardiac muscle).

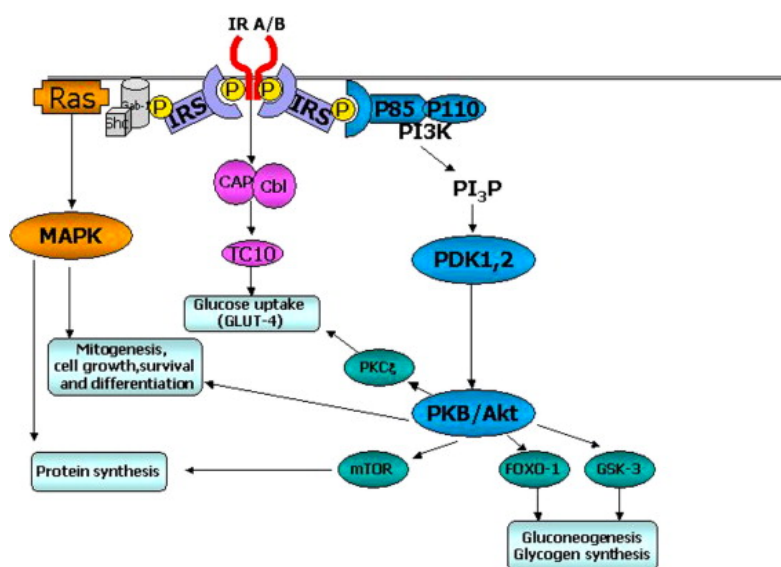


Figure 4.6 PKB/Akt-mediated intracellular insulin signalling. Abbreviations: PKB/ Akt (protein kinase B), PKC (protein kinase C), GLUT- 4 (glucose transporter 4), MAPK (mitogen-activated protein kinase), IRS (insulin receptor substrate), PI3K (3-phosphoinositide kinase), PDK1,2 (protein D kinase 1, 2), GSK-3 (glycogen synthase kinase-3). Adapted with permission (Leclercq et al. 2007).

The present study observed that the hepatic total PKB/Akt levels were constant in all the experimental groups and remained unchanged (Figure 3.78). However, PKB/Akt phosphorylation was significantly depressed in

the HCD control group and HCD HAART-treated groups compared to their respective controls (Figure 3.79). This observation is intriguing, because dietary effects seemed to impact negatively on hepatocyte PKB/Akt activation. No differences in phosphorylated PKB/Akt were observed in the Saroglitazar groups. However, when the phospho- PKB/Akt / total PKB/Akt ratio was evaluated, it was observed that the HAART-treated groups (lean and obese) had significantly lower ratios compared to the HAART + Saroglitazar-treated groups (Figure 3.80). This finding contradicts the earlier observation that PIs and NRTIs did not alter phosphorylation of PKB/Akt in the lean groups. Furthermore, no functional derangements (based on biochemical analysis of liver enzymes, serum glucose and insulin concentrations) were observed that could explain this finding. Therefore, this is an area that future studies ought to investigate further. The reduction in PKB/Akt phosphorylation in the HCD HAART group supports the observations made earlier that these experimental animals also manifested with insulin resistance and histologically with features of steatosis and hepatitis. Improved phosphorylation of PKB/Akt in the Saroglitazar-treated groups explains the reversal or protection from HAART-induced hepatic steatosis and insulin resistance (based on HOMA-IR). This observation was also made in the aortic phosphorylation of PKB/Akt.

In summary, the present study presents evidence that aortic phosphorylation of PKB/Akt is depressed in HAART therapy (both lean and HCD rats). Similarly, hepatic phosphorylation of PKB/Akt is depressed in HCD control and HCD HAART-treated animals. However, this downregulation is limited by co-administration of HAART (LPV / r and AZT / 3TC) with Saroglitazar and was associated with improved endothelial-mediated acetylcholine-induced aortic relaxation and improvement in insulin resistance (lowering of HOMA-IR) with improved liver histology. In the cardiac tissue, similar observations were made following ischaemia reperfusion, although baseline phosphorylation of PKB/Akt was not altered.

4.13.3 eNOS

4.13.3.1 Cardiac eNOS

Reduced expression of cardiac eNOS has been implicated in CVD and cardiac hypertrophy (Brede et al. 2003). Additionally, disturbances in insulin signalling have been implicated in altered cardiac eNOS signalling (Koricanac et al. 2011). The role of PIs and NRTIs in eNOS signalling derangements has been reviewed (see sections 1.5.4.2 and 1.2.4). The present study did not observe any differences in either total or phosphorylated eNOS before induction of ischaemia. However, following ischaemia and subsequent reperfusion, the phospho-eNOS was significantly reduced in the HCD HAART-treated animals compared to the HCD control animals (Figure 3.58 A). The lean and HCD HAART + Saroglitazar-treated groups also showed increased eNOS phosphorylation compared to the lean and HCD Saroglitazar-treated groups (Figure 3.58 B). The phospho-eNOS / total eNOS ratio was significantly higher in the HCD group compared to the HCD HAART group. Also, both lean and HCD HAART-treated animals showed reduced phospho-eNOS / total eNOS ratios compared to lean and HCD HAART + Saroglitazar-treated animals (Figure 3.59).

Ischaemia interferes with cardiac substrates required for energy metabolism and therefore activates protective mechanisms that aim to improve cardiac function and blood flow in the strained state. An increase in eNOS activity is one of the ways in which the cardiac endothelium responds to increase NO production and improve not only blood flow but also inhibit apoptosis and promote other proliferative pathways (see section 1.2.4). Therefore, from the above findings, we infer that, as suggested by other studies (Zhou & Gurley 2006; Zhou et al. 2005; Lipshultz et al. 2012), LPV/ r and AZT /3TC therapy impairs the cardiac eNOS response to ischaemic insult and this was improved when animals on HAART were co-treated with a dual PPAR agonist, Saroglitazar. To the best of our knowledge, this is a novel finding.

Possible mechanisms that have been postulated to interfere with eNOS activity in HAART include increased oxidative stress as a result of NRTI-mediated mitochondrial damage (Zhou et al. 2005) and activation of mononuclear cell recruitment (Dressman et al. 2003). Observations made on the PKB/Akt signalling in cardiac, aortic and liver tissues indicate that there is consistent upregulation of PKB/Akt activity when Saroglitazar is combined with HAART. PKB/Akt is a well-documented inducer of eNOS phosphorylation (Shiojima & Walsh 2002) and therefore, this may explain eNOS upregulation following ischaemia-reperfusion.

4.13.3.2 Aortic eNOS

The aortic expression of total eNOS and phosphorylation are shown in Figure 3.70. The phospho-eNOS / total eNOS ratio shows a clear reduction in the HAART groups (lean and HCD) and increased ratios in the Saroglitazar-treated groups (lean and HCD HAART + Saro and, lean and HCD Saroglitazar) compared to the HAART-treated groups. Therefore, HAART-mediated reduction in eNOS activation was ameliorated by co-therapy with Saroglitazar (HAART + Saro). Perhaps the most striking observation in terms of both eNOS activation and endothelial performance is the downregulation of phospho-eNOS in the HCD HAART group that was accompanied by poor endothelial-mediated acetylcholine-induced aortic relaxation. In addition, the HCD HAART + Saroglitazar-treated animals showed an increase in phosphorylation of eNOS that may explain the improved endothelial-mediated acetylcholine-induced aortic relaxation (Figure 3.48 B).

The eNOS phosphorylation findings correspond to the phosphorylation of PKB/Akt (discussed 4.13.2.2) thereby underscoring the interplay between PKB/Akt and eNOS in both cardiac and aortic tissues protection. We therefore postulate that the dual PPAR α , γ -mediated upregulation of these signalling proteins (PKB / Akt and eNOS) in HAART, is a possible mechanism underlying the functional and structural amelioration of HAART-induced NAFLD and cardiac / vascular dysfunction.

4.13.4 MAPKs: p38 and Erk 1 / 2

The roles played by these important intracellular signalling proteins are reviewed in section 1.5.7.3.

4.13.4.1 Cardiac Erk 1 / 2

There were no changes observed in the baseline cardiac expression of total and phosphorylated Erk 1 / 2 (Figure 3.62). This finding was unexpected because previous studies using the same HCD have demonstrated increased Erk 1 / 2 activation in diet-induced obese animals compared to the lean control animals (Salie et al. 2014). However, although the diet compositions were similar, the DIO rats were 21 % heavier than the control rats in the aforementioned study by Salie et al. (2014) compared to the present study mass difference of 15 %. Following 20 minutes of global ischaemia and 10 minutes of reperfusion, the total Erk 1 / 2 expression remained the same across the experimental groups. However, phosphorylation of Erk 1 / 2 was significantly higher in the HCD control group compared to the lean control and HCD HAART groups (Figure 3.64 A). This observation is consistent with previous studies that have evaluated the role of Erk 1 / 2 in ischaemia-reperfusion and in preconditioned hearts (Salie et al. 2014); however, we are not aware of any studies conducted in the context of HAART. This is in support of the obesity paradox in cardiovascular protection, and possible mechanisms of this observation are the insulin-mediated pre-conditioning since the animals were hyperinsulinaemic (Hausenloy and Yellon 2007).

We did not observe changes in Erk 1 / 2 expression or activation following dual PPAR stimulation in either lean or obese rats, and similarly, no changes were observed in the HAART-treated animals. Although no previous studies have focused on this area, it is interesting to note, that despite marked phosphorylation in PKB/Akt and eNOS in these Saroglitazar-treated animals, no impact was observed on Erk 1 / 2 activity. The role of activated Erk 1 / 2 has previously been demonstrated in cardioprotection and it is a key player in the RISK pathway (Hausenloy et al. 2005; Hausenloy & Yellon 2007; Tsang et al. 2004), which mediates the antiapoptotic and reduction of ROS-mediated damage during reperfusion.

4.13.4.2 Aortic Erk 1 / 2

The aortic Erk 1 / 2 expression and activation findings were surprising because, although the aortic tissues in the HCD HAART + Saroglitazar group were associated with marked activation of PKB/Akt and eNOS, no significant differences were observed in Erk 1 / 2 activity. The reason for this observation remains unclear because there is ample evidence to support the protective role of Erk 1 / 2 activation in the vascular endothelium and promotion of angiogenesis and endothelial proliferation which go hand in hand with PKB/Akt activation (Secchiero et al. 2003; Mavria et al. 2006).

4.13.4.3 Hepatic Erk 1 / 2

Erk 1 / 2 MAPK signalling in the liver is involved in diverse cellular processes. Previous studies have documented both protective and detrimental effects of Erk 1 / 2 activation. Through activation by stress and inflammatory stimuli, JNK and Erk 1 / 2 activation has been shown to induce insulin resistance in NAFLD (Malhi et al. 2006; Tarantino & Caputi 2011). On the other hand, Erk 1 / 2 activation has been implicated in mediating an anti-apoptotic role in ROS-induced caspase activation by JNK (de la Rosa et al. 2006). In the

present study, it was observed that phosphorylation of Erk 1 / 2 was increased in both lean and HCD HAART-treated groups compared to the lean and HCD control groups, and no differences were observed in the Saroglitazar-treated groups (Figure 3.81). The ratio of phospho-Erk 1 / 2 : total Erk 1 / 2 was also increased in the lean and HCD HAART-treated animals compared to their respective controls (Figure 3.82). The phospho-Erk 1 / 2 : total Erk 1 / 2 ratio was higher in the HCD HAART group compared to the HCD HAART + Saro and no other differences were observed. These findings are corroborated by a previous study by Fatani et al. (2011) where it was observed that despite induction of obesity in Wistar rats (marked with increased body weight, IP fat and TGs) using a highly palatable (fat) diet, no differences in activation of Erk 1 / 2 in the liver were observed. However, the animals developed insulin resistance as observed in the present study. No previous studies have explored the role of HAART in this context (to the best of our knowledge).

Activation of Erk 1 / 2 by LPV + AZT / 3TC in both lean and obese animals is a novel observation and although it correlates with steatosis in the HCD HAART-treated group, the lean HAART group did not develop such features.

4.13.4.4 Cardiac p38 MAPK

No changes were observed in the pre-and post-ischaemia cardiac activation of p38 MAPK. Both total p38 expression and phosphorylation were equal in all the experimental groups. This finding was unexpected because previous studies have demonstrated that the induction of ischaemia activates p38 MAPK. A study by Ma et al. (1999) clearly showed that 10 minutes-reperfused rabbit hearts following 30 mins of global ischaemia showed increased activation of p38 MAPK and was associated with increased apoptosis. Subsequently, apoptosis was reduced following p38 MAPK inhibition. Although our protocol only induced global ischaemia for 20 mins, no changes in p38 MAPK activation were observed after 10 minutes of reperfusion in either control or HCD treated and untreated animals. Data on the effects HAART on p38 MAPK expression in ischaemia-reperfusion is limited and therefore comparisons with other findings were not feasible. However, we are of the opinion that this signalling protein may not be implicated in the diet and HAART-mediated effects on isolated perfused rat hearts.

4.13.5 PGC 1 α and PPAR α

Cardiac PGC-1 α and PPAR α expressions were not altered by either diet, HAART or *in vivo* PPAR α and γ stimulation before induction of ischaemia (Table 3.9). Additionally, no changes were observed in the hepatic expression of PGC-1 α and PPAR α (Table 3.10). Although there is a paucity of data from previous studies to make comparisons in this context, this finding was unexpected because as already stated (section 1.5.1 and section 1.5.2), PGC-1 α and PPAR α play a major role in glucose and lipid regulation in metabolic syndrome (Tonstad et al. 2007; Ratzu et al. 2008).

Although cardiac post-ischaemia PGC-1 α and PPAR α expression was not significantly different among the experimental groups, PGC-1 α expression was higher following ischaemia-reperfusion compared to the pre-ischaemia expression levels. This has been demonstrated before (Butterick et al. 2016) where pioglitazone (a

TZD) improved PGC-1 α signalling, although no improvements in infarct sizes or blood flow were observed in this swine model of MI. Interestingly, the HCD HAART group showed the highest percentage increase in the expression of PGC-1 α following ischaemia compared to the pre-ischaemia levels.

Involvement of PIs and NRTIs in both cardiovascular and metabolic abnormalities is linked to PGC-1 α and PPAR α / γ downregulation leading to insulin resistance, NAFLD and lipodystrophy (Carr et al. 1998; Giralt et al. 2006). The present study has also demonstrated the induction of insulin resistance in HCD and HAART-treated animals despite normal blood glucose concentrations. Furthermore, there was demonstrable steatosis in the liver that was also associated with mild inflammatory changes in the HCD HAART-exposed animals.

Aortic PGC-1 α expression was higher in the lean HAART + Saroglitazar-treated group compared to the lean HAART group. In addition, PGC-1 α expression was higher in the HCD Saroglitazar-treated group compared to lean Saroglitazar group. No differences were observed between the HCD control and lean control group. No significant differences were observed between HCD HAART + Saro and HCD HAART-treated groups. The findings are difficult to explain because it has been observed that overexpression of PGC-1 α is associated with increased NO levels, which activate mitochondrial biogenesis complementing the role played by PGC-1 α (Nisoli 2003; Kodlec et al. 2017). Therefore, when comparing the aortic reactivity and PGC-1 α signalling, the expectation was that the HCD HAART + Saroglitazar-treated group which showed improved relaxation compared to HCD HAART would have displayed better PGC-1 α expression. However, the hyper-contractile response of the aortic rings from the lean Saroglitazar group demonstrates a possible link to the observed reduced PGC-1 α expression. However, the aortic rings from the HCD HAART group with poor relaxation values did not show significant reduction in PGC-1 α expression compared to HCD HAART + Saro.

4.13.6 I κ B α

A review on the implications of I κ B α in the present study has been supplied in section 1.5.3. Cardiac expression of I κ B α did not differ among the experimental groups before ischaemia-reperfusion. Following 20 minutes of global ischaemia and 10 minutes of retrograde reperfusion, it was observed that all groups had increased I κ B α expression compared to the pre-ischaemia expression. The percentage change was highest in the HCD HAART + Saro group (Table 3.9). Although the post-ischaemia mean I κ B α expressions did not differ, we infer that the increased percentage change in the HCD HAART + Saro group was an indication of increased inhibition of NF κ B which has been shown to offer protection during ischaemia-reperfusion (Valen et al. 2001). Although this inhibition has been shown to improve cardiac function and reduce infarct sizes (Saini et al. 2005), the present study only observed a reduction in infarct sizes in HCD control and HCD HAART groups in comparison to the control group without demonstrable improvement in cardiac function.

Although hepatic NF κ B expression has previously been shown to be high in steatohepatitis, the hepatic changes in the present study did not result in demonstrable changes in the hepatic I κ B α expression. This finding warrants further investigation into the inflammatory mediators (serum markers) in the liver tissue. This was outside the scope of the present study.

Aortic I κ B α expression was only significantly decreased in the lean Saroglitazar-treated group compared to the lean control (Figure 3.75). This finding is consistent with the aortic reactivity studies which indicated that the lean Saro group had increased phenylephrine-induced aortic contraction compared to the other groups. Furthermore, this group also showed marked reduction in the expression of PGC-1 α . The effects of LPV/r + AZT / 3TC were not reflected in the aortic I κ B α expression. The combination of ARVs used in the present study has not been previously investigated in this context; however, since it is known that PIs and NRTIs are associated with endothelial dysfunction and atherosclerosis (Zhou & Gurley 2006; Zhou et al. 2005), the anticipated effect was a reflection of increased aortic inflammatory processes which are stimulated in I κ B α and NF κ B signalling pathways. This was not observed in the present study.

4.13.7 NADPH p22-phox, cleaved caspase 3 and cleaved PARP

4.13.7.1 p22-phox

The role of p22-phox in the induction of aberrant cell proliferation, generation of ROS, migration and inflammatory responses (Griendling et al. 2000) is of great interest in hepatic, cardiac and endothelial / vascular physiology (Section 1.5.7.1). In the present study, it was observed that the pre-ischaemia expression of p22-phox did not differ among the experimental groups. However, following ischaemia-reperfusion, p22-phox was significantly decreased in the lean and HCD HAART + Saroglitazar-treated groups compared to the lean and HCD HAART-treated groups (Figure 3.67). Similarly, the expression of aortic p22-phox was significantly elevated in the HCD HAART and lean HAART groups compared to the respective untreated control groups (Figure 3.77). Aortic p22-phox expression in the HAART + Saroglitazar-treated groups remained unchanged. No changes were observed in hepatic p22-phox expression in any of the experimental groups.

The above findings are consistent with the increased oxidative stress in vascular endothelium and cardiomyocytes posed by chronic use of LPV / r and NRTIs (Videla et al. 2004; Reyskens & Essop 2014). Additionally, previous studies have observed a clear correlation between the risk / severity of atherosclerotic disease (CAD) and elevated levels of p22-phox. Therefore, the above findings accurately reflect the observation made on the poor endothelial-mediated acetylcholine-induced aortic relaxation in the HCD animals treated with HAART (increased p22-phox) and improved endothelial-mediated acetylcholine-induced aortic relaxation in Saroglitazar co-administration with PI and NRTIs (reduced p22-phox). The lack of altered hepatic p22-phox expression is explained by the observation that the steatosis was mild-moderate and was associated with only mild-moderate inflammation. Increased p22-phox expression has been associated with advanced NASH (Videla et al. 2004).

4.13.7.2 Cleaved PARP and cleaved caspase 3

The roles played by these two proteins in both normal and altered physiology are described in section (1.5.7.2). Although they are important in mediating effective DNA repair (PARP) and apoptosis (caspase 3), their uncontrolled activation is implicated in cell death and impaired mitochondrial biogenesis.

The present study did not observe any significant differences in the aortic and hepatic expression of either cleaved PARP or cleaved caspase 3 expression. However, post-ischaemic cardiac expression of cleaved caspase 3 was significantly higher in the HCD HAART group compared to the HCD control and HCD HAART + Saro groups (Figure 3.68 A and B). Similarly, the expression of caspase 3 was significantly higher in lean HAART-treated animals compared to the lean HAART + Saro group (Figure 3.68 B). Following ischaemia and reperfusion cleaved PARP expression was higher in the HCD control group compared to the lean control, and treatment with HAART in both lean and HCD groups significantly increased the expression of cleaved PARP. The increase was more pronounced in the HCD HAART-treated group (Figure 3.69 A). Also, the expression of cleaved PARP was significantly lower in the HCD HAART + Saro group compared to the lean HAART + Saro and HCD Saro groups (Figure 3.69 B). It is important to note that infarct sizes measured in these experimental groups did not correlate well with PARP activation, hence raising more questions on the role of PARP.

High fat feeding has been shown to increase PARP activity, and although the short-term consequences protect the cells, long-term effects lead to cell death and mitochondrial dysfunction (Bai & Cantó 2012). Figure 4.7 below illustrates the short-and long-term effects of activation and inhibition of PARP.

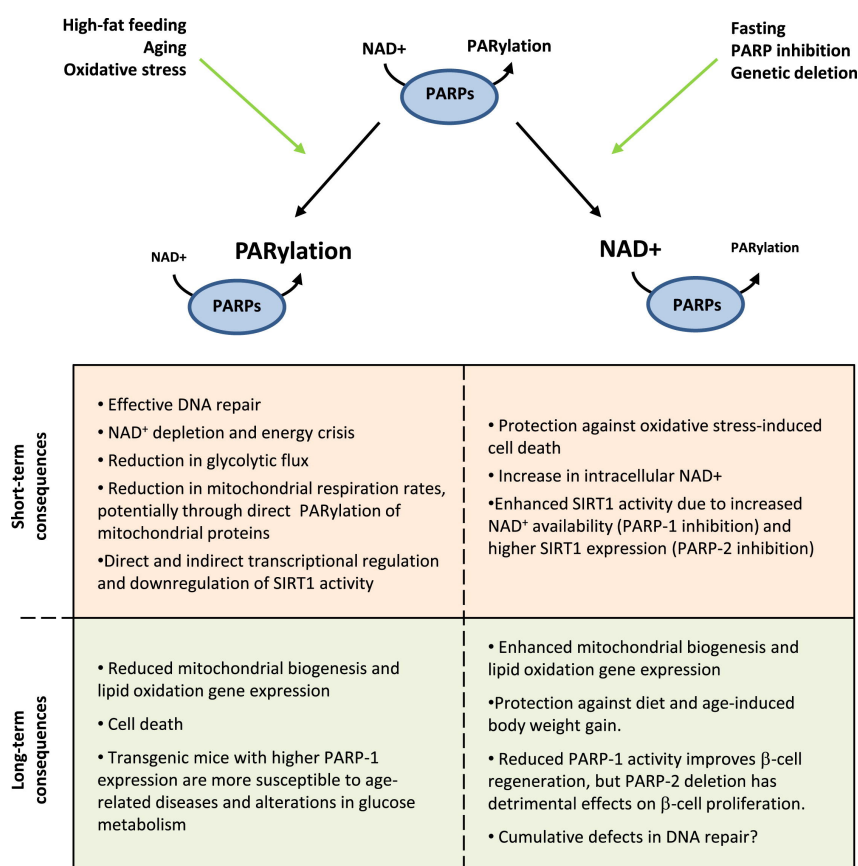


Figure 4.7 Showing short-term and long-term consequences of PARP activation (by high-fat feeding, aging and oxidative stress) and PARP inhibition by (fasting, PARP inhibitors, genetic deletion. Abbreviations: NAD⁺ (Nicotinamide adenine dinucleotide), PARP (poly (ADP)-ribose polymerase), PAR (poly (ADP-ribose) polymers), SIRT1 (Sirtuin 1). Adapted with permission from Bai & Cantó (2012).

The role of HAART in the induction of DNA damage, genomic instability, mitochondrial dysfunction and eventual cell loss through increased apoptosis has been described in numerous cells, such as hepatocytes, endothelial cells and immune cells (Lewis et al. 2001; Badley 2005; Zhou et al. 2005). Furthermore, the mitochondrial damage induced by NRTIs further drives cellular oxidative damage rendering the cell dysfunctional (Liu et al. 2015). All these factors activate PARP and caspase-mediated pathways that lead to eventual cell death through necrosis (PARP), apoptosis (PARP and cleaved caspase 3) or both (Tewari et al. 1995; Adaikalakoteswari et al. 2007). Although this HAART combination (LPV / r and AZT / 3TC) has not previously been investigated in this context, our findings concur with studies that have implicated PIs and NRTIs in aggravating cardiomyocyte damage following ischaemia-reperfusion (increase in apoptosis possibly driven by upregulation of PARP and caspase pathways). We propose that the mechanisms involved are similar to the long-term effects of HFD and oxidative stress on PARP activation (Figure 4.7). Furthermore, the present study provides new evidence that combining PIs +NRTIs with a dual PPAR α , γ agonist (Saroglitazar) leads to a decrease in both cleaved PARP and cleaved caspase 3 expression, which are more pronounced in HCD treated groups.

4.14 Summary

The highly palatable HCD induced visceral obesity as evidenced by increased weight gain (from the 6th week of feeding programme) and increased % IP fat as a result of consumption of more food (hyperphagia). Obesity in this HCD model was also accompanied by hyperinsulinaemia and insulin resistance, hypertriglyceridaemia and elevated liver mass as opposed to the standard rat chow. Treatment with HAART or Saroglitazar did not have any effects on water and food consumption in either the lean or obese animals and similarly no effects were observed in total body mass. However, co-treatment of HAART + Saroglitazar led to a reduction in the percentage IP fat content in both lean and HCD groups. Although the HCD diet did not induce any changes in the cardiac mass, HAART induced an increase in cardiac mass in the obese animals and this was limited by co-treatment with Saroglitazar.

HAART-induced hyperinsulinaemia and insulin resistance in obese rats was improved with Saroglitazar co-treatment. Saroglitazar treatment with or without HAART did not alter serum TGs. Similarly, HAART treatment in both lean and obese animals was not associated with altered serum TG concentrations. HAART treatment in obese animals induced FFA oxidation as evidenced by elevated levels of serum CD in obese rats treated with HAART. However, this effect was limited in combined HAART and Saroglitazar therapy.

Untreated obese animals also presented with mild steatosis, however, six-weeks of LP V / r + 3TC / AZT treatment in obese rats led to the development of moderate steatosis that was associated with moderate inflammation but no fibrotic, necrotic or neoplastic changes. Combined Saroglitazar with HAART limited these hepatic changes, but did not translate into improvement in the liver transaminases and aminotransferases levels.

HCD did not impair cardiac functional performance before and after ischaemia reperfusion. Untreated obese rats had smaller infarct sizes compared to the lean animals and intriguingly, infarct sizes in HAART-treated obese rats were smaller compared to the untreated obese animals. The cardiac functional performance in the HCD HAART group was poor (reduced cardiac output and total work) compared to lean animals treated with HAART. Additionally, post ischaemia expression of Erk1/2, PKB / Akt, AMPK and eNOS signalling proteins was downregulated whereas expression of p22-phox and caspase 3 was accentuated. Combination of HAART with Saroglitazar, however, upregulated the expression of Erk1/2, PKB / Akt, AMPK and eNOS signalling proteins and downregulated caspase 3 and p22-phox expression.

Obese rats treated with HAART demonstrated poor endothelial-dependent acetylcholine-induced aortic relaxation, whereas combination of Saroglitazar with HAART improved the aortic relaxation. HAART treatment in obese rats reduced aortic activation of eNOS, PKB / Akt and was associated with high expression of p22-phox. However, Saroglitazar combined with HAART in HCD rats led to upregulation of eNOS, PKB / Akt and downregulation of p22-phox expression.

Although we have shown clear association between the modulation of these signalling proteins and the various pathophysiological states investigated, future studies should use specific inhibitors of these proteins to show that there is effectively a role of a specific protein in the effect observed with different treatments. In addition, we recognise the limitation of using neither an *in vivo* model of ischemia-reperfusion nor an animal model infected with the virus. These factors should be considered in future studies.

Table 4.1 A and B Summary of the main study findings (corresponding colour codes indicate comparisons made between two experimental groups and ↑ and ↓ refer to increase or decrease following comparisons between paired groups).

Table 4.1 A) Summary of the main findings								
176 Wistar rats randomized into 2 groups (n = 88 / group)								
Parameters assessed	Standard diet (lean group)				High calorie diet (HCD) group			
Water intake (mL/rat/day)	↑				↓			
Food intake (g/rat/day)	↓				↑			
Total body mass (g)	-				↑			
After 10 weeks, standard diet and HCD groups further randomized into 4 groups and started on drug treatment								
Experimental groups (n = 22 / group)	Lean control (Vehicle, H ₂ O)	Lean HAART	Lean HAART + Saro	Lean Saro	HCD control (Vehicle, H ₂ O)	HCD HAART	HCD HAART + Saro	HCD SARO
Food intake (g/rat/day)	-	-	-	-	↑	↑	↑	↑
Water intake (mL/rat/day)	↑	↑	↑	↑	↓	↓	↓	↓
Total body mass (g)	↓	↓	↓	↓	↑	↑	↑	↑
End of 16 weeks of feeding program and (last 6 weeks) of drug treatment biometric parameters								
Total body mass (g)	↓	↓	↓	↓	↑	↑	↑	↑
IP fat (% of total body mass)	↓	↓	↓	↓	↑	↑	↑	↑
Normalised cardiac mass (mg/mm)		↓	↓			↑	↑	
Normalised liver mass (mg/mm)	↓				↑			
Blood and serum parameters								
Random > Fasting blood glucose	↑	↑	↑	↑	↑	↑	↑	↑
Fasting insulin (μIU/L)	↓	↓		↓	↑	↑	↓	↑
HOMA-IR	↓	↓		↓	↑	↑	↓	↑
TGs (mmol / L)	↓				↑			
Normalised CD (μmol/mmol)	↑	↑	↓	↑	↑	↑	↓	↓
Normalised TBARS (μmol/mmol)					↑			↓
S-ALP (IU/L)						↓		↑
Cardiac performance								
Qa (ml/min)		↑				↓	↑	
% Qa recovery						↓	↑	
CO (ml/min)		↑				↓	↑	
% CO recovery						↓	↑	↑
Wt (mW)		↑				↓		
% Wt recovery						↓	↑	
Infarct sizes								
% infarct size	↑				↓	↓		
Liver tissue histology								
Steatosis	↓				↑	↑	↓	↓
Steatohepatitis	-	-	-	-	-	↑	↓	

Table 4.1 B) Summary of the main findings								
Experimental groups	Lean control	Lean HAART	Lean HAART + Saro	Lean Saro	HCD control	HCD HAART	HCD HAART + Saro	HCD SARO
Parameter								
Vascular reactivity								
Contraction E _{max}		↓		↑	↓	↓	↓	↓
Relaxation R _{max}	↓				↑			
					↑	↓		
Relaxation Log EC ₅₀						↑	↓	
					↓	↑	↓	↑
Protein Expression and Activation								
AMPK activation								
Cardiac (Pre-ischaemia)	↑				↓			
		↑				↓		
Cardiac (post-ischaemia)			↓	↑			↓	↑
Liver			↑			↓		
						↓	↑	
eNOS activation								
Cardiac (Post-ischaemia)		↑	↑	↓	↑	↓	↑	↓
		↓	↑			↓	↑	
Aorta	↑	↓			↑	↓		
			↓	↑		↓	↑	
PKB/Akt activation								
Cardiac (post-ischaemia)	↑	↓			↑	↓		
		↓	↑			↓	↑	
Aorta	↓	↓	↑		↑	↓	↑	
				↑	↑	↓		↓
Liver PKB/Akt	↑	↓	↑		↓	↓	↑	
IκBα expression								
Aorta	↑			↓				
PGC-1α expression								
Aorta		↓	↑	↓				↑
Erk 1/2 activation								
Cardiac (post-ischaemia)	↑				↑			
					↑	↓		
Liver	↓	↑			↓	↑		
						↑	↓	
p22-phox expression								
Cardiac (Post-ischaemia)		↓	↑			↑	↓	
						↑		
Aorta	↓	↑			↓	↑		
Caspase 3 expression								
Cardiac (Post-ischaemia)		↓			↓	↑		
		↑	↓			↑	↓	
Cleaved PARP expression								
Cardiac (Post-ischaemia)	↓		↑		↑		↓	
	↓	↑			↓	↑		

Having discussed the present study findings, the subsequent chapter (chapter 5) draws conclusions based on the research question and study hypotheses. Also, the present study limitations and future directions on this research topic are indicated.

Chapter 5 : Final Conclusion

5.1 Conclusion

In this controlled experimental study, we set out to answer two questions: (i), whether treatment with HAART (LPV / r + AZT / 3TC) for six weeks would lead to NAFLD with concomitant development of cardiac and vascular dysfunction in lean / obese male Wistar rats compared to non-treated rats and (ii), whether co-treatment with a dual PPAR α and γ agonist, Saroglitazar, for the same duration of time, would limit HAART-induced NAFLD and subsequent cardiovascular outcomes. In addition, we aimed to test whether the null hypothesis would hold true i.e., that HAART has no effects on the development of NAFLD and CVD and that co-treatment with Saroglitazar has no effects on liver and cardiovascular system. Based on the study findings, we have made several conclusions according to the experimental objectives.

The high calorie diet model we employed successfully induced visceral obesity in male Wistar rats through hyperphagia and was marked with insulin resistance, hypertriglyceridaemia, increased IP fat, and increased CD. Following HAART therapy for six weeks, these derangements persisted and were limited when Saroglitazar was co-administered with HAART in the obese animals. Obesity also presented with mild features of steatosis, however, six-weeks of LPV / r+3TC / AZT treatment in obese rats led to development of moderate steatosis that was associated with moderate inflammation but not fibrotic, necrotic or neoplastic changes. Therefore, this combination of PIs and NRTIs led to the development NAFLD.

Combined Saroglitazar with HAART limited these hepatic changes, but did not translate into an improvement in the liver transaminases and aminotransferases levels. Therefore, we infer that the Saroglitazar-mediated protection from steatosis and steatohepatitis is via improved fat distribution (\downarrow IP fat) and amelioration of insulin resistance through upregulation of hepatic AMPK, PKB / AKT activity.

Despite the metabolic alterations induced by obesity, the findings of the present study failed to provide evidence of adverse effects by the high calorie diet on cardiac functional performance before and after ischaemia reperfusion. In fact, obese rats presented with smaller infarct sizes compared to the lean animals. Furthermore, HAART-treated obese rats developed smaller left ventricular infarct sizes following ischaemia and reperfusion, compared to the untreated obese animals. Therefore, we infer that the high serum insulin concentrations appeared to protect the treated and untreated obese rats from developing increased large infarct sizes, possibly through the insulin preconditioning phenomenon. However, obese animals treated with HAART presented with reduced cardiac output and total work compared to lean animals treated with HAART and this decline in function was associated with downregulation of protective signalling cascades i.e., Erk1/2, and PKB / Akt (RISK pathway), AMPK and eNOS signalling proteins and high oxidative stress as evidenced by increased expression of p22-phox. In support of our alternate hypothesis, co-administration of Saroglitazar with HAART limited this derangement (HAART-induced cardiac dysfunction) and lead to upregulation of

post-ischaemia Erk1/2, and PKB / Akt (RISK), AMPK and eNOS signalling proteins. These proteins are known to mediate improved cardiomyocyte efficiency and protection against reperfusion injury following an ischaemic insult. Additionally, post-ischaemia expression of p22-phox was downregulated when Saroglitazar was co-administered with HAART in obese animals indicating protection from oxidative stress posed by LPV / r + 3TC / AZT.

Therefore, we have presented novel evidence that a combination of LPV / r + AZT / 3TC impairs the myocardial response to an ischaemic insult in obese rats but co-treatment with Saroglitazar offers protection. We deduce that patients on HAART after an acute MI event, may be unable to competently activate cardio-protective mechanisms and therefore dual PPAR α / γ stimulation may have clinical potential in ameliorating this dysfunction.

Vascular reactivity studies indicated that obesity improved endothelial performance (better endothelial-mediated acetylcholine-induced aortic relaxation compared to lean animals). Therefore, the present study has provided more evidence supporting the 'obesity paradox' in cardiovascular protection, whereas obese rats treated with HAART demonstrated poor endothelial-mediated relaxation. However, combination of Saroglitazar with HAART improved this dysfunction and we consider this to be of novel potential therapeutic value for HAART-induced endothelial dysfunction in obese patients. We have established that HAART treatment in obese rats downregulates aortic activation of eNOS, PKB / Akt and upregulates expression of p22-phox thereby indicating reduced NO and increased oxidative stress that is associated with poor endothelial-mediated acetylcholine-induced aortic relaxation. However, these effects were ameliorated in Saroglitazar and HAART co-therapy through upregulation of eNOS, PKB / Akt and downregulation of p22-phox expression.

From the present study findings, we conclude that treatment of male Wistar rats with LPV / r (68.57/17.14 mg/kg/day) + AZT/3TC (51.43/25.71 mg/kg/day) for six weeks is not by itself a major risk factor for CVD, but that it potentiates the risks associated with high caloric diet-induced obesity. The PIs and NRTIs combination did not by itself induce altered cardiac functional performance or vascular reactivity, but aggravated the HCD effects. These findings suggest that the monitoring of cardiovascular risk factors in obese patients on HAART therapy is important, and that the introduction of appropriate mitigating measures such as co-treatment with a dual PPAR α and γ agonist, Saroglitazar, be investigated further for potential clinical use. We have demonstrated that the metabolic, functional and signalling disturbances in the liver, heart and aorta in obese Wistar rats treated with HAART are interlinked and are partially limited by co-treatment with a dual PPAR α and γ agonist, Saroglitazar (0.4 mg/kg/day).

5.2 Study limitations

Although the study was largely a success, there are a few things that would have improved the overall success. Suffice it to say, all the activities set out in this controlled experimental study were undertaken and all the objectives achieved.

As frequently stated in our discussion, there is a paucity of knowledge in this topic, especially on the mechanisms that mediate the HAART-induced liver, aorta and cardiac abnormalities in the setting of obesity. Although epidemiological studies and clinical trials have provided strong evidence linking these conditions, the surface is barely scratched when it comes to the pathophysiological mechanisms.

Although the *ex vivo* working heart is an excellent technique of assessing cardiac contractility and AMI, we are of the opinion that it would have been more valuable to assess the cardiac structure and performance periodically (every 4 weeks) for example through echocardiography in an *in vivo* ischemia-reperfusion model to generate more translatable findings. This is an area that future studies should focus on.

Due to budgetary constraints, the Western blot experiments had to be conducted in different sets (four experimental groups per 15-well gel plates (n = 3 / group), for the liver and heart tissues. Although the aims we set out were all accomplished, this took a long period of time compared to the aorta Western blot experiments which were conducted using 26-well pre-cast gel plates. We prioritized (with the limited funds) the aorta tissue Western blot analysis (26-well pre-cast gel plates) because the amount of protein concentration is low in aorta tissue without perivascular adipose tissue and therefore separating the groups would have demanded duplicating the limited tissue lysates which was not feasible.

As already stated, we only conducted our experiments on male Wistar rats due to time and budgetary restrictions since inclusion of female rats would have demanded larger sample sizes to account for the hormonal variations. Obesity, metabolic and CVD complications are also prevalent in female patients on HAART therapy and therefore understanding of the underlying pathophysiological mechanisms is important. Perhaps, this is an area that should be evaluated in future studies.

The present protocol evaluated HAART effects on young rats. Although this did not limit what we set out to achieve, we are of the opinion that extension of this protocol would have led to development of overt liver changes such as severe steatohepatitis and fibrosis based on our findings. Effects of HAART on older obese rats (to represent the ageing human population) have not been studied. In addition, use of HIV animal model would have provided more insight in this context and should be considered in the future.

Because only limited serum volumes could be collected, the type and number of serum analyses conducted had to be determined carefully. This is because, the animals could not be bled periodically so as not to introduce confounding effects in cardiovascular physiology. Additionally, analysis of circulating drug concentrations would have provided crucial data to correlate with the metabolites assessed. Therefore, larger sample sizes could have offered more options although this would have come at a cost to an already restricted budget.

No fatty acids were included in the perfusion buffer. Although this important factor was considered during the formulation of this protocol, inclusion of fatty acids would have required a significant addition of study animals and cost to the already restricted budgetary allocation. Inclusion of a fatty acid buffer should be considered in future studies.

5.3 Future directions

As mentioned, the surface is barely scratched in this topic area and the present study focused only on parameters relevant in assessment of NAFLD, CVD and aortic reactivity studies. For example, an *in vivo* model of MI – reperfusion would generate interesting results to corroborate our findings. Additionally, radiological cardiac performance monitoring through echocardiography and electrocardiography would be another venture in this topic.

Other parameters that should be considered in future studies include: investigation of histology of the heart and determination of cardiac lipids and glycogen. Adipose tissue histology should also be investigated in PI-based HAART regimen. Since HAART has been shown to interfere with the inflammatory pathways, serum inflammatory markers should be evaluated. Additionally, the present study investigated HAART effects following six weeks of therapy. Future studies should focus also on longer treatment protocols because the human population on HAART is ageing and the effects in obesity therefore differ.

Investigations on vascular reactivity should also investigate signalling cascades following induction of contraction and relaxation to have clearer understanding on changes that occur following drug phenylephrine-induced aortic contraction and acetylcholine-induced aortic relaxation. In addition, the endothelial (without the other vascular components) measurements of AMPK, PKB / Akt and eNOS ought to be evaluated because this area was outside the scope present study. Future experiments should also consider evaluation of these physiological processes on female rats.

As previously stated, evaluation of the serum drug concentrations during the treatment period should be considered in future studies in the context of HAART because the high rate of metabolism in rodents may greatly impact their effectiveness.

Future studies should also evaluate the role of dual PPAR α / γ stimulation in cardio-protection following AMI. This research area is currently ongoing in our laboratory where cardio-protection in ischaemia-reperfusion is being investigated targeting the PPAR α , γ stimulation in pre-and post-conditioned hearts.

5.4 Research outputs so far

Conference and science meetings contribution

Year: 2016

Authors: F. Kamau, H. Strijdom, D. Blackhurst, P. Waweru, R. Salie.

Reference: Peroxisome proliferator-activated receptors α/γ stimulation is beneficial in combined antiretroviral therapy.

(Oral presentation)

Physiology Society of Southern Africa, 44th Conference, Cape Town, South Africa. 2016.

Year: 2016

Authors: F. Kamau, H. Strijdom, D. Blackhurst, P. Waweru, R. Salie.

Reference: Peroxisome proliferator-activated receptors α/γ stimulation is beneficial in combined antiretroviral therapy.

(Oral presentation)

Annual Research Day, Faculty of Health Sciences, Stellenbosch University, 2016.

Year: 2016

Authors: F. Kamau, H. Strijdom, D Blackhurst, P. Waweru, R. Salie.

Reference: PPAR α/γ agonist, Ameliorates Metabolic Derangements in Obese rats on HAART.




(Oral presentation)

Biomedical Research and Innovation Platform (BRIP), SAMRC Annual Science Symposium. 2016.

Addenda

Addendum A, Rat chow and HCD certificates of analysis.

Addendum A, 1 Certificate of rat chow analysis.

		1st Floor, Fairweather House, 176 Sir Lowry Road, Cape Town 8001 Telephone : +27 21 465-6996/7 E-mail: chem@microchem.co.za		 	
Co .Reg. 2007/010539/07 Vat No. 4330239049				T0393	
CERTIFICATE OF ANALYSIS					
Client's Reporting Address: Department of Food Science Private Bag X1 Matieland 7602 Client's Telephone #: 021 938 9391 Client's Fax #:		Our Lab Ref #: 2013-06-25-039 Client: Stellenbosch University Requested by: Prof A Lochner E-mail address: alo@sun.ac.za Product: Control Chow Sampling Method Barcode No of Samples: Production Date: 24/06/2013 Sample Condition: SEALED Date Received: 25/06/2013 Date Validated: 16/07/2013		Our Sample ID : AC92365 Client Samp #: 1 Batch Code: Sell By Date: Order Number: PROF A LOCHNER	
ANALYSIS RESULTS	1	2	Average	MoU (%)	Test Method Ref
Moisture (g/100g)	10.95	10.84	10.9	0.70	S.O.P.C. No. 1#
Ash (g/100g)	5.66	5.72	5.7	5.00	S.O.P.C. No. 2#
Total Fat (g/100g)	4.65	4.91	4.8	2.60	S.O.P.C. No. 25#
Saturated Fat (g/100g)	0.87	0.91	0.9	2.60	S.O.P.C. No. 25#
Mono-Unsaturated Fat (g/100g)	1.42	1.51	1.5	2.60	S.O.P.C. No. 25#
Poly-Unsaturated Fat (g/100g)	2.37	2.50	2.4	2.60	S.O.P.C. No. 25#
Trans Fatty Acids (g/100g)	0.000	0.000	0.00	2.60	S.O.P.C. No. 25#
Omega 3 Fatty Acids (g/100g)	0.23	0.25	0.2	2.60	S.O.P.C. No. 25#
ALA (g/100g)	0.23	0.25	0.2	2.60	S.O.P.C. No. 25#
EPA (g/100g)	0.00	0.00	0.0	2.60	S.O.P.C. No. 25#
DHA (g/100g)	0.00	0.00	0.0	2.60	S.O.P.C. No. 25#
DPA (g/100g)	0.00	0.00	0.0	2.60	S.O.P.C. No. 25#
Omega 6 Fatty acids (g/100g)	2.13	2.25	2.2	2.60	S.O.P.C. No. 25#
Cholesterol (mg/100 g)	2.99	2.94	3	4.70	S.O.P.C. No. 26#
% Protein (6.25)	16.96	17.22	17.1	1.90	S.O.P.C. No. 36#
Nitrogen (g/100g)	2.71	2.75	2.7	1.90	S.O.P.C. No. 36#
Total Dietary Fibre (g/100g)	26.98	26.88	26.9	1.30	S.O.P.C. No. 20#
% Carbohydrate	34.80	34.43	34.6	C*	S.O.P.C. No. 21
Total Sugar (g/100g)	6.65	6.54	6.6	2.90	S.O.P.C. No. 27#
Fructose (g/100g)	0.51	0.49	0.5	2.90	S.O.P.C. No. 27#
Glucose (g/100g)	0.76	0.77	0.8	2.90	S.O.P.C. No. 27#
Sucrose (g/100g)	5.39	5.28	5.3	2.90	S.O.P.C. No. 27#
Maltose (g/100g)	0.00	0.00	0.0	2.90	S.O.P.C. No. 27#
Lactose (g/100g)	0.00	0.00	0.0	2.90	S.O.P.C. No. 27#
Energy (kJ/100 g)	1268	1275	1272		S.O.P.C. No. 22
Sodium (mg/100 g)	188.75	178.40	184	7.56	S.O.P.C. No. 45#
COMMENTS					

Confirmed by:



Technical Signatory

P Rubuz Date: 16-Jul-13

These results relate only to the items tested. Total Dietary Fibre content determined by AOAC Method 991.43
 MoU = Measurement of Uncertainty. C* = By calculation.




= SANAS Accredited Method.

Tests without the # mark in this report are "Not SANAS Accredited" and are not included in the SANAS Schedule of
 Accreditation for this laboratory.

Opinions and interpretations expressed herein are outside the scope of SANAS accreditation. This certificate shall not be reproduced
 except with the approval of the laboratory. The integrity of results reported are only valid from sample receipt by the laboratory.

Page 1 of 1


Addendum A, 2 Certificate of HCD analysis.

 Specialized Lab Services Co.Reg. 2007/010539/07 Vat No. 4330239049	1st Floor, Fairweather House, 176 Sir Lowry Road, Cape Town 8001 Telephone : +27 21 465-6996/7 E-mail: chem@microchem.co.za	  Testing Laboratory T0393
	CERTIFICATE OF ANALYSIS	

Client's Reporting Address: Department of Food Science Private Bag X1 Matieland 7602 Client's Telephone #: 021 938 9391 Client's Fax #:	Our Lab Ref #: 2013-06-25-039 Client: Stellenbosch University Requested by: Prof A Lochner E-mail address: alo@sun.ac.za Product: High Fat Diet Sampling Method Barcode No of Samples: Production Date: 24/06/2013 Sample Condition: SEALED Date Received: 25/06/2013 Date Validated: 16/07/2013	Our Sample ID : AC92367 Client Samp #: 3 Batch Code: Sell By Date: 2013/06/26 Order Number: PROF A LOCHNER
--	--	---

ANALYSIS RESULTS	1	2	Average	MoU (%)	Test Method Ref
Moisture (g/100g)	26.74	26.26	26.5	0.70	S.O.P.C. No. 1#
Ash (g/100g)	2.49	2.40	2.4	5.00	S.O.P.C. No. 2#
Total Fat (g/100g)	12.26	10.73	11.5	2.60	S.O.P.C. No. 25#
Saturated Fat (g/100g)	8.09	7.01	7.6	2.60	S.O.P.C. No. 25#
Mono-Unsaturated Fat (g/100g)	3.07	2.65	2.9	2.60	S.O.P.C. No. 25#
Poly-Unsaturated Fat (g/100g)	1.10	1.06	1.1	2.60	S.O.P.C. No. 25#
Trans Fatty Acids (g/100g)	0.000	0.000	0.00	2.60	S.O.P.C. No. 25#
Omega 3 Fatty Acids (g/100g)	0.08	0.07	0.1	2.60	S.O.P.C. No. 25#
ALA (g/100g)	0.08	0.07	0.1	2.60	S.O.P.C. No. 25#
EPA (g/100g)	0.00	0.00	0.0	2.60	S.O.P.C. No. 25#
DHA (g/100g)	0.00	0.00	0.0	2.60	S.O.P.C. No. 25#
DPA (g/100g)	0.00	0.00	0.0	2.60	S.O.P.C. No. 25#
Omega 6 Fatty acids (g/100g)	1.02	0.99	1.0	2.60	S.O.P.C. No. 25#
Cholesterol (mg/100 g)	13.12	12.43	13	4.70	S.O.P.C. No. 26#
% Protein (6.25)	7.86	8.72	8.3	1.90	S.O.P.C. No. 36#
Nitrogen (g/100g)	1.26	1.40	1.3	1.90	S.O.P.C. No. 36#
Total Dietary Fibre (g/100g)	9.29	9.27	9.3	1.30	S.O.P.C. No. 20#
% Carbohydrate	41.36	42.62	42.0	C*	S.O.P.C. No. 21
Total Sugar (g/100g)	24.64	24.06	24.4	2.90	S.O.P.C. No. 27#
Fructose (g/100g)	0.74	0.78	0.8	2.90	S.O.P.C. No. 27#
Glucose (g/100g)	1.00	1.09	1.0	2.90	S.O.P.C. No. 27#
Sucrose (g/100g)	20.75	19.99	20.4	2.90	S.O.P.C. No. 27#
Maltose (g/100g)	0.00	0.00	0.0	2.90	S.O.P.C. No. 27#
Lactose (g/100g)	2.14	2.20	2.2	2.90	S.O.P.C. No. 27#
Energy (kJ/100 g)	1365	1344	1354		S.O.P.C. No. 22
Sodium (mg/100 g)	110	107	108	7.56	S.O.P.C. No. 45#

COMMENTS


 Confirmed by: _____
 Technical Signatory

P Rubuz Date: 16-Jul-13

These results relate only to the items tested. Total Dietary Fibre content determined by AOAC Method 991.43
 MoU = Measurement of Uncertainty. C* = By calculation.

= SANAS Accredited Method.

Tests without the # mark in this report are "Not SANAS Accredited" and are not included in the SANAS Schedule of Accreditation for this laboratory.

Opinions and interpretations expressed herein are outside the scope of SANAS accreditation. This certificate shall not be reproduced except with the approval of the laboratory. The integrity of results reported are only valid from sample receipt by the laboratory.

Addendum B HCD preparation.

To prepare HCD, standard rat chow (300 g) was mixed in 125 mL of warm water with 70 g of household sugar. The chow was left to soak for about an hour and then mixed with melted vegetable fat, Holsum™ (2 X 125 g) and four cans of full cream condensed milk (4 X 385 g / can) then preserved at 4 degrees. Below are the nutritional values of Holsum™ butter and condensed milk.

Nutritional value of Holsum™ / 100 g

-Energy (kJ)	3700
-Protein	0
-Glycaemic Carbohydrates (g)	0
-Total fat (g)	100
-of which saturated fat (g)	67.8
-trans fat (g)	<1
-Monosaturated fat (g)	26.4
-Dietary fibre (g)	0
-Total Sodium (mg)	0
-Vitamin A (µg)	1380
-Vitamin D (µg)	15

Nutritional value of Condensed milk / 100 g

-Energy (kJ)	1381
-Protein	6.5
-Glycaemic Carbohydrates (g)	54
of which total sugar (g)	54
-Total fat (g)	8.7
-of which saturated fat (g)	5.5
-trans fat (g)	-
-Monosaturated fat (g)	-
-Dietary fibre (g)	0
-Total Sodium (mg)	125
-Calcium (mg)	284

Addendum C Description of phenylephrine and acetylcholine drug preparation for organ (aorta) bath perfusion system.

Phenylephrine

0.002 g Phenylephrine in 10 ml of 0.9 % saline = 1 mM stock

Acetylcholine

0.0182 g acetylcholine in 10 ml of 0.9 % saline = 10 mM (Stock A)

Dilution:

1 ml of Stock A in 9 ml 0.9 % saline = 1 mM (Stock B)

1 ml of Stock B in 9 ml 0.9 % saline = 1 mM (Stock C)

Phenylephrine and acetylcholine stock preparation.

Phenylephrine:

- 2.5 μ L of stock (100nM Phe)
- 5 μ L of stock (300nM Phe)
- 5 μ L of stock (500nM Phe)
- 7.5 μ L of stock (800nM Phe)
- 5 μ L of stock (1 μ M Phe)

(Total volume = 25 μ L)

Acetylcholine:

- 7.5 μ L of Stock C (30nM Ach)
- 17.5 μ L of Stock C (100nM Ach)
- 42.5 μ L of Stock C (300nM Ach)
- 14.3 μ L of Stock B (1 μ M Ach)
- 220 μ L of Stock B (10 μ M Ach)

(Total volume = 301.8 μ L)

Phenylephrine and acetylcholine cumulative doses preparation.

Addendum D Antibodies (Ab).

Antibody	Manufacturer	Dilutions
I κ B α	Cell Signalling Technology®	1:1000 (TBS-tween)
PGC-1 α	Cell Signalling Technology®	1:1000 (Signal boost)
PPAR α	Abcam Biotechnology®	1:1000 (1 % fat free milk in TBS-tween)
Cleaved PARP	Cell Signalling Technology®	1:500 (TBS-tween)
Cleaved caspase 3	Cell Signalling Technology®	1:1000 (TBS-tween)
p22-Phox	Santa Cruz Biotechnology®	1:1000 (1 % fat free milk in TBS-tween)
eNOS (total and phosphorylated Ab)	Cell Signalling Technology®	1:1000 (Signal boost)
Erk 1 / 2 (total and phosphorylated Ab)	Cell Signalling Technology®	1:1000 (TBS-tween)
p38 (total and phosphorylated Ab)	Cell Signalling Technology®	1:1000 (TBS-tween)
PKB/Akt (total and phosphorylated Ab)	Cell Signalling Technology®	1:1000 (TBS-tween)
AMPK (total and phosphorylated Ab)	Cell Signalling Technology®	1:1000 (TBS-tween)

Antibodies distributed by Anatech Instruments (pty) limited, South Africa (*Cell signalling Biotechnology, Inc., Massachusetts, USA and Santa Cruz Biotechnology, Inc., Texas, USA*) and Biocom biotech (pty) limited, South Africa (*Abcam Biotechnology®, Cambridge, UK*).

Secondary antibody (*AEC Amersham, Buckinghamshire, United Kingdom*) (Dilution 1:4000 TBS-tween for all primary antibodies except for PGC-1 α and total and phosphorylated eNOS which were diluted in signal boost (1:4000) as previously described.

Addendum E Rat mortality report.

Following the oral gavage procedure, the following 12 deaths categorized as per the experimental groups (shown below) were reported. Post-mortem examinations revealed that the cause of death was because of aspiration of the turbid drug mixture as evidenced by presence of the drug concoction along the respiratory tract. Deaths were random and occurred within 1-4 hours following gavage except for 2 cases where rats were isolated following development of dyspnoea after gavage and died after 8 hours.

Group	Lean Control	HCD Control	Lean HAART	HCD HAART	Lean HAART + Saro	HCD HAART + Saro	Lean Saro	HCD Saro
Deaths	0	0	4	2	2	4	0	0

Chapter 6 : Bibliography

(Harvard referencing system)

- Adaikalakoteswari, A., Rema, M., Mohan, V. and Balasubramanyam, M., 2007. Oxidative DNA damage and augmentation of poly (ADP-ribose) polymerase/nuclear factor-kappa B signaling in patients with type 2 diabetes and microangiopathy. *The international journal of biochemistry & cell biology*, 39(9), pp.1673-1684.
- Agrawal, R., 2014. The first approved agent in the glitazar's class: Saroglitazar. *Current drug targets*, 15 (2), pp.151-155.
- Akinbami, A., Balogun, B., Balogun, M., Dosunmu, O., Oshinaike, O., Adediran, A. and Adegboyega, K., 2012. Chest X-ray findings in HIV-infected Highly Active Antiretroviral Treatment (HAART)-naïve patients. *Pan African Medical Journal*, 12(1), pp.78-84.
- Alessi, D. R., Andjelkovic, M., Caudwell, B., Cron, P., Morrice, N., Cohen, P., 1996. Mechanism of activation of protein kinase B by insulin and IGF-1. *The EMBO journal*, 15(23), pp.6541-6551.
- Amarasinghe, G. K., De Guzman, R. N., Turner, R. B., Chancellor, K. J., Wu, Z. R. and Summers, M. F., 2000. NMR structure of the HIV-1 nucleocapsid protein bound to stem-loop SL2 of the Ψ -RNA packaging signal. implications for genome recognition. *Journal of Molecular Biology*, 301(2), pp.491–511.
- Amorosa, V., Synnestvedt, M., Gross, R., Friedman, H., MacGregor, R. R., Gudonis, D., et al., 2005. A tale of 2 epidemics: the intersection between obesity and HIV infection in Philadelphia. *J Acquir Immune Defic Syndr*, 39(5), pp. 557–561.
- An, D. & Rodrigues, B., 2006. Role of changes in cardiac metabolism in development of diabetic cardiomyopathy. *American Journal of Physiology-Heart and Circulatory Physiology*, 291(4), pp.H1489–H1506.
- Angulo, P., 2007. GI Epidemiology: nonalcoholic fatty liver disease. *Alimentary Pharmacology & Therapeutics*, 25(8), pp.883–889.
- Antman, E., Bassand, J. P., Klein, W., Ohman, M., Lopez Sendon, J. L., Rydén, L. et al., 2000. Myocardial infarction redefined - A consensus document of The Joint European Society of Cardiology/American College of Cardiology Committee for the redefinition of myocardial infarction. *Journal of the American College of Cardiology*, 36(3), pp.959–969.
- Antunes, L.C., Elkfury, J.L., Jornada, M.N., Foletto, K.C. and Bertoluci, M.C., 2016. Validation of HOMA-IR in a model of insulin-resistance induced by a high-fat diet in Wistar rats. *Archives of endocrinology and metabolism*, 60(2), pp.138-142.
- Aragno, M., Tomasinelli, C.E., Vercellinatto, I., Catalano, M.G., Collino, M., Fantozzi, R., Danni, O. and Boccuzzi, G., 2009. SREBP-1c in nonalcoholic fatty liver disease induced by Western-type high-fat diet plus fructose in rats. *Free Radical Biology and Medicine*, 47(7), pp.1067-1074.
- Arany, Z., He, H., Lin, J., Hoyer, K., Handschin, C., Toka, O., et al., 2005. Transcriptional coactivator PGC-1 α controls the energy state and contractile function of cardiac muscle. *Cell Metabolism*, 1(4), pp.259–271.
- Araya, J., Rodrigo, R., Videla, L. a, Thielemann, L., Orellana, M., Pettinelli, P., et al., 2004. Increase in long-chain polyunsaturated fatty acid n - 6/n - 3 ratio in relation to hepatic steatosis in patients with non-alcoholic fatty liver disease. *Clinical science (London, England : 1979)*, 106(6), pp.635–643.
- Assy, N., Kaita, K., Mymin, D., Levy, C., Rosser, B. and Minuk, G., 2000. Fatty infiltration of liver in hyperlipidemic patients. *Digestive Diseases and Sciences*, 45(10), pp.1929–1934.
- Asztalos, B.F., Schaefer, E.J., Horvath, K.V., Cox, C.E., Skinner, S., Gerior, J., et al., 2006. Protease inhibitor-based HAART, HDL, and CHD-risk in HIV-infected patients. *Atherosclerosis*, 184(1), pp.72-77.
- Auouet, M., Delaflotte, S. and Braquet, P., 1989. Increased influence of endothelium in obese Zucker rat aorta. *Journal of pharmacy and pharmacology*, 41(12), pp.861-864.

- Avena, N.M., Rada, P. and Hoebel, B.G., 2008. Evidence for sugar addiction: behavioral and neurochemical effects of intermittent, excessive sugar intake. *Neuroscience & Biobehavioral Reviews*, 32(1), pp.20-39.
- Ayala, A., Muñoz, M.F. and Argüelles, S., 2014. Lipid peroxidation: production, metabolism, and signaling mechanisms of malondialdehyde and 4-hydroxy-2-nonenal. *Oxidative medicine and cellular longevity*, 2014(360438), p.11-42.
- Azumi, H., Inoue, N., Takeshita, S., Rikitake, Y., Kawashima, S., Hayashi, Y., 1999. Expression of NADH/NADPH oxidase p22 phox in human coronary arteries. *Circulation*, 100(14), pp.1494-1498.
- Badimon, J. J., Fuster, V., Chesebro, J. H. and Badimon, L., 1993. Coronary atherosclerosis. A multifactorial disease. *Circulation*, 87(3 Suppl), pp.II3-16.
- Badley, A.D., 2005. In vitro and in vivo effects of HIV protease inhibitors on apoptosis. *Cell death and differentiation*, 12(S1), pp.924-931.
- Baggaley, R. F., Boily, M. C., White, R. G. and Alary, M., 2006. Risk of HIV-1 transmission for parenteral exposure and blood transfusion: a systematic review and meta-analysis. *Aids*, 20(6), pp.805-812.
- Bai, P. and Cantó, C., 2012. The role of PARP-1 and PARP-2 enzymes in metabolic regulation and disease. *Cell metabolism*, 16(3), pp.290-295.
- Bakan, A. and Bahar, I., 2009. The intrinsic dynamics of enzymes plays a dominant role in determining the structural changes induced upon inhibitor binding. *Proceedings of the National Academy of Sciences*, 106(34), pp.14349-14354.
- Ballestri, S., Lonardo, A., Bonapace, S., Byrne, C. D., Loria, P. and Targher, G., 2014. Risk of cardiovascular, cardiac and arrhythmic complications in patients with non-alcoholic fatty liver disease, *World journal of gastroenterology*: WJG, 20(7), pp. 1724-1745.
- Balzarini, J., Naesens, L. & Clercq, E. De., 1998. New antivirals - mechanism of action and resistance development. *Current opinion in biotechnology*, 1, pp.535-546.
- Banerjee, T., Pensi, T., Banerjee, D. and Grover, G., 2010. Impact of HAART on survival, weight gain and resting energy expenditure in HIV-1-infected children in India. *Annals of tropical paediatrics*, 30(1), pp.27-37.
- Barnes, D.M., 1986. Promising results halt trial of anti-AIDS drug. *American Association for the Advancement of Science*, 234, pp.15-17.
- Barnett, S.F., Bilodeau, M.T. and Lindsley, C.W., 2005. The Akt/PKB family of protein kinases: a review of small molecule inhibitors and progress towards target validation. *Current topics in medicinal chemistry*, 5(2), pp.109-125.
- Baron, S. J., Li, J., Russell, R. R., Neumann, D., Miller, E. J., Tuerk, R., et al., 2005. Dual mechanisms regulating AMPK kinase action in the ischaemic heart. *Circulation research*, 96(3), pp.337-345.
- Barre-Sinoussi, F., Chermann, J. C., Rey, F., Nugeyre, M. T., Chamaret, S., Gruest, J., et al., 1983. Isolation of a T-lymphotropic retrovirus from a patient at risk for acquired immune deficiency syndrome (AIDS). *Science*, 220(4599), pp.868-871.
- Bavinger, C., Bendavid, E., Niehaus, K., Olshen, R. a., Olkin, I., Sundaram, V., et al., 2013. Risk of Cardiovascular Disease from Antiretroviral Therapy for HIV: A Systematic Review. *PLoS ONE*, 8(3), pp.1243-1248.
- Bayraktutan, U., Blayney, L. and Shah, A.M., 2000. Molecular characterization and localization of the NAD (P) H oxidase components gp91-phox and p22-phox in endothelial cells. *Arteriosclerosis, thrombosis, and vascular biology*, 20(8), pp.1903-1911.
- Beaglehole, R. & Bonita, R., 2008. Global public health: a scorecard. *The Lancet*, 372(9654), pp.1988-1996.
- Bell, F.P., Adamson, I.L. and Schwartz, C.J., 1974. Aortic endothelial permeability to albumin: focal and regional patterns of uptake and transmural distribution of 131I-albumin in the young pig. *Experimental and molecular pathology*, 20(1), pp.57-68.
- Bell, R.M., Mocanu, M.M. and Yellon, D.M., 2011. Retrograde heart perfusion: the Langendorff technique of isolated heart perfusion. *Journal of molecular and cellular cardiology*, 50(6), pp.940-950.

- Bergman, R.N., Stefanovski, D., Buchanan, T.A., Sumner, A.E., Reynolds, J.C., Sebring, N.G., Xiang, A.H. and Watanabe, R.M., 2011. A better index of body adiposity. *Obesity*, 19(5), pp.1083-1089.
- Bertz, R., Renz, C., Foit, C., Swerdlow, J., Ye, X., Jasinsky, O., et al., 2001. Steady-state pharmacokinetics of Kaletra (lopinavir/ritonavir 400/100 mg BID) in HIV-infected subjects when taken with food. In *Second International Workshop on Clinical Pharmacology of HIV Therapy, Noordwijk, The Netherlands*, Abstract (No. 3-10).
- Bhatia, L. S., Curzen, N. P., Calder, P. C. and Byrne, C. D., 2012. Non-alcoholic fatty liver disease: A new and important cardiovascular risk factor? *European Heart Journal*, 33(10), pp.1190-1200.
- Bica, I., McGovern, B., Dhar, R., Stone, D., McGowan, K., Scheib, R., et al., 2001. Increasing mortality due to end-stage liver disease in patients with human immunodeficiency virus infection. *Clinical infectious diseases : an official publication of the Infectious Diseases Society of America*, 32(3), pp.492-497.
- Blake, G.J. & Ridker, P.M., 2002. Inflammatory bio-markers and cardiovascular risk prediction. *J Int Med*, 252, pp.283-94.
- Blümer, R.M., van Vonderen, M.G., Sutinen, J., Hassink, E., Ackermans, M., van Agtmael, M.A., Yki-Jarvinen, H., Danner, S.A., Reiss, P. and Sauerwein, H.P., 2008. Zidovudine/lamivudine contributes to insulin resistance within 3 months of starting combination antiretroviral therapy. *Aids*, 22(2), pp.227-236.
- Bogner, J.R., Vielhauer, V., Beckmann, R.A., Michl, G., Wille, L., Salzberger, B. and Goebel, F.D., 2001. Stavudine versus zidovudine and the development of lipodystrophy. *JAIDS Journal of Acquired Immune Deficiency Syndromes*, 27(3), pp.237-244.
- Bohl, S., Medway, D.J., Schulz-Menger, J., Schneider, J.E., Neubauer, S. and Lygate, C.A., 2009. Refined approach for quantification of in vivo ischaemia-reperfusion injury in the mouse heart. *American Journal of Physiology-Heart and Circulatory Physiology*, 297(6), pp.H2054-H2058.
- Boucher, C. A., Cammack, N., Schipper, P., Schuurman, R., Rouse, P., Wainberg, M. A., et al., 1993. High-level resistance to (-) enantiomeric 2'-deoxy-3'-thiacytidine in vitro is due to one amino acid substitution in the catalytic site of human immunodeficiency virus type 1 reverse transcriptase. *Antimicrobial Agents & Chemotherapy*, 37(10), pp.2231-2234.
- Bowie, A. & O'Neill, L. a., 2000. Oxidative stress and nuclear factor- κ B activation. *Biochemical Pharmacology*, 59(1), pp.13-23.
- Boza, C., Riquelme, A., Ibañez, L., Duarte, I., Norero, E., Viviani, P., et al., 2005. Predictors of nonalcoholic steatohepatitis (NASH) in obese patients undergoing gastric bypass. *Obesity Surgery*, 15(8), pp.1148-1153.
- Bozzette, S.A., Ake, C.F., Tam, H.K., Phippard, A., Cohen, D., Scharfstein, D.O. and Louis, T.A., 2008. Long-term survival and serious cardiovascular events in HIV-infected patients treated with highly active antiretroviral therapy. *JAIDS Journal of Acquired Immune Deficiency Syndromes*, 47(3), pp.338-341.
- Bradford, M.M., 1976. A rapid and sensitive method for the quantitation of microgram quantities of protein utilizing the principle of protein-dye binding. *Analytical biochemistry*, 72(1-2), pp.248-254.
- Brede, M., Roell, W., Ritter, O., Wiesmann, F., Jahns, R., Haase, A., Fleischmann, B.K. and Hein, L., 2003. Cardiac hypertrophy is associated with decreased eNOS expression in angiotensin AT2 receptor-deficient mice. *Hypertension*, 42(6), pp.1177-1182.
- Bridges, E. G., Dutschman, G. E., Gullen, E. A. and Cheng, Y. C., 1996. Favorable interaction of β -l (-) nucleoside analogues with clinically approved anti-HIV nucleoside analogues for the treatment of human immunodeficiency virus. *Biochemical Pharmacology*, 51(6), pp.731-736.
- Brien, S.I.O., 1996. HIV causes AIDS: Koch's postulates fulfilled Guest editorial. *Current Opinion in Immunology 1996*, 8:613-618 ©, pp.613-618.
- Brik, A. & Wong, C.-H., 2003. HIV-1 protease: mechanism and drug discovery. *Org. Biomol. Chem.*, 1, pp.5-14.
- Brinkman, K., Smeitink, J. a, Romijn, J. a and Reiss, P., 1999. Mitochondrial toxicity induced by nucleoside-analogue reverse- transcriptase inhibitors is a key factor in the pathogenesis of antiretroviral-therapy-related lipodystrophy. *Lancet*, 354(9184), pp.1112-1115.

- Brown, T.T., Li, X., Cole, S.R., Kingsley, L.A., Palella, F.J., Riddler, S.A., et al., 2005. Cumulative exposure to nucleoside analogue reverse transcriptase inhibitors is associated with insulin resistance markers in the Multicenter AIDS Cohort Study. *Aids*, 19(13), pp.1375-1383.
- Buchanan, J., Mazumder, P.K., Hu, P., Chakrabarti, G., Roberts, M.W., Yun, et al., 2005. Reduced cardiac efficiency and altered substrate metabolism precedes the onset of hyperglycemia and contractile dysfunction in two mouse models of insulin resistance and obesity. *Endocrinology*, 146(12), pp.5341-5349.
- Butt, A. A., Chang, C.-C., Kuller, L., Goetz, M. B., Leaf, D., Rimland, D., et al., 2011. Risk of heart failure with human immunodeficiency virus in the absence of prior diagnosis of coronary heart disease. *Archives of Internal Medicine*, 171(United States RF-37 LG-English PT-Journal: Article DD-20110520), pp.737-743.
- Butterick, T. A., Stone, L. H., Duffy, C., Holley, C., Cabrera, J. A., Crampton, M., et al., 2016. Pioglitazone increases PGC1- α signaling within chronically ischaemic myocardium. *Basic Research in Cardiology*, 111(3), pp.37-52.
- Byrne, C.D. & Targher, G., 2015. Review NAFLD: A multisystem disease. *Journal of Hepatology*, 62(1), pp.S47-S64.
- Byrne, C.D., 2012. Dorothy Hodgkin Lecture 2012 Non-alcoholic fatty liver disease, insulin resistance and ectopic fat: A new problem in diabetes management. *Diabetic Medicine*, 29(9), pp.1098-1107.
- Cai, D., Yuan, M., Frantz, D. F., Melendez, P. A., Hansen, L., Lee, J., et al., 2005. Local and systemic insulin resistance resulting from hepatic activation of IKK- β and NF- κ B. *Nature medicine*, 11(2), p.183.
- Cao, J., Sodhi, K., Puri, N., Monu, S.R., Rezzani, R. and Abraham, N.G., 2011. High fat diet enhances cardiac abnormalities in SHR rats: Protective role of heme oxygenase-adiponectin axis. *Diabetology & metabolic syndrome*, 3(1), p.37.
- Carael, M., Van De Perre, P. H., Lepage, P. H., Allen, S., Nsengumuremyi, F., Van Goethem, C., et al., 1988. Human immunodeficiency virus transmission among heterosexual couples in Central Africa. *AIDS (London, England)*, 2(3), pp.201-205.
- Carpentier, A., Patterson, B.W., Uffelman, K.D., Salit, I. and Lewis, G.F., 2005. Mechanism of highly active anti-retroviral therapy-induced hyperlipidemia in HIV-infected individuals. *Atherosclerosis*, 178(1), pp.165-172.
- Carr, A., Samaras, K., Burton, S., Law, M., Freund, J., Chisholm, D.J. and Cooper, D.A., 1998. A syndrome of peripheral lipodystrophy, hyperlipidaemia and insulin resistance in patients receiving HIV protease inhibitors. *Aids*, 12(7), pp.F51-F58.
- Carr, A., Samaras, K., Chisholm, D.J. and Cooper, D.A., 1998. Pathogenesis of HIV-1-protease inhibitor-associated peripheral lipodystrophy, hyperlipidaemia, and insulin resistance. *The Lancet*, 351(9119), pp.1881-1883.
- Castelli, W.P., 1988. Cholesterol and lipids in the risk of coronary artery disease--the Framingham Heart Study. *The Canadian journal of cardiology*, 4 Suppl A, pp.5A-10A.
- Centers for Disease Control (CDC), 1985. Revision of the case definition of acquired immunodeficiency syndrome for national reporting--United States. *MMWR. Morbidity and mortality weekly report*, 34(25), p.373.
- Chakrabarti, R., Misra, P., Vikramadithyan, R.K., Premkumar, M., Hiriyan, J., Datla, S.R., et al., 2004. Antidiabetic and hypolipidemic potential of DRF 2519—a dual activator of PPAR- α and PPAR- γ . *European journal of pharmacology*, 491(2), pp.195-206.
- Chalasani, N., Younossi, Z., Lavine, J. E., Diehl, A. M., Brunt, E. M., Cusi, K., et al., 2012. The diagnosis and management of non-alcoholic fatty liver disease: Practice guideline by the American Gastroenterological Association, American Association for the Study of Liver Diseases, and American College of Gastroenterology. *Gastroenterology*, 142(7), pp.1592-1609.
- Chalasani, N., Younossi, Z., Lavine, J.E., Diehl, A.M., Brunt, E.M., Cusi, K., et al., 2012. The diagnosis and management of non-alcoholic fatty liver disease: Practice Guideline by the American Association for the Study of Liver Diseases, American College of Gastroenterology, and the American Gastroenterological Association. *Hepatology*, 55(6), pp.2005-2023.
- Chan, D. C., Fass, D., Berger, J. M. and Kim, P. S., 1997. Core Structure of gp41 from the HIV Envelope Glycoprotein. *Cell*, 89(2), pp.263-273.

- Chang, K.S. and Stevens, W.C., 1992. Endothelium-dependent increase in vascular sensitivity to phenylephrine in long-term streptozotocin diabetic rat aorta. *British journal of pharmacology*, 107(4), pp.983-990.
- Charneau, P., Mirambeau, G., Roux, P., Paulous, S., Buc, H. and Clavel, F., 1994. HIV-1 reverse transcription. A termination step at the center of the genome. *Journal of molecular biology*, 241, pp.651-662.
- Chen, C.-H., Nien, C.-K., Yang, C.-C. and Yeh, Y.-H., 2010. Association Between Nonalcoholic Fatty Liver Disease and Coronary Artery Calcification. *Digestive Diseases and Sciences*, 55(6), pp.1752-1760.
- Chen, C., Lu, X.H., Yan, S., Chai, H. and Yao, Q., 2005. HIV protease inhibitor ritonavir increases endothelial monolayer permeability. *Biochemical and biophysical research communications*, 335(3), pp.874-882.
- Chen, L., Jarujaron, S., Wu, X., Sun, L., Zha, W., Liang, G., Wang, X., et al., 2009. HIV protease inhibitor lopinavir-induced TNF- α and IL-6 expression is coupled to the unfolded protein response and ERK signaling pathways in macrophages. *Biochemical pharmacology*, 78(1), pp.70-77.
- Choi, S. & Diehl, A.M., 2005. Role of inflammation in nonalcoholic steatohepatitis. *Curr.Opin.Gastroenterol.*, 21(0267-1379), pp.702-707.
- Chung, M. H., Drake, A. L., Richardson, B. a, Reddy, A., Thiga, J., Sakr, S. R., et al., 2009. Impact of prior HAART use on clinical outcomes in a large Kenyan HIV treatment program. *Current HIV research*, 7(4), pp.441-446.
- Cichy, S.B., Uddin, S., Danilkovich, A., Guo, S., Klippel, A. and Unterman, T.G., 1998. Protein kinase B/Akt mediates effects of insulin on hepatic insulin-like growth factor-binding protein-1 gene expression through a conserved insulin response sequence. *Journal of Biological Chemistry*, 273(11), pp.6482-6487.
- Clarkson, P.M. and Thompson, H.S., 2000. Antioxidants: what role do they play in physical activity and health? *The American journal of clinical nutrition*, 72(2), pp.637s-646s.
- Cloyd, M.W., Chen, J.J. and Wang, L., 2000. How does HIV cause AIDS? The homing theory. *Molecular Medicine Today*, 6(3), pp.108-111.
- Cohen, I. S., Anderson, D. W., Virmani, R., Reen, B. M., Macher, A. M., Sennesh, J., et al., 1986. Congestive Cardiomyopathy in Association with the Acquired Immunodeficiency Syndrome. *New England Journal of Medicine*, 315(10), pp.628-630.
- Cohen, P.S., Schmidtmyerova, H., Dennis, J., Dubrovsky, L., Sherry, B., Tracey, K.J., et al., 1997. The critical role of p38 MAP kinase in T cell HIV-1 replication. *Molecular Medicine*, 3(5), pp.339-346.
- Corbit, J. D., & Stellar, E., 1964. Palatability, food intake, and obesity in normal and hyperphagic rats. *Journal of Comparative and Physiological Psychology*, 58(1), pp 63-67.
- Crespo, J., Cayón, A., Fernández-Gil, P., Hernández-Guerra, M., Mayorga, M., Domínguez-Díez, A., Fernández-Escalante, J.C. and Pons-Romero, F., 2001. Gene expression of tumor necrosis factor α and TNF-receptors, p55 and p75, in nonalcoholic steatohepatitis patients. *Hepatology*, 34(6), pp.1158-1163.
- Crum-Cianflone, N. F., Roediger, M., Eberly, L. E., Landrum, M. L., Ganesan, A., Weintrob, A. C., et al., 2011. Obesity among HIV-Infected persons: Impact of weight on CD4 cell count. *Aids*, 24(7), pp.1069-1072.
- Crum-Cianflone, N., Dilay, A., Collins, G., Asher, D., Campin, R., Medina, S., et al., 2009. Nonalcoholic fatty liver disease among HIV-infected persons. *Journal of acquired immune deficiency syndromes (1999)*, 50(5), pp.464-473.
- Crum-Cianflone, N., Roediger, M. P., Eberly, L., Headd, M., Marconi, V., Ganesan, A., et al., 2010. Increasing Rates of Obesity among HIV-Infected Persons during the HIV Epidemic. *PLoS ONE*, 5(4), p.e10106.
- Crum-Cianflone, N., Tejjidor, R., Medina, S., Barahona, I. and Ganesan, A., 2008. Obesity among patients with HIV: the latest epidemic. *AIDS patient care and STDs*, 22(12), pp.925-930.
- Cunha, R., Weber, R., Sabin, C.A., Friis-Moller, N., Reiss, P., El-Sadr, W.M., et al., 2006. Liver-related deaths in persons infected with the human immunodeficiency virus: the D: A: D study. *Arch Intern Med*, 166(15), pp.1632-41.
- Dai, H., Wang, W., Tang, X., Chen, R., Chen, Z., Lu, Y., et al., 2016. Association between homocysteine and non-alcoholic fatty liver disease in Chinese adults: a cross-sectional study. *Nutrition Journal*, 15(1), pp.102-111.

- Dal Maso, L., Polesel, J., Serraino, D., Lise, M., Piselli, P., Falcini, F., et al., 2009. Pattern of cancer risk in persons with AIDS in Italy in the HAART era. *British journal of cancer*, 100(5), pp.840-847.
- Das, K., Das, K., Mukherjee, P. S., Ghosh, A., Ghosh, S., Mridha, A. R., et al., 2010. Nonobese population in a developing country has a high prevalence of nonalcoholic fatty liver and significant liver disease. *Hepatology*, 51(5), pp.1593–1602.
- Day, C.P. & James, O.F.W., 1998. Steatohepatitis: A tale of two “Hits”? *Gastroenterology*, 114(4 I), pp.842–845.
- Day, L., Shikuma, C. & Gerschenson, M., 2004. Mitochondrial injury in the pathogenesis of antiretroviral-induced hepatic steatosis and lactic acidemia. *Mitochondrion*, 4(2–3), pp.95–109.
- de la Rosa, L.C., Schoemaker, M.H., Vrenken, T.E., Buist-Homan, M., Havinga, R., Jansen, P.L. and Moshage, H., 2006. Superoxide anions and hydrogen peroxide induce hepatocyte death by different mechanisms: involvement of JNK and ERK MAP kinases. *Journal of hepatology*, 44(5), pp.918-929.
- de Murcia, G., Schreiber, V., Molinete, M., Saulier, B., Poch, O., Masson, M., et al., 1994. Structure and function of poly (ADP-ribose) polymerase. *Molecular and cellular biochemistry*, 138(1-2), pp.15-24.
- Dean, J.L., Brook, M., Clark, A.R. and Saklatvala, J., 1999. p38 mitogen-activated protein kinase regulates cyclooxygenase-2 mRNA stability and transcription in lipopolysaccharide-treated human monocytes. *Journal of Biological Chemistry*, 274(1), pp.264-269.
- Del Ben, M., Baratta, F., Polimeni, L. and Angelico, F., 2012. Non-alcoholic fatty liver disease and cardiovascular disease: epidemiological, clinical and pathophysiological evidences. *Internal and emergency medicine*, 7(3), pp.291-296.
- Delerive, P., Fruchart, J.C. and Staels, B., 2001. Peroxisome proliferator-activated receptors in inflammation control. *Journal of Endocrinology*, 169(3), pp.453-459.
- Deprez, J., Vertommen, D., Alessi, D. R., Hue, L. and Rider, M. H., 1997. Phosphorylation and Activation of Heart 6-Phosphofructo-2-kinase by Protein Kinase B and Other Protein Kinases of the Insulin Signaling Cascades. *Journal of Biological Chemistry*, 272(28), pp.17269–17275.
- Deshpande, A., Toshniwal, H., Joshi, S. and Jani, R.H., 2016. A prospective, multicentre, open-label single-arm exploratory study to evaluate efficacy and safety of saroglitazar on hypertriglyceridemia in HIV associated lipodystrophy. *PloS one*, 11(1), p.e0146222.
- Diehl, A.M., 2005. Cytokines and the pathogenesis of non-alcoholic steatohepatitis. *Gut*, 54(2), pp.303–306.
- Dinauer, M. C., Pierce, E. A., Bruns, G. A., Curnutte, J. T. and Orkin, S. H., 1990. Human neutrophil cytochrome b light chain (p22-phox). Gene structure, chromosomal location, and mutations in cytochrome-negative autosomal recessive chronic granulomatous disease. *Journal of Clinical Investigation*, 86(5), pp.1729-1737.
- Doenst, T., Nguyen, T.D. and Abel, E.D., 2013. Cardiac metabolism in heart failure. *Circulation research*, 113(6), pp.709-724.
- Dressman, J., Kincer, J., Matveev, S.V., Guo, L., Greenberg, R.N., Guerin, T., et al., 2003. HIV protease inhibitors promote atherosclerotic lesion formation independent of dyslipidemia by increasing CD36-dependent cholesteryl ester accumulation in macrophages. *Journal of Clinical Investigation*, 111(3), pp.389-397.
- Dreyer, C. & Krey, G., 1992. Control of the Peroxisomal P-Oxidation Pathway by a Novel Family of Nuclear Hormone Receptors. *Cell*, 68, pp.879–887.
- du Toit, E.F., Smith, W., Muller, C., Strijdom, H., Stouthammer, B., Woodiwiss, A.J., Lochner, A., 2008. Myocardial susceptibility to ischaemic-reperfusion injury in a prediabetic model of dietary-induced obesity. *American Journal of Physiology-Heart and Circulatory Physiology*, 294(5), pp.H2336-H2343.
- Durand, M., Sheehy, O., Baril, J.-G., Leloir, J. and Tremblay, C. L., 2011. Association Between HIV Infection, Antiretroviral Therapy, and Risk of Acute Myocardial Infarction: A Cohort and Nested Case–Control Study Using Québec’s Public Health Insurance Database. *JAIDS Journal of Acquired Immune Deficiency Syndromes*, 57(3), pp.245–253.
- Egger, M., Hirschel, B., Francioli, P., Sudre, P., Wirz, M., Flepp, M., 1997. Impact of new antiretroviral combination

- therapies in HIV infected patients in Switzerland: prospective multicentre study. Swiss HIV Cohort Study. *BMJ (Clinical research ed.)*, 315(7117), pp.1194–1199.
- Ek, J., Andersen, G., Urhammer, S.A., Gaede, P.H., Drivsholm, T., Borch-Johnsen, K., et al., 2001. Mutation analysis of peroxisome proliferator-activated receptor- γ coactivator-1 (PGC-1) and relationships of identified amino acid polymorphisms to type II diabetes mellitus. *Diabetologia*, 44(12), pp.2220-2226.
- Ekstedt, M., Franzén, L. E., Mathiesen, U. L., Thorelius, L., Holmqvist, M., Bodemar, G., et al., 2006. Long-term follow-up of patients with NAFLD and elevated liver enzymes. *Hepatology*, 44(4), pp.865–873.
- Esposito, D. & Craigie, R., 1999. HIV Integrase Structure and Function. *Advances in Virus Research*, 52, pp.319–333.
- Esterbauer, H., Striegl, G., Puhl, H. and Rotheneder, M., 1989. Continuous monitoring of in vitro oxidation of human low-density lipoprotein. *Free radical research communications*, 6(1), pp.67-75.
- Fatani, S., Itua, I., Clark, P., Wong, C. and Naderali, E.K., 2011. The effects of diet-induced obesity on hepatocyte insulin signaling pathways and induction of non-alcoholic liver damage. *International journal of general medicine*, 4, pp.211-219.
- Fauci, A.S., 2007. 25 Years of HIV/AIDS Science: Reaching the Poor with Research Advances. *Cell*, 131(3), pp.429–432.
- Félétou, M. & Vanhoutte, P.M., 2006. Endothelial dysfunction: a multifaceted disorder. *Am J Physiol Heart Circ Physiol*, 291, pp.H985–H1002.
- Ferdinandy, P., Schulz, R. & Baxter, G.F., 2007. Interaction of cardiovascular risk factors with myocardial ischaemia/reperfusion injury, preconditioning, and postconditioning. *Pharmacological Reviews*, 59(4), pp.418–458.
- Fernández-Hernando, C., Ackah, E., Yu, J., Suárez, Y., Murata, T., Iwakiri, Y., et al., 2007. Loss of Akt1 Leads to Severe Atherosclerosis and Occlusive Coronary Artery Disease. *Cell Metabolism*, 6(6), pp.446–457.
- Fernández-hernando, C., József, L., Jenkins, D., Di, A. and Sessa, W. C., 2010. NIH Public Access cardiac dysfunction during atherosclerosis. *Arteriosclerosis & Thrombosis*, 29(12), pp.2033–2040.
- Ferré, P., 2004. The biology of peroxisome proliferator-activated receptors. *Diabetes*, 53(suppl 1), pp.S43-S50.
- Fillmore, N., Mori, J. & Lopaschuk, G.D., 2014. Mitochondrial fatty acid oxidation alterations in heart failure, ischaemic heart disease and diabetic cardiomyopathy. *British Journal of Pharmacology*, 171(8), pp.2080–2090.
- Finck, B.N. and Kelly, D.P., 2006. PGC-1 coactivators: inducible regulators of energy metabolism in health and disease. *Journal of Clinical Investigation*, 116(3), pp.615-622.
- Fischl, M. A., Richman, D. D., Grieco, M. H., Gottlieb, M. S., Volberding, P. A., Laskin, O. L., et al., 1987. The Efficacy of Azidothymidine (AZT) in the Treatment of Patients with AIDS and AIDS-Related Complex. *New England Journal of Medicine*, 317(4), pp.185–191.
- Folkman, J., 1995. Angiogenesis in cancer, vascular, rheumatoid and other disease. *Nat Med*, 1(1), pp.27–30.
- Fonarow, G.C., Srikanthan, P., Costanzo, M.R., Cintron, G.B., Lopatin, M. and ADHERE Scientific Advisory Committee and Investigators., 2007. An obesity paradox in acute heart failure: analysis of body mass index and in-hospital mortality for 108927 patients in the Acute Decompensated Heart Failure National Registry. *American heart journal*, 153(1), pp.74-81.
- Fonseca, V., 2003. Effect of thiazolidinediones on body weight in patients with diabetes mellitus. *The American journal of medicine*, 115(8), pp.42-48.
- Friis-Møller, N., Reiss, P., Sabin, C. a, Weber, R., Monforte, A. d'Arminio, El-Sadr, W., et al., 2007. Class of antiretroviral drugs and the risk of myocardial infarction. *The New England journal of medicine*, 356(17), pp.1723–1735.
- Friis-Møller, N., Weber, R., Reiss, P., Thiébaud, R., Kirk, O., d'Arminio Monforte, A., et al., 2003a. Cardiovascular disease risk factors in HIV patients - association with antiretroviral therapy. Results from the DAD study. *AIDS (London, England)*, 17(8), pp.1179–1193.

- Friis-Moller N., Weber R., Sabin CA., Reiss, P., El-Sadr, W., Thiébaud, R., et al., 2003b. Combination antiretroviral therapy and the risk of myocardial infarction. *N Engl J Med*, 349 (21), pp.1993-2003 [Erratum, *N Engl J Med* 2004;350, pp.955.]
- Fujio, Y. and Walsh, K., 1999. Akt mediates cytoprotection of endothelial cells by vascular endothelial growth factor in an anchorage-dependent manner. *Journal of Biological Chemistry*, 274(23), pp.16349-16354.
- Fujioka, S., Matsuzawa, Y., Tokunaga, K. and Tarui, S., 1987. Contribution of intra-abdominal fat accumulation to the impairment of glucose and lipid metabolism in human obesity. *Metabolism*, 36(1), pp.54-59.
- Fukui, T., Ishizaka, N., Rajagopalan, S., Laursen, J.B., Capers, Q., Taylor, W.R., Harrison, D.G., de Leon, H., Wilcox, J.N. and Griendling, K.K., 1997. p22phox mRNA expression and NADPH oxidase activity are increased in aortas from hypertensive rats. *Circulation research*, 80(1), pp.45-51.
- Furchgott, R.F. and Zawadzki, J.V., 1980. The obligatory role of endothelial cells in the relaxation of arterial smooth muscle by acetylcholine. *Nature*, 288(5789), pp.373-376.
- Furchgott, R.F., 1955. The pharmacology of vascular smooth muscle. *Pharmacological Reviews*, 7(2), pp.183-265.
- Furchgott, R.F., 1983. Role of endothelium in responses of vascular smooth muscle. *Circulation research*, 53(5), pp.557-573.
- Furman, P. a, Fyfe, J. a, St Clair, M. H., Weinhold, K., Rideout, J. L., Freeman, G. a., 1986. Phosphorylation of 3'-azido-3'-deoxythymidine and selective interaction of the 5'-triphosphate with human immunodeficiency virus reverse transcriptase. *Proceedings of the National Academy of Sciences of the United States of America*, 83(21), pp.8333-8337.
- Gaggini, M., Morelli, M., Buzzigoli, E., DeFronzo, R. A., Bugianesi, E. and Gastaldelli, A., 2013. Non-alcoholic fatty liver disease (NAFLD) and its connection with insulin resistance, dyslipidemia, atherosclerosis and coronary heart disease. *Nutrients*, 5(5), pp.1544-1560.
- Gaines Das, R. and North, D., 2007. Implications of experimental technique for analysis and interpretation of data from animal experiments: outliers and increased variability resulting from failure of intraperitoneal injection procedures. *Laboratory animals*, 41(3), pp.312-320.
- Gallo, R. C., Salahuddin, S. Z., Popovic, M., Shearer, G. M., Kaplan, M., Haynes, B. F., et al., 1984. Frequent detection and isolation of cytopathic retroviruses (HTLV-III) from patients with AIDS and at risk for AIDS. *Science*, 224(4648), pp.500-503.
- Gallo, R. C., Sarin, P. S., Gelmann, E. P., Robert-Guroff, M., Richardson, E., Kalyanaraman, V. S. et al., 1983. Isolation of human T-cell leukemia virus in acquired immune deficiency syndrome (AIDS). *Science*, 220(4599), pp.865-867.
- Gavrilova, O., Haluzik, M., Matsusue, K., Cutson, J.J., Johnson, L., Dietz, K.R., et al., 2003. Liver peroxisome proliferator-activated receptor γ contributes to hepatic steatosis, triglyceride clearance, and regulation of body fat mass. *Journal of Biological Chemistry*, 278(36), pp.34268-34276.
- Gerber, H.P., McMurtrey, A., Kowalski, J., Yan, M., Keyt, B.A., Dixit, V. and Ferrara, N., 1998. Vascular endothelial growth factor regulates endothelial cell survival through the phosphatidylinositol 3'-kinase/Akt signal transduction pathway requirement for Flk-1/KDR activation. *Journal of Biological Chemistry*, 273(46), pp.30336-30343.
- Ghosh, S. and Baltimore, D., 1990. Activation In Vitro of NF-(kappa) B by Phosphorylation of Its Inhibitor I (kappa) B. *Nature*, 344(6267), pp.678-689.
- Gidez, L.I., Miller, G.J., Burstein, M., Slagle, S. and Eder, H.A., 1982. Separation and quantitation of subclasses of human plasma high density lipoproteins by a simple precipitation procedure. *Journal of Lipid Research*, 23(8), pp.1206-1223
- Gil, A., Aguilera, C. M., Gil-Campos, M. and Cañete, R., 2007. Altered signalling and gene expression associated with the immune system and the inflammatory response in obesity. *British Journal of Nutrition*, 98(S1), pp.S121-S126.
- Gilbert, P. B., McKeague, I. W., Eisen, G., Mullins, C., Guéye-NDiaye, A., Mboup, S., et al., 2003. Comparison of HIV-1 and HIV-2 infectivity from a prospective cohort study in Senegal. *Statistics in Medicine*, 22(4), pp.573-593.

- Giralt, M., Domingo, P., Guallar, J. P., Rodriguez de la Concepción, M. L., Alegre, M., Domingo, J. C., et al., 2006. HIV-1 infection alters gene expression in adipose tissue, which contributes to HIV-1/HAART-associated lipodystrophy. *Antiviral therapy*, 11, pp.729–740.
- Goland, S., Shimoni, S., Zornitzki, T., Knobler, H., Azoulai, O., Lutaty, G., et al., 2006. Cardiac Abnormalities as a New Manifestation of Nonalcoholic Fatty Liver Disease: Echocardiographic and Tissue Doppler Imaging Assessment. *Journal of Clinical Gastroenterology*, 40(10), pp.949–955.
- Gottlieb, M. S., Schroff, R., Schanker, H. M., Weisman, J. D., Fan, P. T., Wolf, R. A., et al., 1981. Pneumocystis carinii Pneumonia and Mucosal Candidiasis in Previously Healthy Homosexual Men. *New England Journal of Medicine*, 305(24), pp.1425–1431.
- Griendling, K.K., Sorescu, D. and Ushio-Fukai, M., 2000. NAD (p) h Oxidase. *Circulation research*, 86(5), pp.494-501.
- Grundy, S.M. and Denke, M.A., 1990. Dietary influences on serum lipids and lipoproteins. *Journal of lipid research*, 31(7), pp.1149-1172.
- Guehi, C., Badjé, A., Gabillard, D., Ouattara, E., Koulé, S. O., Moh, R., et al., 2016. High prevalence of being Overweight and Obese HIV - infected persons, before and after 24 months on early ART in the ANRS 12136 Temprano Trial. *AIDS Research and Therapy*, 13(1), pp.354-366.
- Günthard, H.F., Saag, M.S., Benson, C.A., Del Rio, C., Eron, J.J., Gallant, J.E., et al., 2016. Antiretroviral drugs for treatment and prevention of HIV infection in adults: 2016 recommendations of the International Antiviral Society–USA panel. *Jama*, 316(2), pp.191-210.
- Gupta, D., Varma, S. & Khandelwal, R.L., 2007. Long-term effects of tumor necrosis factor- α treatment on insulin signaling pathway in HepG2 cells and HepG2 cells overexpressing constitutively active Akt/PKB. *Journal of Cellular Biochemistry*, 100(3), pp.593–607.
- Hackam, D.G. and Anand, S.S., 2003. Emerging risk factors for atherosclerotic vascular disease: a critical review of the evidence. *Jama*, 290(7), pp.932-940.
- Hafizur, R.M., Raza, S.A. and Aquuel, A., 2015. A “Humanized” rat model of pre-diabetes by high fat diet-feeding to weaning wistar rats. *Integr. Obes. Diabetes*, 1, pp.44-48.
- Hallsworth, K., Hollingsworth, K. G., Thoma, C., Jakovljevic, D., Macgowan, G. a., Anstee, Q. M., et al., 2013. Cardiac structure and function are altered in adults with non-alcoholic fatty liver disease. *Journal of Hepatology*, 58(4), pp.757–762.
- Hamaguchi, M., Kojima, T., Takeda, N., et al., 2005. The metabolic syndrome as a predictor of nonalcoholic fatty liver disease. *Annals of Internal Medicine*, 143(10), pp.722–728.
- Hanada, M., Feng, J. and Hemmings, B.A., 2004. Structure, regulation and function of PKB/AKT—a major therapeutic target. *Biochimica et Biophysica Acta (BBA)-Proteins and Proteomics*, 1697(1), pp.3-16.
- Hardie, D. G., Scott, J. W., Pan, D. A. and Hudson, E. R., 2003. Management of cellular energy by the AMP-activated protein kinase system. *FEBS letters*, 546(1), pp.113–120.
- Hardie, D.G., 2008. AMPK: a key regulator of energy balance in the single cell and the whole organism. *International journal of obesity*, 32(S4), pp.S7-S12.
- Hardie, D.G., 2011. AMP-activated protein kinase-an energy sensor that regulates all aspects of cell function. *Genes and Development*, 25(18), pp.1895–1908.
- Hashimoto, E., 2006. Diagnostic criteria for non-alcoholic steatohepatitis. *Nihon rinsho. Japanese journal of clinical medicine*, 64(6), pp.1025-1032.
- Hashimoto, E., Tokushige, K. & Ludwig, J., 2014. Diagnosis and classification of non-alcoholic fatty liver disease and non-alcoholic steatohepatitis: Current concepts and remaining challenges. *Hepatology research: the official journal of the Japan Society of Hepatology*, pp.20–28.
- Hausenloy, D.J. & Yellon, D.M., 2007. Reperfusion injury salvage kinase signalling: Taking a RISK for cardioprotection. *Heart Failure Reviews*, 12(3–4), pp.217–234.

- Hausenloy, D.J. and Yellon, D.M., 2004. New directions for protecting the heart against ischaemia–reperfusion injury: targeting the Reperfusion Injury Salvage Kinase (RISK)-pathway. *Cardiovascular research*, 61(3), pp.448-460.
- Hausenloy, D.J., Tsang, A. & Yellon, D.M., 2005. The reperfusion injury salvage kinase pathway: A common target for both ischaemic preconditioning and postconditioning. *Trends in Cardiovascular Medicine*, 15(2), pp.69–75.
- Hazra, S., Xiong, S., Wang, J., Rippe, R. A., Chatterjee, V. K. K. and Tsukamoto, H., 2004. Peroxisome Proliferator-activated Receptor γ Induces a Phenotypic Switch from Activated to Quiescent Hepatic Stellate Cells. *Journal of Biological Chemistry*, 279(12), pp.11392–11401.
- Herceg, Z. and Wang, Z.Q., 1999. Failure of poly (ADP-ribose) polymerase cleavage by caspases leads to induction of necrosis and enhanced apoptosis. *Molecular and cellular biology*, 19(7), pp.5124-5133.
- Hill, A. and Balkin, A., 2009. Risk factors for gastrointestinal adverse events in HIV treated and untreated patients. *AIDS Rev*, 11(1), pp.30-38.
- Hirosumi, J., Tuncman, G., Chang, L., Görgün, C. Z., Uysal, K. T., Maeda, K., 2002. A central role for JNK in obesity and insulin resistance. *Nature*, 420(6913), pp.333–336.
- Hitti, E., Iakovleva, T., Brook, M., Deppenmeier, S., Gruber, A.D., Radzioch, D., Clark, A.R., Blackshear, P.J., Kotlyarov, A. and Gaestel, M., 2006. Mitogen-activated protein kinase-activated protein kinase 2 regulates tumor necrosis factor mRNA stability and translation mainly by altering tristetraprolin expression, stability, and binding to adenine/uridine-rich element. *Molecular and cellular biology*, 26(6), pp.2399-2407.
- Hsiou, Y., Ding, J., Das, K., Clark, A. D., Hughes, S. H. and Arnold, E., 1996. Structure of unliganded HIV-1 reverse transcriptase at 2.7 Å resolution: Implications of conformational changes for polymerization and inhibition mechanisms. *Structure*, 4(7), pp.853–860.
- Hui, J. M., Hodge, A., Farrell, G. C., Kench, J. G., Kriketos, A. and George, J., 2004. Beyond insulin resistance in NASH: TNF- α or adiponectin? *Hepatology*, 40(1), pp.46–54.
- Hussain, M.B. and Marshall, I., 1997. Characterization of α 1-adrenoceptor subtypes mediating contractions to phenylephrine in rat thoracic aorta, mesenteric artery and pulmonary artery. *British journal of pharmacology*, 122(5), pp.849-858.
- IJpenberg, A., Jeannin, E., Wahli, W. and Desvergne, B., 1997. Polarity and specific sequence requirements of peroxisome proliferator-activated receptor (PPAR)/retinoid X receptor heterodimer binding to DNA A functional analysis of the malic enzyme gene PPAR response element. *Journal of Biological Chemistry*, 272(32), pp.20108-20117.
- Jacobs, M.D. and Harrison, S.C., 1998. Structure of an I κ B α /NF- κ B complex. *Cell*, 95(6), pp.749-758.
- Jäger, S., Handschin, C., Pierre, J. S.- and Spiegelman, B. M., 2007. AMP-activated protein kinase (AMPK) action in skeletal muscle via direct phosphorylation of PGC-1 α . *Proceedings of the National Academy of Sciences*, 104(29), pp.12017–12022.
- Jaime, P.C., Florindo, A.A., Latorre, M.D.R.D.D. and Segurado, A.A.C., 2006. Central obesity and dietary intake in HIV/AIDS patients. *Revista de saude publica*, 40(4), pp.634-640.
- Jain, M.R., Giri, S.R., Trivedi, C., Bhoi, B., Rath, A., Vanage, G., et al., 2015. Saroglitazar, a novel PPAR α / γ agonist with predominant PPAR α activity, shows lipid-lowering and insulin-sensitizing effects in preclinical models. *Pharmacology research & perspectives*, 3(3), p.e00136.
- James, P.T., Leach, R., Kalamara, E. and Shayeghi, M., 2001. The worldwide obesity epidemic. *Obesity*, 9(S11), pp.228-233.
- Jani, R.H., Kansagra, K., Jain, M.R. and Patel, H., 2013. Pharmacokinetics, safety, and tolerability of saroglitazar (ZYH1), a predominantly PPAR α agonist with moderate PPAR γ agonist activity in healthy human subjects. *Clinical drug investigation*, 33(11), pp.809-816.
- Jani, R.H., Pai, V., Jha, P., Jariwala, G., Mukhopadhyay, S., Bhansali, A. and Joshi, S., 2014. A multicenter, prospective, randomized, double-blind study to evaluate the safety and efficacy of Saroglitazar 2 and 4 mg compared with

- placebo in type 2 diabetes mellitus patients having hypertriglyceridemia not controlled with atorvastatin therapy (PRESS VI). *Diabetes technology & therapeutics*, 16(2), pp.63-71.
- Jayakody, R.L., Senaratne, M.P.J., Thomson, A.B.R. and Kappagoda, C.T., 1985. Cholesterol feeding impairs endothelium-dependent relaxation of rabbit aorta. *Canadian journal of physiology and pharmacology*, 63(9), pp.1206-1209.
- Jensen, T. E., Rose, A. J., Jørgensen, S. B., Brandt, N., Schjerling, P., Wojtaszewski, J. F. P., et al., 2007. Possible CaMKK-dependent regulation of AMPK phosphorylation and glucose uptake at the onset of mild tetanic skeletal muscle contraction. *American journal of physiology. Endocrinology and metabolism*, 292(5), pp.E1308–E1317.
- Jentzsch, A.M., Bachmann, H., Fürst, P. and Biesalski, H.K., 1996. Improved analysis of malondialdehyde in human body fluids. *Free Radical Biology and Medicine*, 20(2), pp.251-256.
- Jespersen, B., Tykocki, N.R., Watts, S.W. and Cobbett, P.J., 2015. Measurement of smooth muscle function in the isolated tissue bath-applications to pharmacology research. *Journal of visualized experiments: JoVE*, (95), pe52324.
- Jones, S.A., O'Donnell, V.B., Wood, J.D., Broughton, J.P., Hughes, E.J. and Jones, O.T., 1996. Expression of phagocyte NADPH oxidase components in human endothelial cells. *American Journal of Physiology-Heart and Circulatory Physiology*, 271(4), pp.H1626-H1634.
- Kadlec, A. O., Chabowski, D. S., Ait-Aissa, K., Hockenberry, J. C., Otterson, M. F., Durand, M. J., et al., 2017. PGC-1 α (Peroxisome Proliferator-Activated Receptor γ Coactivator 1- α) Overexpression in Coronary Artery Disease Recruits NO and Hydrogen Peroxide During Flow-Mediated Dilatation and Protects Against Increased Intraluminal Pressure. *Hypertension*, 70(1), pp.166–173.
- Kannel, W. & Mc Gee, D., 1979. Diabetes and Cardiovascular Risk Factors : The Framingham Study. *Circulation*, 59(1), pp.8–13.
- Kannel, W., Dawber, T., Kagan, A., Revotskie, N., Stokes, J. and III., 1961. Factors of risk in the development of coronary heart disease—six-year follow-up experience: The framingham study. *Annals of Internal Medicine*, 55(1), pp.33–50.
- Kannel, W.B., McGee, D. & Gordon, T., 1976. A general cardiovascular risk profile: The Framingham study. *The American Journal of Cardiology*, 38(1), pp.46–51.
- Kannel, W.B., Wolf, P.A., Castelli, W.P. and D'Agostino, R.B., 1987. Fibrinogen and risk of cardiovascular disease: the Framingham Study. *Jama*, 258(9), pp.1183-1186.
- Kant, A.K., Graubard, B.I. and Atchison, E.A., 2009. Intakes of plain water, moisture in foods and beverages, and total water in the adult US population—nutritional, meal pattern, and body weight correlates: National Health and Nutrition Examination Surveys 1999–2006. *The American journal of clinical nutrition*, 90(3), pp.655-663.
- Kaufmann, S.H., Desnoyers, S., Ottaviano, Y., Davidson, N.E. and Poirier, G.G., 1993. Specific proteolytic cleavage of poly (ADP-ribose) polymerase: an early marker of chemotherapy-induced apoptosis. *Cancer research*, 53(17), pp.3976-3985.
- Kawano, Y. and Cohen, D.E., 2013. Mechanisms of hepatic triglyceride accumulation in non-alcoholic fatty liver disease. *Journal of gastroenterology*, 48(4), pp.434-441.
- Kellam, P., Boucher, C. a & Larder, B. a, 1992. Fifth mutation in human immunodeficiency virus type 1 reverse transcriptase contributes to the development of high-level resistance to zidovudine. *Proceedings of the National Academy of Sciences of the United States of America*, 89(5), pp.1934–1938.
- Kelly, I.E., Han, T.S., Walsh, K. and Lean, M.E., 1999. Effects of a thiazolidinedione compound on body fat and fat distribution of patients with type 2 diabetes. *Diabetes care*, 22(2), pp.288-293.
- Kempf, D. J., Marsh, K. C., Denissen, J. F., McDonald, E., Vasavanonda, S., Flentge, C. A., et al., 1995. ABT-538 is a potent inhibitor of human immunodeficiency virus protease and has high oral bioavailability in humans. *Proceedings of the National Academy of Sciences of the United States of America*, 92(7), pp.2484–2488.
- Kewn, S., Veal, G. J., Hoggard, P. G., Barry, M. G. and Back, D. J., 1997. Lamivudine (3TC) phosphorylation and drug interactions in vitro. *Biochemical Pharmacology*, 54(5), pp.589–595.

- Kitamura, T., Kitamura, Y., Kuroda, S., Hino, Y., Ando, M., Kotani, K., et al., 1999. Insulin-induced phosphorylation and activation of cyclic nucleotide phosphodiesterase 3B by the serine-threonine kinase Akt. *Molecular and cellular biology*, 19(9), pp.6286–6296.
- Knaapen, M., Kootte, R. S., Zoetendal, E. G., de Vos, W. M., Dallinga-Thie, G. M., Levi, M., et al., 2013. Obesity, non-alcoholic fatty liver disease, and atherothrombosis: A role for the intestinal microbiota? *Clinical Microbiology and Infection*, 19(4), pp.331–337.
- Koo, S.-H., Satoh, H., Herzig, S., Lee, C.-H., Hedrick, S., Kulkarni, et al., 2004. PGC-1 promotes insulin resistance in liver through PPAR- α -dependent induction of TRB-3. *Nature Medicine*, 10(5), pp.530–534.
- Kopelman, P., 2007. Health risks associated with overweight and obesity. *Obesity reviews*, 8(s1), pp.13-17.
- Koricanac, G., Tepavcevic, S., Zakula, Z., Milosavljevic, T., Stojiljkovic, M. and Isenovic, E.R., 2011. Interference between insulin and estradiol signaling pathways in the regulation of cardiac eNOS and Na⁺/K⁺-ATPase. *European journal of pharmacology*, 655(1), pp.23-30.
- Kota, B.P., Huang, T.H.W. and Roufogalis, B.D., 2005. An overview on biological mechanisms of PPARs. *Pharmacological Research*, 51(2), pp.85-94.
- Kwiterovich, P.O., 2000. The metabolic pathways of high-density lipoprotein, low-density lipoprotein, and triglycerides: a current review. *The American journal of cardiology*, 86(12), pp.5-10.
- Kwong, P. D., Wyatt, R., Robinson, J., Sweet, R. W., Sodroski, J. and Hendrickson, W. a., 1998. Structure of an HIV gp120 envelope glycoprotein in complex with the CD4 receptor and a neutralizing human antibody. *Nature*, 393(June), pp.648–659.
- La Fleur, S.E., Luijendijk, M.C.M., Van Der Zwaal, E.M., Brans, M.A.D. and Adan, R.A.H., 2014. The snacking rat as model of human obesity: effects of a free-choice high-fat high-sugar diet on meal patterns. *International Journal of Obesity*, 38(5), pp.643-649.
- Lage, R., Diéguez, C., Vidal-Puig, A. and López, M., 2008. AMPK: a metabolic gauge regulating whole-body energy homeostasis. *Trends in molecular medicine*, 14(12), pp.539-549.
- Lai, K. K., Gang, D. L., Zawacki, J. K. and Cooley, T. P., 1991. Fulminant hepatic failure associated with 2', 3'-dideoxyinosine (ddI). *Ann Intern Med*, 115(4), pp.283–284.
- Lake, J.E., Wohl, D., Scherzer, R., Grunfeld, C., Tien, P.C., Sidney, S. and Currier, J.S., 2011. Regional fat deposition and cardiovascular risk in HIV infection: the FRAM study. *AIDS care*, 23(8), pp.929-938.
- Lakey, W. C., Yang, L. Y., Yancy, W., Chow, S. C. and Hicks, C. B., 2013. Short communication: from wasting to obesity: initial antiretroviral therapy and weight gain in HIV-infected persons. *AIDS Res Hum Retroviruses*, 29(3), pp.435–440.
- Larder, B.A., Kemp, S.D. & Harrigan, P.R., 1995. Potential Mechanism for Sustained Antiretroviral Efficacy of AZT-3TC Combination Therapy. *American Association for the Advancement of Science Stable*, 269(5224), pp.696–699.
- Lavie, C.J., Osman, A.F., Milani, R.V. and Mehra, M.R., 2003. Body composition and prognosis in chronic systolic heart failure: the obesity paradox. *American Journal of Cardiology*, 91(7), pp.891-894.
- Lawlor, M.A. & Alessi, D.R., 2001. PKB/Akt. *Journal of cell science*, 114(16), pp.2903–2910.
- Leclercq, I.A., Morais, A.D.S., Schroyen, B., Van Hul, N. and Geerts, A., 2007. Insulin resistance in hepatocytes and sinusoidal liver cells: mechanisms and consequences. *Journal of hepatology*, 47(1), pp.142-156.
- Lee, J. Y., Kim, K. M., Lee, S. G., Yu, E., Lim, Y. S., Lee, H. C., et al., 2007. Prevalence and risk factors of non-alcoholic fatty liver disease in potential living liver donors in Korea: A review of 589 consecutive liver biopsies in a single center. *Journal of Hepatology*, 47(2), pp.239–244.
- Lehman, J.J., Barger, P.M., Kovacs, A., Saffitz, J.E., Medeiros, D.M. and Kelly, D.P., 2000. Peroxisome proliferator-activated receptor γ coactivator-1 promotes cardiac mitochondrial biogenesis. *Journal of Clinical Investigation*, 106(7), p.847.

- Leite, N. C., Salles, G. F., Araujo, A. L. E., Villela-Nogueira, C. A. and Cardoso, C. R. L., 2009. Prevalence and associated factors of non-alcoholic fatty liver disease in patients with type-2 diabetes mellitus. *Liver International*, 29(1), pp.113–119.
- Lemoine, M., Barbu, V., Girard, P.M., Kim, M., Bastard, J.P., Wendum, D., et al., 2006. Altered hepatic expression of SREBP-1 and PPAR γ is associated with liver injury in insulin-resistant lipodystrophic HIV-infected patients. *Aids*, 20(3), pp.387-395.
- Leonardini, A., Laviola, L., Perrini, S., Natalicchio, A. and Giorgino, F., 2009. Cross-Talk between PPAR and Insulin Signaling and Modulation of Insulin Sensitivity. *PPAR research*, 2009(2009) pe818945,12.
- Leone, T. C., Lehman, J. J., Finck, B. N., Schaeffer, P. J., Wende, A. R., Boudina, S., et al., 2005. PGC-1 α deficiency causes multi-system energy metabolic derangements: Muscle dysfunction, abnormal weight control and hepatic steatosis. *PLoS Biology*, 3(4), pp.0672–0687.
- Lewis, W., Copeland, W.C. & Day, B.J., 2001. Mitochondrial DNA Depletion, Oxidative Stress, and Mutation: Mechanisms Of Dysfunction from Nucleoside Reverse Transcriptase Inhibitors. *Laboratory investigation*, 81(6), pp.777–790.
- Li, Y., Xu, S., Mihaylova, M.M., Zheng, B., Hou, X., Jiang, B., Park, O., Luo, Z., Lefai, E., Shyy, J.Y.J. and Gao, B., 2011. AMPK phosphorylates and inhibits SREBP activity to attenuate hepatic steatosis and atherosclerosis in diet-induced insulin-resistant mice. *Cell metabolism*, 13(4), pp.376-388.
- Liebermeister, H., Battersby, E.J. and Morgan, H.E., 1967. Effect of pressure development on oxygen consumption by isolated rat heart. *American Journal of Physiology--Legacy Content*, 212(4), pp.804-814.
- Lillie, R.D. and Ashburn, L.L., 1943. Supersaturated solutions of fat stains in dilute isopropanol for demonstration of acute fatty degeneration not shown by Herxheimer's technique. *Arch Pathol*, 36, pp.432-440.
- Lillie, R.D., 1944. Various Oil Soluble Dyes as Pat Stains in the Supersaturated Isopropanol Technic. *Stain Technology*, 19(2), pp.55-58.
- Lin, J., Puigserver, P., Donovan, J., Tarr, P. and Spiegelman, B. M., 2002. Peroxisome proliferator-activated receptor γ coactivator 1 β (PGC-1 β), a novel PGC-1-related transcription coactivator associated with host cell factor. *Journal of Biological Chemistry*, 277(3), pp.1645–1648.
- Lin, T.S. & Prusoff, W.H., 1978. Synthesis and biological activity of several amino analogues of thymidine. *Journal of medicinal chemistry*, 21(1), pp.109–112.
- Lipshultz, S. E., Mas, C. M., Henkel, J. M., Franco, V. I., Fisher, S. D. and Miller, T. L., 2012. HAART to Heart: Highly active antiretroviral therapy and the risk of cardiovascular disease in HIV-infected or exposed children and adults. *Expert Rev. Anti Infect. Ther.*, 10(6), pp.661–674.
- Liu, Y., Shim, E., Crespo-Mejias, Y., Nguyen, P., Gibbons, A., Liu, D., et al., 2015. Cardiomyocytes are Protected from Antiretroviral Nucleoside Analog-Induced Mitochondrial Toxicity by Overexpression of PGC-1 α . *Cardiovascular Toxicology*, 15(3), pp.224–231.
- Liu, Y., Wan, Q., Guan, Q., Gao, L. and Zhao, J., 2006. High-fat diet feeding impairs both the expression and activity of AMPKa in rats' skeletal muscle. *Biochemical and biophysical research communications*, 339(2), pp.701–707.
- Lizardi-Cervera, J., Chavez-Tapia, N. C., Pérez-Bautista, O., Ramos, M. H. and Uribe, M., 2007. Association among C-reactive protein, fatty liver disease, and cardiovascular risk. *Digestive Diseases and Sciences*, 52(9), pp.2375–2379.
- Lochner, A., Genade, S. and Moolman, J.A., 2003. Ischaemic preconditioning: infarct size is a more reliable endpoint than functional recovery. *Basic research in cardiology*, 98(5), pp.337-346.
- Locker, N., Chamond, N. & Sargueil, B., 2011. A conserved structure within the HIV gag open reading frame that controls translation initiation directly recruits the 40S subunit and eIF3. *Nucleic Acids Research*, 39(6), pp.2367–2377.
- Logani, M.K. and Davies, R.E., 1980. Lipid oxidation: biologic effects and antioxidants—a review. *Lipids*, 15(6), pp.485-495.

- Logie, L., Ruiz-Alcaraz, A.J., Keane, M., Woods, Y.L., Bain, J., Marquez, R., Alessi, D.R. and Sutherland, C., 2007. Characterization of a protein kinase B inhibitor in vitro and in insulin-treated liver cells. *Diabetes*, 56(9), pp.2218-2227.
- Lumsden, R.H. & Bloomfield, G.S., 2016. The Causes of HIV-Associated Cardiomyopathy: A Tale of Two Worlds. *BioMed Research International*, 2016(2016), p.e8196560-9.
- Lüscher, T.F. & Vanhoutte, P.M., 1991. The endothelium: modulator of cardiovascular function, Boca Raton, *FLCRC press*.
- Ma, X.L., Kumar, S., Gao, F., Loudon, C.S., Lopez, B.L., Christopher, T.A., Wang, C., Lee, J.C., Feuerstein, G.Z. and Yue, T.L., 1999. Inhibition of p38 mitogen-activated protein kinase decreases cardiomyocyte apoptosis and improves cardiac function after myocardial ischaemia and reperfusion. *Circulation*, 99(13), pp.1685-1691.
- Maartens, G., Celum, C., Lewin, S. R., Town, C. and Africa, S., 2014. Seminar HIV infection : epidemiology , pathogenesis , treatment , and prevention. *The Lancet*, 384(9939), pp.258–271.
- Machado, M., Marques-Vidal, P. & Cortez-Pinto, H., 2006. Hepatic histology in obese patients undergoing bariatric surgery. *Journal of Hepatology*, 45(4), pp.600–606.
- Maia Leite, L.H. & De Mattos Marinho Sampaio, A.B., 2010. Progression to overweight, obesity and associated factors after antiretroviral therapy initiation among Brazilian persons with HIV/AIDS. *Nutricion Hospitalaria*, 25(4), pp.635–640.
- Malhi, H., Bronk, S.F., Werneburg, N.W. and Gores, G.J., 2006. Free fatty acids induce JNK-dependent hepatocyte lipoapoptosis. *Journal of Biological Chemistry*, 281(17), pp.12093-12101.
- Marais, E., Genade, S., Salie, R., Huisamen, B., Maritz, S., Moolman, J.A. and Lochner, A., 2005. The temporal relationship between p38 MAPK and HSP27 activation in ischaemic and pharmacological preconditioning. *Basic research in cardiology*, 100(1), pp.35-47.
- Marks, G., Crepaz, N. & Janssen, R.S., 2006. Estimating sexual transmission of HIV from persons aware and unaware that they are infected with the virus in the USA. *AIDS (London, England)*, 20(10), pp.1447–1450.
- Marsin, A. S., Bertrand, L., Rider, M. H., Deprez, J., Beauvoys, C., Vincent, M. F., et al., 2000. Phosphorylation and activation of heart PFK-2 by AMPK has a role in the stimulation of glycolysis during ischaemia. *Current biology*, 10(20), pp.1247–1255.
- Mathers, C.D. and Loncar, D., 2006. Projections of global mortality and burden of disease from 2002 to 2030. *PLoS medicine*, 3(11), p.e442.
- Matthews, D.R., Hosker, J.P., Rudenski, A.S., Naylor, B.A., Treacher, D.F. and Turner, R.C., 1985. Homeostasis model assessment: insulin resistance and β -cell function from fasting plasma glucose and insulin concentrations in man. *Diabetologia*, 28(7), pp.412-419.
- Matthews, L. T., Giddy, J., Ghebremichael, M., Hampton, J., Guarino, A. J., Ewusi, A., et al., 2011. A risk-factor guided approach to reducing lactic acidosis and hyperlactatemia in patients on antiretroviral therapy. *PLoS ONE*, 6(4), p.e18736.
- Mavria, G., Vercoulen, Y., Yeo, M., Paterson, H., Karasarides, M., Marais, R., Bird, D. and Marshall, C.J., 2006. ERK-MAPK signaling opposes Rho-kinase to promote endothelial cell survival and sprouting during angiogenesis. *Cancer cell*, 9(1), pp.33-44.
- Mazen, A., Murcia, J.M.D., Molinete, M., Simonin, F., Gradwohl, G., Poirier, G. and de Murcia, G., 1989. Poly (ADP-ribose) polymerase: a novel finger protein. *Nucleic acids research*, 17(12), pp.4689-4698.
- Mazumder, P.K., O'Neill, B.T., Roberts, M.W., Buchanan, J., Yun, U.J., Cooksey, R.C., Boudina, S. and Abel, E.D., 2004. Impaired cardiac efficiency and increased fatty acid oxidation in insulin-resistant ob/ob mouse hearts. *Diabetes*, 53(9), pp.2366-2374.
- McComsey, G.A., Moser, C., Currier, J., Ribaldo, H.J., Paczuski, P., Dubé, M.P., Kelesidis, T., Rothenberg, J., Stein, J.H. and Brown, T.T., 2016. Body composition changes after initiation of raltegravir or protease inhibitors: ACTG A5260s. *Clinical Infectious Diseases*, 62(7), pp.853-862.

- McDougal, J. S., Nicholson, J. K., Cross, G. D., Cort, S. P., Kennedy, M. S. and Mawle, A. C., 1986. Binding of the human retrovirus HTLV-III/LAV/ARV/HIV to the CD4 (T4) molecule: conformation dependence, epitope mapping, antibody inhibition, and potential for idiotypic mimicry. *The Journal of Immunology*, 137(9), pp.2937-2944.
- McGovern, B. H., Ditelberg, J. S., Taylor, L. E., Gandhi, R. T., Christopoulos, K. a, Chapman, S., et al., 2006. Hepatic steatosis is associated with fibrosis, nucleoside analogue use, and hepatitis C virus genotype 3 infection in HIV-seropositive patients. *Clinical infectious diseases: an official publication of the Infectious Diseases Society of America*, 43(3), pp.365–372.
- Mehta, S. H., Thomas, D. L., Torbenson, M., Brinkley, S., Mirel, L., Chaisson, R. E., et al., 2005. The effect of antiretroviral therapy on liver disease among adults with HIV and hepatitis C coinfection. *Hepatology (Baltimore, Md.)*, 41(1), pp.123–131.
- Meininger, G., Hadigan, C., Rietschel, P. and Grinspoon, S., 2002. Body-composition measurements as predictors of glucose and insulin abnormalities in HIV-positive men. *The American journal of clinical nutrition*, 76(2), pp.460-465.
- Melanson, E.L., Astrup, A. and Donahoo, W.T., 2009. The relationship between dietary fat and fatty acid intake and body weight, diabetes, and the metabolic syndrome. *Annals of Nutrition and Metabolism*, 55(1-3), pp.229-243.
- Michael, L.F., Wu, Z., Cheatham, R.B., Puigserver, P., Adelmant, G., Lehman, J.J., Kelly, D.P. and Spiegelman, B.M., 2001. Restoration of insulin-sensitive glucose transporter (GLUT4) gene expression in muscle cells by the transcriptional coactivator PGC-1. *Proceedings of the National Academy of Sciences*, 98(7), pp.3820-3825.
- Mihaylova, M.M. & Shaw, R.J., 2011. The AMP-activated protein kinase (AMPK) signaling pathway coordinates cell growth, autophagy, & metabolism. *Nature cell biology*, 13(9), pp.1016-1023.
- Mitsuya, H. & Broder, S., 1986. Inhibition of the in vitro infectivity and cytopathic effect of human T-lymphotropic virus type III/lymphadenopathy-associated virus (HTLV-III/LAV) by 2',3'-dideoxynucleosides. *Proceedings of the National Academy of Sciences of the United States of America*, 83(6), pp.1911–1915.
- Mitsuya, H., Weinholdt, K. J., Furmant, P. A., Clairt, M. H. S., Lehrmant, S. N., Gallo, R. C., et al., 1985. 3'-Azido-3'-deoxythymidine (BW A509U): An antiviral agent that inhibits the infectivity and cytopathic effect of human T-lymphotropic virus type III/lymphadenopathy-associated virus in vitro. *Proc. Natl. Acad. Sci. USA*, 82(20), pp.7096–7100.
- Mocroft, A., Ledergerber, B., Katlama, C., Kirk, O., Reiss, P.D., Monforte, A.D.A., and EuroSIDA Study Group., 2003. Decline in the AIDS and death rates in the EuroSIDA study: an observational study. *The Lancet*, 362(9377), pp.22-29.
- Molla, A., Korneyeva, M., Gao, Q., Vasavanonda, S., Schipper, P. J., Mo, H. M., et al., 1996. Ordered accumulation of mutations in HIV protease confers resistance to ritonavir. *Nature medicine*, 2(7), pp.760–766.
- Monaco, C., Andreakos, E., Kiriakidis, S., Mauri, C., Bicknell, C., Foxwell, B., Cheshire, N., et al., 2004 Canonical pathway of nuclear factor k B activation selectively regulates proinflammatory and prothrombotic responses in human atherosclerosis, *Proceedings of the National Academy of Sciences*, 101 (15) pp. 5634-5639.
- Moore, A., Herrera, G., Nyamongo, J., Lackritz, E., Granade, T., Nahlen, B., et al., 2001. Estimated risk of HIV transmission by blood transfusion in Kenya. *Lancet*, 358(9282), pp.657–660.
- Moran, A. E., Forouzanfar, M. H., Roth, G. A., Mensah, G. A., Ezzati, M., Murray, C. J. L., et al., 2014. Temporal trends in ischaemic heart disease mortality in 21 world regions, 1980 to 2010: The global burden of disease 2010 study. *Circulation*, 129(14), pp.1483–1492.
- Moran, V.H., Leathard, H.L. and Coley, J., 2000. Cardiovascular functioning during the menstrual cycle. *Clinical Physiology and Functional Imaging*, 20(6), pp.496-504.
- Morse, C. G., McLaughlin, M., Matthews, L., Proshan, M., Thomas, F., Gharib, A. M., et al., 2015. Nonalcoholic steatohepatitis and hepatic fibrosis in HIV-1-monoinfected adults with elevated aminotransferase levels on antiretroviral therapy. *Clinical Infectious Diseases*, 60(10), pp.1569–1578.

- Motoshima, H., Goldstein, B. J., Igata, M. and Araki, E., 2006. AMPK and cell proliferation—AMPK as a therapeutic target for atherosclerosis and cancer. *The Journal of physiology*, 574(1), pp.63–71.
- Nagendran, J., Waller, T.J. & Dyck, J.R.B., 2013. AMPK signalling and the control of substrate use in the heart. *Molecular and Cellular Endocrinology*, 366(2), pp.180–193.
- Nagiah, S., Phulukdaree, A. & Chuturgoon, A., 2015. Mitochondrial and Oxidative Stress Response in HepG2 Cells Following Acute and Prolonged Exposure to Antiretroviral Drugs. *Journal of Cellular Biochemistry*, 116(9), pp.1939–1946.
- Nair, A.B. and Jacob, S., 2016. A simple practice guide for dose conversion between animals and human. *Journal of basic and clinical pharmacy*, 7(2), pp.27-31.
- Nduhirabandi, F., Huisamen, B., Strijdom, H., Blackhurst, D. and Lochner, A., 2014. Short-term melatonin consumption protects the heart of obese rats independent of body weight change and visceral adiposity. *Journal of pineal research*, 57(3), pp.317-332.
- Nisoli, E., 2003. Mitochondrial Biogenesis in Mammals: The Role of Endogenous Nitric Oxide. *Science*, 299(5608), pp.896–899.
- Oakes, N.D., Cooney, G.J., Camilleri, S., Chisholm, D.J. and Kraegen, E.W., 1997. Mechanisms of liver and muscle insulin resistance induced by chronic high-fat feeding. *Diabetes*, 46(11), pp.1768-1774.
- Oberdorfer, P., Sittiwangkul, R., Puthanakit, T., Pongprot, Y. and Sirisanthana, V., 2008. Dilated cardiomyopathy in three HIV-infected children after initiation of antiretroviral therapy. *Pediatrics International*, 50(2), pp.251-254.
- Olano, J. P., Borucki, M. J., Wen, J. W. and Haque, A. K., 1995. Massive hepatic steatosis and lactic acidosis in a patient with AIDS who was receiving zidovudine. *Clinical infectious diseases*, 21(4), pp.973–976.
- Ouchi, Y., Han, S.Z., Kim, S., Akishita, M., Kozaki, K., Toba, K. and Orimo, H., 1996. Augmented contractile function and abnormal Ca²⁺ handling in the aorta of Zucker obese rats with insulin resistance. *Diabetes*, 45(Supplement 3), pp.S55-S58.
- Ouwens, D.M., Boer, C., Fodor, M., De Galan, P., Heine, R.J., Maassen, J.A. and Diamant, M., 2005. Cardiac dysfunction induced by high-fat diet is associated with altered myocardial insulin signalling in rats. *Diabetologia*, 48(6), pp.1229-1237.
- Pai, J. K., Pischon, T., Ma, J., Manson, J. E., Hankinson, S. E., Joshipura, K., et al., 2004. Inflammatory markers and the risk of coronary heart disease in men and women. *New England Journal of Medicine*, 351(25), pp.2599–2610.
- Palella Jr, F. J., Delaney, K. M., Moorman, A. C., Loveless, M. O., Fuhrer, J., Satten, G. A., et al., 1998. Declining morbidity and mortality among patients with advanced human immunodeficiency virus infection. *New England Journal of Medicine*, 338(13), pp.853–860.
- Palmer, R.M.J., Ashton, D.S. & Moncada, S., 1988. Vascular endothelial cells synthesize nitric oxide from L-arginine. *Nature*, 333(6174), pp.664–666.
- Pancani, T., Anderson, K.L., Brewer, L.D., Kadish, I., DeMoll, C., Landfield, P.W., Blalock, E.M., Porter, N.M. and Thibault, O., 2013. Effect of high-fat diet on metabolic indices, cognition, and neuronal physiology in aging F344 rats. *Neurobiology of aging*, 34(8), pp.1977-1987.
- Pang, J., Choi, Y. and Park, T., 2008. Ilex paraguariensis extract ameliorates obesity induced by high-fat diet: potential role of AMPK in the visceral adipose tissue. *Archives of biochemistry and biophysics*, 476(2), pp.178-185.
- Panel on Antiretroviral Guidelines for Adults and Adolescents. Guidelines for the Use of Antiretroviral Agents in Adults and Adolescents Living with HIV. *Department of Health and Human Services*. (Available at <http://www.aidsinfo.nih.gov/ContentFiles/AdultandAdolescentGL.pdf>, “Accessed: 30/12/2017”).
- Panza, J. A., Quyyumi, A. A., Brush, J. E. and Epstein, S. E., 1990. Abnormal Endothelium-Dependent Vascular Relaxation in Patients with Essential Hypertension. *New England Journal of Medicine*, 323(1), pp.22–27.
- Pascual, F. & Coleman, R.A., 2016. Fuel availability and fate in cardiac metabolism: A tale of two substrates. *Biochimica et Biophysica Acta - Molecular and Cell Biology of Lipids*, 1861(10), pp.1425–1433.

- Patsch, J.R., Miesenböck, G., Hopferwieser, T., Mühlberger, V., Knapp, E., Dunn, J.K., Gotto, A.M. and Patsch, W., 1992. Relation of triglyceride metabolism and coronary artery disease. Studies in the postprandial state. *Arteriosclerosis, Thrombosis, and Vascular Biology*, 12(11), pp.1336-1345.
- Pearson, T. A., Mensah, G. A., Alexander, R. W., Anderson, J. L., Cannon, R. O., Criqui, M., et al., 2003. Markers of inflammation and cardiovascular disease: Application to clinical and public health practice: A statement for healthcare professionals from the centers for disease control and prevention and the American Heart Association. *Circulation*, 107(3), pp.499-511.
- Pelkonen, R., Nikkilä, E.A., Koskinen, S., Penttinen, K. and Sarna, S., 1977. Association of serum lipids and obesity with cardiovascular mortality. *Br Med J*, 2(6096), pp.1185-1187.
- Pereira, V. X., de Abreu, L. C., Valenti, V. E., Raimundo, R. D., Henrique Silva, M., Rocha Oliveira, F., et al., 2015. The lipodystrophy syndrome as a risk marker for cardiovascular disease in patients with HIV / AIDS treated with HAART. *International Archives of Medicine*, 78 (8), pp.11-16.
- Pérez Rodrigo, C., 2013. Current mapping of obesity. *Nutrición hospitalaria*, 28 (S5), pp.21-31.
- Pickavance, L.C., Tadayyon, M., Widdowson, P.S., Buckingham, R.E. and Wilding, J.P.H., 1999. Therapeutic index for rosiglitazone in dietary obese rats: separation of efficacy and haemodilution. *British journal of pharmacology*, 128(7), pp.1570-1576.
- Piepoli, M. F., Hoes, A. W., Agewall, S., Albus, C., Brotons, C., Catapano, A. L., et al., 2016. 2016 European Guidelines on cardiovascular disease prevention in clinical practice. *European Heart Journal*, 37(29), pp.2315-2381.
- Prashanth, M., Ganesh, H. K., Vima, M. V, John, M., Bandgar, T., Joshi, S. R., et al., 2009. Prevalence of nonalcoholic fatty liver disease in patients with type 2 diabetes mellitus. *J Assoc Physicians India*, 57(April), pp.205-210.
- Price, D.T. and Loscalzo, J., 1999. Cellular adhesion molecules and atherogenesis I. *The American journal of medicine*, 107(1), pp.85-97.
- Price, J.C., Seaberg, E.C., Latanich, R., Budoff, M.J., Kingsley, L.A., Post, W.S. and Thio, C.L., et al., 2014. Risk factors for fatty liver in the Multicenter AIDS Cohort Study. *The American journal of gastroenterology*, 109(5), pp.695-701.
- Pryor, W.A. and Castle, L., 1984. Chemical methods for the detection of lipid hydroperoxides. *Methods in enzymology*, 105, pp.293-299.
- Puchner, S. B., Lu, M. T., Mayrhofer, T., Liu, T., Pursnani, A., Ghoshhajra, B. B., et al., 2015. High-Risk Coronary Plaque at Coronary CT Angiography Is Associated with Nonalcoholic Fatty Liver Disease, Independent of Coronary Plaque and Stenosis Burden: Results from the ROMICAT II Trial. *Radiology*, 274(3), pp.693-701.
- Pujades-Rodriguez, M., Timmis, A., Stogiannis, D., Rapsomaniki, E., Denaxas, S., Shah, A., et al., 2014. Socioeconomic deprivation and the incidence of 12 cardiovascular diseases in 1.9 million women and men: Implications for risk prediction and prevention. *PLoS ONE*, 9 (8), p.e104671.
- Qi, D. & Young, L.H., 2015. AMPK: energy sensor and survival mechanism in the ischaemic heart. *Trends in Endocrinology & Metabolism*, 26(8), pp.422-429.
- Qian, J. & Fulton, D., 2013. Post-translational regulation of endothelial nitric oxide synthase in vascular endothelium. *Frontiers in Physiology*, 4 pp.347-358.
- Rahmouni, K., Correia, M.L., Haynes, W.G. and Mark, A.L., 2005. Obesity-associated hypertension. *Hypertension*, 45(1), pp.9-14.
- Ratziu, V., Giral, P., Jacqueminet, S., Charlotte, F., Hartemann-Heurtier, A., Serfaty, L., et al., 2008. Rosiglitazone for Nonalcoholic Steatohepatitis: One-Year Results of the Randomized Placebo-Controlled Fatty Liver Improvement with Rosiglitazone Therapy (FLIRT) Trial. *Gastroenterology*, 135(1), pp.100-110.
- Razali, N., Dewa, A., Asmawi, M.Z., Ismail, Z., Manshor, N.M. and Hassan, Z., 2013. Vascular reactivity on aortic rings of spontaneously hypertensive rats treated with methanolic and water extracts of *Ficus deltoidea*. *Journal of Experimental & Integrative Medicine*, 3(2), pp.93-102.

- Reeves JD, D.R., 2002. Human immunodeficiency virus type 2. *The Journal of general virology*, 83(2002), pp.1253–1265.
- Regier, D.S., Greene, D.G., Sergeant, S., Jesaitis, A.J. and McPhail, L.C., 2000. Phosphorylation of p22 phox Is Mediated by Phospholipase D-dependent and-independent Mechanisms correlation of NADPH activity and p22phox phosphorylation. *Journal of Biological Chemistry*, 275(37), pp.28406-28412.
- Reitz, M.S. and Gallo, R.C., 2015. Human immunodeficiency viruses. *Mandell, Douglas, and Bennett's principles and practice of infectious diseases. 8th ed. Philadelphia, PA: Elsevier Saunders*.
- Remaley, A.T., Rust, S., Rosier, M., Knapper, C., Naudin, L., Broccardo, C., Peterson, K.M., et al., 1999. Human ATP-binding cassette transporter 1 (ABC1): genomic organization and identification of the genetic defect in the original Tangier disease kindred. *Proceedings of the National Academy of Sciences*, 96(22), pp.12685-12690.
- Review, C. & Communication, S., 2017. Antiretroviral Drugs for Treatment and Prevention of HIV Infection in Adults 2016 *Recommendations of the International Antiviral Society–USA Panel*, 316(2), pp.191–210.
- Reyskens, K.M., Fisher, T.L., Schisler, J.C., O'Connor, W.G., Rogers, A.B., Willis, M.S., et al., 2013. Cardio-metabolic effects of HIV protease inhibitors (lopinavir/ritonavir). *PloS one*, 8(9), p.e73347.
- Reyskens, K.M.S.E. & Essop, M.F., 2014. HIV protease inhibitors and onset of cardiovascular diseases: a central role for oxidative stress and dysregulation of the ubiquitin-proteasome system. *Biochimica et biophysica acta*, 1842(2), pp.256–68.
- Reyskens, K.M.S.E. et al., 2013. The Maladaptive Effects of HIV Protease Inhibitors (Lopinavir/Ritonavir) on the Rat Heart. *PloS one*, 8(9), p.e73347.
- Rhee, J., Inoue, Y., Yoon, J. C., Puigserver, P., Fan, M., Gonzalez, F. J., et al., 2003. Regulation of hepatic fasting response by PPARgamma coactivator-1alpha (PGC-1): Requirement for hepatocyte nuclear factor 4alpha in gluconeogenesis. *Pnas*, 100(7), pp.4012–4017.
- Riddle, T. M., Kuhel, D. G., Woollett, L. A., Fichtenbaum, C. J. and Hui, D. Y., 2001. HIV Protease Inhibitor Induces Fatty Acid and Sterol Biosynthesis in Liver and Adipose Tissues Due to the Accumulation of Activated Sterol Regulatory Element-binding Proteins in the Nucleus. *Journal of Biological Chemistry*, 276(40), pp.37514–37519.
- Ridley, S.H., Sarsfield, S.J., Lee, J.C., Bigg, H.F., Cawston, T.E., Taylor, D.J., DeWitt, D.L. and Saklatvala, J., 1997. Actions of IL-1 are selectively controlled by p38 mitogen-activated protein kinase: regulation of prostaglandin H synthase-2, metalloproteinases, and IL-6 at different levels. *The Journal of Immunology*, 158(7), pp.3165-3173.
- Rinella, M.E., 2015. Nonalcoholic Fatty Liver Disease. *Jama*, 313(22), pp.2263-2273.
- Robinson, W. E., Reinecke, M. G., Abdel-Malek, S., Jia, Q. and Chow, S. a., 1996. Inhibitors of HIV-1 replication that inhibit HIV integrase. *Proceedings of the National Academy of Sciences of the United States of America*, 93(June), pp.6326–6331.
- Rogler, G., Brand, K., Vogl, D., Page, S., Hofmeister, R., Andus, T., Knuechel, R., Baeuerle, P.A., Schölmerich, J. and Gross, V., 1998. Nuclear factor κ B is activated in macrophages and epithelial cells of inflamed intestinal mucosa. *Gastroenterology*, 115(2), pp.357-369.
- Russell III, R.R., Li, J., Coven, D.L., Pypaert, M., Zechner, C., Palmeri, M., Giordano, F.J., Mu, J., Birnbaum, M.J. and Young, L.H., 2004. AMP-activated protein kinase mediates ischaemic glucose uptake and prevents postischaemic cardiac dysfunction, apoptosis, and injury. *Journal of Clinical Investigation*, 114(4), pp.495-503.
- Russell, R. R., Bergeron, R., Shulman, G. I. and Young, L. H., 1999. Translocation of myocardial GLUT-4 and increased glucose uptake through activation of AMPK by AICAR. *American Journal of Physiology-Heart and Circulatory Physiology*, 277(2), pp.H643–H649.
- Rydén, M. & Arner, P., 2007. Tumour necrosis factor- α in human adipose tissue - From signalling mechanisms to clinical implications. *Journal of Internal Medicine*, 262(4), pp.431–438.
- Rykx, A., De Kimpe, L., Mikhalap, S., Vantus, T., Seufferlein, T., Vandenneede, J.R. and Van Lint, J., 2003. Protein kinase D: a family affair. *FEBS letters*, 546(1), pp.81-86.

- Sack, M.N., Disch, D.L., Rockman, H.A. and Kelly, D.P., 1997. A role for Sp and nuclear receptor transcription factors in a cardiac hypertrophic growth program. *Proceedings of the National Academy of Sciences*, 94(12), pp.6438-6443.
- Saini, H. K., Xu, Y. J., Zhang, M., Liu, P. P., Kirshenbaum, L. A. and Dhalla, N. S., 2005. Role of tumour necrosis factor- α and other cytokines in ischaemia-reperfusion-induced injury in the heart. *Experimental and Clinical Cardiology*, 10(4), pp.213–222.
- Salie, R., Huisamen, B. and Lochner, A., 2014. High carbohydrate and high fat diets protect the heart against ischaemia/reperfusion injury. *Cardiovascular diabetology*, 13(1), pp.109-116.
- Salie, R., Moolman, J.A. and Lochner, A., 2012. The mechanism of beta-adrenergic preconditioning: roles for adenosine and ROS during triggering and mediation. *Basic research in cardiology*, 107(5), pp.281-289.
- Salonen, J.T., Salonen, R., Seppänen, K., Rauramaa, R. and Tuomilehto, J.H.D.L., 1991. HDL, HDL2, and HDL3 subfractions, and the risk of acute myocardial infarction. A prospective population study in eastern Finnish men. *Circulation*, 84(1), pp.129-139.
- Sambandam, N. & Lopaschuk, G.D., 2003. AMP-activated protein kinase (AMPK) control of fatty acid and glucose metabolism in the ischaemic heart. *Progress in Lipid Research*, 42(3), pp.238–256.
- Samji, H., Cescon, A., Hogg, R.S., Modur, S.P., Althoff, K.N., Buchacz, K., et al., 2013. Closing the gap: increases in life expectancy among treated HIV-positive individuals in the United States and Canada. *PloS one*, 8(12), p.e81355.
- Sato, K., Kitahara, A., Satoh, K., Ishikawa, T., Tatematsu, M. and Ito, N., 1984. The placental form of glutathione S-transferase as a new marker protein for preneoplasia in rat chemical hepatocarcinogenesis. *GANN Japanese Journal of Cancer Research*, 75(3), pp.199-202.
- Scarborough, N.L. and Carrier, G.O., 1983. Increased α 2-adrenoceptor mediated vascular mediated contraction in diabetic rats. *Autonomic and Autacoid Pharmacology*, 3(3), pp.177-183.
- Scheid, M. P. and Woodgett, J. R., 2003. Unravelling the activation mechanisms of protein kinase B/Akt. *FEBS Letters*, 546(1), pp.108–112.
- Schisterman, E.F., Faraggi, D., Browne, R., Freudenheim, J., Dorn, J., Muti, P., et al., 2001. TBARS and cardiovascular disease in a population-based sample. *Journal of cardiovascular risk*, 8(4), pp.219-225.
- Schreiber, S., Nikolaus, S. & Hampe, J., 1998. Activation of nuclear factor B in inflammatory bowel disease. *Gut*, pp.477–484.
- Schuster, I., Thöni, G. J., Edérhy, S., Walther, G., Nottin, S., Vinet, A., et al., 2008. Subclinical cardiac abnormalities in human immunodeficiency virus-infected men receiving antiretroviral therapy. *The American journal of cardiology*, 101(8), pp.1213–1217.
- Secchiero, P., Gonelli, A., Carnevale, E., Milani, D., Pandolfi, A., Zella, D. and Zauli, G., 2003. TRAIL promotes the survival and proliferation of primary human vascular endothelial cells by activating the Akt and ERK pathways. *Circulation*, 107(17), pp.2250-2256.
- Sengupta, P., 2013. The laboratory rat: relating its age with human's. *International journal of preventive medicine*, 4(6), pp.624-630.
- Shackelford, D.B. & Shaw, R.J., 2009. The LKB1-AMPK pathway: metabolism and growth control in tumor suppression. *Nature reviews. Cancer*, 9(8), pp.563-575.
- Sham, H. L., Kempf, D. J., Molla, M. A., Marsh, K. C., Kumar, G. N., Chen, C. M., et al., 1998. ABT-378, a highly potent inhibitor of the human immunodeficiency virus protease. *Antimicrobial agents and chemotherapy*, 42(12), pp.3218–3224.
- Shi, S.R., Liu, C. and Taylor, C.R., 2007. Standardization of immunohistochemistry for formalin-fixed, paraffin-embedded tissue sections based on the antigen-retrieval technique: from experiments to hypothesis. *Journal of Histochemistry & Cytochemistry*, 55(2), pp.105-109.

- Shiojima, I. and Walsh, K., 2002. Role of Akt signaling in vascular homeostasis and angiogenesis. *Circulation research*, 90(12), pp.1243-1250.
- Shiojima, I., Sato, K. & Kenneth, W., 2005. Disruption of Coordinated Tissue Growth and Angiogenesis in the Heart Contributes to the Progression from Adaptive Hypertrophy to Heart Failure. *Journal of Cardiac Failure*, 11(9), p.S278.
- Siddiqui, M. S., Cheang, K. L., Luketic, V. a., Boyett, S., Idowu, M. O., Patidar, K., 2015. Nonalcoholic Steatohepatitis (NASH) Is Associated with a Decline in Pancreatic Beta Cell (β -Cell) Function. *Digestive Diseases and Sciences*, 60(8), pp.2529-2537
- Sotocinal, S.G., Sorge, R.E., Zaloum, A., Tuttle, A.H., Martin, L.J., Wieskopf, J.S., et al, J.J., 2011. The Rat Grimace Scale: a partially automated method for quantifying pain in the laboratory rat via facial expressions. *Molecular pain*, 7(1), p.55.
- South African National Accreditation System (SANS 10386:2008, <http://www.sun.ac.za/research>, “Accessed: 22/08/2017).
- South African Veterinary Council (Veterinary and Para veterinary regulations, (<http://www.savc.org.za/>, “Accessed: 22/08/2017).
- Sriwijitkamol, A., Ivy, J. L., Christ-Roberts, C., DeFronzo, R. A., Mandarino, L. J. and Musi, N., 2006. LKB1-AMPK signaling in muscle from obese insulin-resistant Zucker rats and effects of training. *American Journal of Physiology-Endocrinology and Metabolism*, 290(5), pp.E925–E932.
- St Clair, M. H., Richards, C. A., Spector, T., Weinhold, K. J., Miller, W. H., Langlois, A. J., et al.,1987. 3'-Azido-3'-deoxythymidine triphosphate as an inhibitor and substrate of purified human immunodeficiency virus reverse transcriptase. *Antimicrob Agents Chemother*, 31(12), pp.1972–1977.
- Stein, J.H., Klein, M.A., Bellehumeur, J.L., McBride, P.E., Wiebe, D.A., Otvos, J.D. and Sosman, J.M., 2001. Use of human immunodeficiency virus-1 protease inhibitors is associated with atherogenic lipoprotein changes and endothelial dysfunction. *Circulation*, 104(3), pp.257-262.
- Stensl kken, K.O., Rutkovskiy, A., Kaljusto, M.L., Hafstad, A.D., Larsen, T.S. and Vaage, J., 2009. Inadvertent phosphorylation of survival kinases in isolated perfused hearts: a word of caution. *Basic research in cardiology*, 104(4), pp.412-423.
- Sugioka, Y., Fujii-Kuriyama, Y., Kitagawa, T. and Muramatsu, M., 1985. Changes in polypeptide pattern of rat liver cells during chemical hepatocarcinogenesis. *Cancer research*, 45(1), pp.365-378.
- Sun, B. and Karin, M., 2008. NF- κ B signaling, liver disease and hepatoprotective agents. *Oncogene*, 27(48), pp.6228-6244.
- Sundar, K., Suarez, M., Banogon, P. E. and Shapiro, J. M., 1997. Zidovudine-induced fatal lactic acidosis and hepatic failure in patients with acquired immunodeficiency syndrome: report of two patients and review of the literature. *Critical care medicine*, 25(8), pp.1425–1430.
- Sundaram, M., Saghayam, S., Priya, B., Venkatesh, K.K., Balakrishnan, P., Shankar, E.M., et al., 2008. Changes in antioxidant profile among HIV-infected individuals on generic highly active antiretroviral therapy in southern India. *International Journal of Infectious Diseases*, 12(6), pp.61-66.
- Sundquist, W.I. and Kr usslich, H.G., 2012. HIV-1 assembly, budding, and maturation. *Cold Spring Harbor perspectives in medicine*, 2(7), p.a006924.
- Suzuki, A., Angulo, P., Lymp, J., St. Sauver, J., Muto, A., Okada, T., et al., 2005. Chronological development of elevated aminotransferases in a nonalcoholic population. *Hepatology*, 41(1), pp.64–71.
- Takagi, H., Matsui, Y., Hirotsu, S., Sakoda, H., Asano, T. and Sadoshima, J., 2007. AMPK mediates autophagy during myocardial ischaemia in vivo. *Autophagy*, 3(4), pp.405–407.
- Tamilarasan, K. P., Temmel, H., Das, S. K., Al Zoughbi, W., Schauer, S., Vesely, P. W., et al., 2012. Skeletal muscle damage and impaired regeneration due to LPL-mediated lipotoxicity. *Cell death & disease*, 3(7), p.e354.

- Tan, Q., Zhu, Y., Li, J., Chen, Z., Han, G. W., Kufareva, I., et al., 2013. Structure of the CCR5 Chemokine Receptor–HIV Entry Inhibitor Maraviroc Complex. *Science*, 341(6152), pp.1387-1390.
- Tang, H., Vasselli, J.R., Wu, E.X., Boozer, C.N. and Gallagher, D., 2002. High-resolution magnetic resonance imaging tracks changes in organ and tissue mass in obese and aging rats. *American Journal of Physiology-Regulatory, Integrative and Comparative Physiology*, 282(3), pp.R890-R899.
- Tanuma, J., Ishizaki, A., Gatanaga, H., Kikuchi, Y., Kimura, S., Hiroe, M. and Oka, S., 2003. Dilated cardiomyopathy in an adult human immunodeficiency virus type 1–Positive patient treated with a zidovudine-containing antiretroviral regime. *Clinical Infectious Diseases*, 37(7), pp.e109-e111.
- Tarantino, G. and Caputi, A., 2011. JNKs, insulin resistance and inflammation: A possible link between NAFLD and coronary artery disease. *World journal of gastroenterology: WJG*, 17(33), pp.3785-3794.
- Targher, G., Bertolini, L., Poli, F., Rodella, S., Scala, L., Tessari, R., et al., 2005. Nonalcoholic fatty liver disease and risk of future cardiovascular events among type 2 diabetic patients. *Diabetes*, 54(12), pp.3541-3546.
- Targher, G., Bertolini, L., Scala, L., Zoppini, G., Zenari, L. and Falezza, G., 2005. Non-alcoholic hepatic steatosis and its relation to increased plasma biomarkers of inflammation and endothelial dysfunction in non-diabetic men. Role of visceral adipose tissue. *Diabetic Medicine*, 22(10), pp.1354–1358.
- Targher, G., Byrne, C. D., Lonardo, A., Zoppini, G. and Barbui, C., 2016. Non-alcoholic fatty liver disease and risk of incident cardiovascular disease : A meta-analysis. *Journal of Hepatology*, 65(3), pp.589–600.
- Tchernof, A. and Després, J.P., 2013. Pathophysiology of human visceral obesity: an update. *Physiological reviews*, 93(1), pp.359-404.
- Teilmann, A.C., Madsen, A.N., Holst, B., Hau, J., Rozell, B. and Abelson, K.S.P., 2014. Physiological and pathological impact of blood sampling by retro-bulbar sinus puncture and facial vein phlebotomy in laboratory mice. *PLoS one*, 9(11), p.e113225.
- Tesfamariam, B.E.L.A.Y., Jakubowski, J.A. and Cohen, R.A., 1989. Contraction of diabetic rabbit aorta caused by endothelium-derived PGH₂-TxA₂. *American Journal of Physiology-Heart and Circulatory Physiology*, 257(5), pp.H1327-H1333.
- Tewari, M., Quan, L.T., O'Rourke, K., Desnoyers, S., Zeng, Z., Beidler, D.R., et al., 1995. Yama/ CPP32 β , a mammalian homolog of CED-3, is a CrmA-inhibitable protease that cleaves the death substrate poly (ADP-ribose) polymerase. *Cell*, 81(5), pp.801-809.
- Than, N.N. & Newsome, P.N., 2015. A concise review of non-alcoholic fatty liver disease. *Atherosclerosis*, 239(1), pp.192–202.
- Tisdale, M., Kemp, S. D., Parry, N. R. and Larder, B. a., 1993. Rapid in vitro selection of human immunodeficiency virus type 1 resistant to 3'-thiacytidine inhibitors due to a mutation in the YMDD region of reverse transcriptase. *Proceedings of the National Academy of Sciences of the United States of America*, 90(12), pp.5653–5656.
- Tonstad, S., Retterstøl, K., Ose, L., Öhman, K.P., Lindberg, M.B. and Svensson, M., 2007. The dual peroxisome proliferator–activated receptor α/γ agonist tesaglitazar further improves the lipid profile in dyslipidemic subjects treated with atorvastatin. *Metabolism*, 56(9), pp.1285-1292.
- Traupe, T., Lang, M., Goettsch, W., Münter, K., Morawietz, H., Vetter, W. and Barton, M., 2002. Obesity increases prostanoid-mediated vasoconstriction and vascular thromboxane receptor gene expression. *Journal of hypertension*, 20(11), pp.2239-2245.
- Treeprasertsuk, S., Lopez-Jimenez, F. & Lindor, K.D., 2011. Nonalcoholic fatty liver disease and the coronary artery disease. *Digestive Diseases and Sciences*, 56(1), pp.35–45.
- Trevisan, M., Browne, R., Ram, M., Muti, P., Freudenheim, J., Carosella, A.M. and Armstrong, D., 2001. Correlates of markers of oxidative status in the general population. *American journal of epidemiology*, 154(4), pp.348-356.
- Troll, J.G., 2011. Approach to dyslipidemia, lipodystrophy, and cardiovascular risk in patients with HIV infection. *Current Atherosclerosis Reports*, 13(1), pp.51–56.

- Tsang, A., Hausenloy, D.J., Mocanu, M.M. and Yellon, D.M., 2004. Postconditioning: a form of “modified reperfusion” protects the myocardium by activating the phosphatidylinositol 3-kinase-Akt pathway. *Circulation research*, 95(3), pp.230-232.
- Tsiodras, S., Mantzoros, C., Hammer, S. and Samore, M., 2000. Effects of protease inhibitors on hyperglycemia, hyperlipidemia, and lipodystrophy: a 5-year cohort study. *Archives of internal medicine*, 160(13), pp.2050-2056.
- Tu, Z., Moss-Pierce, T., Ford, P. and Jiang, T.A., 2013. Rosemary (*Rosmarinus officinalis* L.) extract regulates glucose and lipid metabolism by activating AMPK and PPAR pathways in HepG2 cells. *Journal of agricultural and food chemistry*, 61(11), pp.2803-2810.
- UNAIDS (Joint United Nations Program on HIV/AIDS), 2014. Fast-Track Ending the AIDS epidemic by 2030. *Unaid*, pp.1–40.
- UNICEF, 2004. UNAIDS (Joint United Nations Program on HIV/AIDS). *WHO (World Health Organization), and Médecins sans Frontières*. (Available at http://www.unaids.org/sites/default/files/media_asset/jc645-sources_prices_en_0.pdf, “Accessed: 16/09/2017”).
- Uretsky, S., Messerli, F.H., Bangalore, S., Champion, A., Cooper-DeHoff, R.M., Zhou, Q. and Pepine, C.J., 2007. Obesity paradox in patients with hypertension and coronary artery disease. *The American journal of medicine*, 120(10), pp.863-870.
- Usach, I., Melis, V. & Peris, J.-E., 2013. Non-nucleoside reverse transcriptase inhibitors: a review on pharmacokinetics, pharmacodynamics, safety and tolerability. *Journal of the International AIDS Society*, 16 (1), p.a18567.
- Valen, G., Yan, Z.Q. & Hansson, G.K., 2001. Nuclear factor kappa-B and the heart. *Journal of the American College of Cardiology*, 38(2), pp.307–314.
- Van der Valk, M., Gisolf, E.H., Reiss, P., Wit, F.W.N.M., Japour, A., Weverling, G.J., Danner, S.A. and Prometheus Study Group, 2001. Increased risk of lipodystrophy when nucleoside analogue reverse transcriptase inhibitors are included with protease inhibitors in the treatment of HIV-1 infection. *Aids*, 15(7), pp.847-855.
- Vedanthan, R., Seligman, B. & Fuster, V., 2014. Global perspective on acute coronary syndrome: A burden on the young and poor. *Circulation Research*, 114(12), pp.1959–1975.
- Vega, R.B., Huss, J.M. and Kelly, D.P., 2000. The coactivator PGC-1 cooperates with peroxisome proliferator-activated receptor α in transcriptional control of nuclear genes encoding mitochondrial fatty acid oxidation enzymes. *Molecular and cellular biology*, 20(5), pp.1868-1876.
- Verbeuren, T.J., Jordaens, F.H., Zonnekeyn, L.L., Van Hove, C.E., Coene, M.C. and Herman, A.G., 1986. Effect of hypercholesterolemia on vascular reactivity in the rabbit. I. Endothelium-dependent and endothelium-independent contractions and relaxations in isolated arteries of control and hypercholesterolemic rabbits. *Circulation Research*, 58(4), pp.552-564.
- Vernon, G., Baranova, A. and Younossi, Z.M., 2011. Systematic review: the epidemiology and natural history of non-alcoholic fatty liver disease and non-alcoholic steatohepatitis in adults. *Alimentary pharmacology & therapeutics*, 34(3), pp.274-285.
- Videla, L.A. et al., 2004. Oxidative stress and depletion of hepatic long-chain polyunsaturated fatty acids may contribute to nonalcoholic fatty liver disease. *Free Radical Biology and Medicine*, 37(9), pp.1499–1507.
- Videla, L.A., Rodrigo, R., Orellana, M., Fernandez, V., Tapia, G., Quinones, L., et al., 2004. Oxidative stress-related parameters in the liver of non-alcoholic fatty liver disease patients. *Clinical Science*, 106(3), pp.261-268.
- Vilahir, G. & Badimon, L., 2014. Ischaemia/reperfusion activates myocardial innate immune response: the key role of the toll-like receptor. *Frontiers in Physiology*, 5(12), pp.496-501.
- Vodkin, I. & Loomba, R., 2015. Editorial: NAFLD in HIV infection - Call for action. Authors’ reply. *Alimentary Pharmacology and Therapeutics*, 41(6), p.591-591
- Vodkin, I., Valasek, M. A., Bettencourt, R., Cachay, E. and Loomba, R., 2015. Clinical, biochemical and histological differences between HIV-associated NAFLD and primary NAFLD: A case-control study. *Alimentary Pharmacology and Therapeutics*, 41(4), pp.368–378.

- Walli, R., Herfort, O., Michl, G.M., Demant, T., Jäger, H., Dieterle, C., et al., 1998. Treatment with protease inhibitors associated with peripheral insulin resistance and impaired oral glucose tolerance in HIV-1-infected patients. *Aids*, 12(15), pp.F167-F173.
- Walmsley, S., Bernstein, B., King, M., Arribas, J., Beall, G., Ruane, P., et al., 2002. Lopinavir–ritonavir versus nelfinavir for the initial treatment of HIV infection. *New England Journal of Medicine*, 346(26), pp.2039–2046.
- Wang, H., Naghavi, M., Allen, C., Barber, R. M., Carter, A., Casey, D. C., et al., 2016. Global, regional, and national life expectancy, all-cause mortality, and cause-specific mortality for 249 causes of death, 1980–2015: a systematic analysis for the Global Burden of Disease Study 2015. *The Lancet*, 388(10053), pp.1459–1544.
- Wang, M. & Unger, R.H., 2005. Role of PP2C in cardiac lipid accumulation in obese rodents and its prevention by troglitazone. *American journal of physiology. Endocrinology and metabolism*, 288(1), pp.E216–E221.
- Wang, X., Chai, H., Lin, P.H., Yao, Q. and Chen, C., 2009. Roles and mechanisms of human immunodeficiency virus protease inhibitor ritonavir and other anti-human immunodeficiency virus drugs in endothelial dysfunction of porcine pulmonary arteries and human pulmonary artery endothelial cells. *The American journal of pathology*, 174(3), pp.771-781.
- Webster, I., Salie, R., Marais, E., Fan, W.J., Maarman, G., Huisamen, B. and Lochner, A., 2017. Myocardial susceptibility to ischaemia/reperfusion in obesity: a re-evaluation of the effects of age. *BMC physiology*, 17(1), p.3.
- Whalley, S., Puvanachandra, P., Desai, A. and Kennedy, H., 2007. Hepatology outpatient service provision in secondary care: a study of liver disease incidence and resource costs. *Clinical medicine (London, England)*, 7(2), pp.119–124.
- Wieckowska, A., Papouchado, B. G., Li, Z., Lopez, R., Zein, N. N. and Feldstein, A. E., 2008. Increased hepatic and circulating interleukin-6 levels in human nonalcoholic steatohepatitis. *American Journal of Gastroenterology*, 103(6), pp.1372–1379.
- Willet, W.C., 1994. Diet and health: what should we eat? *Science(Washington)*, 264(5158), pp.532-537.
- Williams, C. D., Stengel, J., Asike, M. I., Torres, D. M., Shaw, J., Contreras, M., et al., 2011. Prevalence of nonalcoholic fatty liver disease and nonalcoholic steatohepatitis among a largely middle-aged population utilizing ultrasound and liver biopsy: A prospective study. *Gastroenterology*, 140(1), pp.124–131.
- Williamson, K., Rebolí, A.C. and Manders, S.M., 1999. Protease inhibitor–induced lipodystrophy. *Journal of the American Academy of Dermatology*, 40(4), pp.635-636.
- Williamson, R. M., Price, J. F., Glancy, S., Perry, E., Nee, L. D., Hayes, P. C., et al., 2011. Prevalence of and risk factors for hepatic steatosis and nonalcoholic fatty liver disease in people with type 2 diabetes: The Edinburgh type 2 diabetes study. *Diabetes Care*, 34(5), pp.1139–1144.
- Wilson, C.R., Tran, M.K., Salazar, K.L., Young, M.E. and Taegtmeyer, H., 2007. Western diet, but not high fat diet, causes derangements of fatty acid metabolism and contractile dysfunction in the heart of Wistar rats. *Biochemical Journal*, 406(3), pp.457-467.
- Wilson, P.W., D'agostino, R.B., Sullivan, L., Parise, H. and Kannel, W.B., 2002. Overweight and obesity as determinants of cardiovascular risk: the Framingham experience. *Archives of internal medicine*, 162(16), pp.1867-1872.
- Wit, F. W. N. M., Weverling, G. J., Weel, J., Jurriaans, S. and Lange, J. M. A., et al., 2002. Incidence of and Risk Factors for Severe Hepatotoxicity Associated with Antiretroviral Combination Therapy. *The Journal of Infectious Diseases*, 186(1), pp.23–31.
- Wolf, A.M. and Colditz, G.A., 1998. Current estimates of the economic cost of obesity in the United States. *Obesity*, 6(2), pp.97-106.
- Wong, K.A. and Lodish, H.F., 2006. A Revised Model for AMP-activated Protein Kinase Structure The α -subunit binds to both the β - and γ -subunits although there is no direct binding between the β - and γ -subunits. *Journal of Biological Chemistry*, 281(47), pp.36434-36442.
- World Health Organization, 2015. *World health statistics 2015*. World Health Organization., (Available at http://www.who.int/gho/publications/world_health_statistics/2015/en/ “Accessed: 08/08/2017”).

- World Health Organization, 2017. *World Health Statistics 2017*: Monitoring Health for The SDGs, (Available at http://www.who.int/gho/publications/world_health_statistics/2017/en/ “Accessed: 30/08/2017”).
- World Health organization. Cardiovascular Diseases. (Available at http://www.who.int/cardiovascular_diseases/en/. “Accessed: 08/08/2017”)
- Woudberg, N.J., Goedecke, J.H. and Lecour, S., 2016. Protection from Cardiovascular Disease Due to Increased High-Density Lipoprotein Cholesterol in African Black Populations: Myth or Reality? *Ethnicity & disease*, 26(4), p.553.
- Wyatt, R. and Sodroski, J., 1998. The HIV-1 envelope glycoproteins: fusogens, antigens, and immunogens. *Science*, 280(5371), pp.1884-1888.
- Yin FC, Spurgeon HA, Rakusan KA, Weisfeldt ML, Lakatta EG.,1982. Use of tibial length to quantify cardiac hypertrophy: application in the aging rat. *American Journal of Physiology-Heart and Circulatory Physiology*. Dec 1;243(6):H941-947.
- Yoon, J.C., Puigserver, P., Chen, G. and Donovan, J., 2001. Control of hepatic gluconeogenesis through the transcriptional coactivator PGC-1. *Nature*, 413(6852), p.131.
- Yu, J., Bian, D., Mahanivong, C., Cheng, R.K., Zhou, W. and Huang, S., 2004. p38 Mitogen-activated protein kinase regulation of endothelial cell migration depends on urokinase plasminogen activator expression. *Journal of Biological Chemistry*, 279(48), pp.50446-50454.
- Yusuf, S., Reddy, S., Ôunpuu, S. and Anand, S., 2001. Global burden of cardiovascular diseases. *Circulation*, 104(23), pp.2855-2864.
- Zatroch, K.K., Knight, C.G., Reimer, J.N. and Pang, D.S., 2017. Refinement of intraperitoneal injection of sodium pentobarbital for euthanasia in laboratory rats (*Rattus norvegicus*). *BMC veterinary research*, 13(1), p.60.
- Zhang, B.B., Zhou, G. & Li, C., 2009. AMPK: An Emerging Drug Target for Diabetes and the Metabolic Syndrome. *Cell Metabolism*, 9(5), pp.407–416.
- Zhou, H., Gurley, E.C., Jarujaron, S., Ding, H., Fang, Y., Xu, Z., Pandak, W.M. and Hylemon, P.B., 2006. HIV protease inhibitors activate the unfolded protein response and disrupt lipid metabolism in primary hepatocytes. *American Journal of Physiology-Gastrointestinal and Liver Physiology*, 291(6), pp.G1071-G1080.
- Zhou, H., Pandak, W. M., Lyall, V., Natarajan, R. and Hylemon, P. B., 2005. HIV protease inhibitors activate the unfolded protein response in macrophages: implication for atherosclerosis and cardiovascular disease. *Molecular pharmacology*, 68(3), pp.690–700.
- Zimmer, H.G., 1998. The isolated perfused heart and its pioneers. *Physiology*, 13(4), pp.203-210
- Ziouzenkova, O., Perrey, S., Marx, N., Bacqueville, D. and Plutzky, J., 2002. Peroxisome proliferator-activated receptors. *Current atherosclerosis reports*, 4(1), pp.59-64.
- Zou, Y., Li, J., Lu, C., Wang, J., Ge, J., Huang, Y., Zhang, L. and Wang, Y., 2006. High-fat emulsion-induced rat model of nonalcoholic steatohepatitis. *Life sciences*, 79(11), pp.1100-1107.